

LUXE's detector system

Noam Tal Hod on behalf of LUXE



WEIZMANN
INSTITUTE
OF SCIENCE



LUXE

Sep 15 2021

Outline

- Introduction (but mostly see Beate's talk!)
- Measurements & Challenges
- Technologies

Eur. Phys. J. Spec. Top.
<https://doi.org/10.1140/epjs/s11734-021-00249-z>

THE EUROPEAN
PHYSICAL JOURNAL
SPECIAL TOPICS

Check for updates

Review

Conceptual design report for the LUXE experiment

H. Abramowicz¹, U. Acosta^{2,3}, M. Altarelli⁴, R. Aßmann⁵, Z. Bai^{6,7}, T. Behnke⁵, Y. Benhammou¹, T. Blackburn⁸, S. Boogert⁹, O. Borysov⁵, M. Borysova^{5,10}, R. Brinkmann⁵, M. Bruschi¹¹, F. Burkart⁵, K. Büßer⁵, N. Cavanagh¹², O. Davidi⁶, W. Decking⁵, U. Dosselli¹³, N. Elkina³, A. Fedotov¹⁴, M. Firlej¹⁵, T. Fiutowski¹⁵, K. Fleck¹², M. Gostkin¹⁶, C. Grojean^{5,30}, J. Hallford^{5,17}, H. Harsh^{18,19}, A. Hartin¹⁷, B. Heinemann^{5,20,a}, T. Heinzl²¹, L. Helary⁵, M. Hoffmann^{5,20}, S. Huang¹, X. Huang^{5,18,20}, M. Idzik¹⁵, A. Ilderton²¹, R. Jacobs⁵, B. Kämpfer^{2,3}, B. King²¹, H. Lahno¹⁰, A. Levanon¹, A. Levy¹, I. Levy²², J. List⁵, W. Lohmann^{5,31}, T. Ma²³, A. J. Macleod²¹, V. Malka⁶, F. Meloni⁵, A. Mironov¹⁴, M. Morandin¹³, J. Moron¹⁵, E. Negodin⁵, G. Perez⁶, I. Pomerantz¹, R. Pöschl²⁴, R. Prasad⁵, F. Quéré²⁵, A. Ringwald⁵, C. Rödel²⁶, S. Rykovanov²⁷, F. Salgado^{18,19}, A. Santra⁶, G. Sarri¹², A. Sävert¹⁸, A. Sbrizzi^{28,32}, S. Schmitt⁵, U. Schramm^{2,3}, S. Schuwalow⁵, D. Seipt¹⁸, L. Shaimerdenova²⁹, M. Shchedrolosiev⁵, M. Skakunov²⁹, Y. Soreq²³, M. Streeter¹², K. Swientek¹⁵, N. Tal Hod⁶, S. Tang²¹, T. Teter^{18,19}, D. Thoden⁵, A. I. Titov¹⁶, O. Tolbanov²⁹, G. Torgrimsson³, A. Tyazhev²⁹, M. Wing^{5,17}, M. Zanetti¹³, A. Zarubin²⁹, K. Zeil³, M. Zepf^{18,19}, and A. Zhemchukov¹⁶

LUXE physics in a nutshell

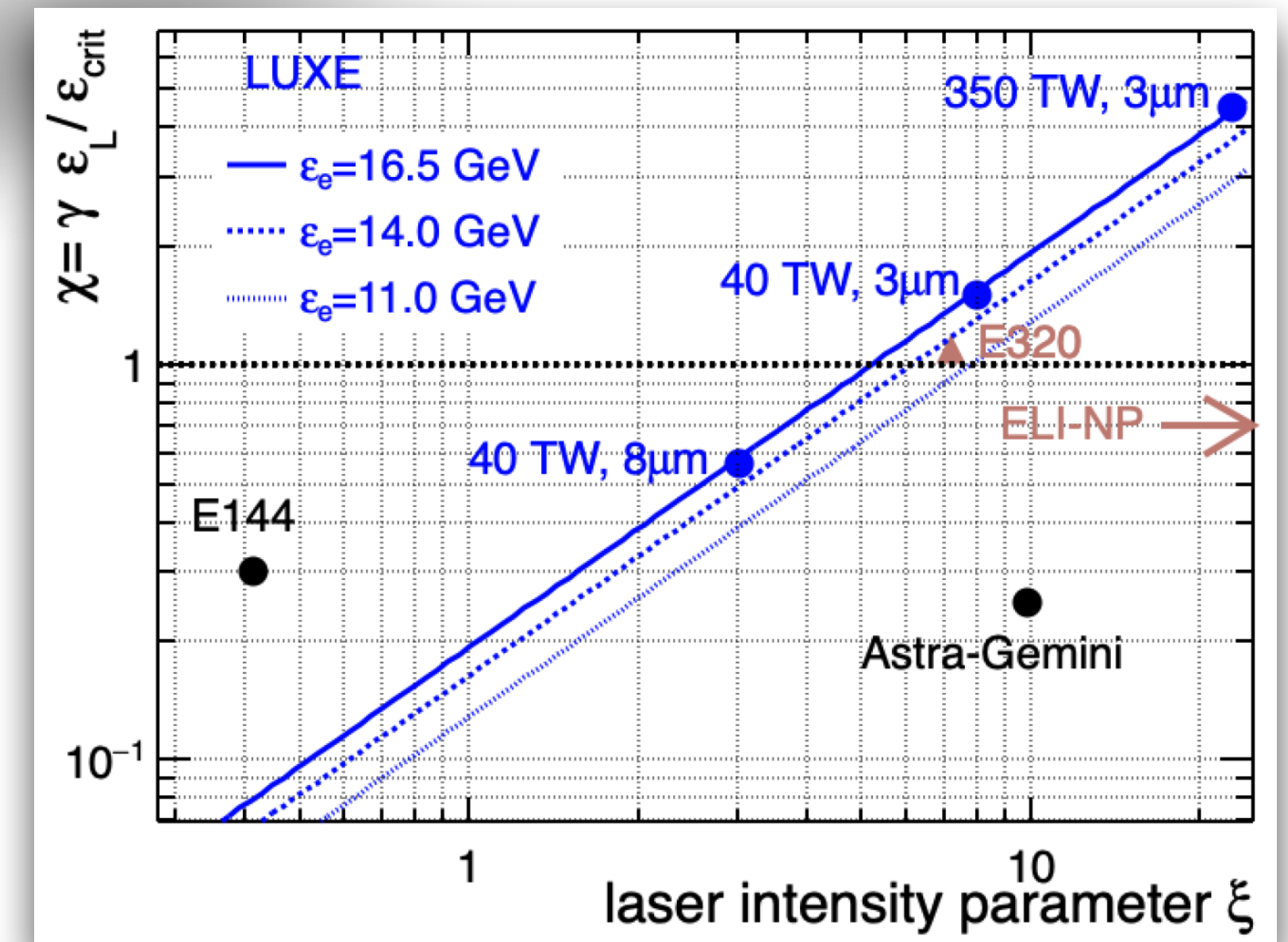
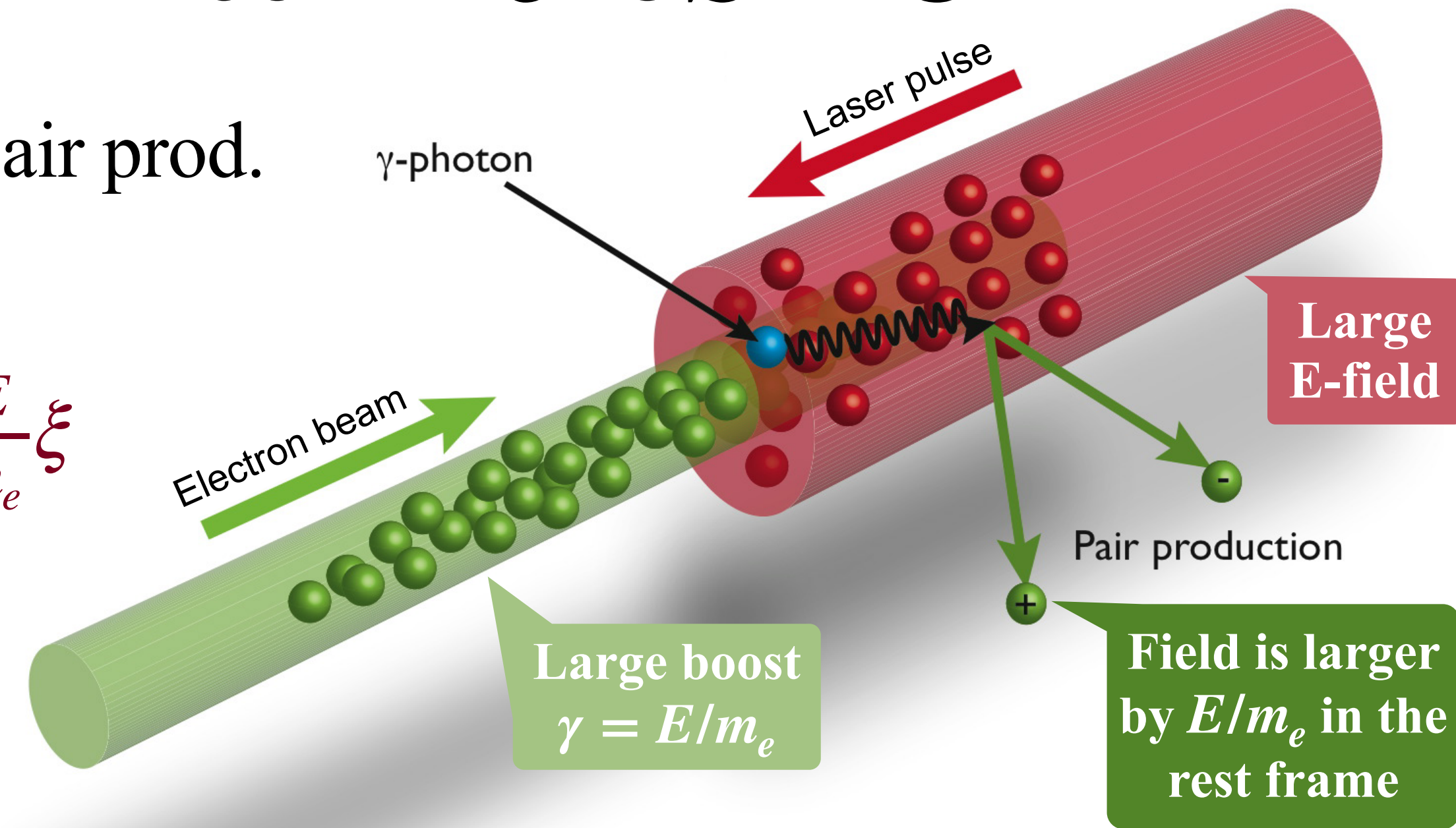
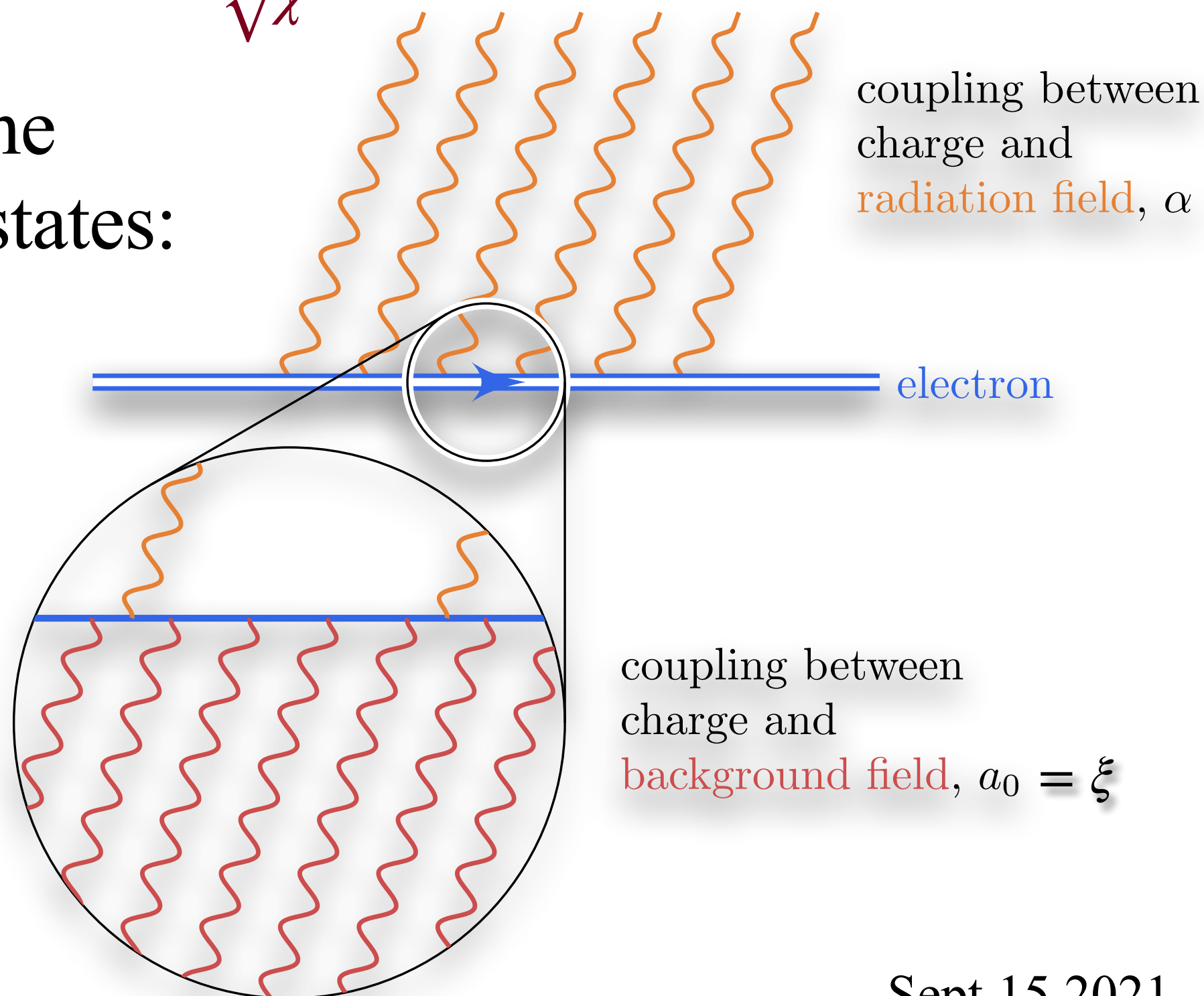
- Nonlinear Compton scat. \longrightarrow Nonlinear Breit-Wheeler pair prod.

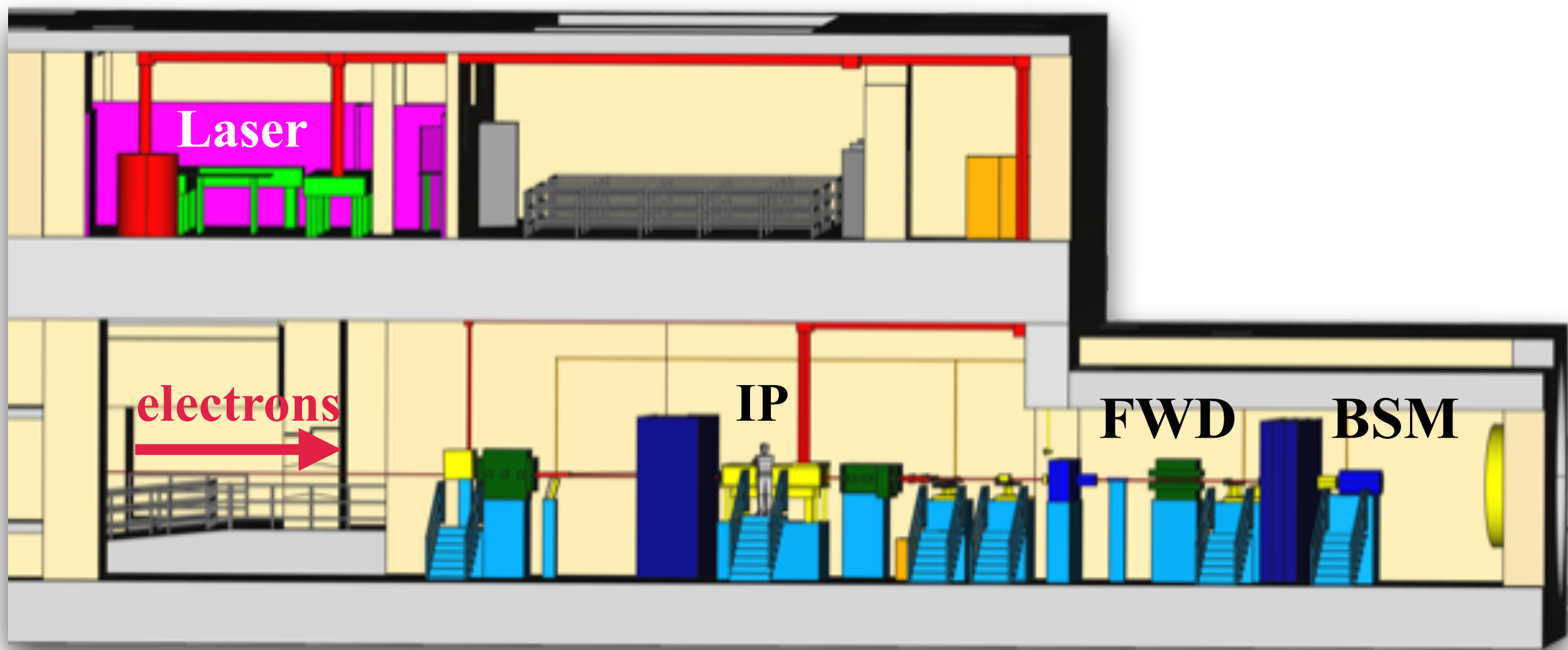
- Characterised by two dimensionless parameters:

- Laser intensity $\xi \propto \frac{\epsilon}{\epsilon_S}$ and Quantum parameter $\chi \propto \frac{E}{m_e} \xi$

- Non-perturbativity: $\xi \geq \frac{1}{\sqrt{\chi}} \gg 1$

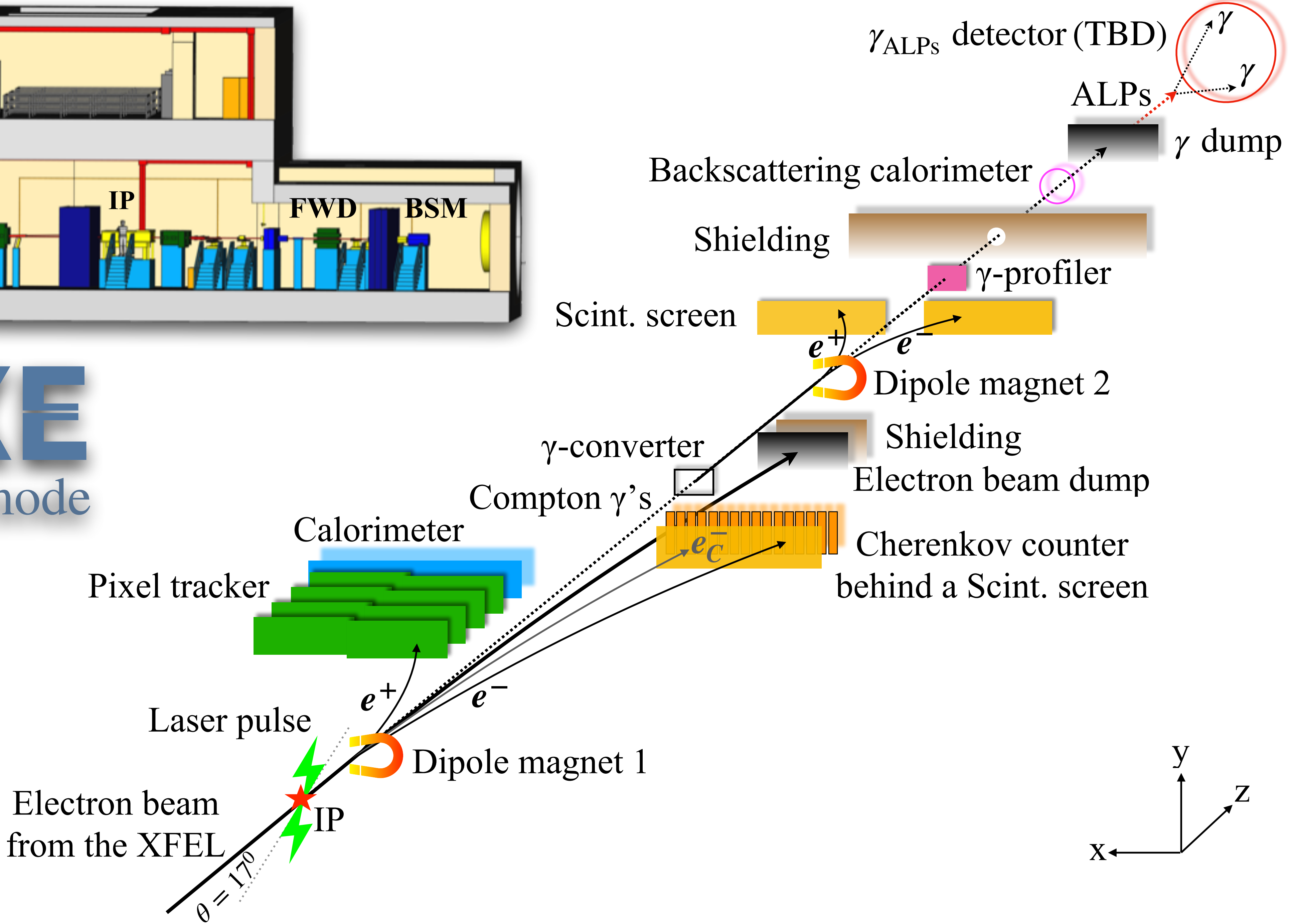
- Fermions inside the pulse are Volkov states:

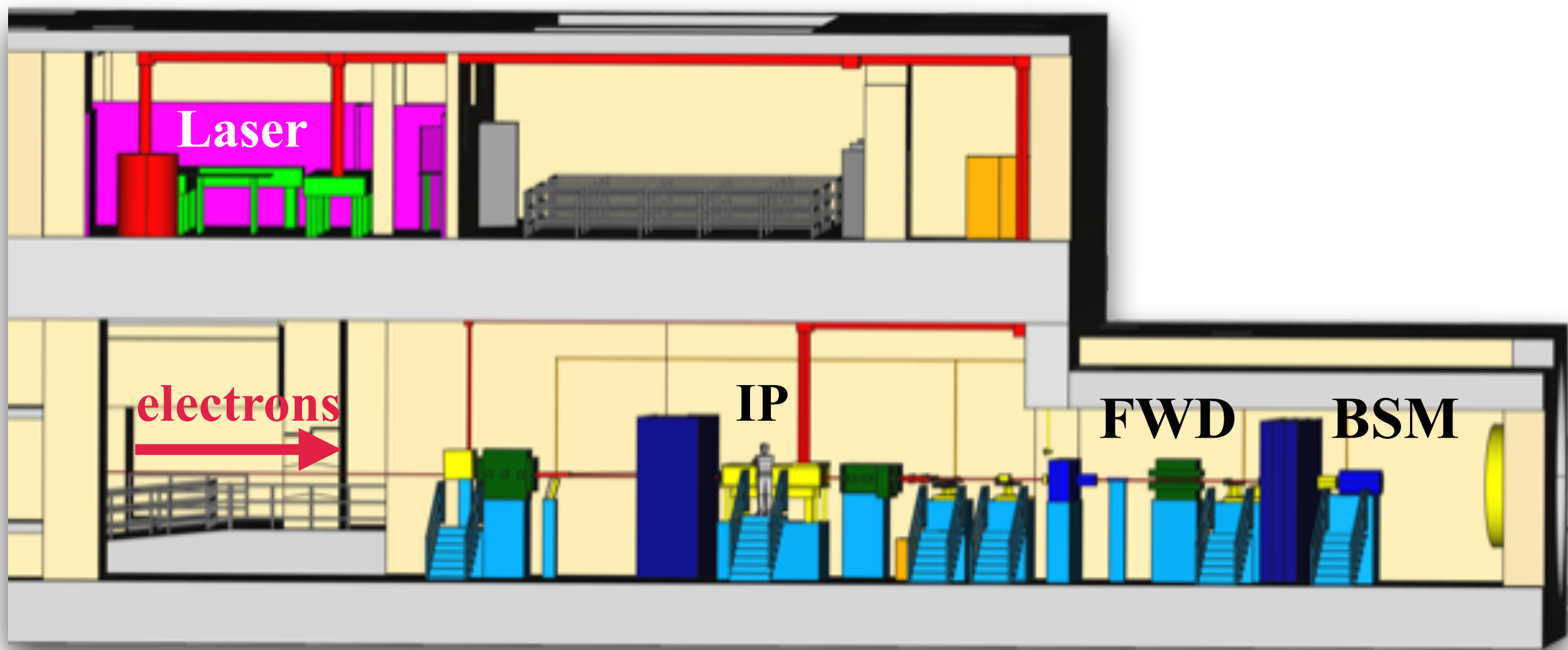




LUXE

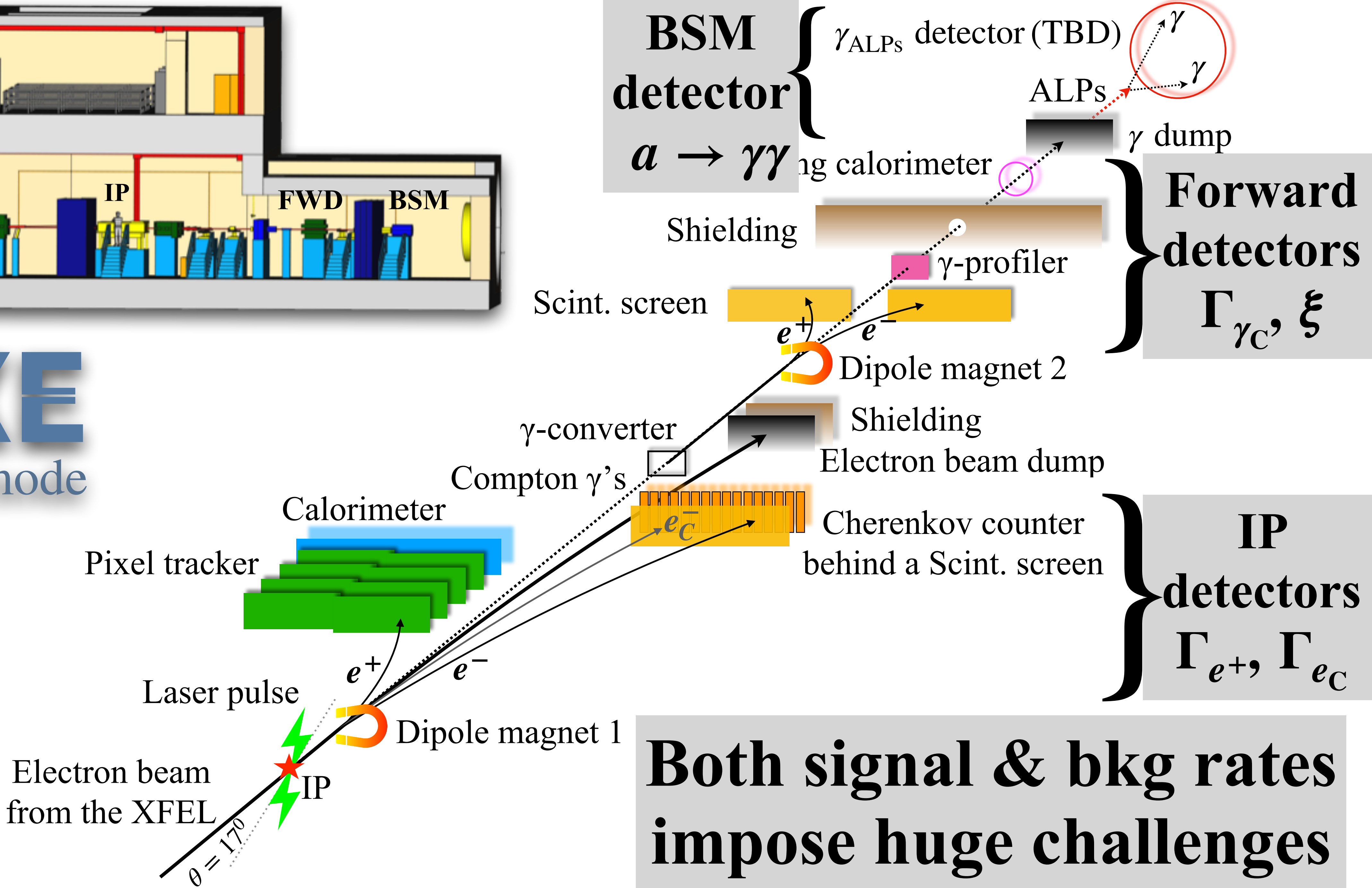
e + laser mode





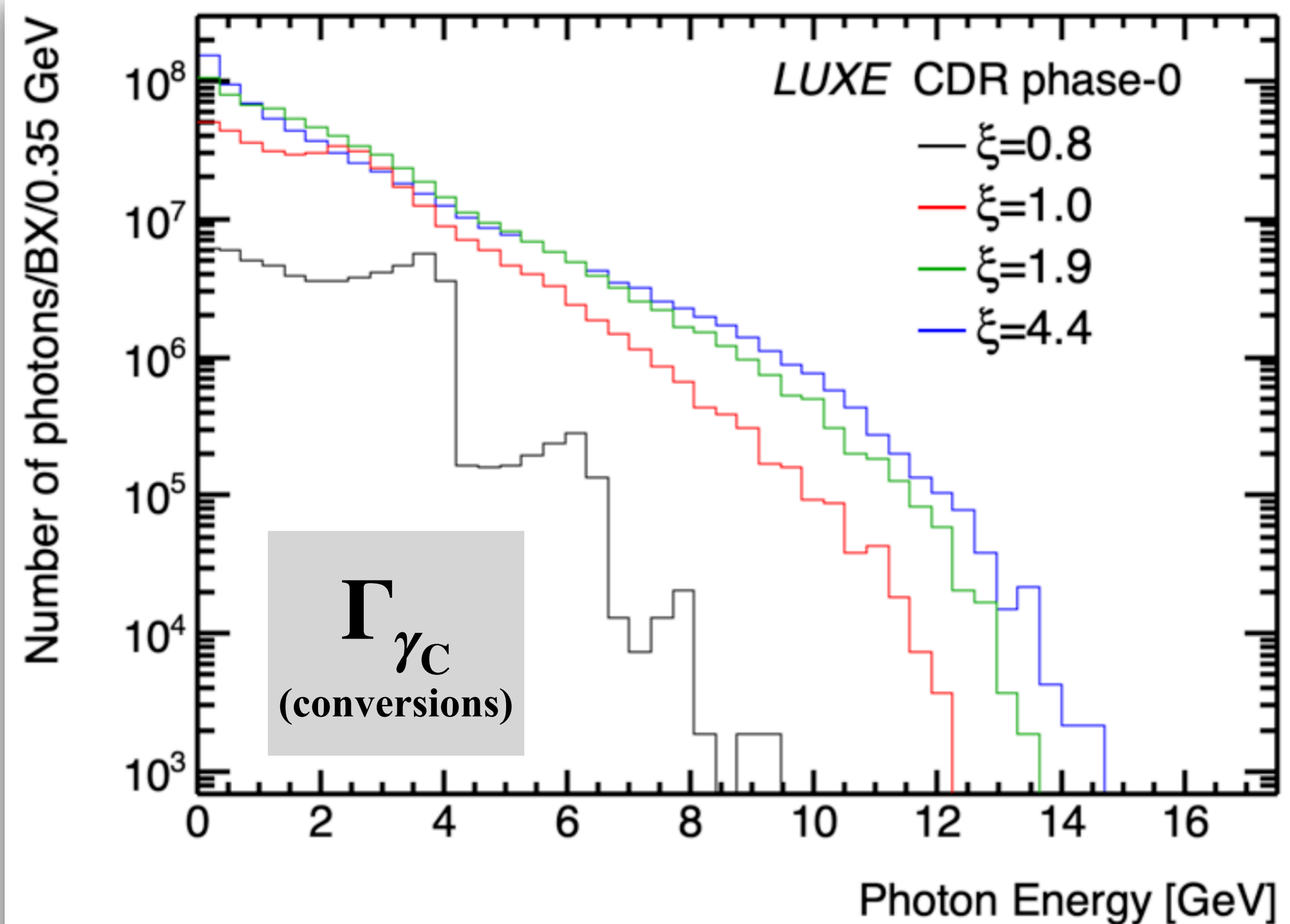
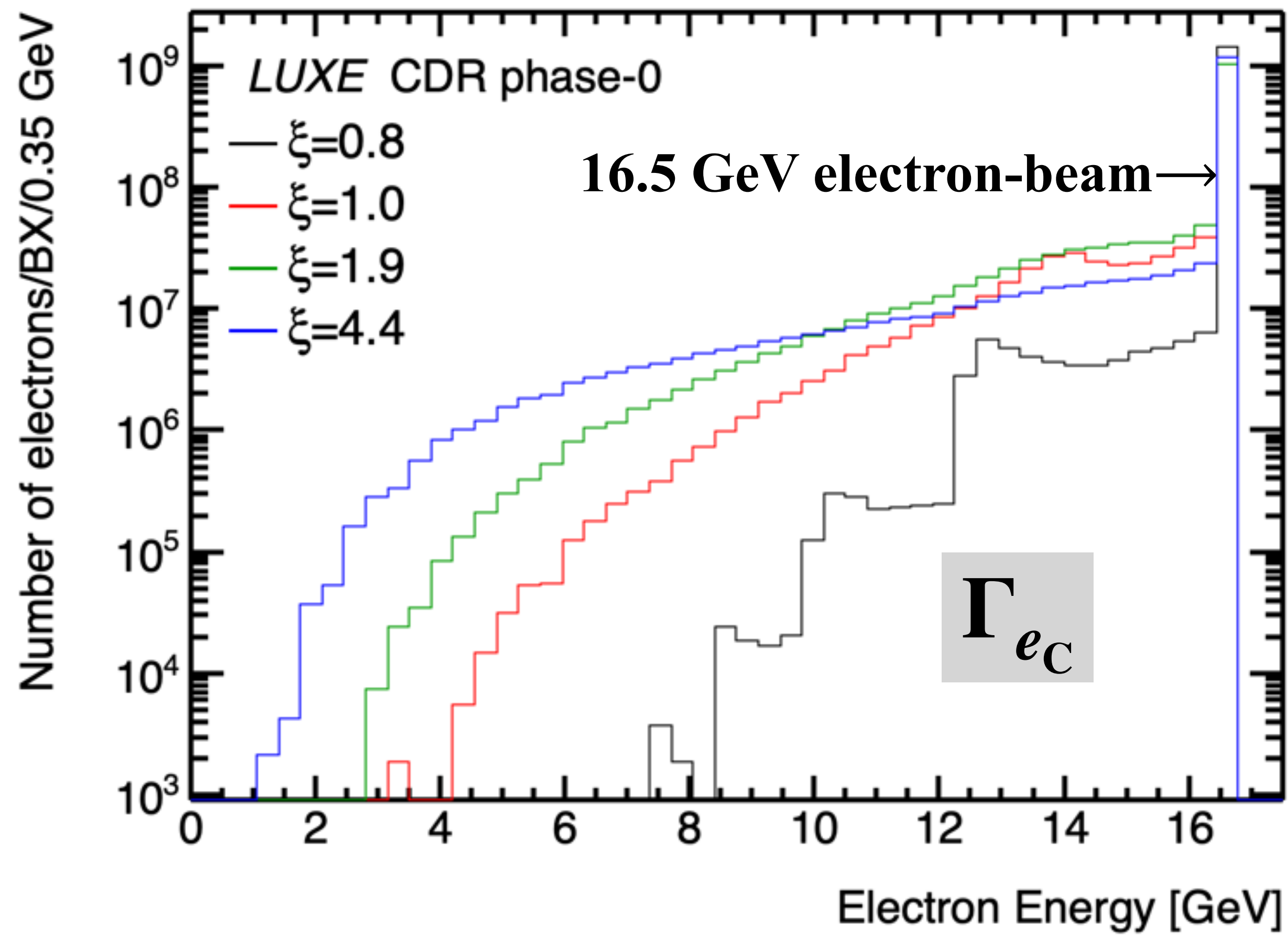
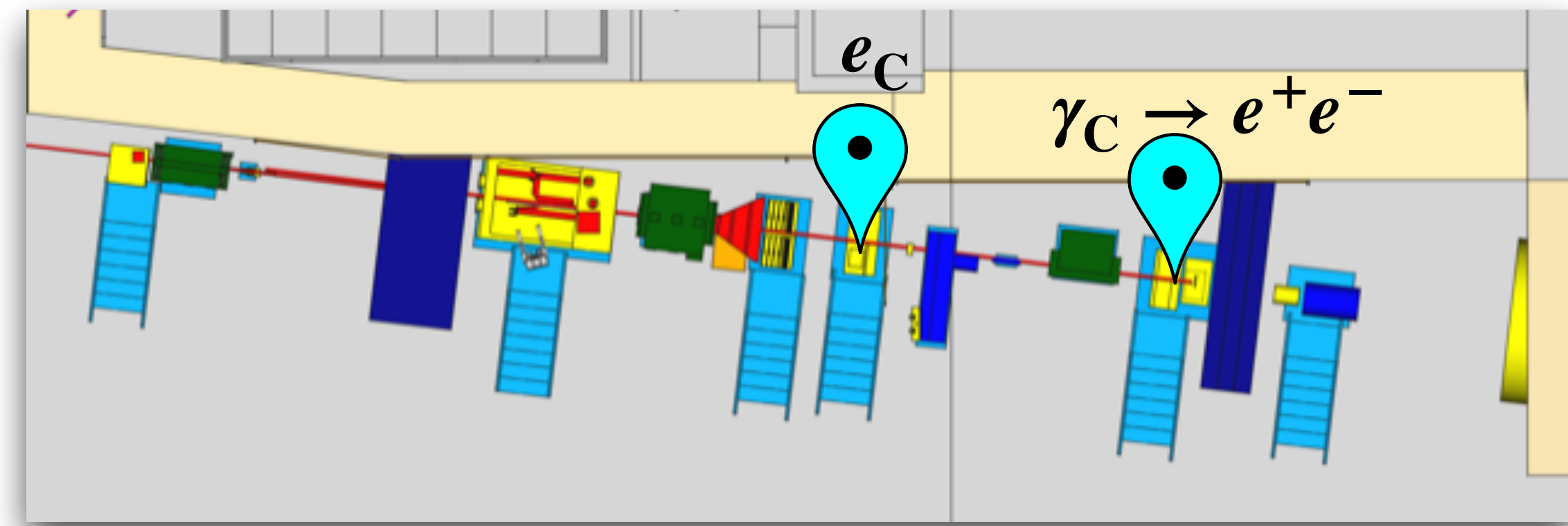
LUXE

e + laser mode

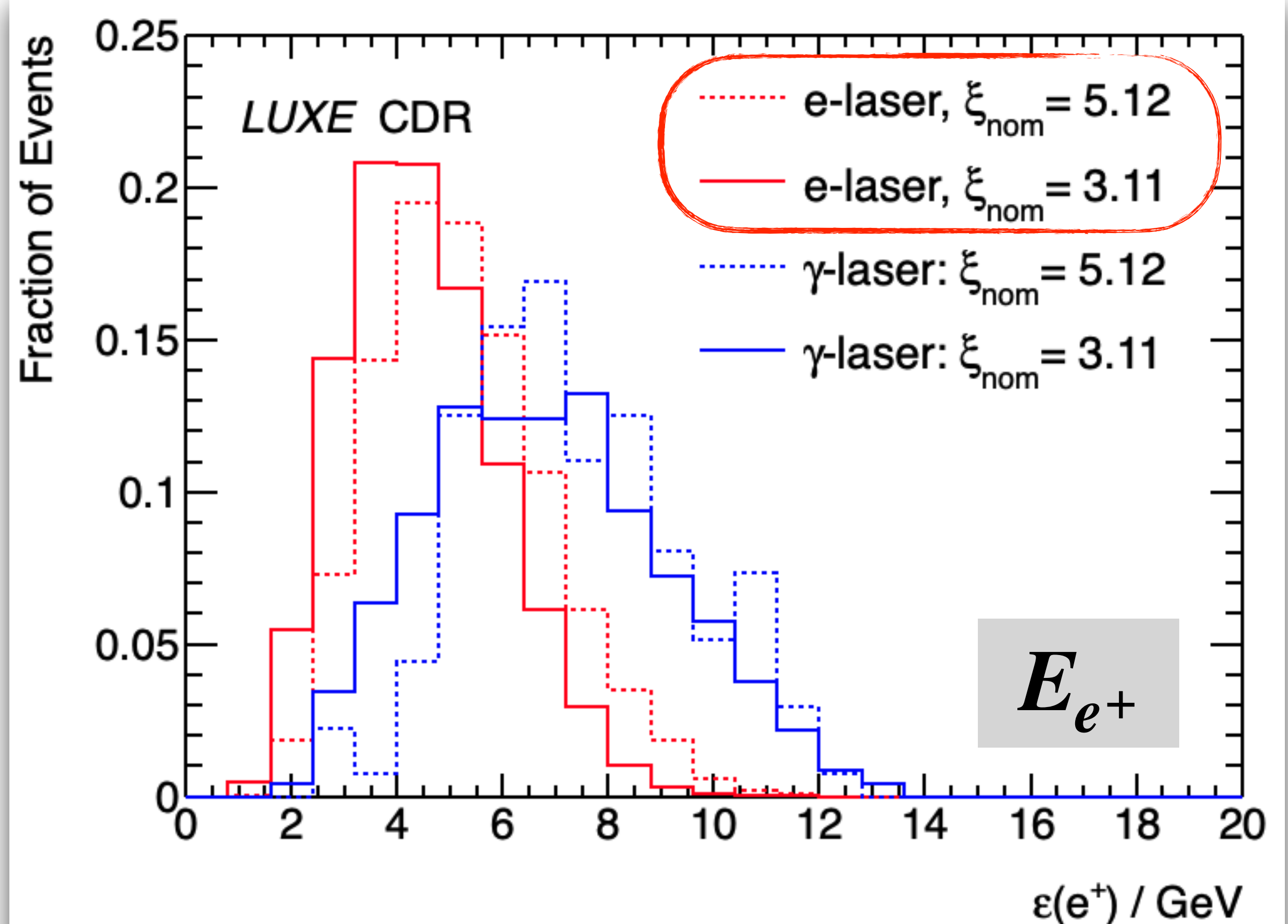
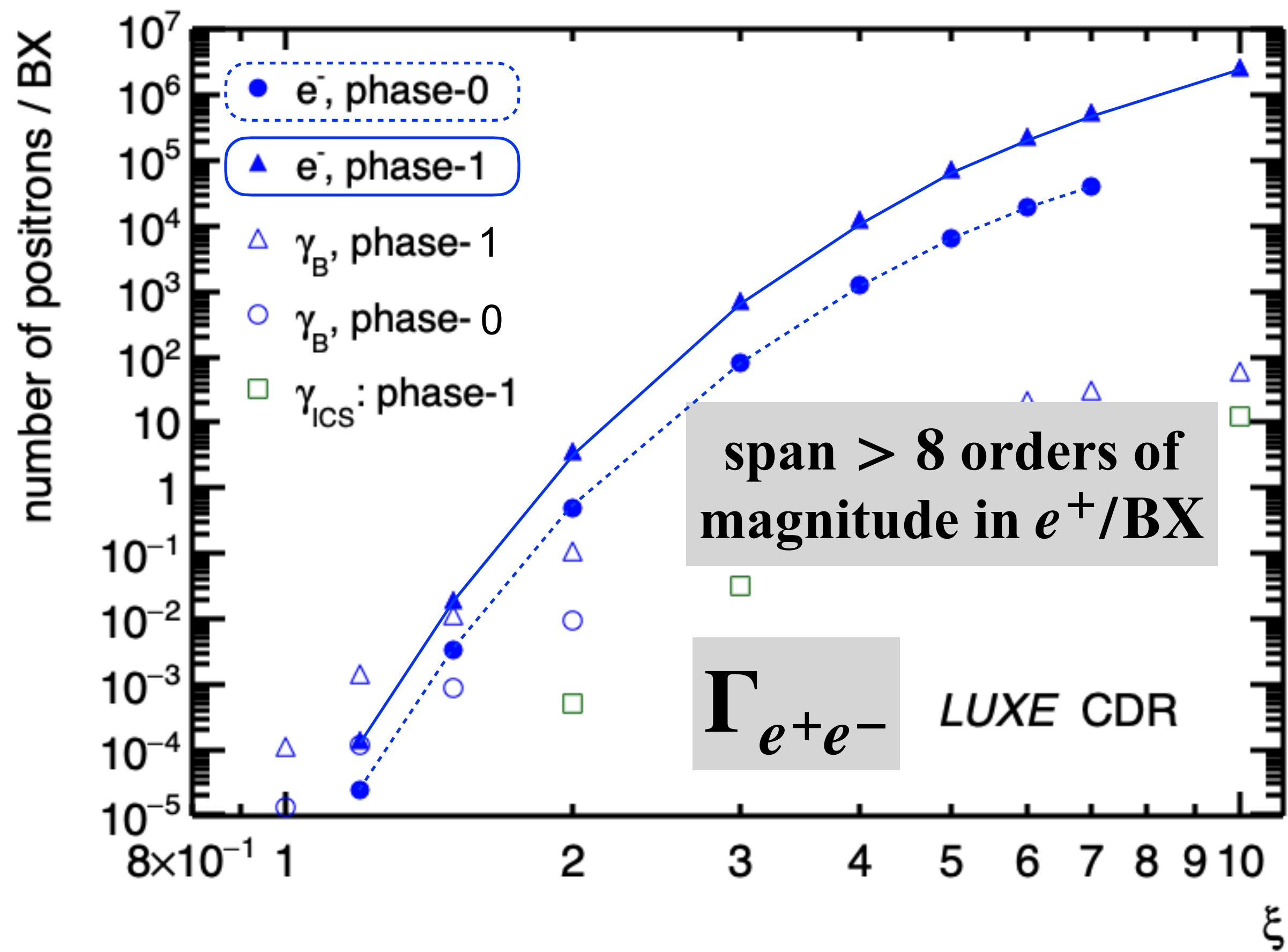
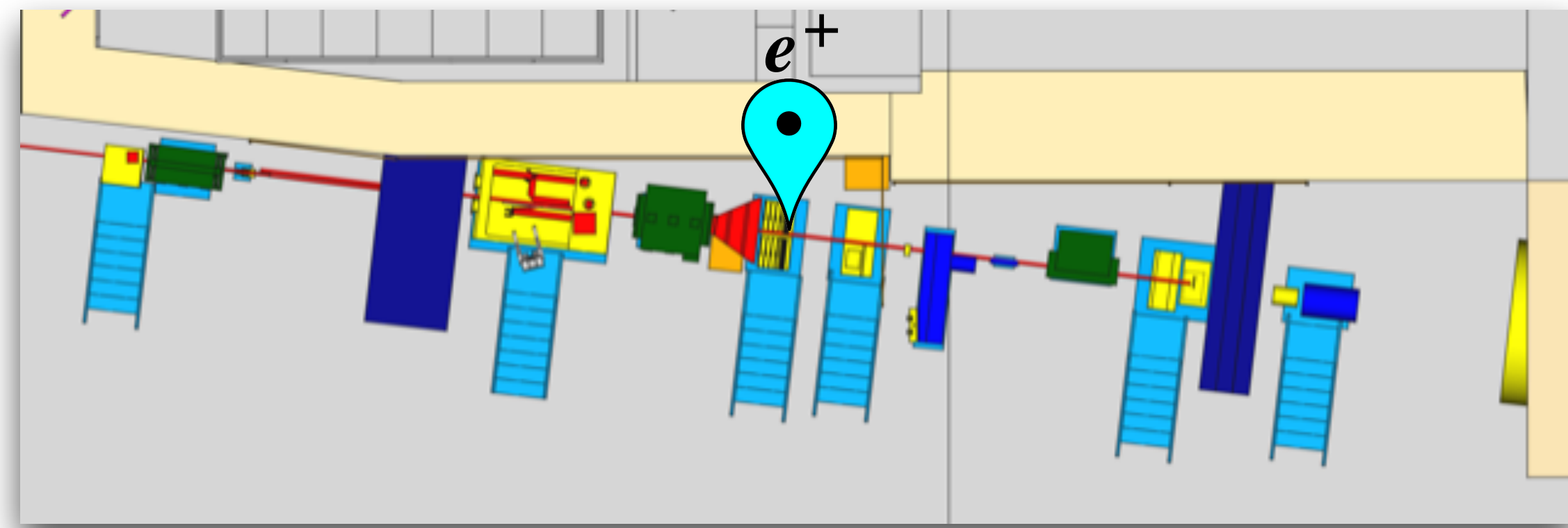


Both signal & bkg rates impose huge challenges

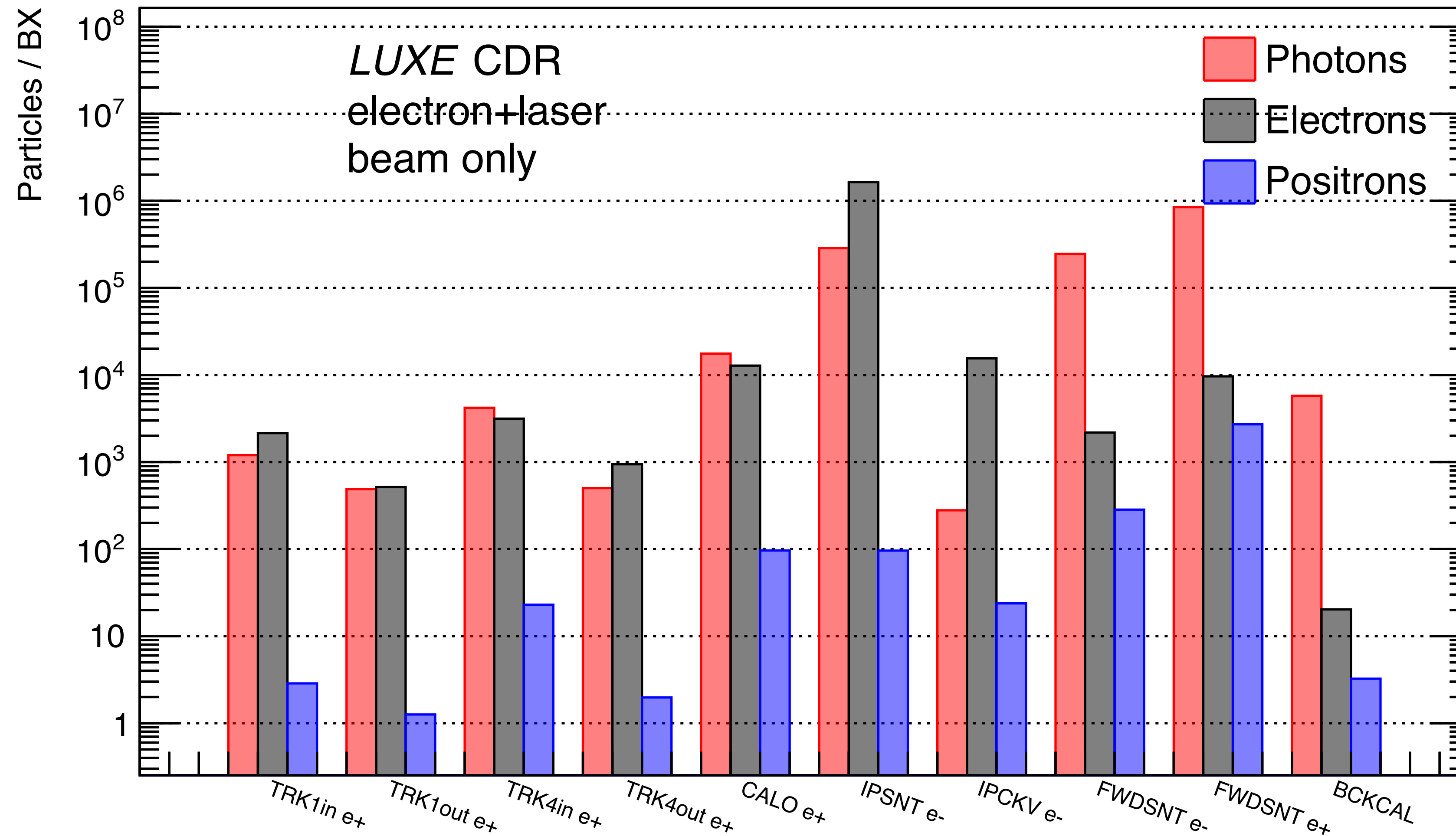
SFQED Signals: Compton e & γ



SFQED Signals: BW $e^+(e^-)$



Bkg rates at the detector faces

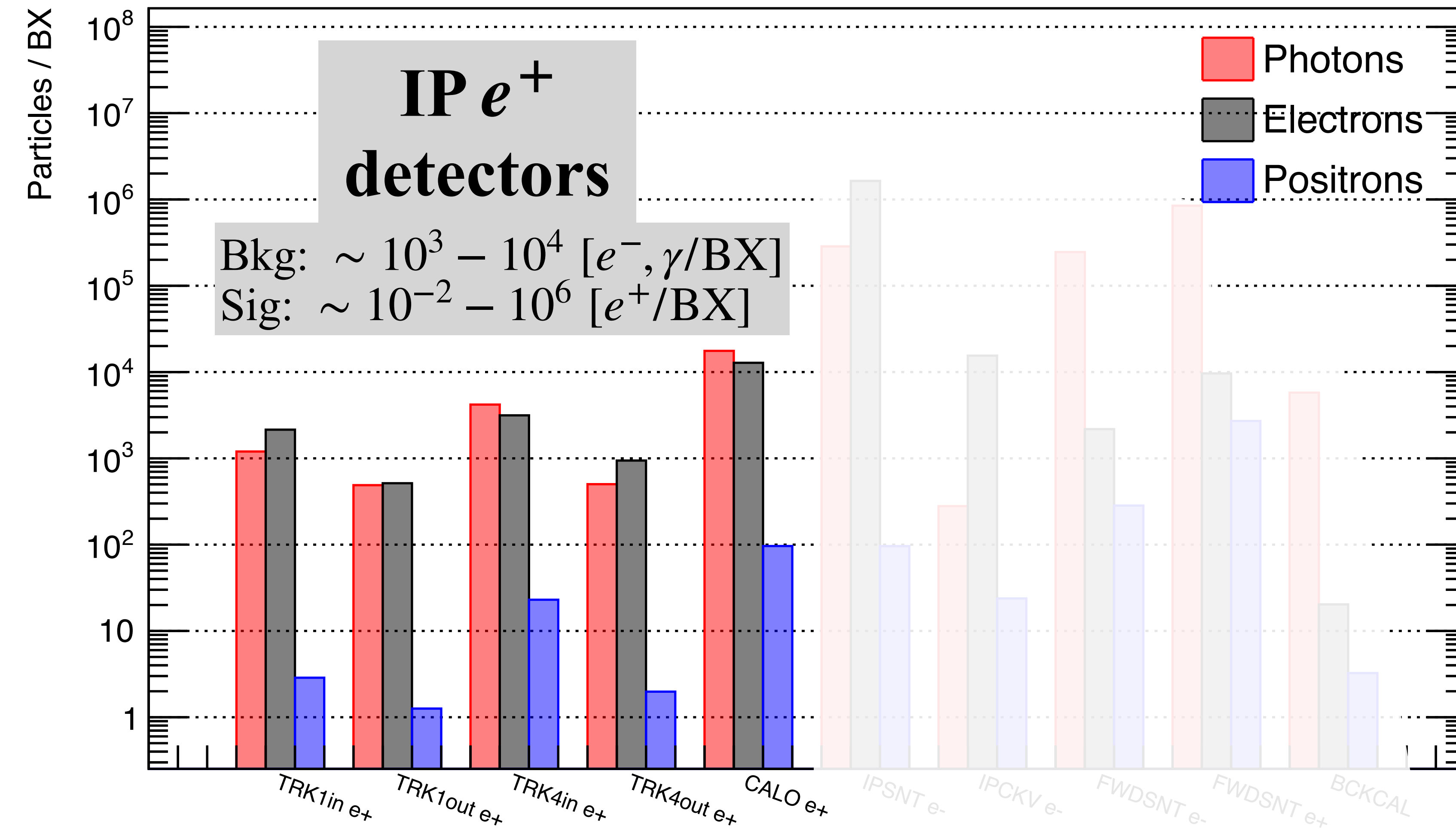


- Full GEANT4 simulation
- beam only (no collisions)
- heavily mitigated with shielding already
- largest source: where the e-beam exits the vacuum

- Not all particles will register an electronic response
 - most very low energetic

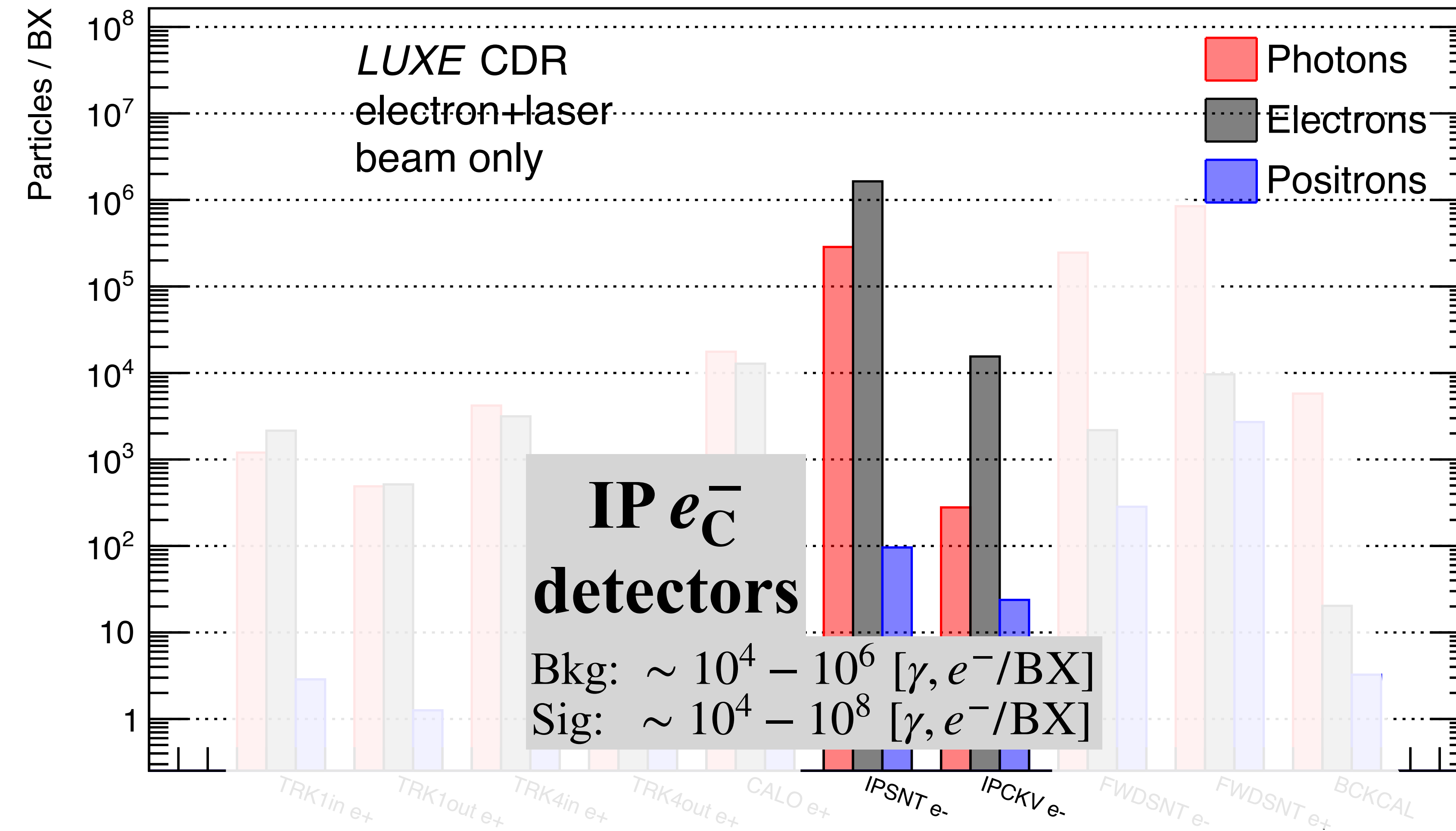
- Still, detectors job is to:
 - massively reject bkg
 - resolve huge signals

Bkg rates at the detector faces



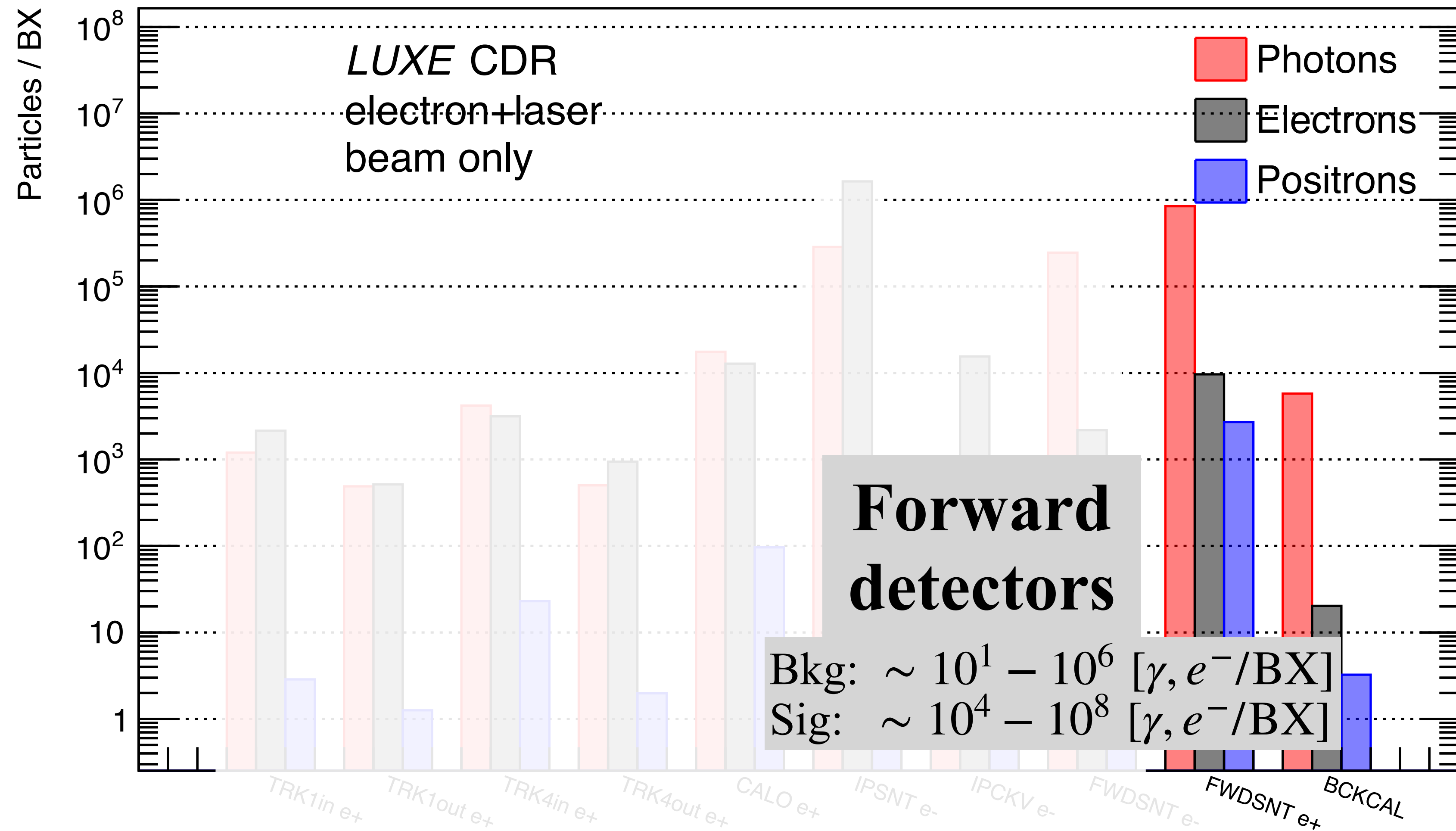
- Full GEANT4 simulation
- beam only (no collisions)
- heavily mitigated with shielding already
- largest source: where the e-beam exits the vacuum
- Not all particles will register an electronic response
 - most very low energetic
- Still, detectors job is to:
 - massively reject bkg
 - resolve huge signals

Bkg rates at the detector faces

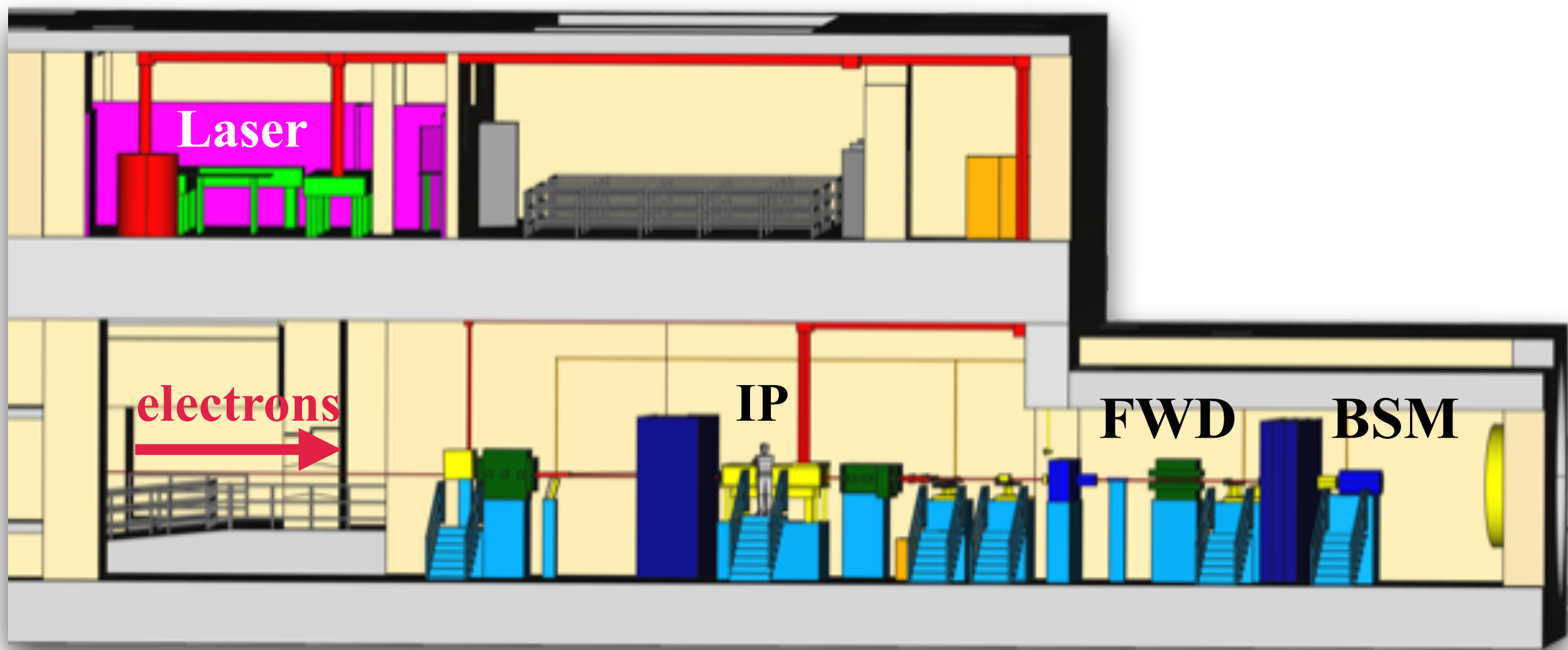


- Full GEANT4 simulation
- beam only (no collisions)
- heavily mitigated with shielding already
- largest source: where the e-beam exits the vacuum
- Not all particles will register an electronic response
 - most very low energetic
- Still, detectors job is to:
 - massively reject bkg
 - resolve huge signals

Bkg rates at the detector faces

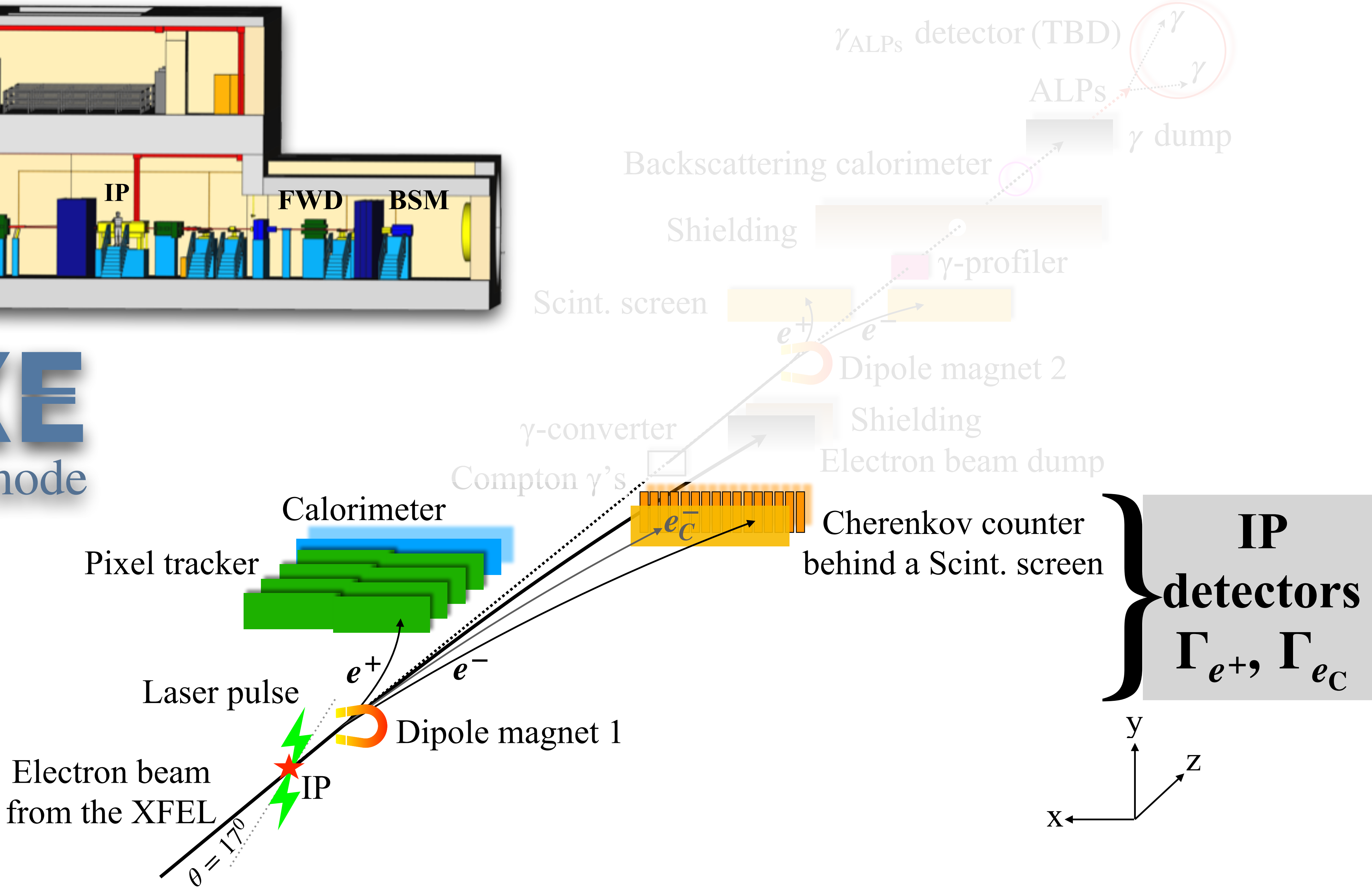


- Full GEANT4 simulation
- beam only (no collisions)
- heavily mitigated with shielding already
- largest source: where the e-beam exits the vacuum
- Not all particles will register an electronic response
 - most very low energetic
- Still, detectors job is to:
 - massively reject bkg
 - resolve huge signals

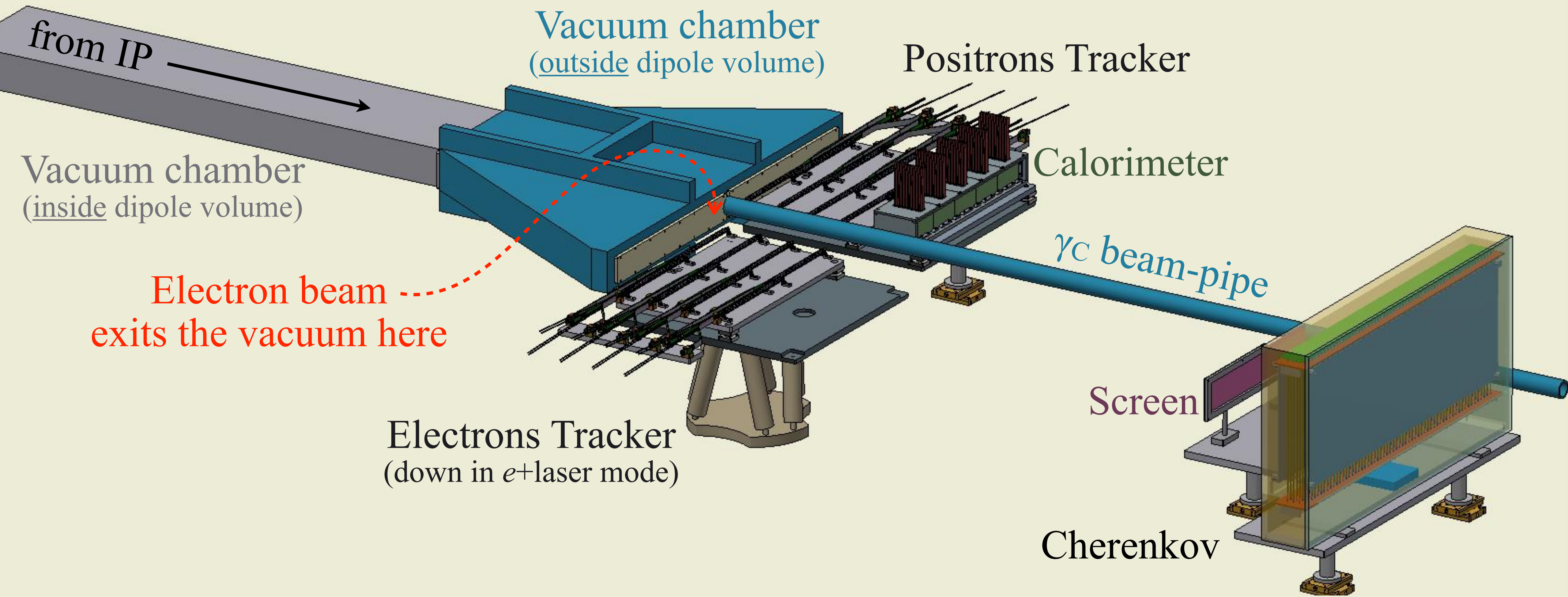


LUXE

e + laser mode

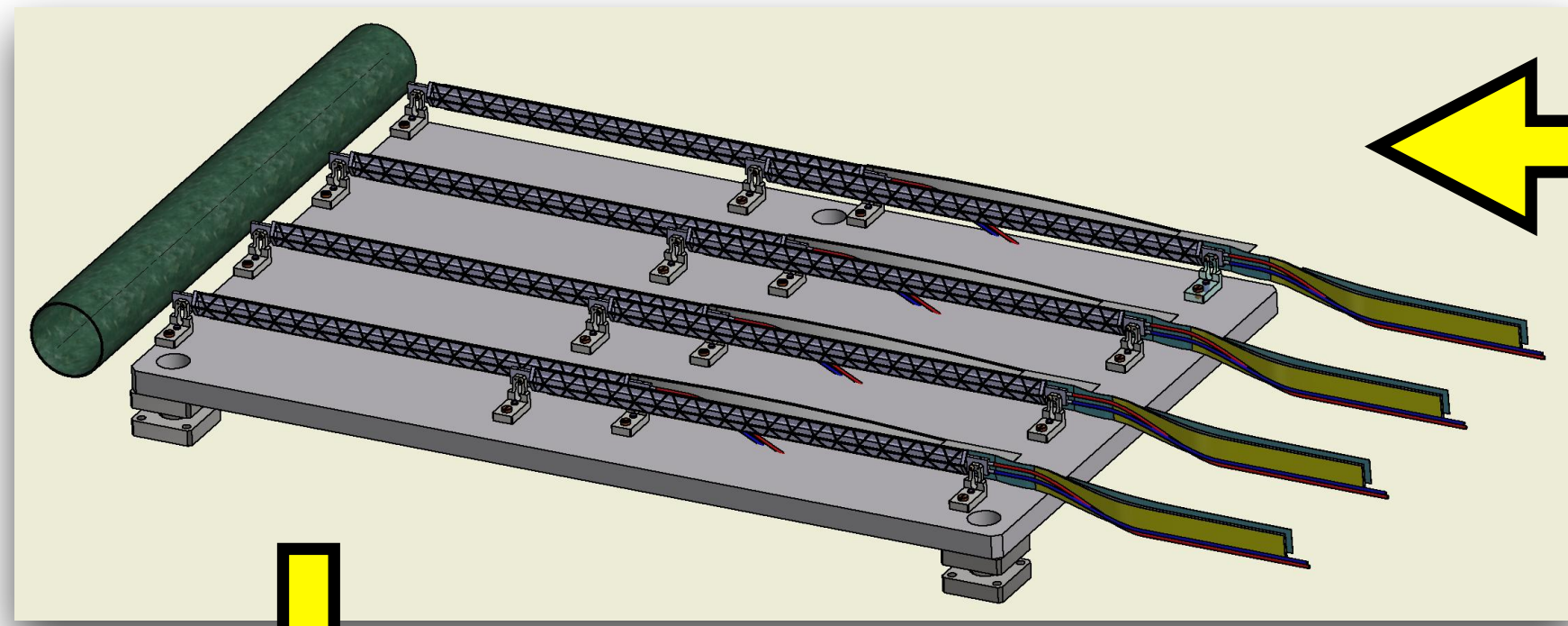


IP detectors - current design

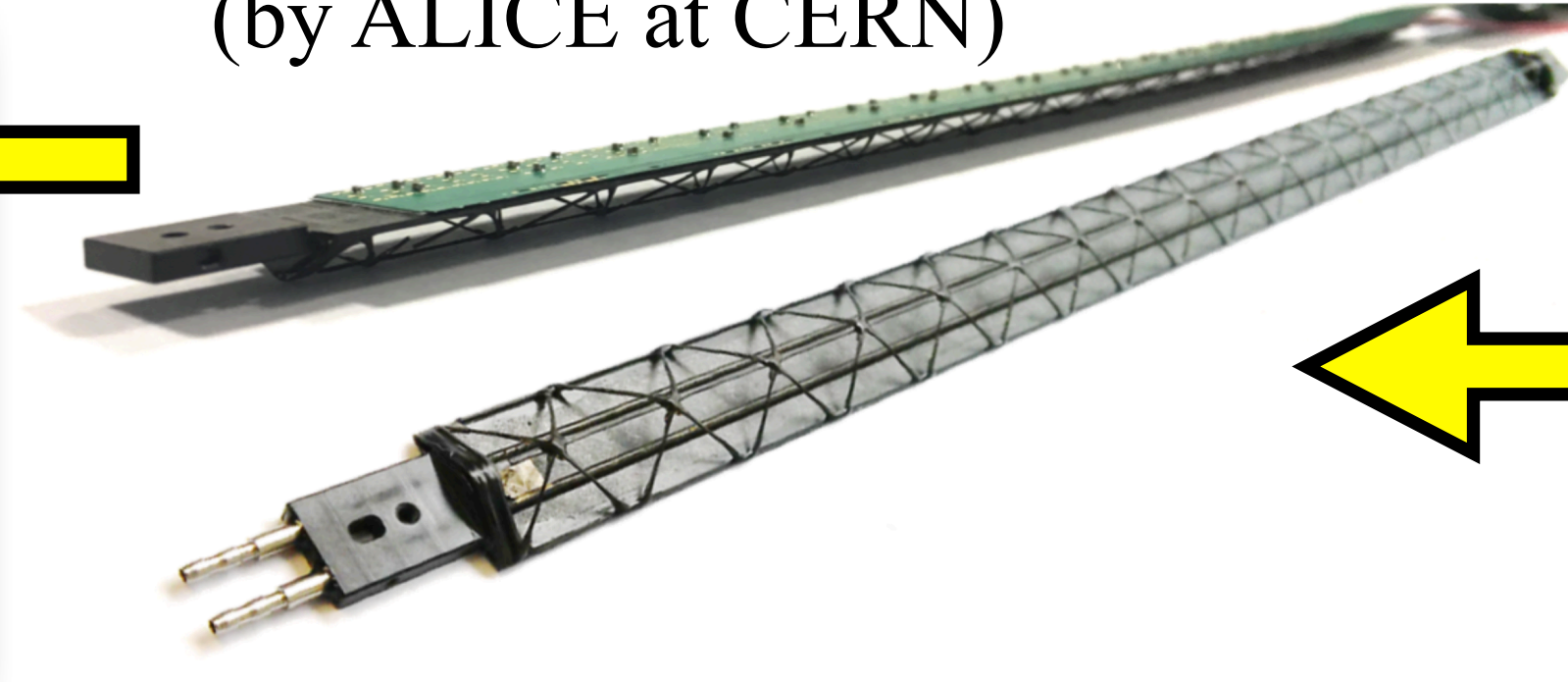


Pixel tracker

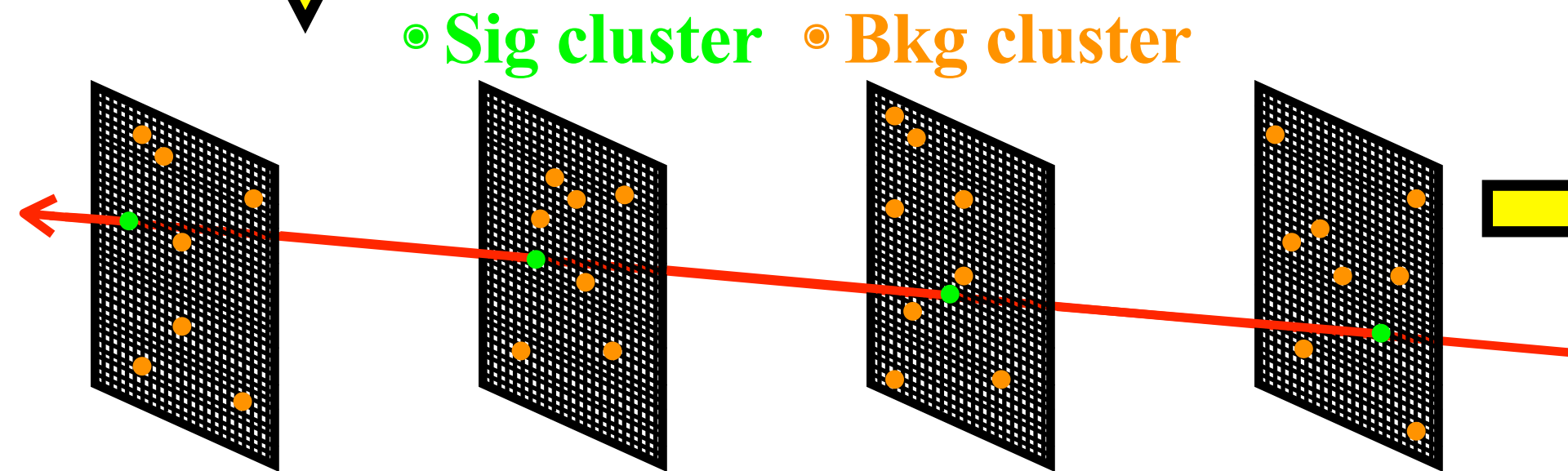
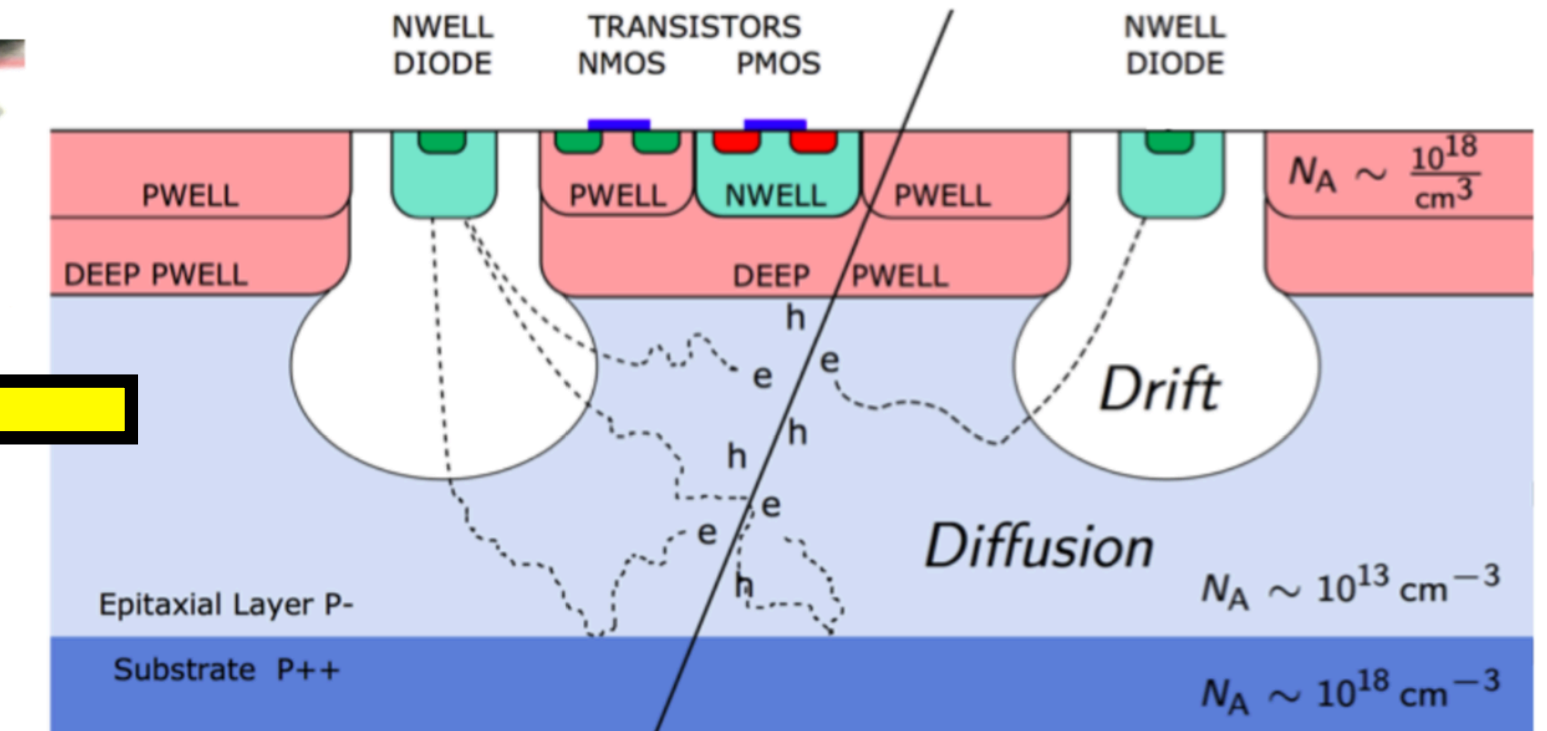
LUXE tracker has 8 staves in each arm of the tracker



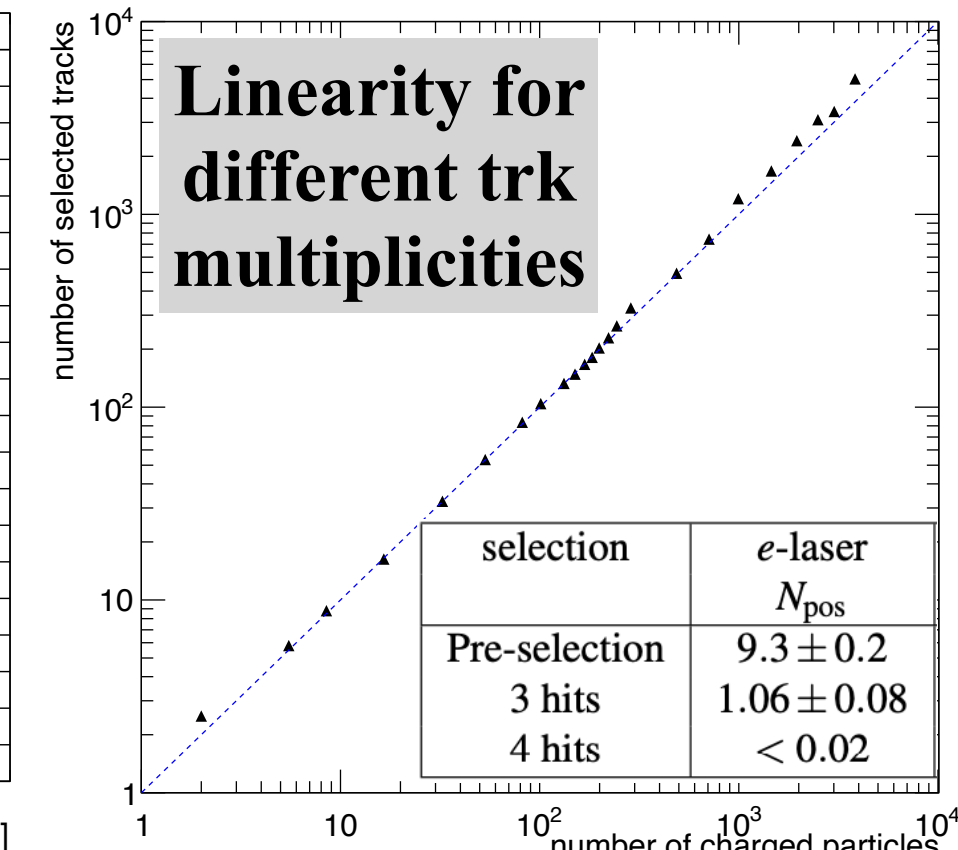
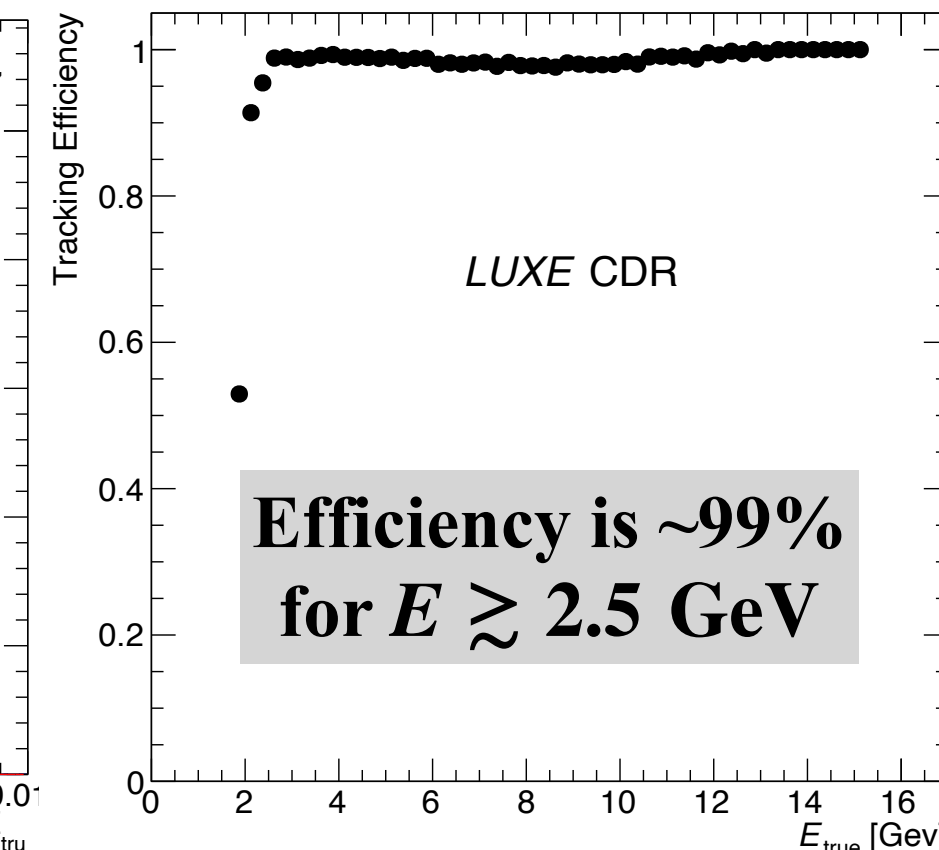
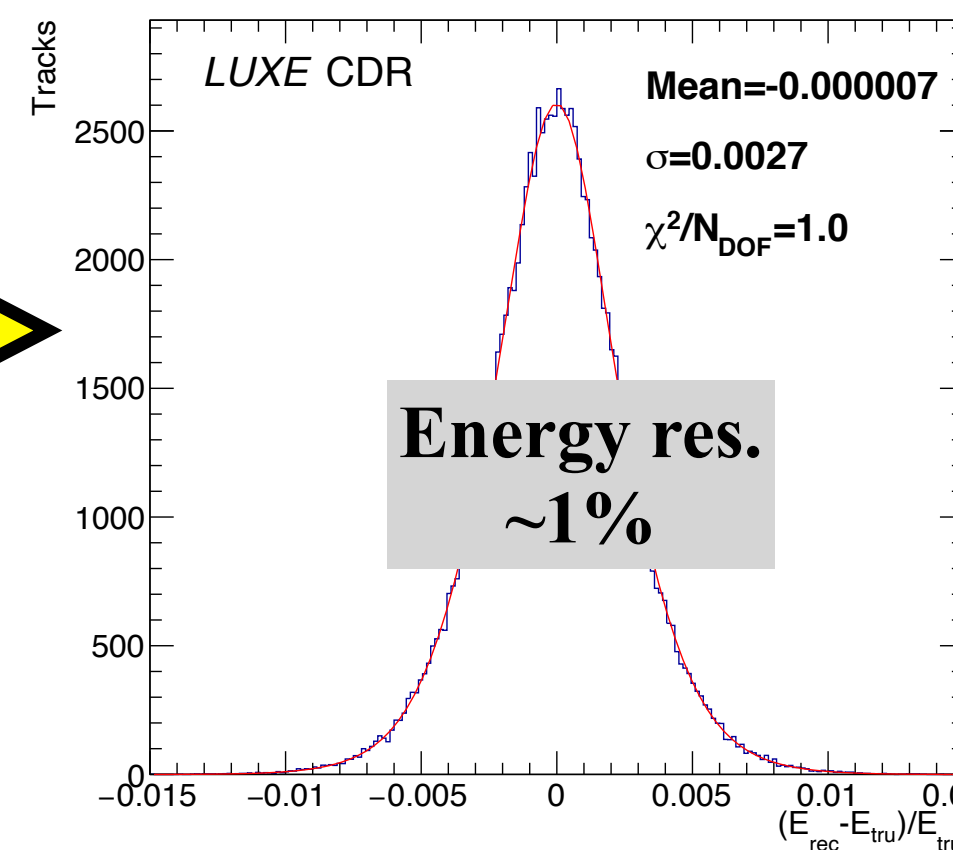
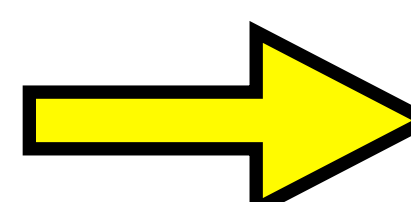
“Stave” has 9 chips (by ALICE at CERN)



ALPIDE: Monolithic Active Pixel Sensor
512x1024 pixels of 27x29 μm^2 in a 3x1.5 cm^2 chip
(by TowerJazz+ALICE at CERN)



● Sig cluster ● Bkg cluster

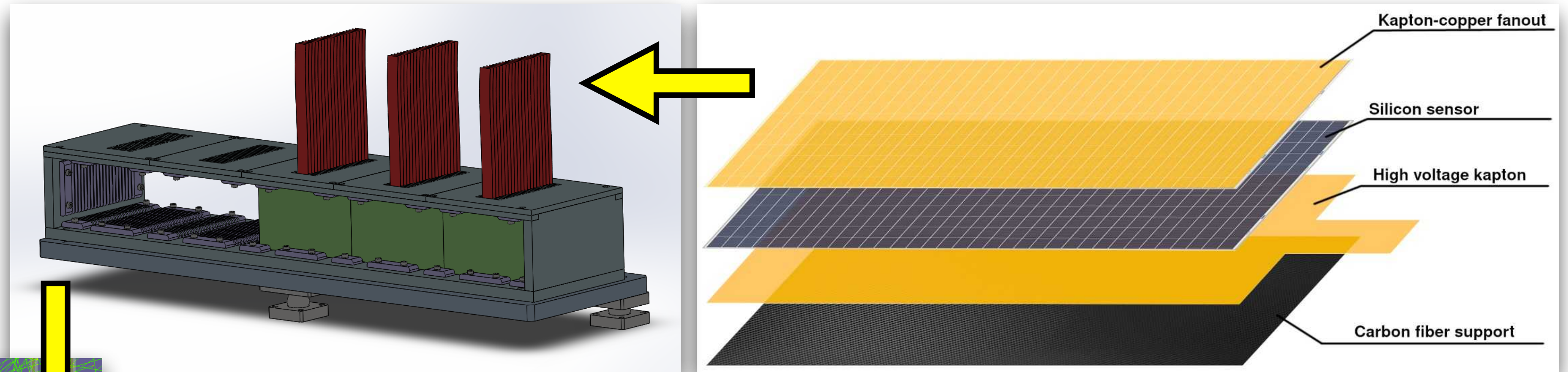


Fired pixels are clustered and tracks are fitted to extract the momentum of the particle using the B – field knowledge

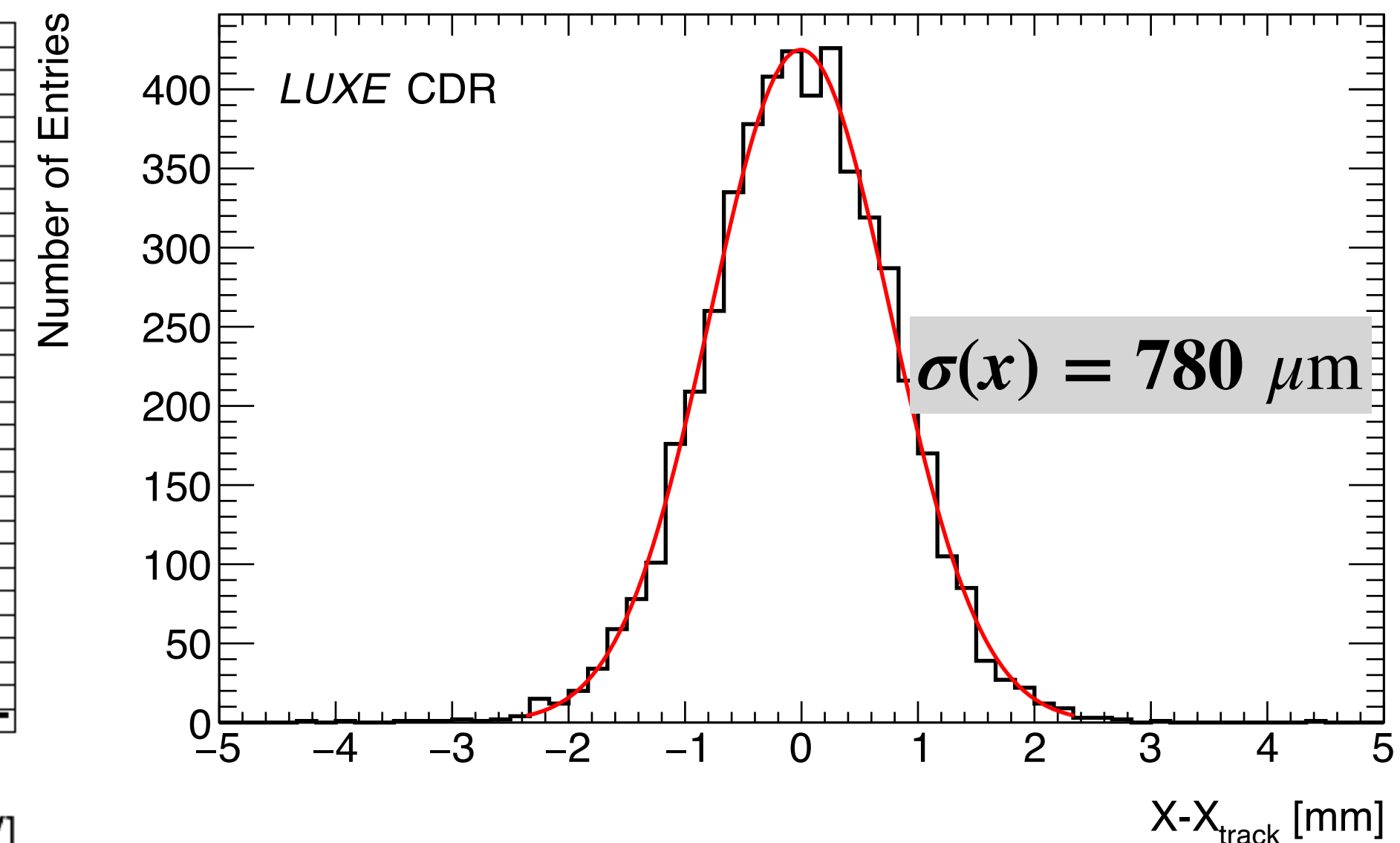
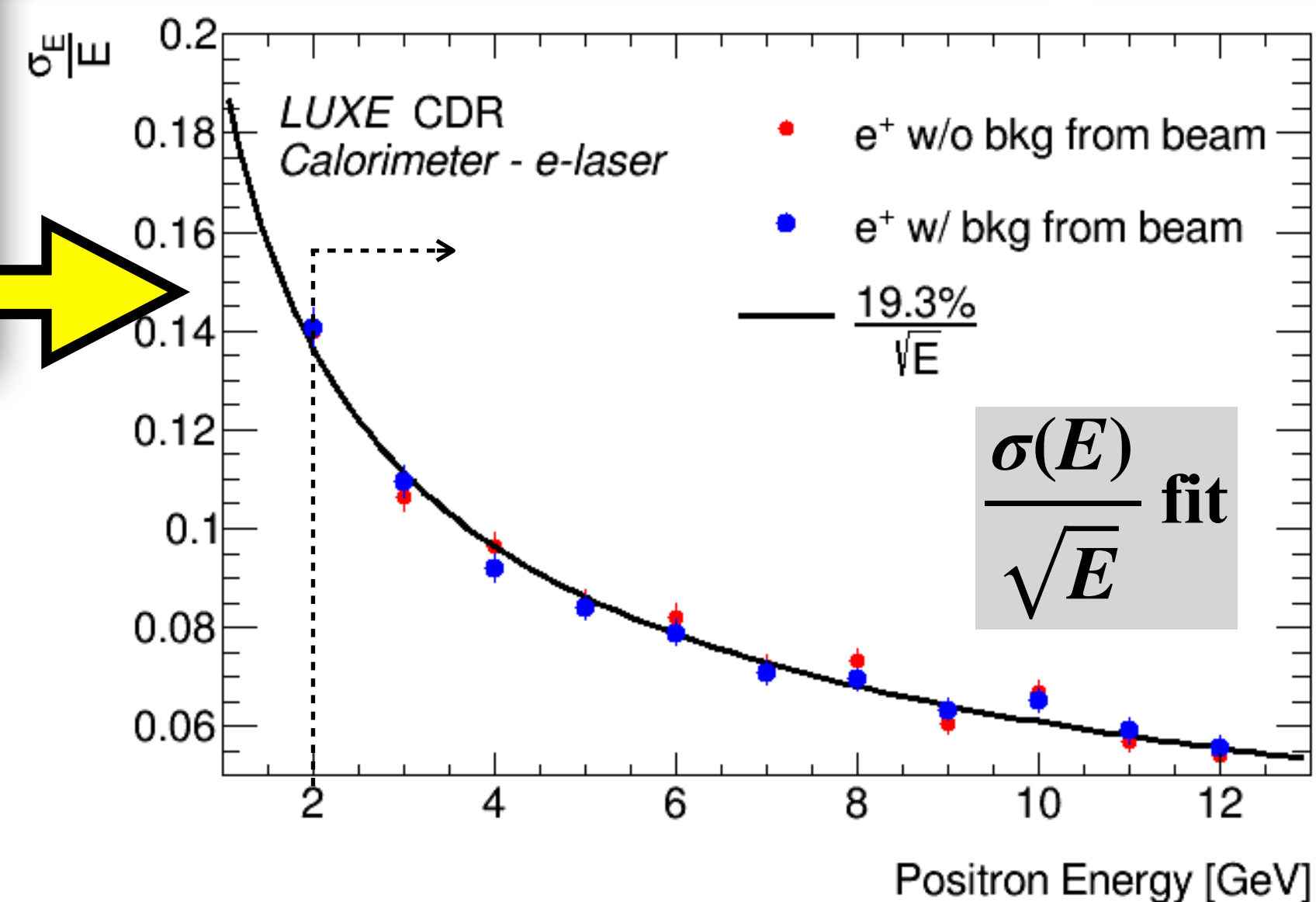
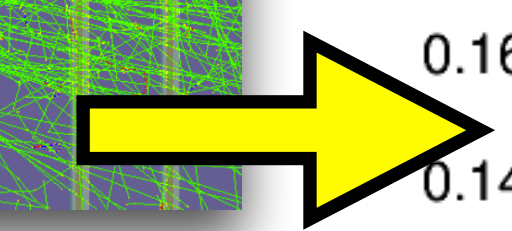
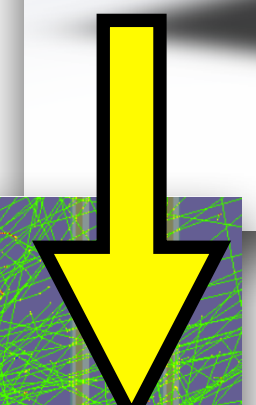
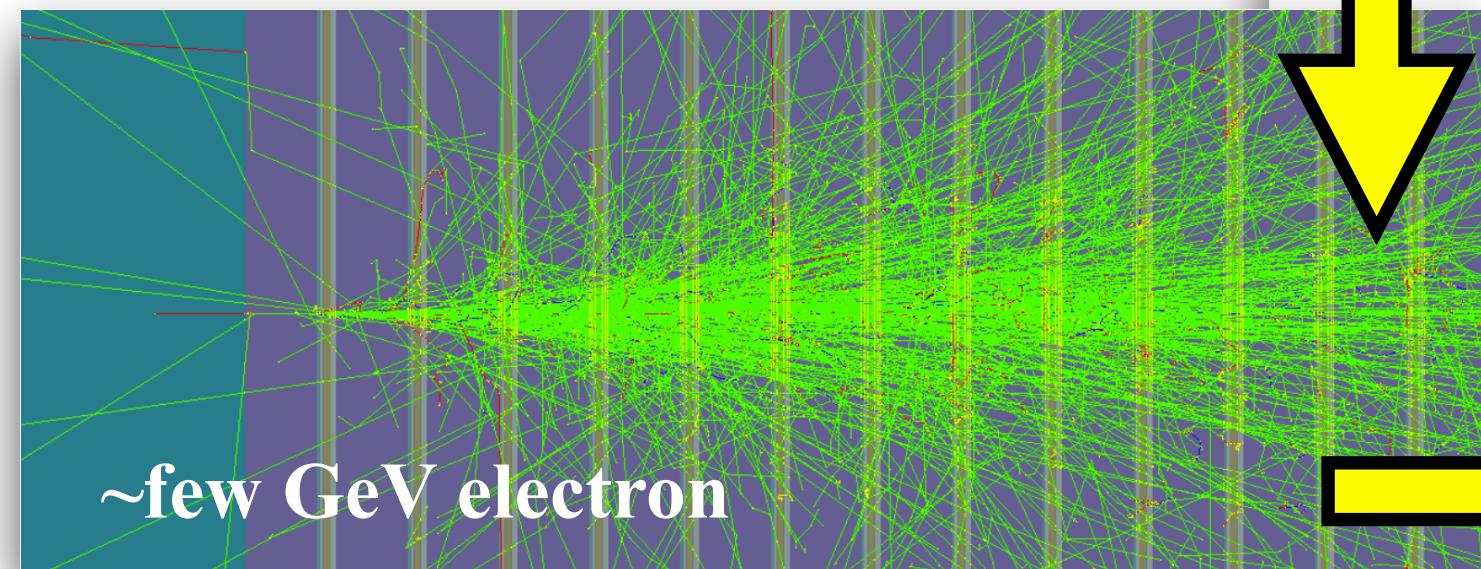
High-granularity compact calorimeter

20 layers of 3.5 mm thick tungsten plates and sensors in 1 mm gaps between plates

Silicon sensor with pad size of $5 \times 5 \text{ mm}^2$ and an assembly thickness of $< 700 \mu\text{m}$



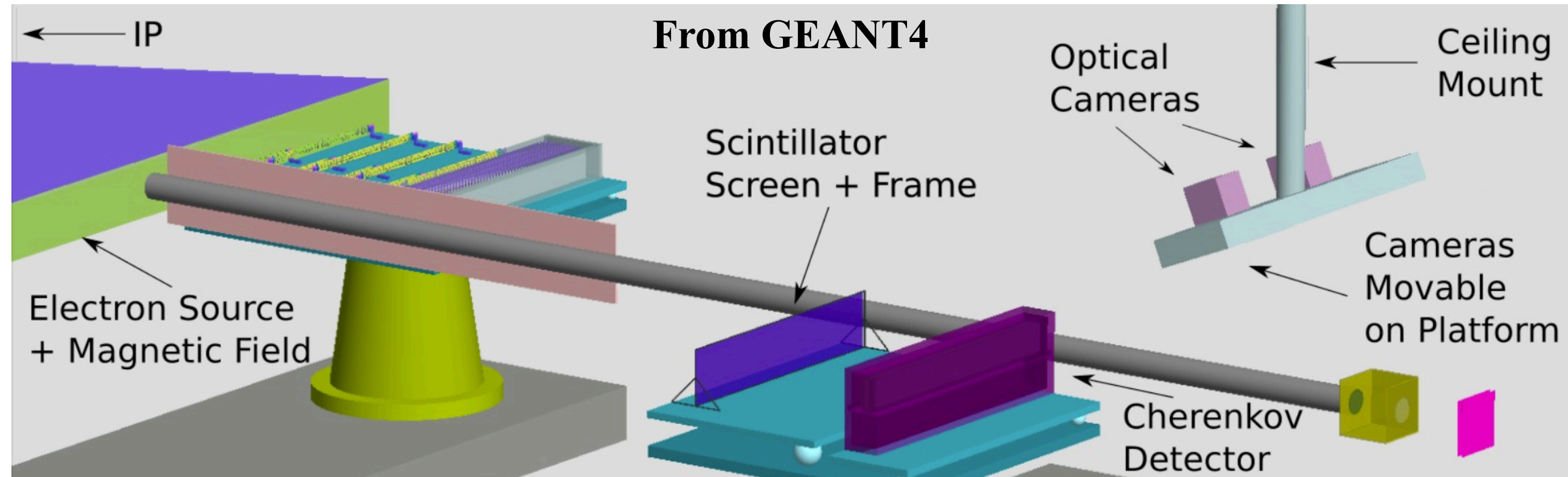
Shower has as small $R_{\text{Molière}}$



Design follows the ILC's FCAL lines but could also converge on the CALICE technology

Scintillating screen & camera

500 μm GadOx: particles depositing energy induce an isotropic and \sim monochromatic ($\sim 545\text{nm}$) fluorescent photons emission



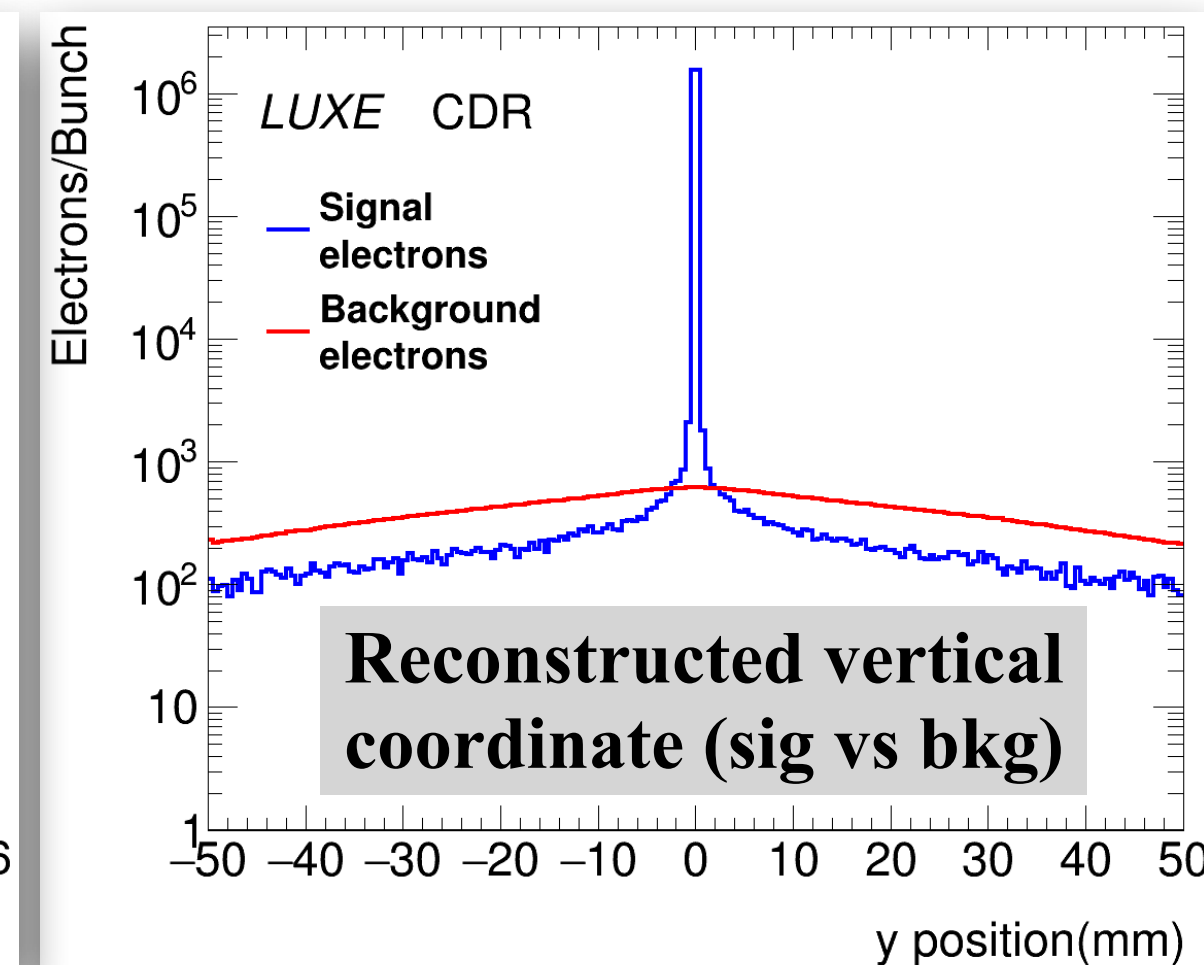
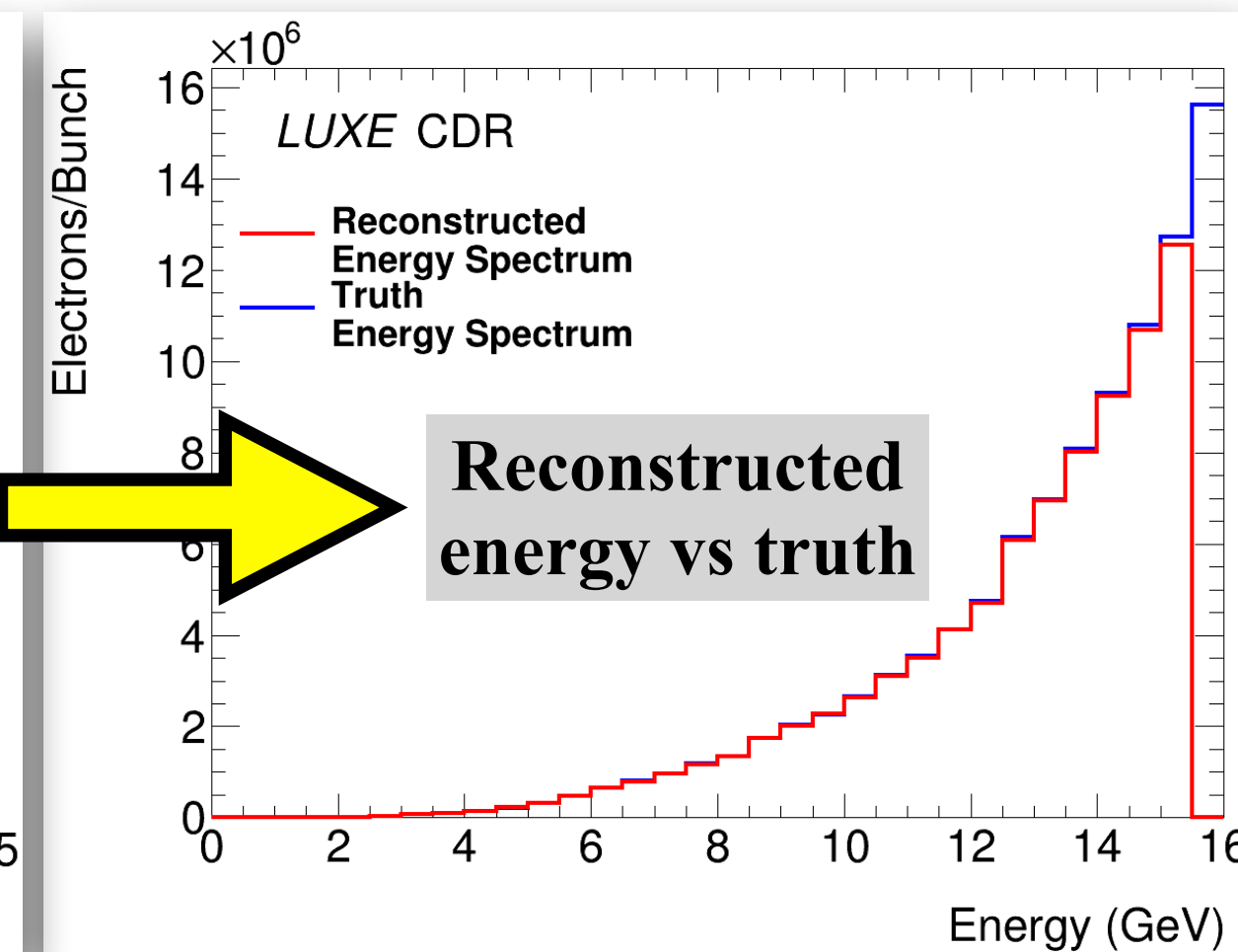
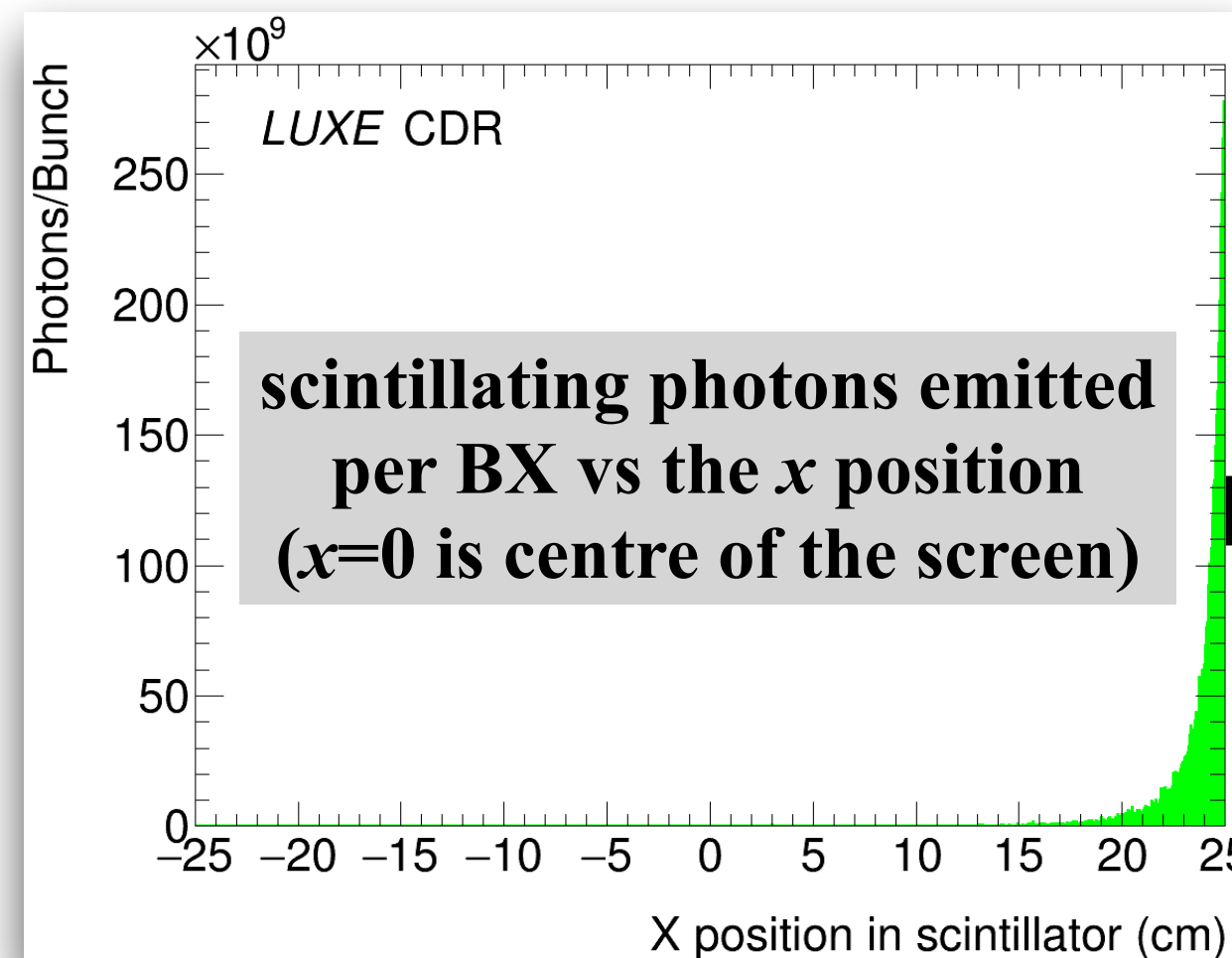
- Terbium-doped Gadolinium Oxysulfide
- high output photon # above the ambient background light

- One 2k-pixel camera: position res. is $< 500 \mu\text{m}$ (better with more cameras)

- Light/charge calibration from measured light curve from testbeam

- Energy determined from the position along the screen and the B-field

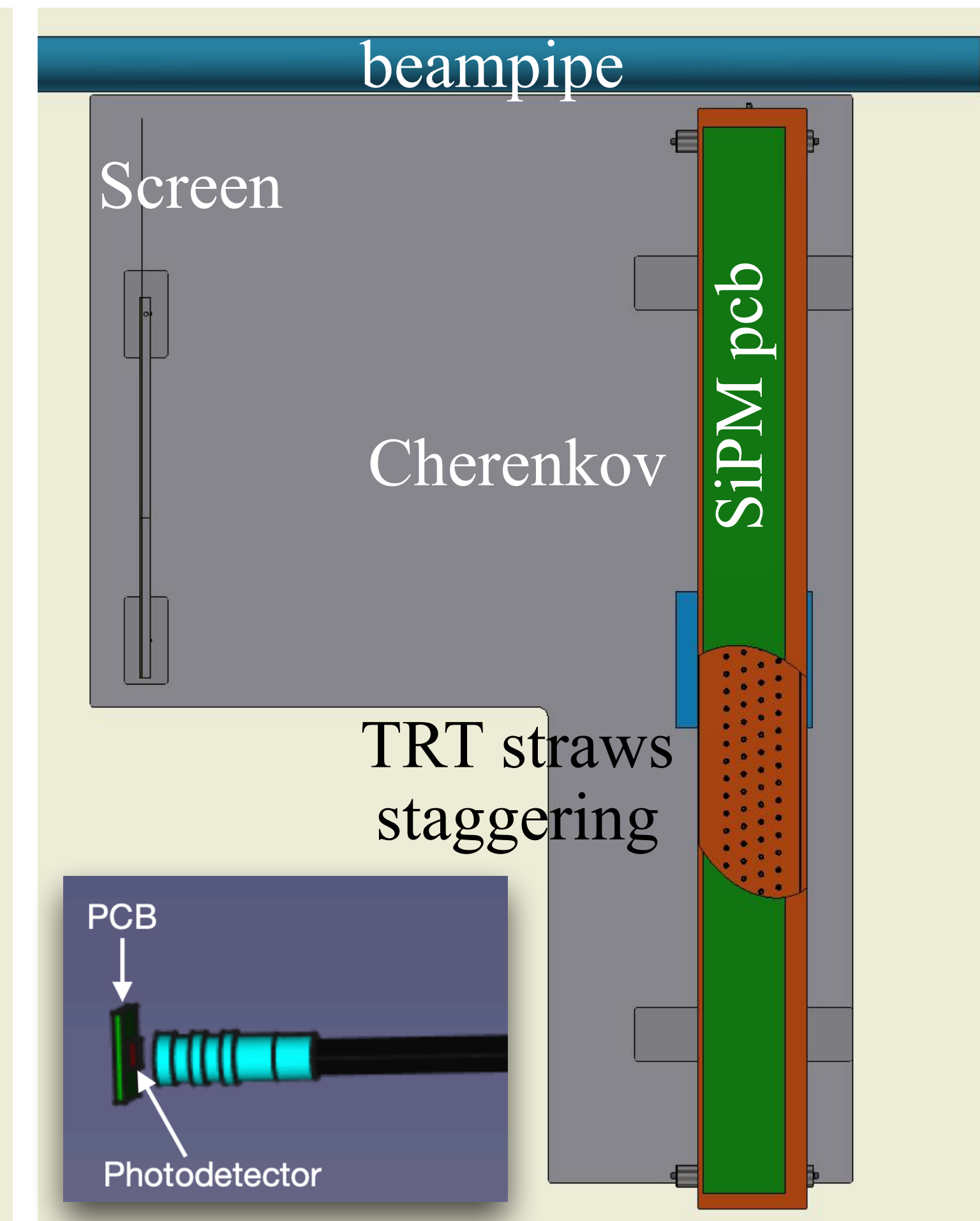
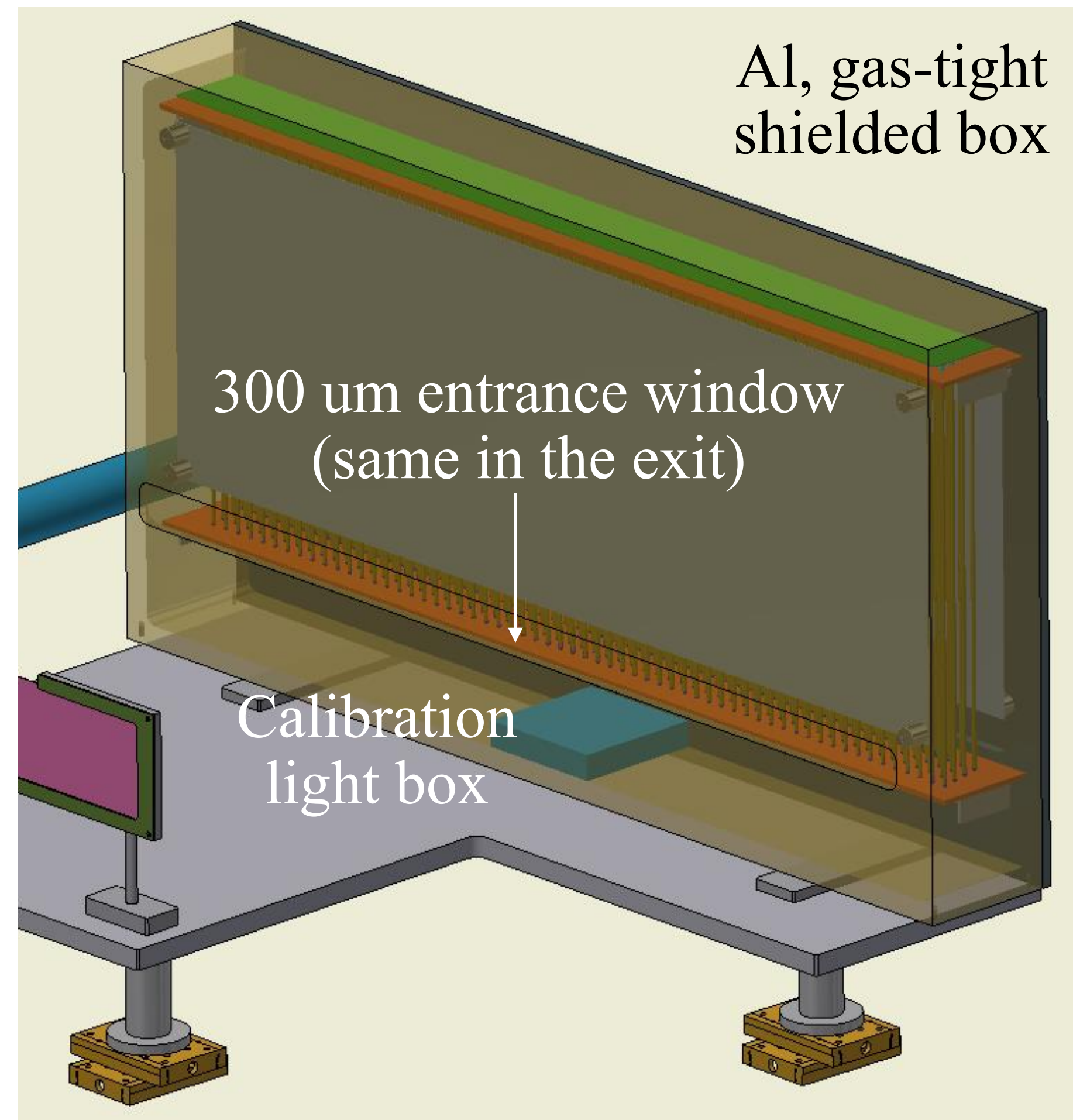
- Linear response up to 350 pC (high fluxes!) demonstrated by AWAKE

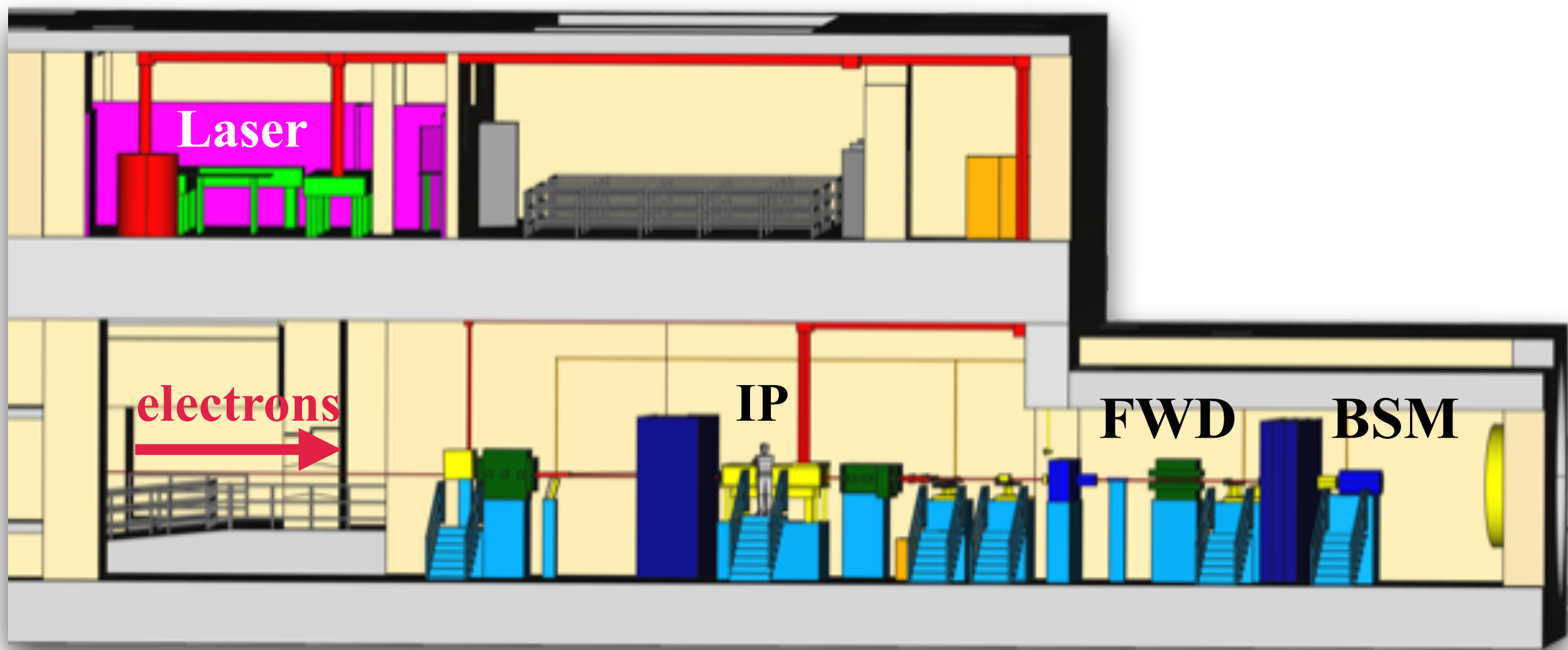


Cherenkov counter

ATLAS spare TRT straws, segmented in a few rows, openly coupled to SiPMs on the top (gas flow) and to fibres for calibration at the bottom

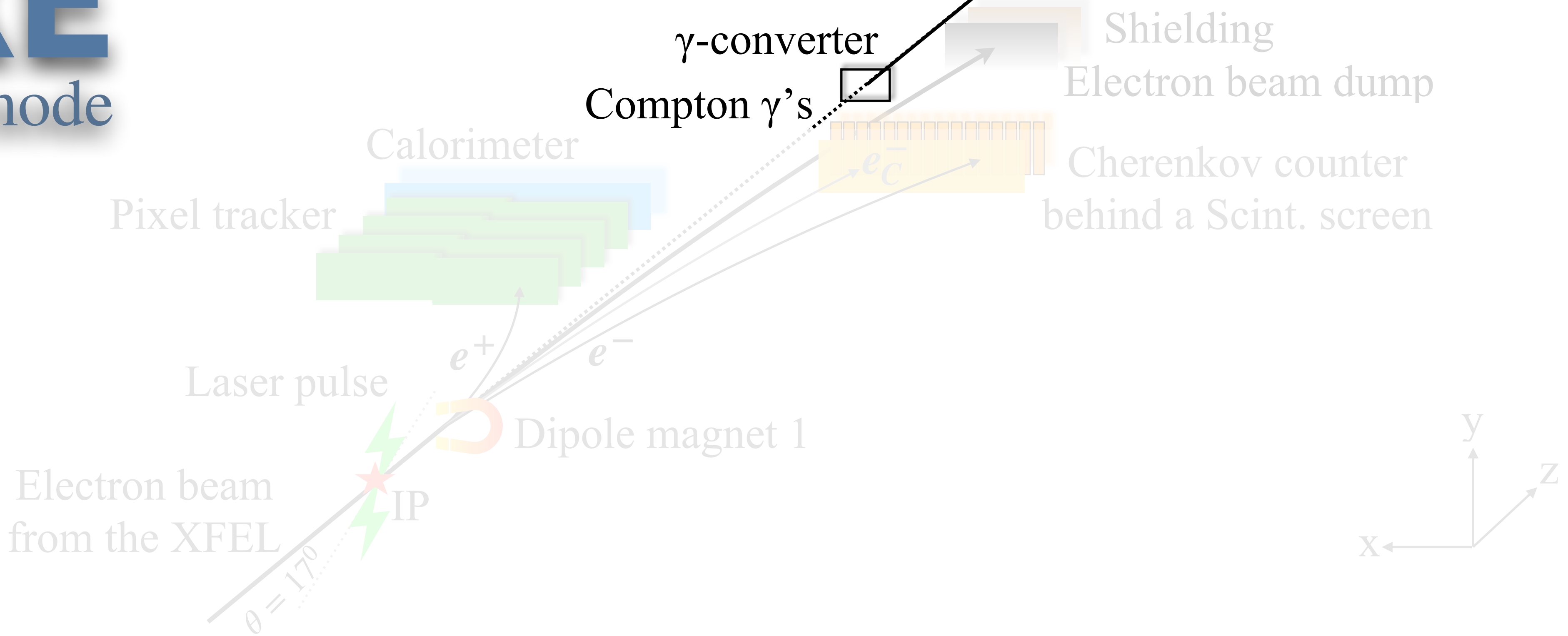
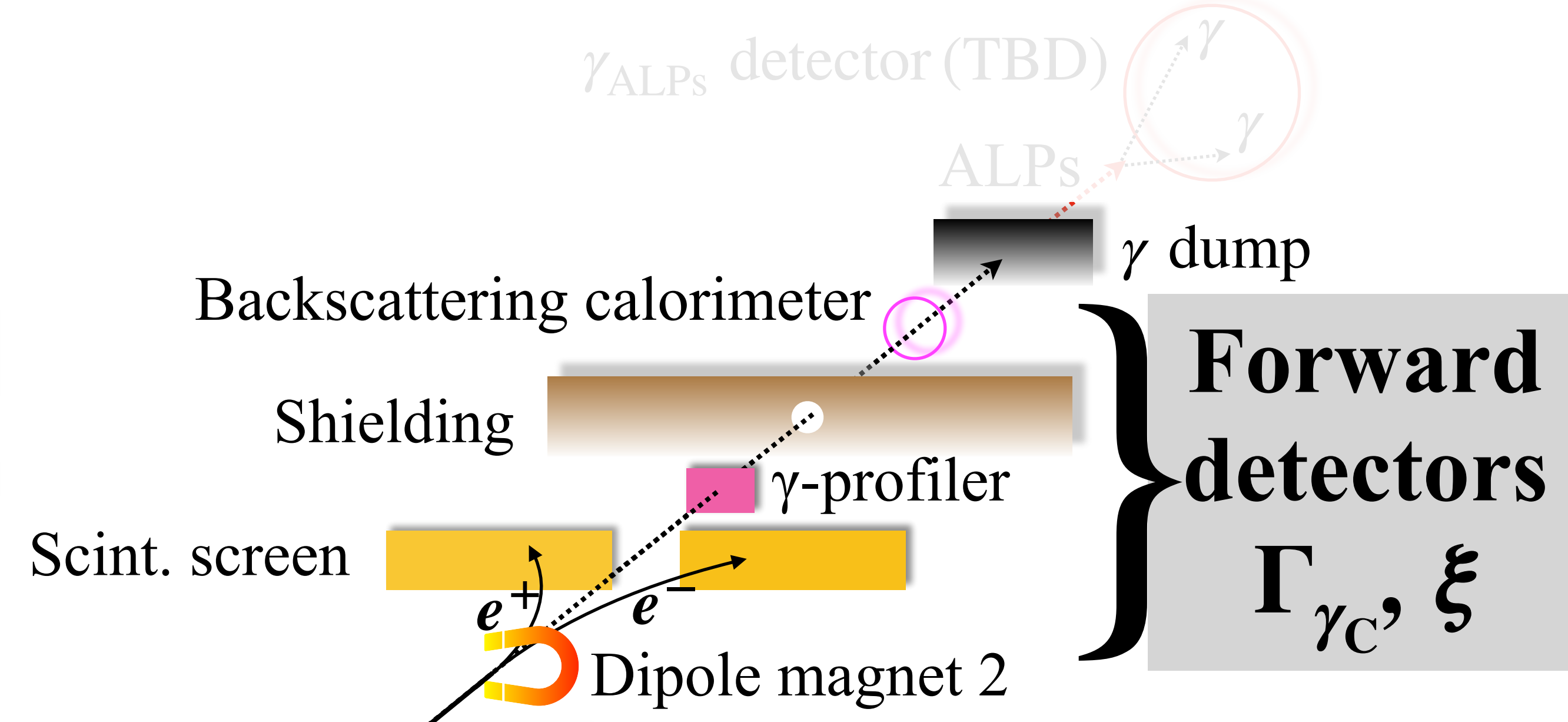
- More agnostic to low-energy (non-signal) particles than the screen
- We don't yet have results for the new TRT concept
- CDR design relied on polarimetry detector for future lepton colliders





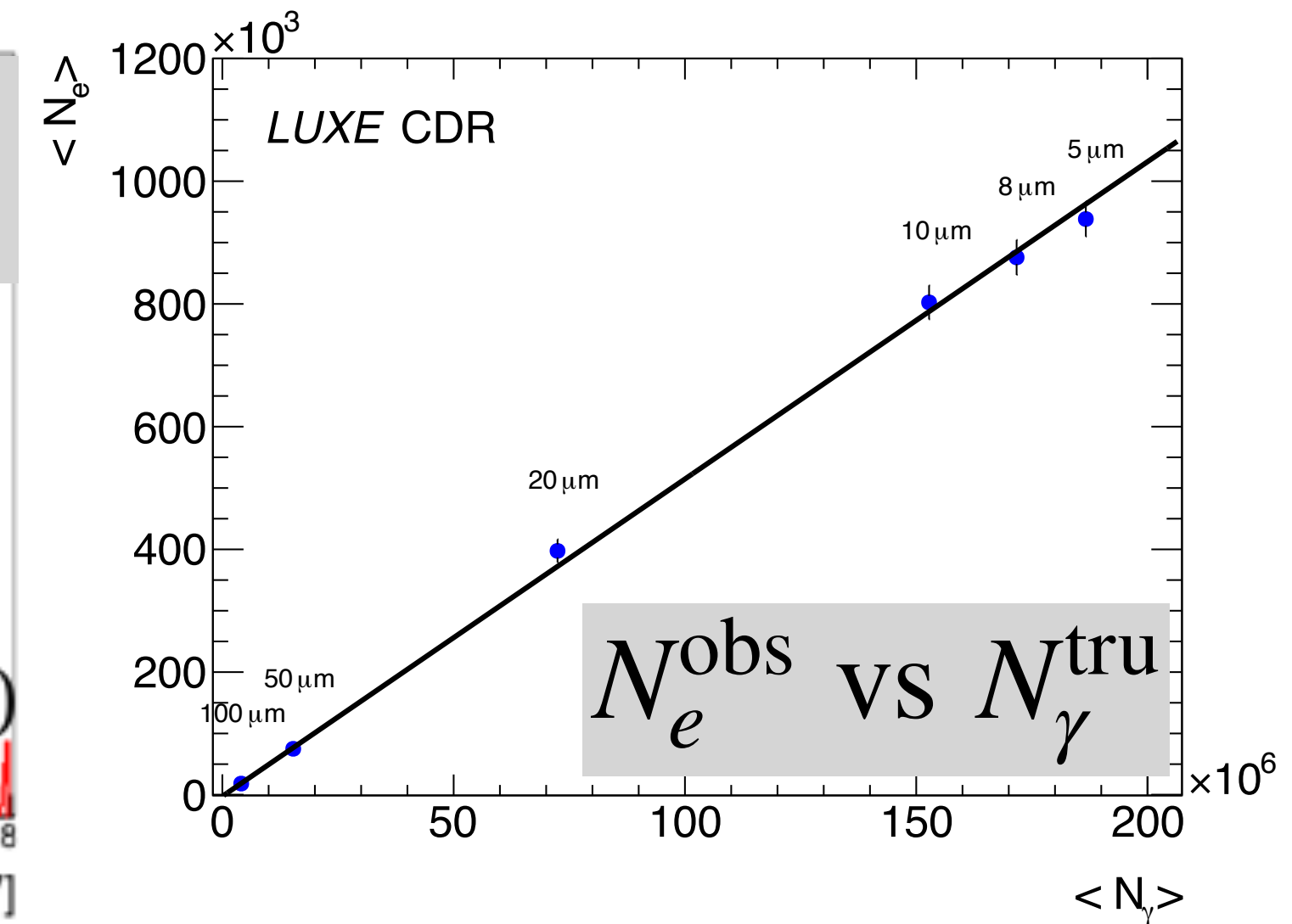
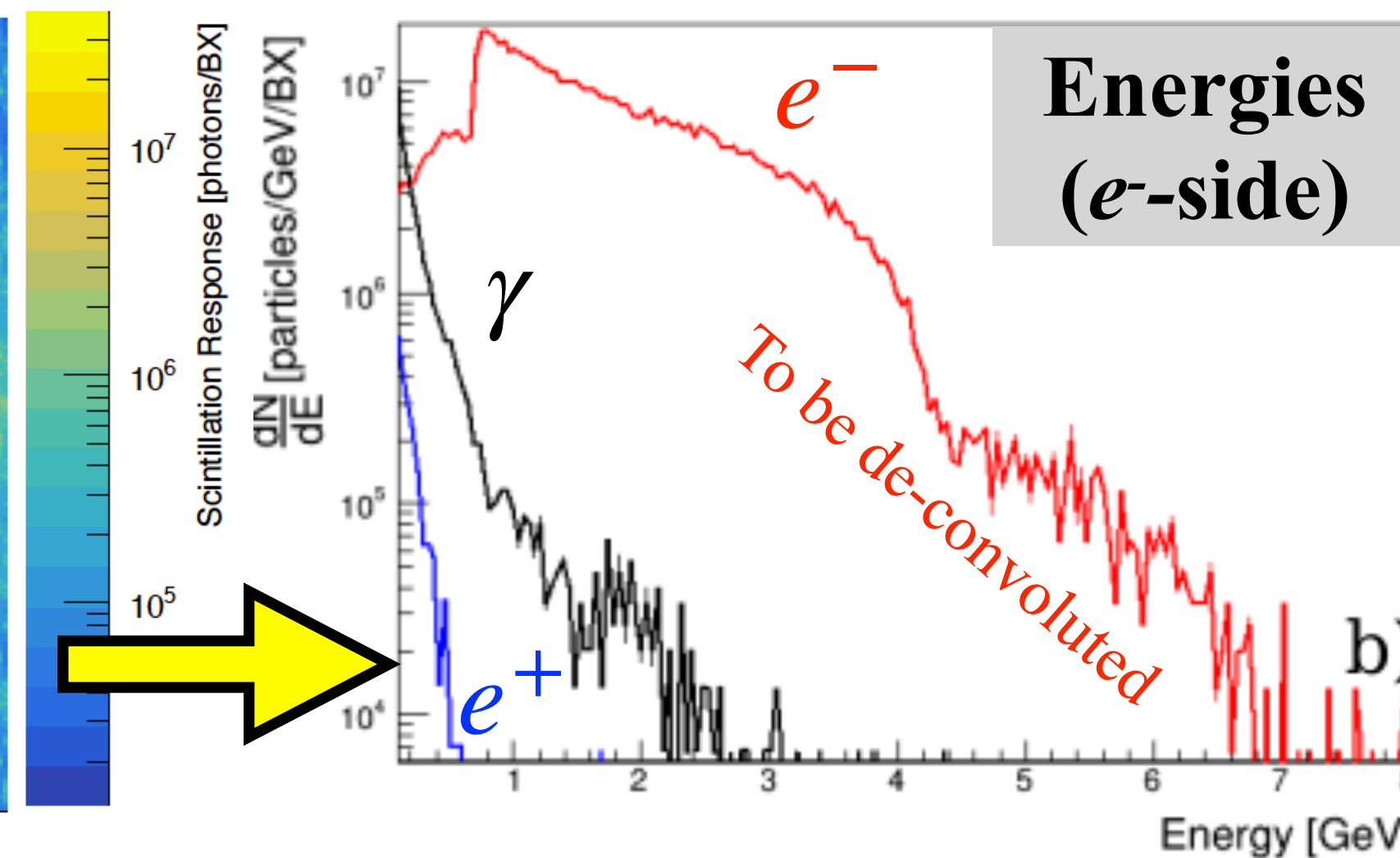
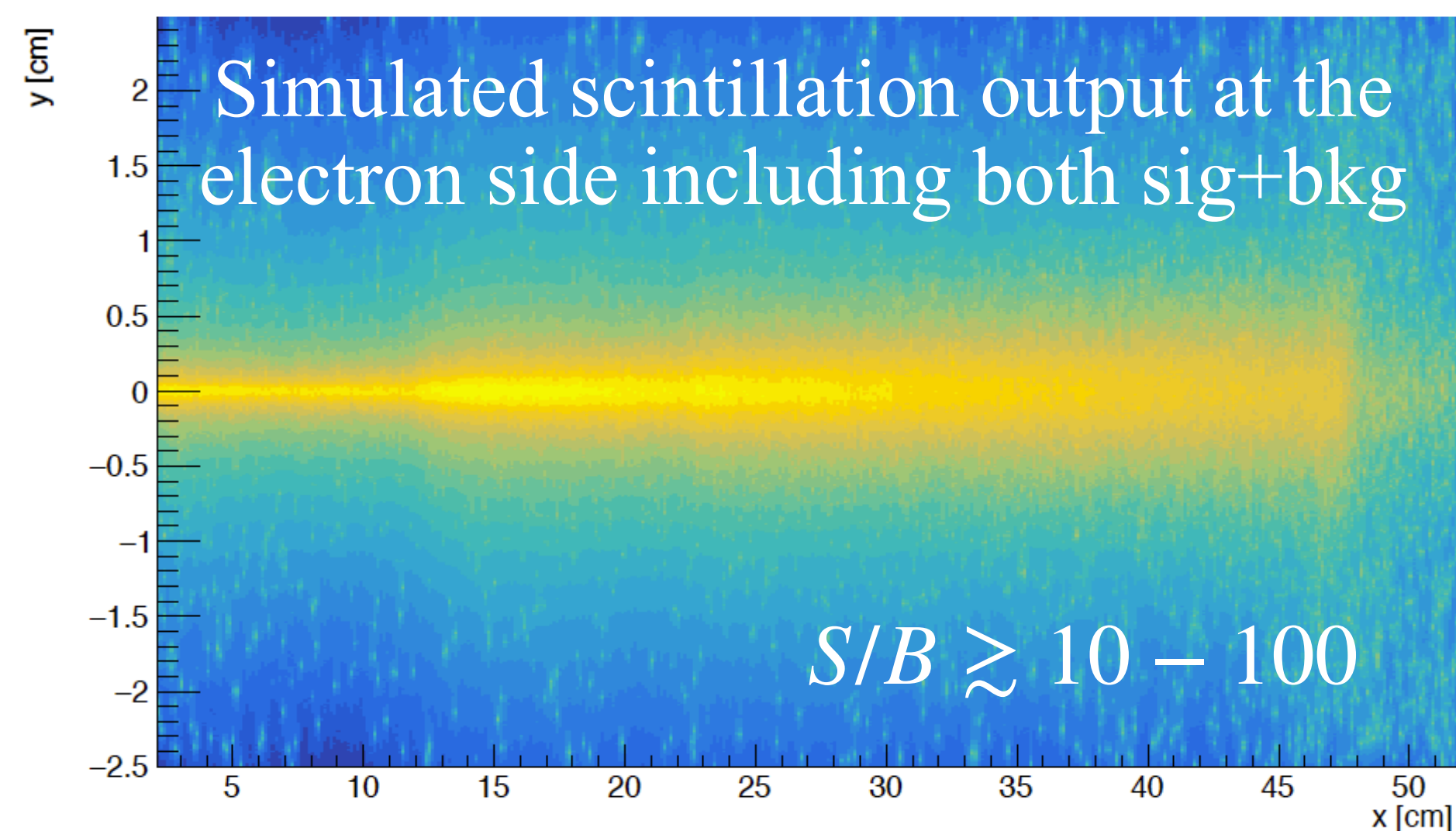
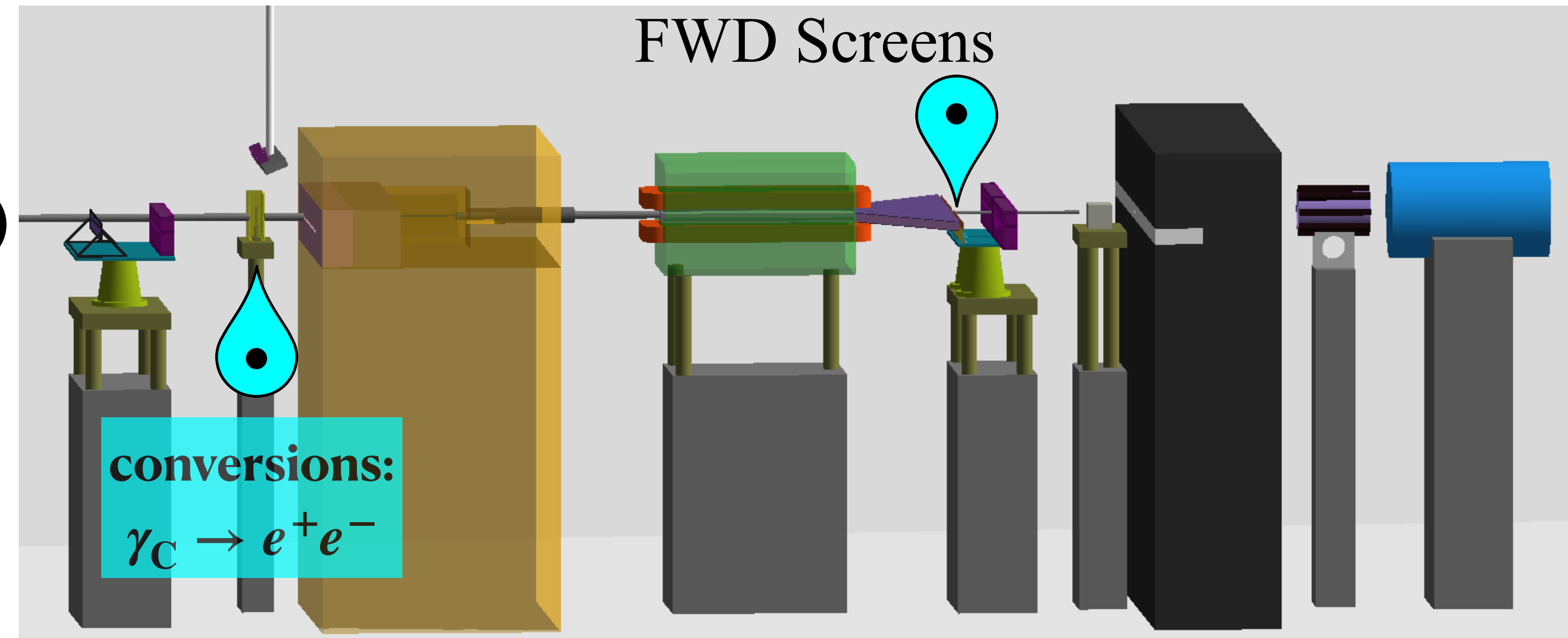
LUXE

e + laser mode



Forward photon spectrometer

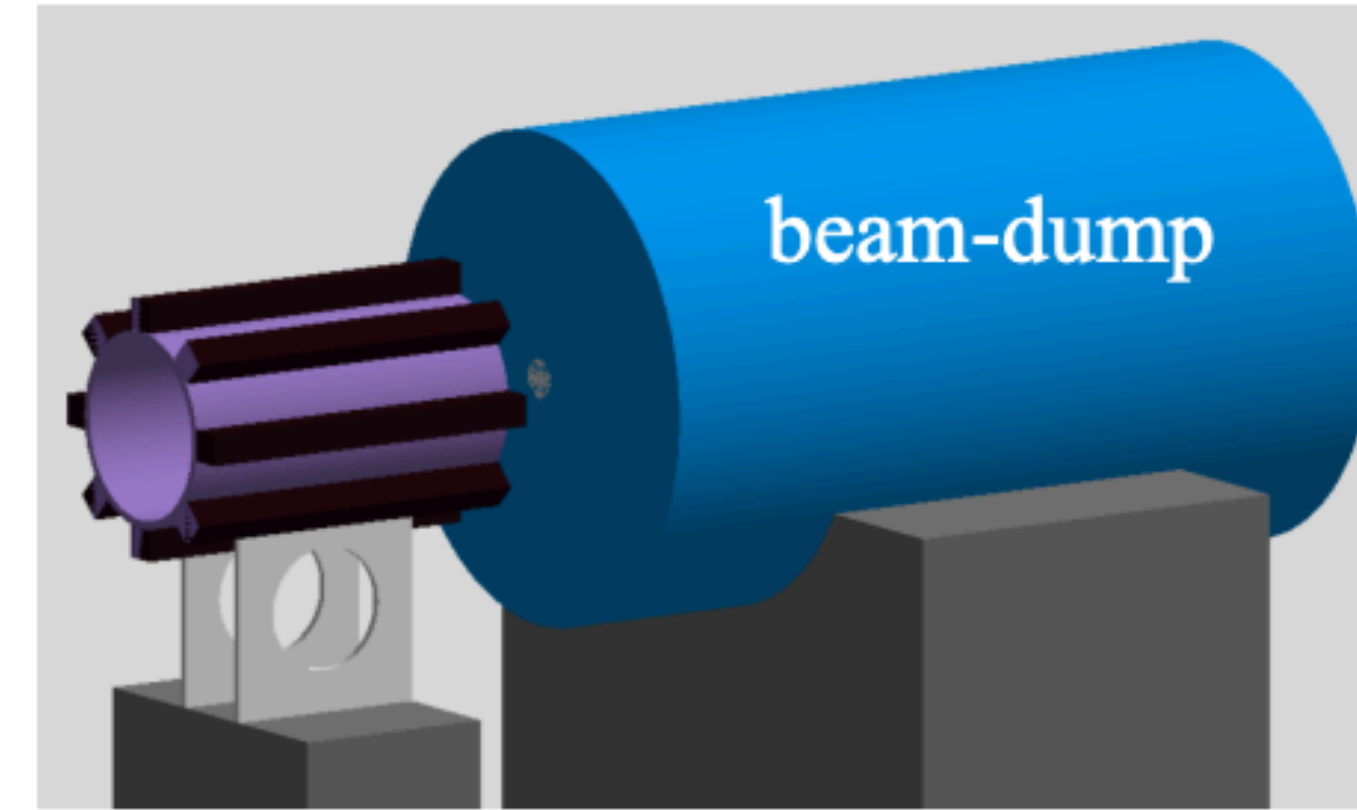
- Same GadOx screen (both sides now!)
- CDR: particles travelling in air (now in vacuum)
 - much more background earlier
 - signal photons were also converted in air
- Possibly measure $dN/dE(x)/dy$ to extract info about the beam shape



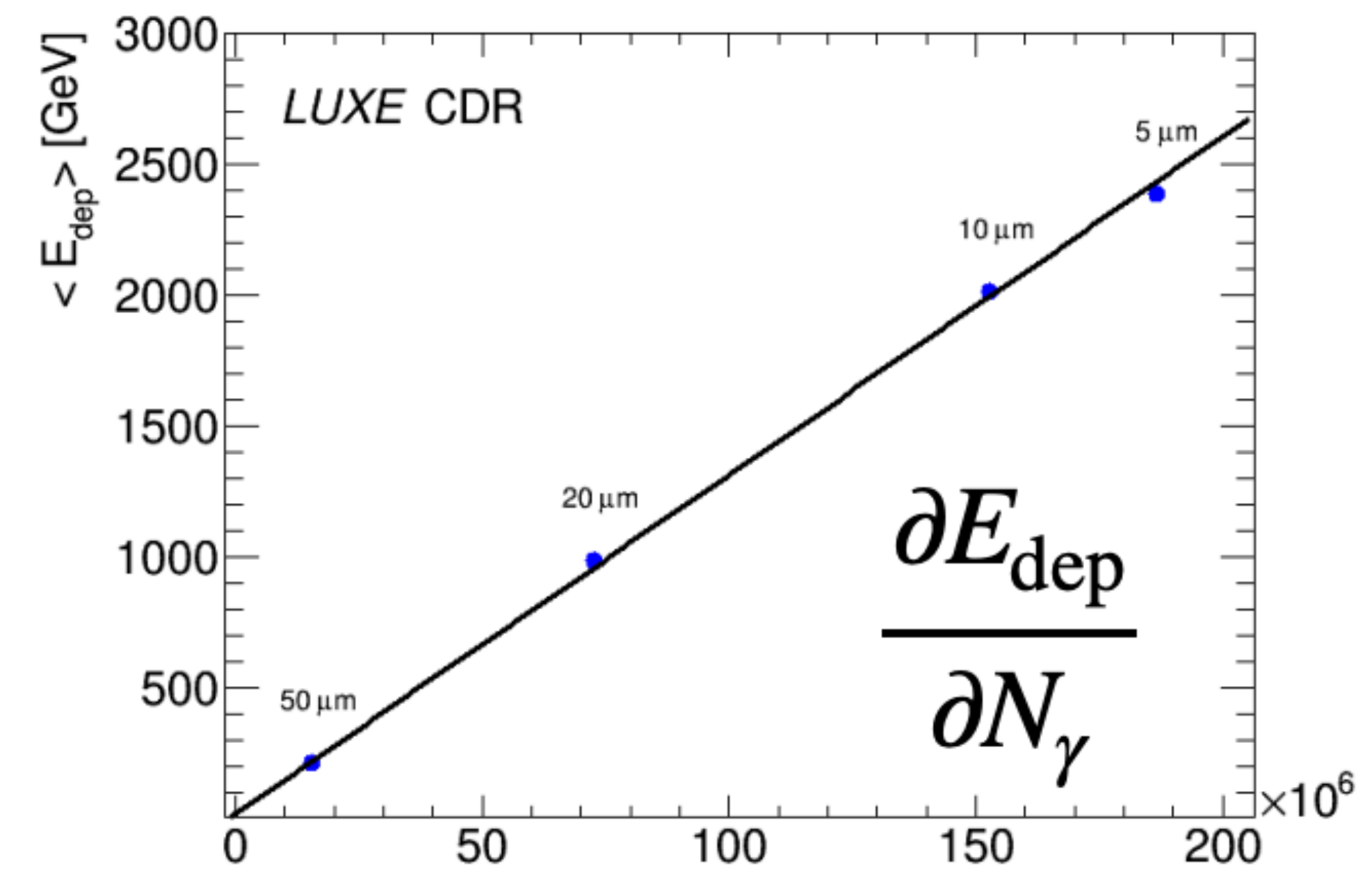
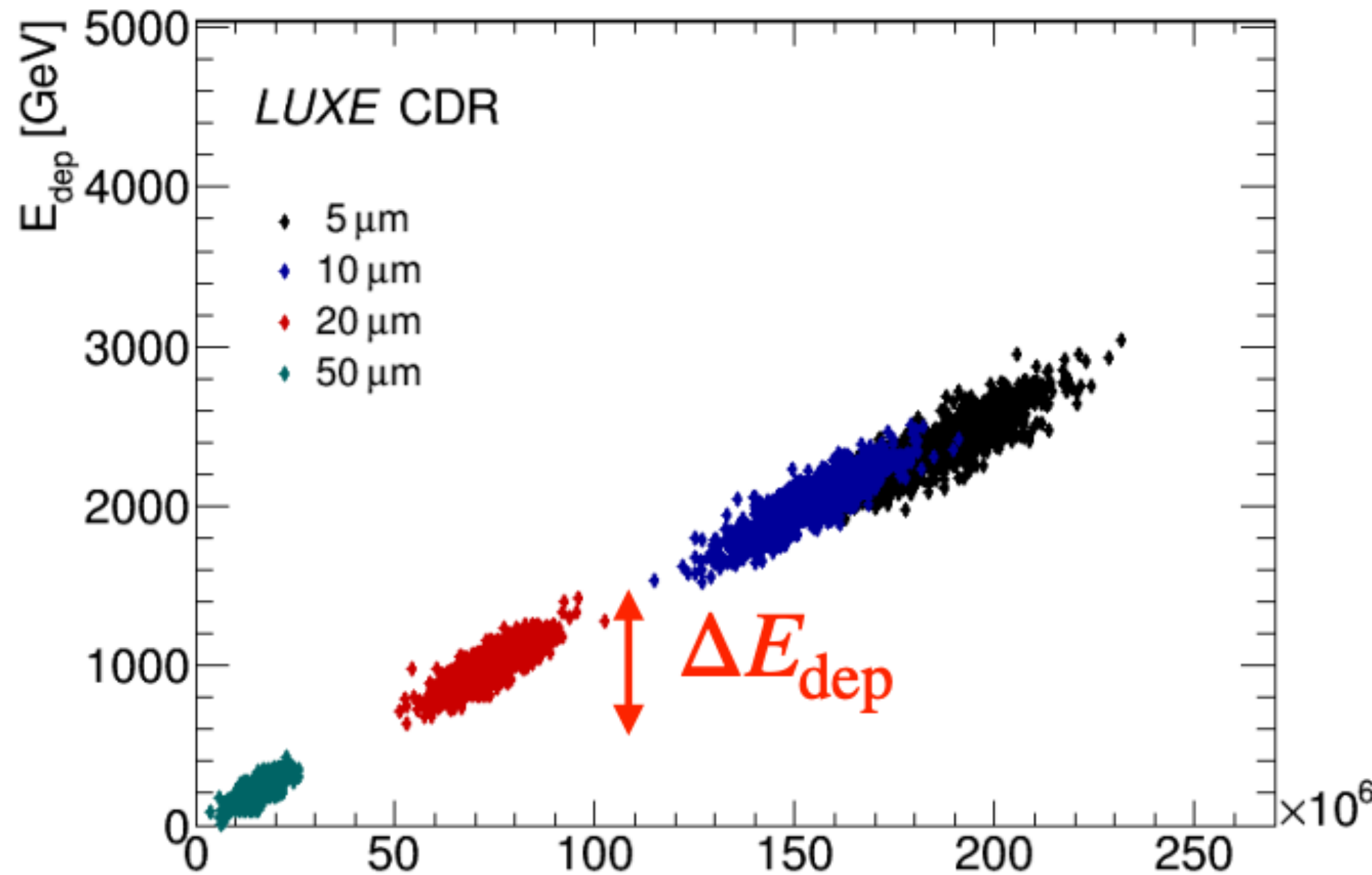
Backscattering calorimeter

- Measure back-scattered energy deposit from the last dump
- Precision in the number of photons is

$$\Delta N_\gamma = \frac{\partial N_\gamma}{\partial E_{\text{dep}}} \Delta E_{\text{dep}}$$
 where the derivative is the slope (MC)
- ΔE_{dep} is the inherent spread of the back-scattered particles
- Typically we can expect that $\Delta N_\gamma / N_\gamma \lesssim 10\%$



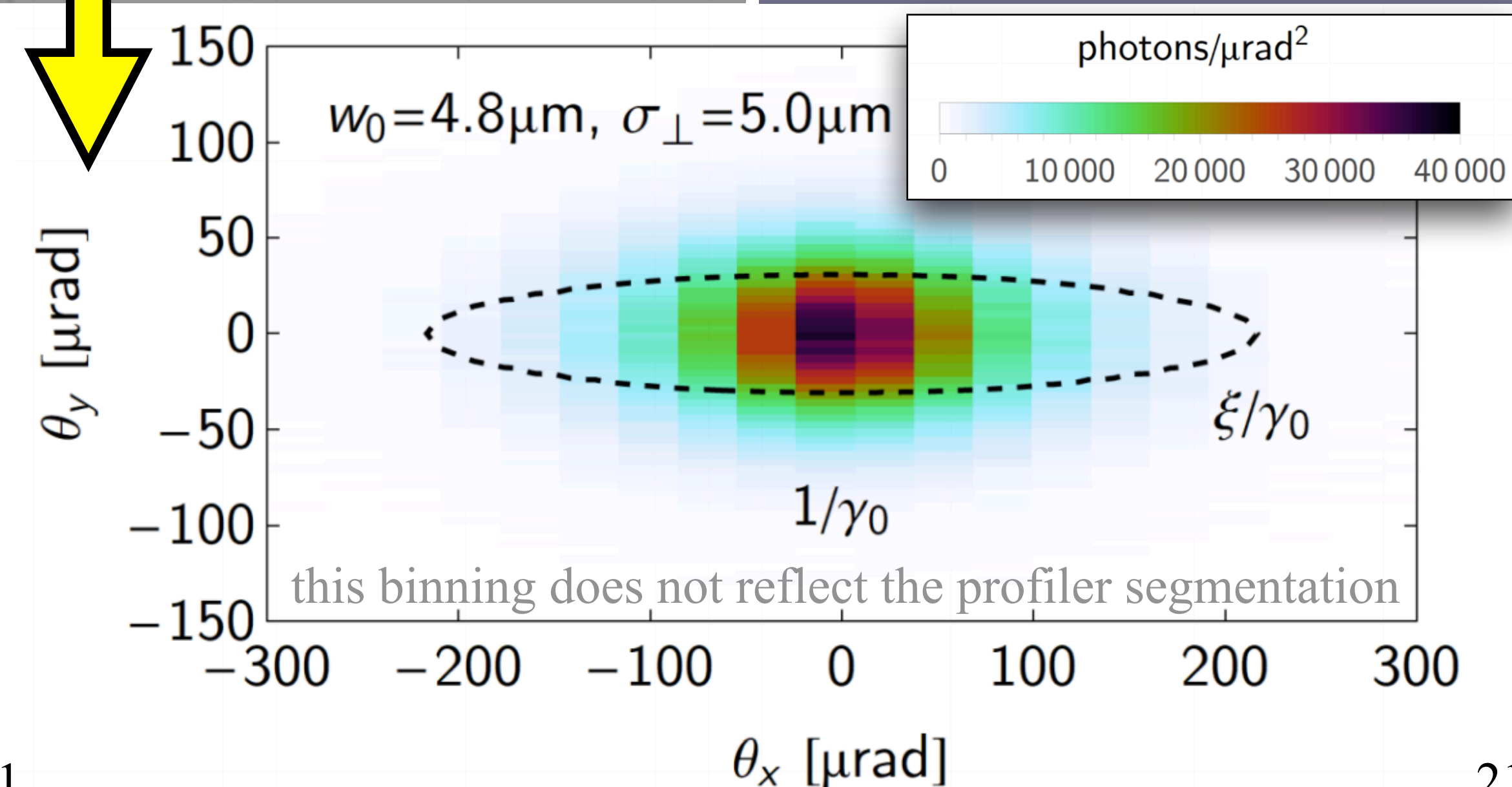
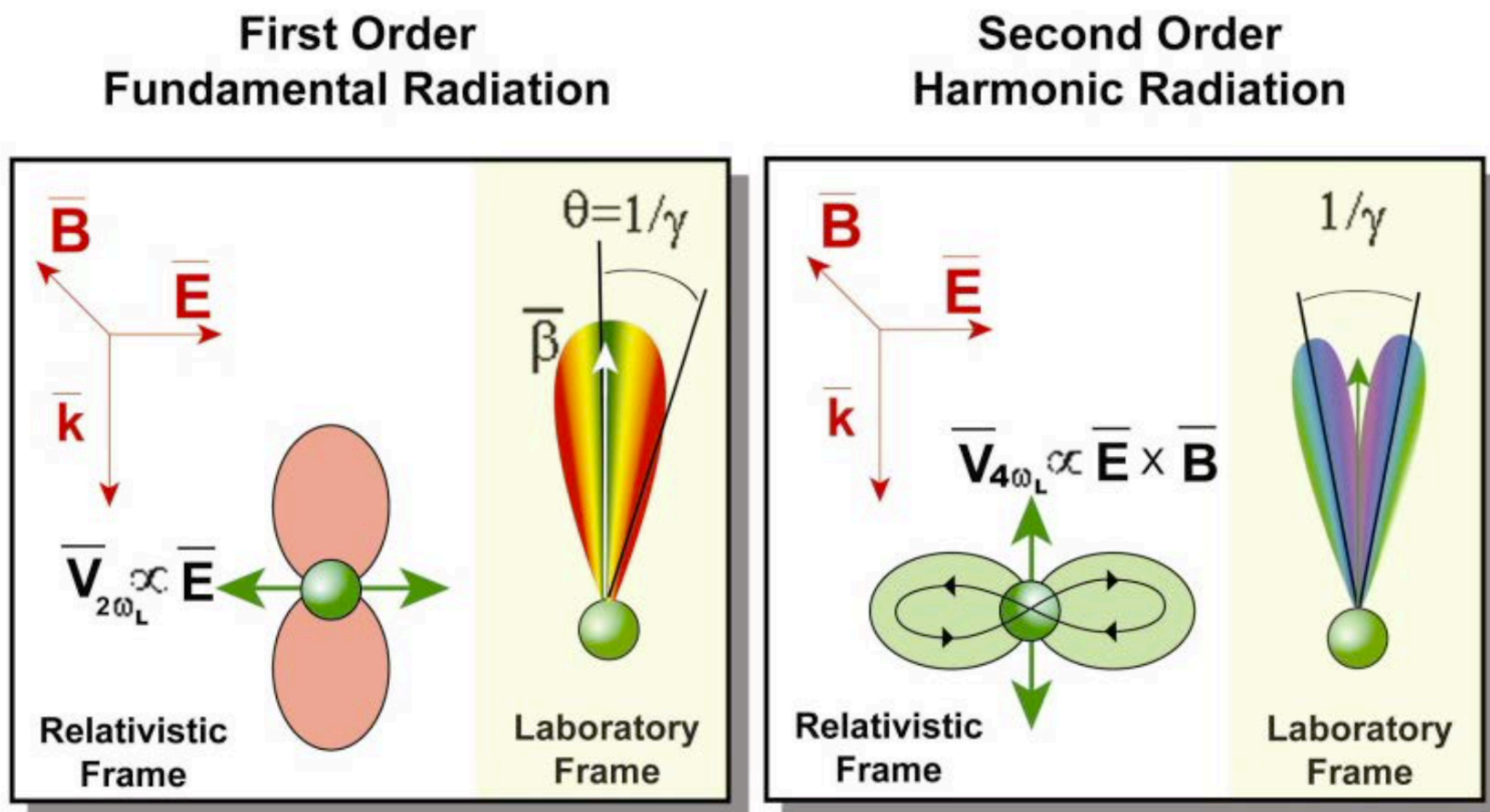
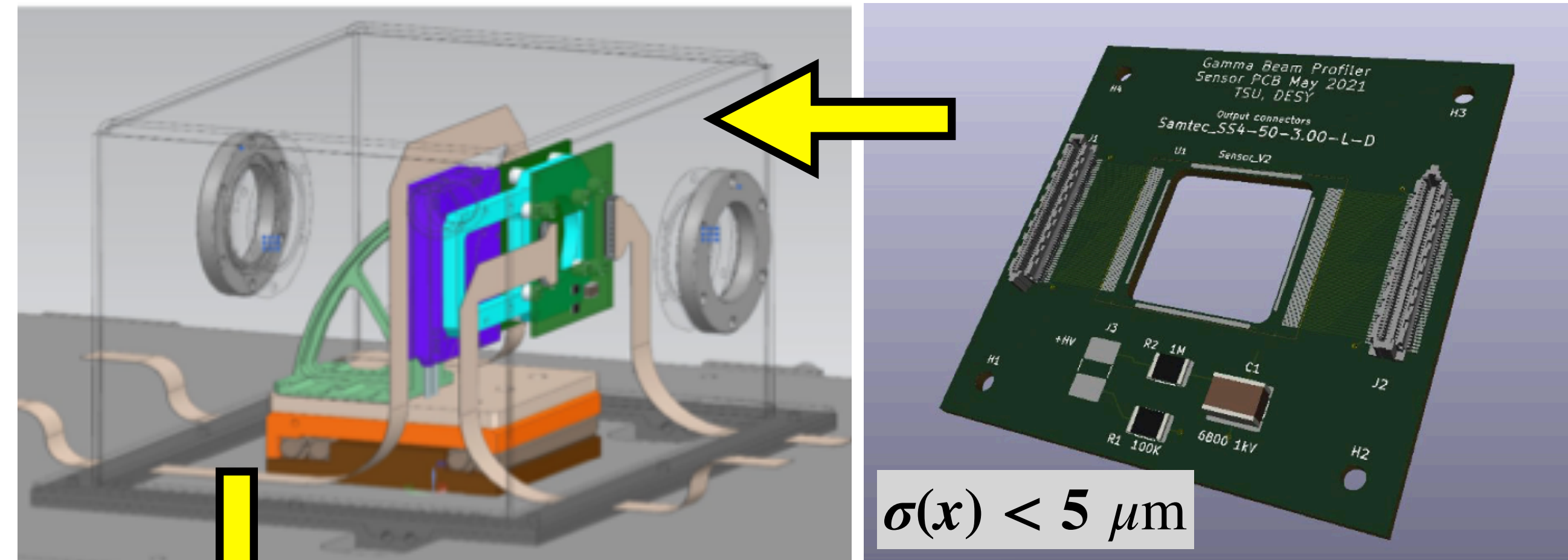
Eight TF-101 type lead-glass blocks of size $3.8 \times 3.8 \times 45 \text{ cm}^3$ connected to PMTs

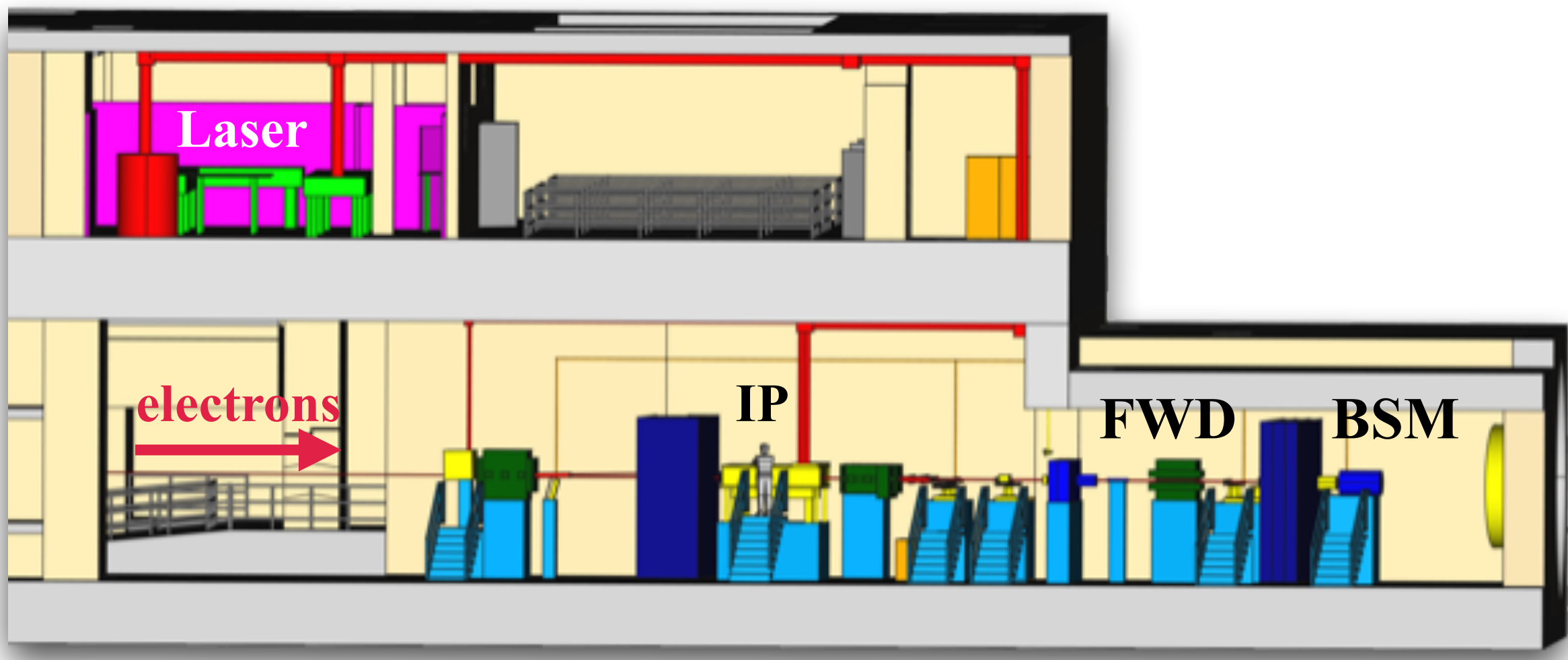


Photon beam profiler

- Measure the beam σ_T and $\sigma_{||}$ to extract ξ value at the IP and measure γ_C rate
- Typical emission angle in the lab frame is $\theta \sim 1/\gamma$
 - LUXE: $\theta \sim 0.031$ mrad so, $\sim 310 \mu\text{m}$ after 10 m
 - For $\xi \gg 1$ there are two relevant angles wrt the polarisation direction: $\theta_{||} \sim \xi/\gamma$ in the and $\theta_{\perp} \sim 1/\gamma$

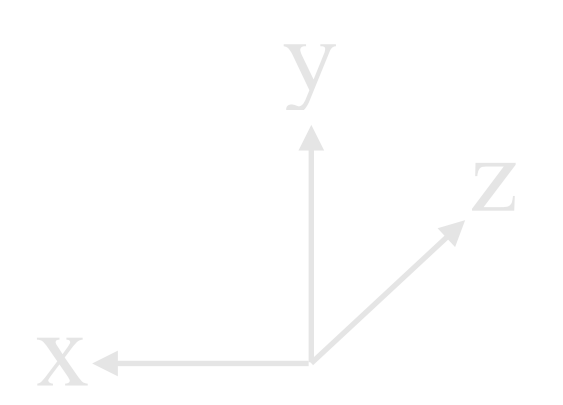
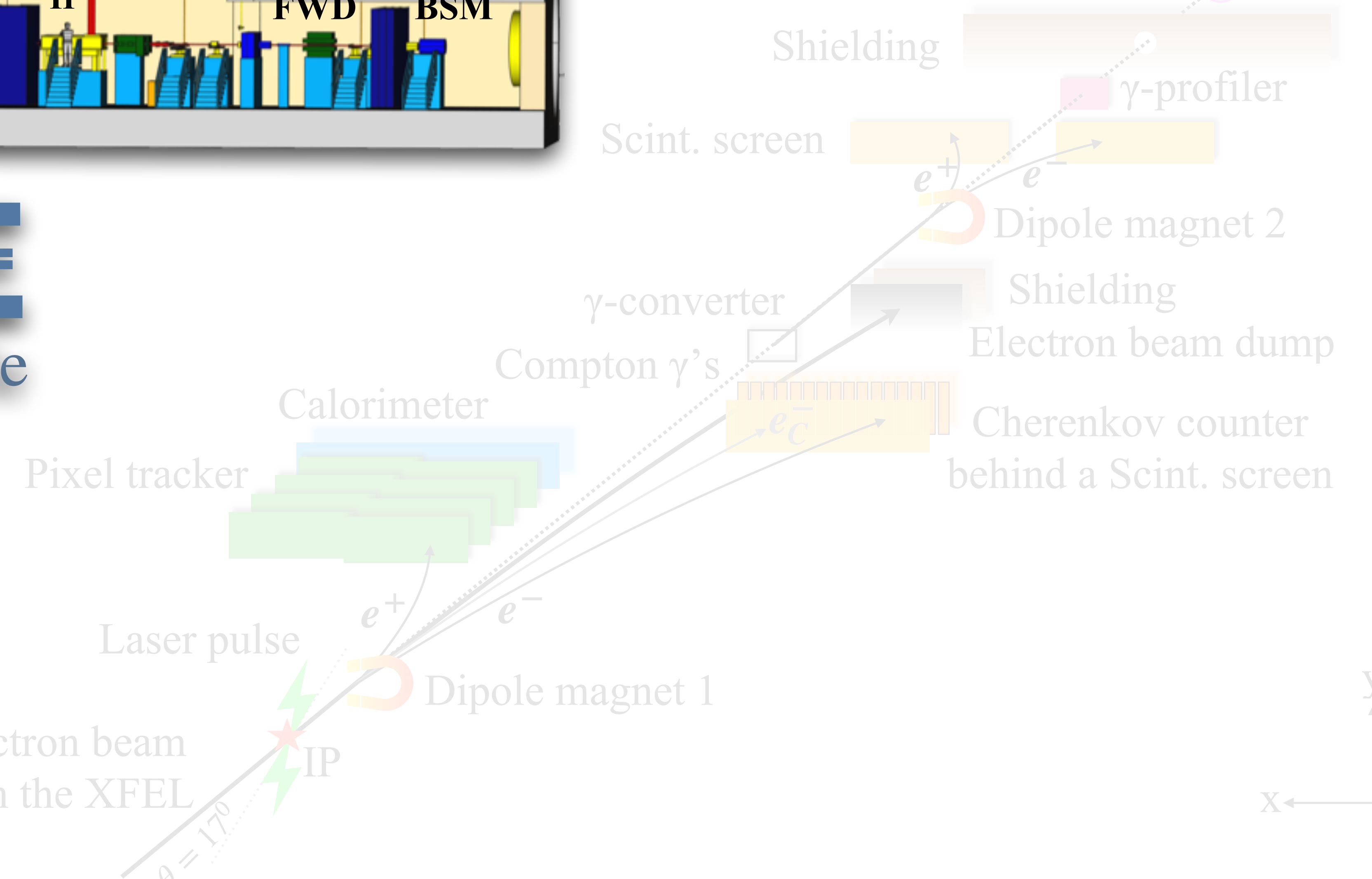
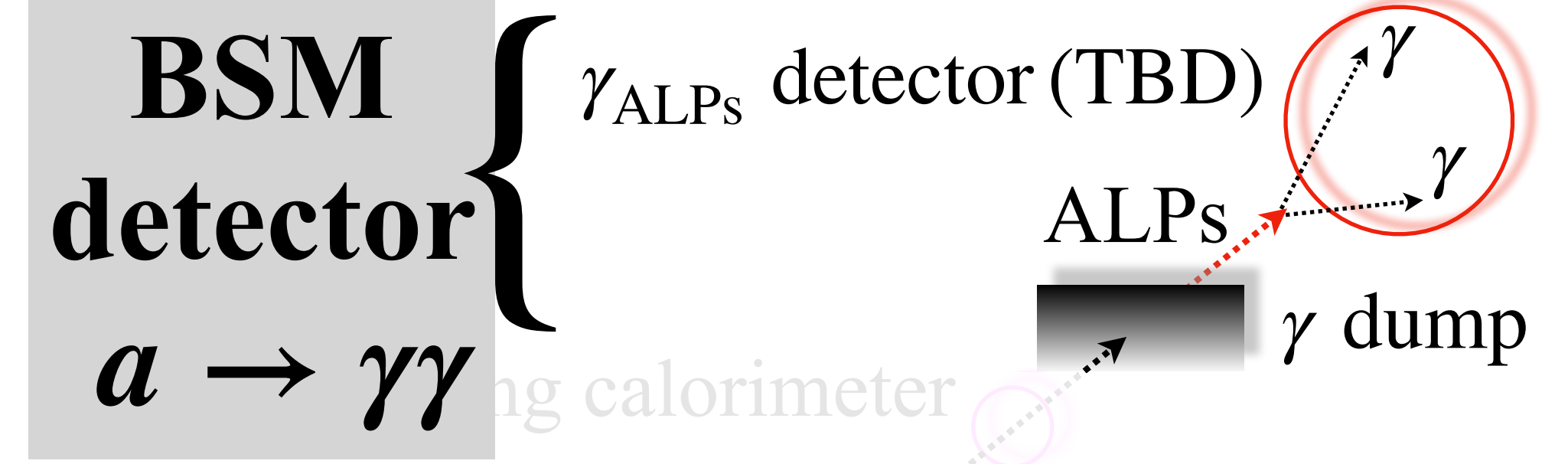
Two orthogonal $2 \times 2 \text{ cm}^2$ and $100 \mu\text{m}$ thick Sapphire strip planes (huge dose!) with $100 \mu\text{m}$ pitch and an analog RO



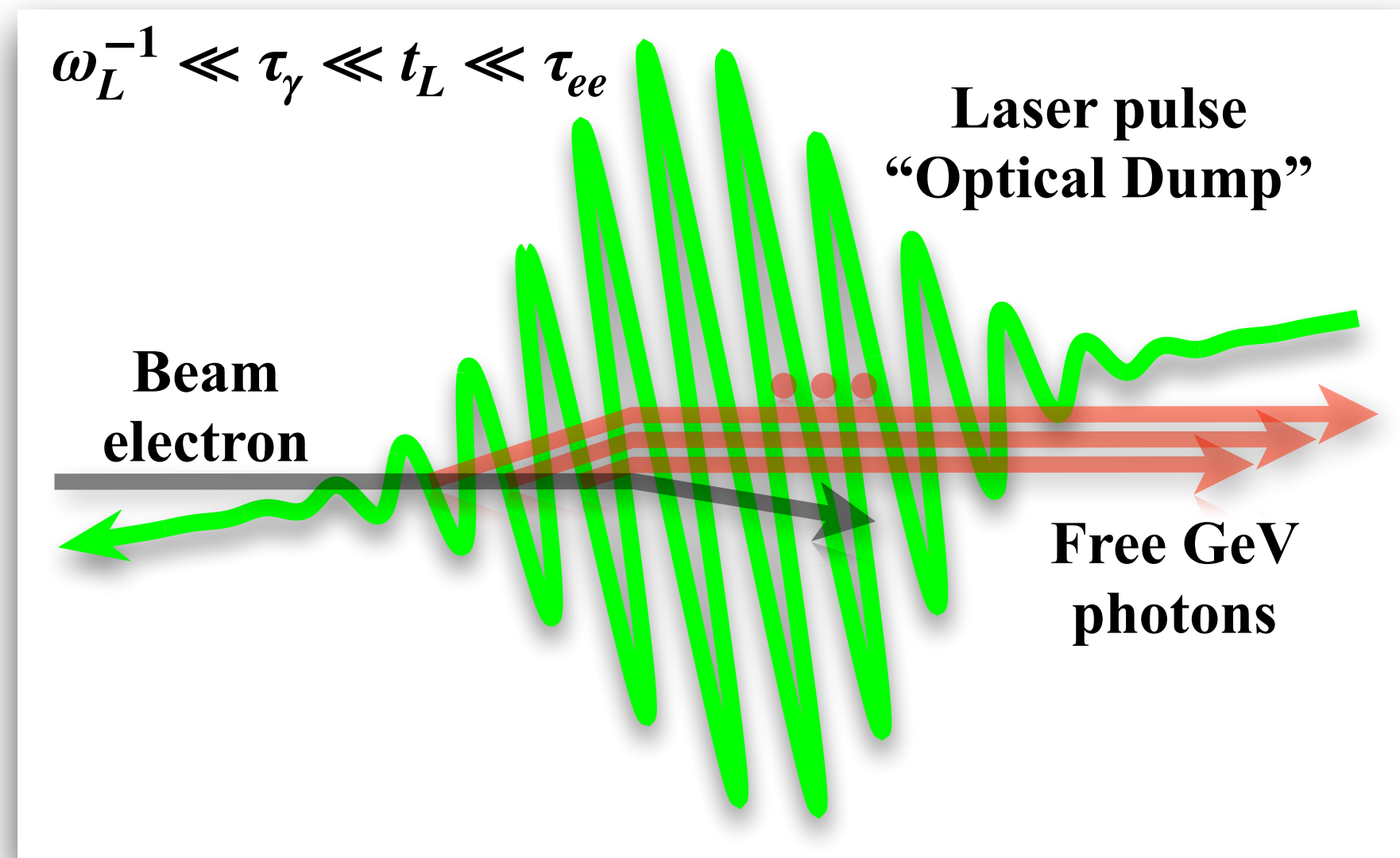


LUXE

e + laser mode

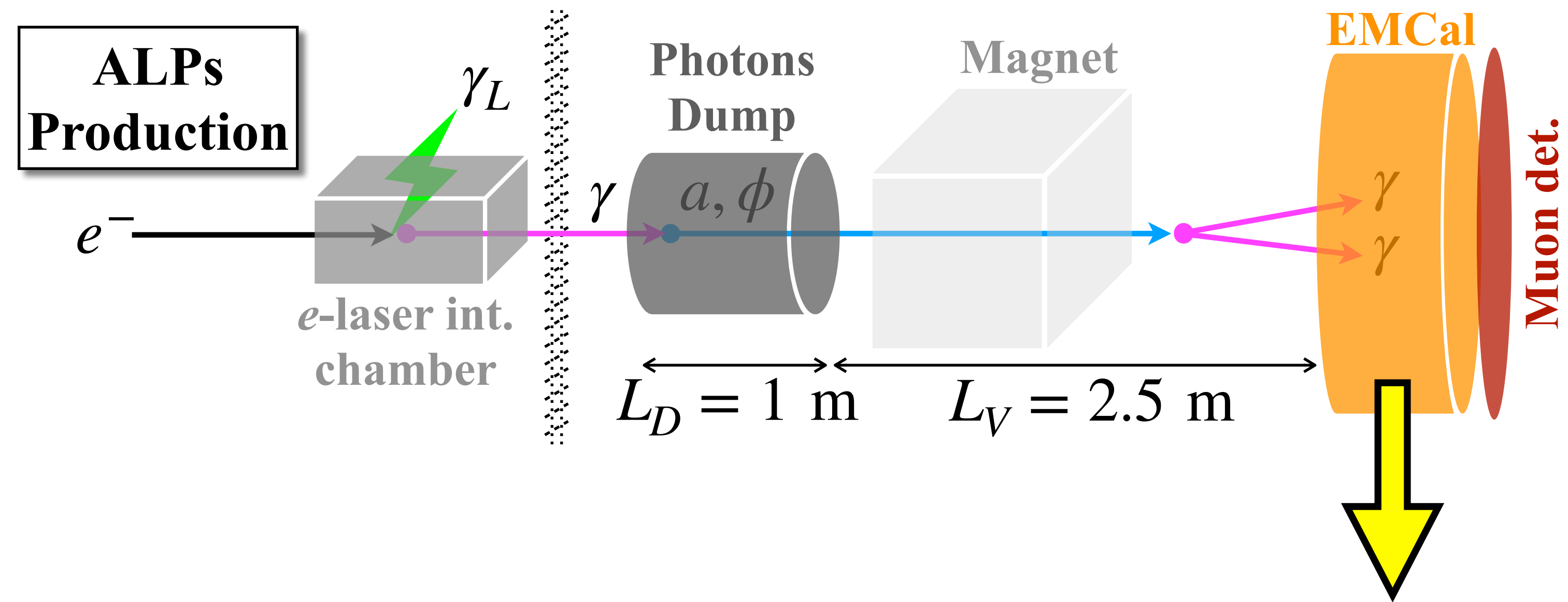


New Physics @ Optical Dump



$N_\gamma/N_e \sim 1.7$ for $E_\gamma > 1$ GeV with $\tau_{\text{pulse}} = 120$ fs and $w_0 = 10$ μm

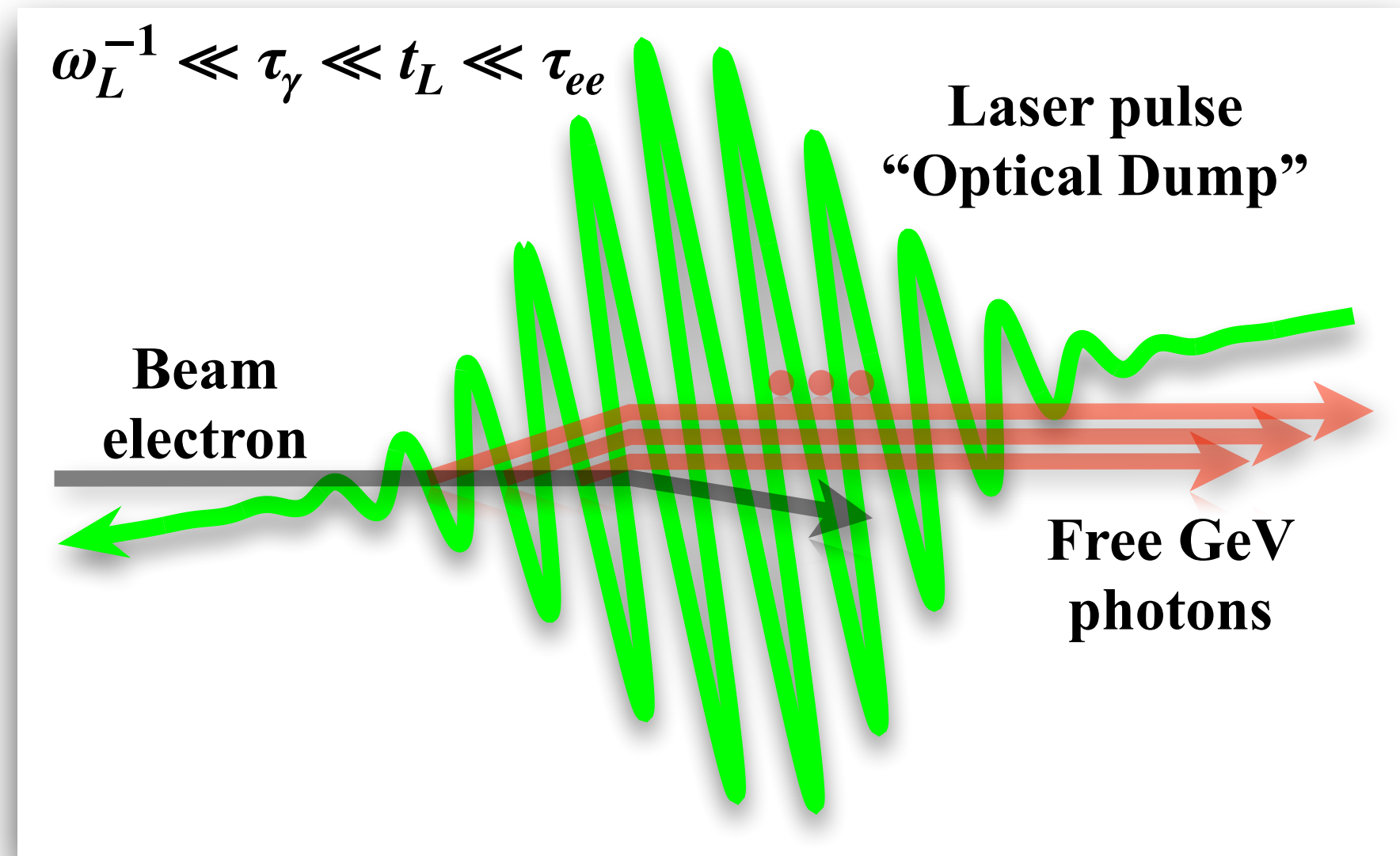
ignore today

$$\mathcal{L}_a = \frac{a}{4\Lambda_a} F_{\mu\nu} \tilde{F}^{\mu\nu} + i g_{ae} a \bar{e} \gamma^5 e$$


EMCal requirements:

- $\sigma_t \sim \mathcal{O}(100$ ps)
- $\sigma_{x,y} \sim \mathcal{O}(100$ $\mu\text{m})$
- $\sigma_\theta \sim \mathcal{O}(10$ mrad)

New Physics @ Optical Dump



$N_\gamma/N_e \sim 1.7$ for $E_\gamma > 1$ GeV with $\tau_{\text{pulse}} = 120$ fs and $w_0 = 10$ μm

ignore today

$$\mathcal{L}_a = \frac{a}{4\Lambda_a} F_{\mu\nu} \tilde{F}^{\mu\nu} + i g_{ae} a \bar{e} \gamma^5 e$$

γ

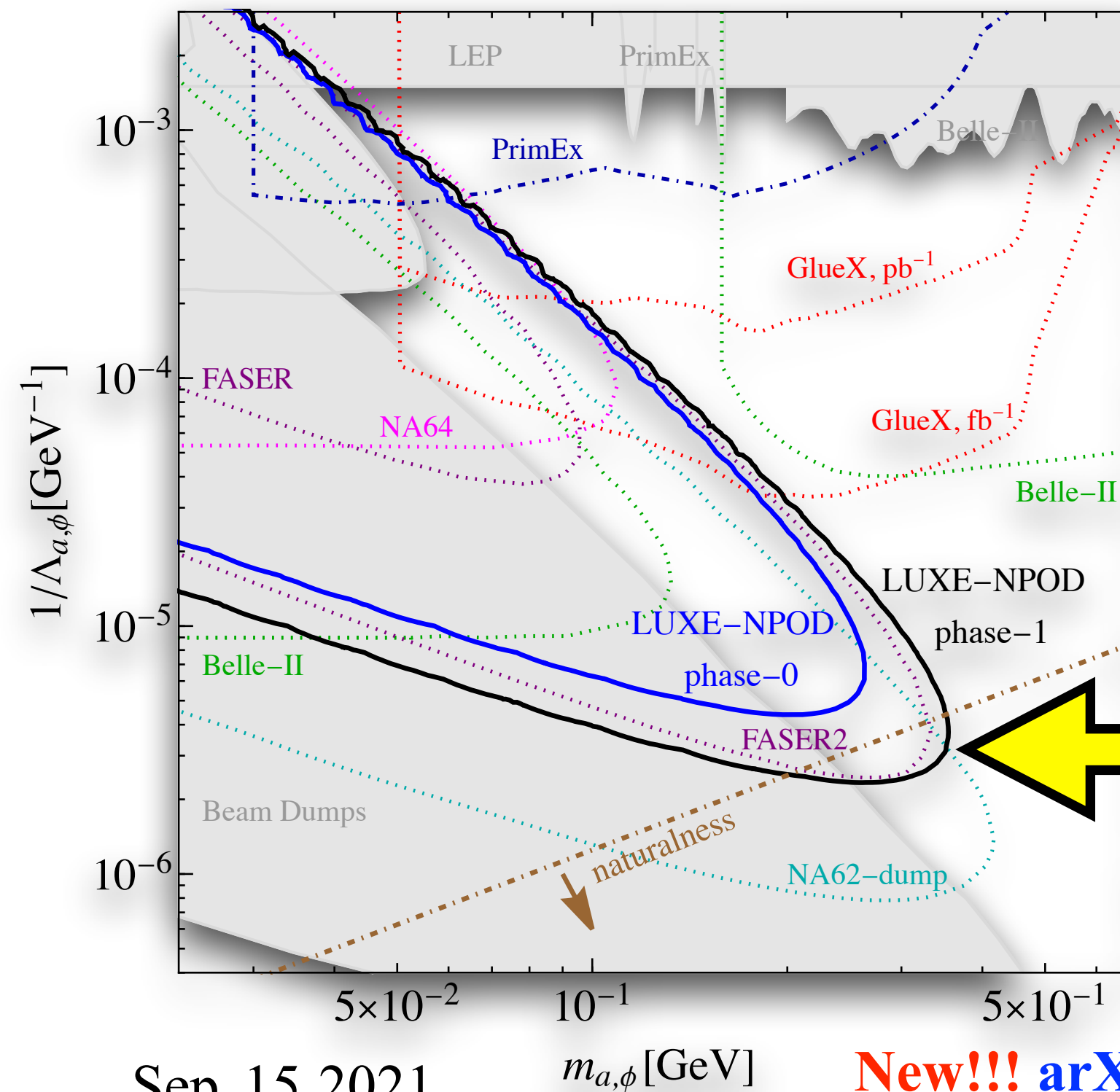
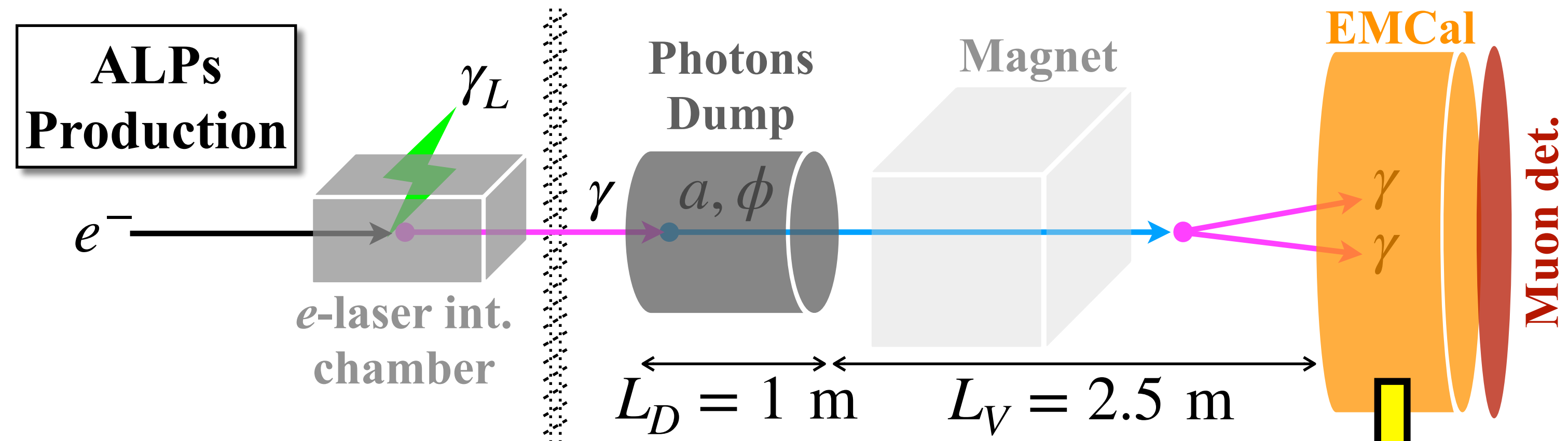
γ^*

a

γ

N

N



EMCal requirements:

- $\sigma_t \sim \mathcal{O}(100$ ps)
- $\sigma_{x,y} \sim \mathcal{O}(100$ $\mu\text{m})$
- $\sigma_\theta \sim \mathcal{O}(10$ mrad)

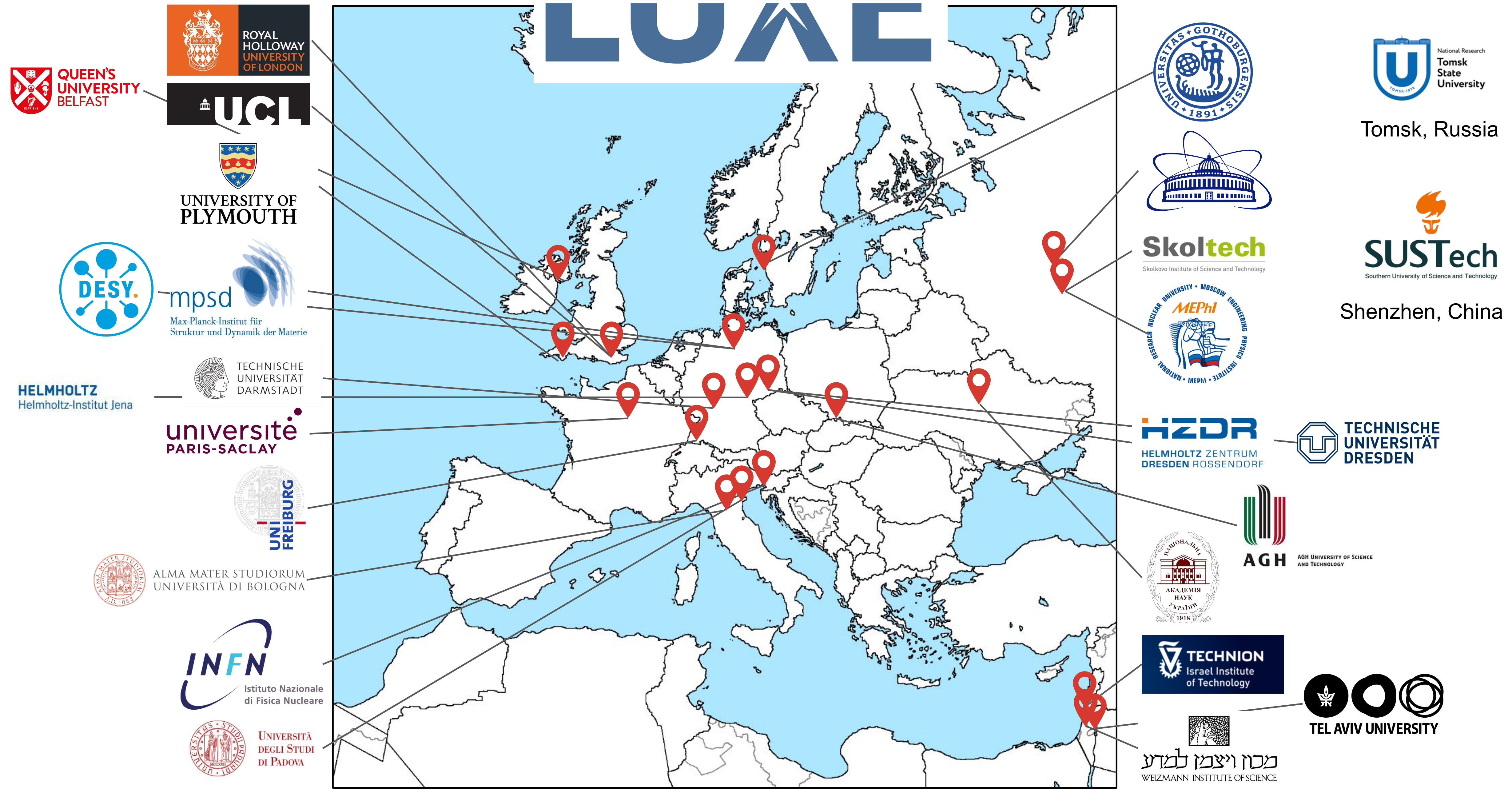
The LUXE-NPOD can be bkg-free and better than other players in the field

Outlook

- ◉ LUXE is a new exciting experiment with a novel baseline plan
 - ◉ test QED predictions in a region of $\xi - \chi$ never explored before cleanly
 - ◉ search for new physics exploiting the optical dump concept
 - ◉ very streamlined: take data in early ~2025
- ◉ The detector system provides redundancy over a huge dynamic range
 - ◉ didn't discuss the detailed analysis techniques (track-fitting, shower characterisation, edge finding, beam profiling algs, etc.)
 - ◉ didn't discuss the γ +laser setup (concepts are very similar)
 - ◉ didn't discuss the DAQ, triggering and combined operation - next time!



LUXE



Backup

What happens in strong fields?

The Schwinger critical field (1951)

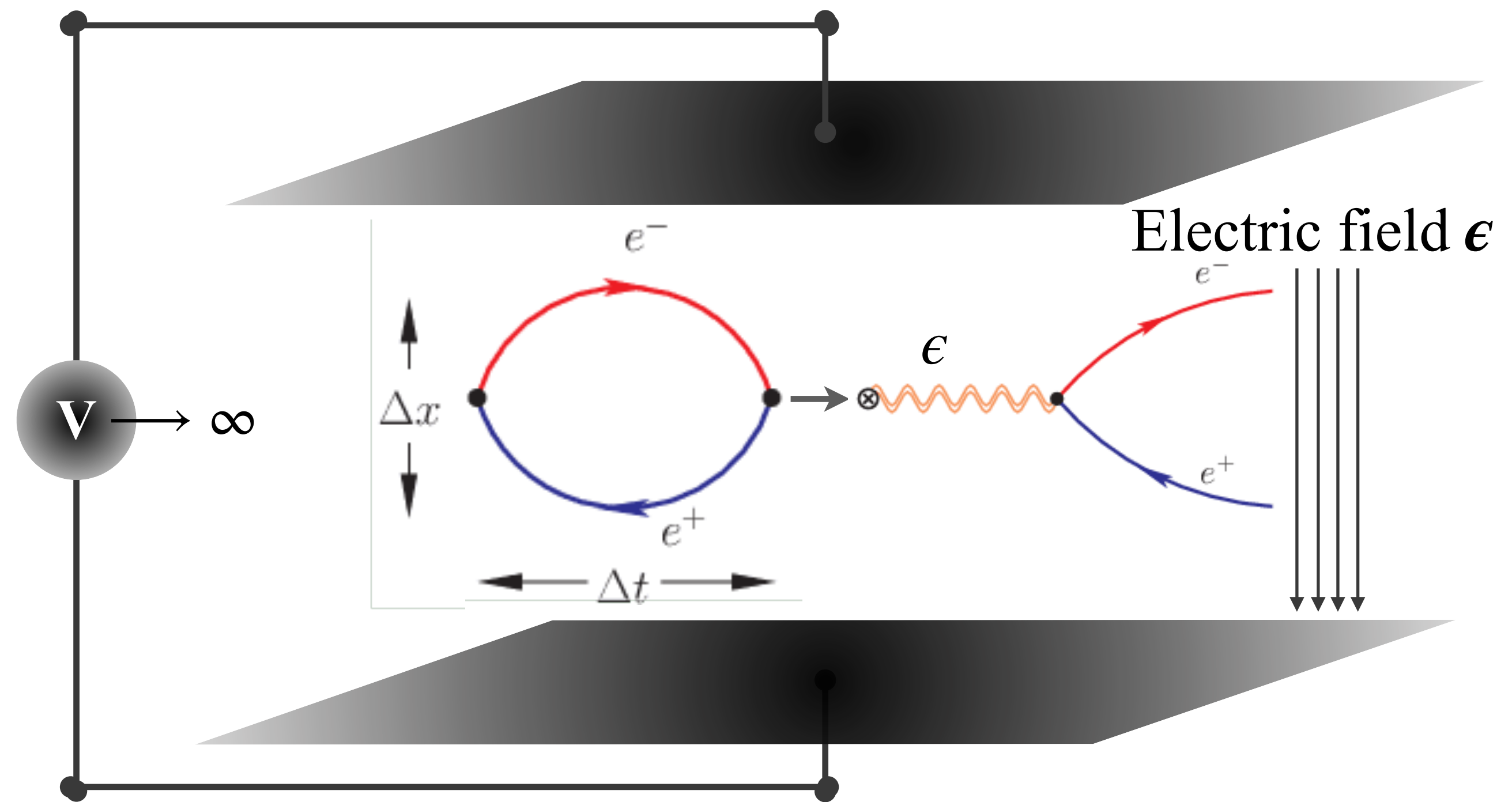
$$\epsilon_S = \frac{m_e^2 c^3}{e \hbar} \simeq 1.32 \cdot 10^{18} \frac{\text{V}}{\text{m}}$$



The probability to materialise one virtual e^+e^- pair from the vacuum

$$P \sim \exp\left(-a \frac{\epsilon_S}{\epsilon}\right) \quad \text{non-perturbative with } \epsilon \longrightarrow \epsilon_S$$

$a = \text{numeric const.}$



History & Impact

1930s — First discussions by Sauter, Heisenberg & Euler

1951 — First calculations by Schwinger: ϵ_S

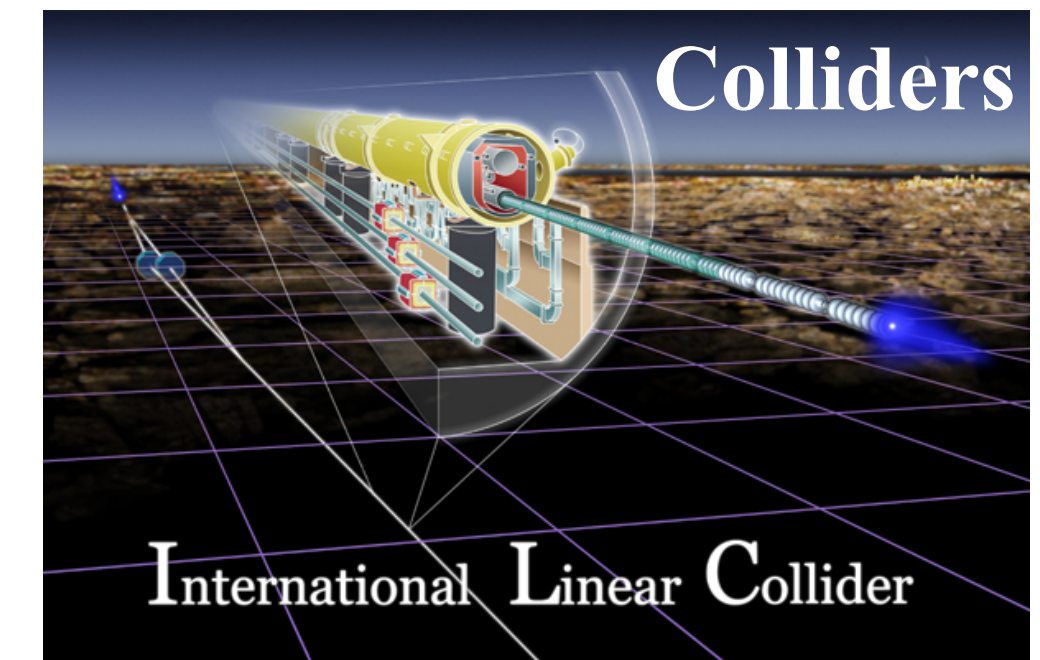
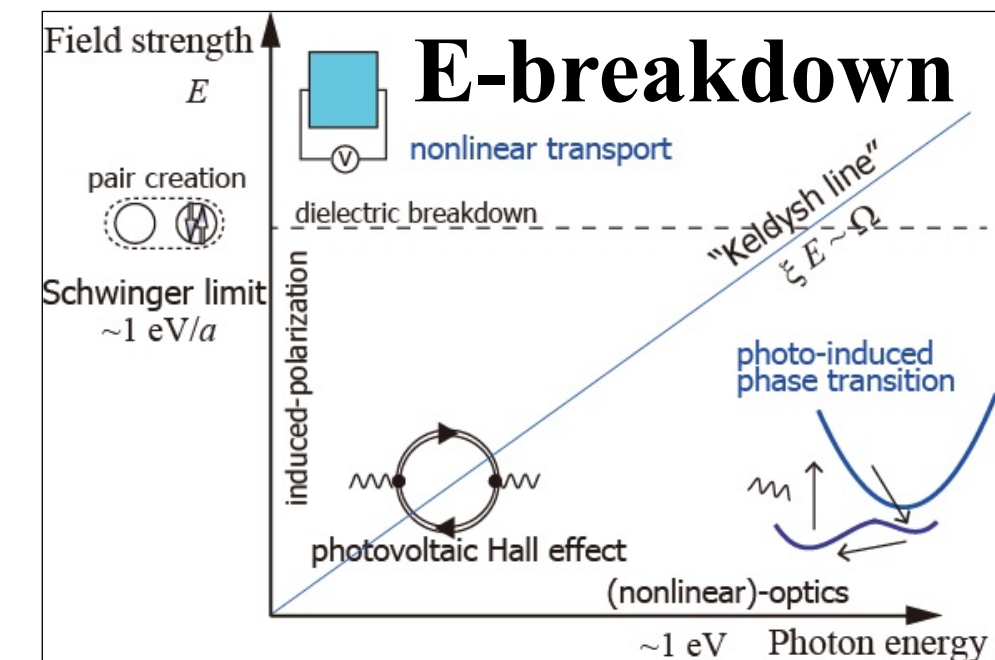
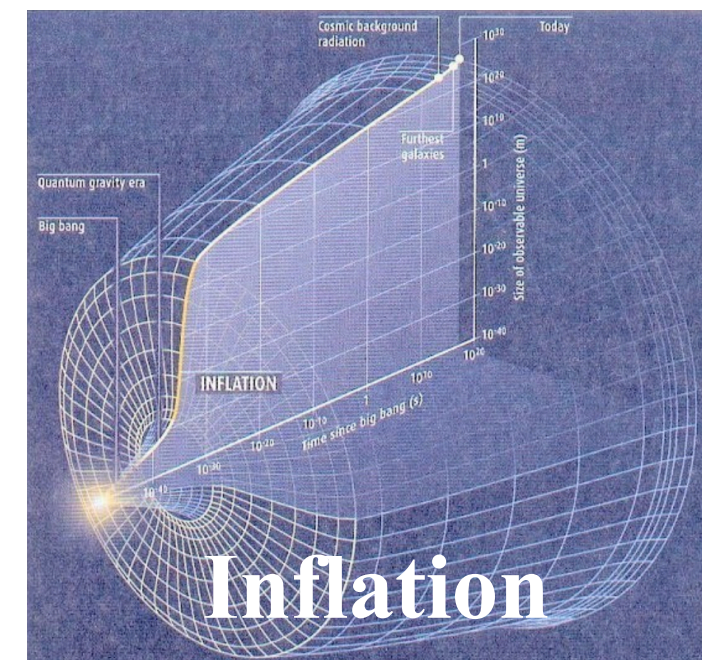
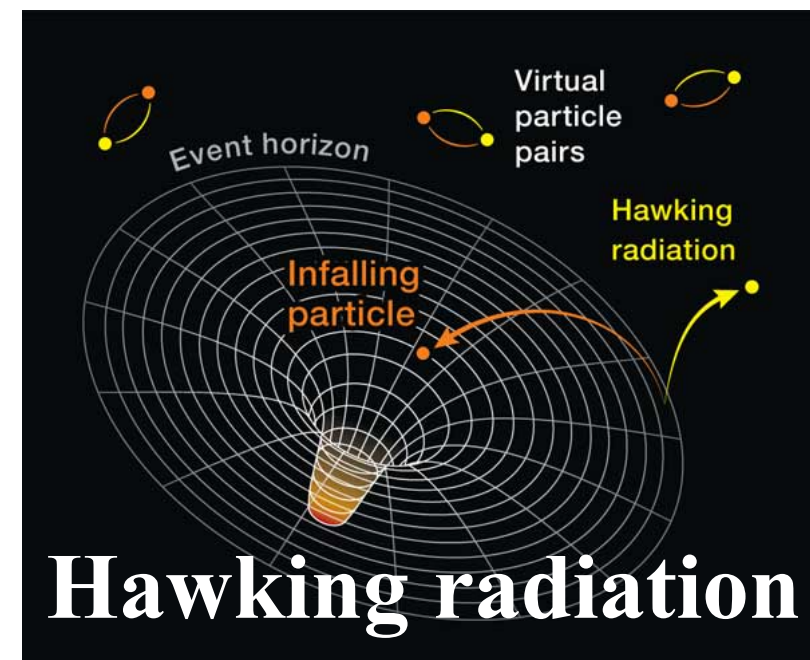
1990s — E144 at SLAC first to approach ϵ_S

2020s — LUXE: reach ϵ_S and go beyond!

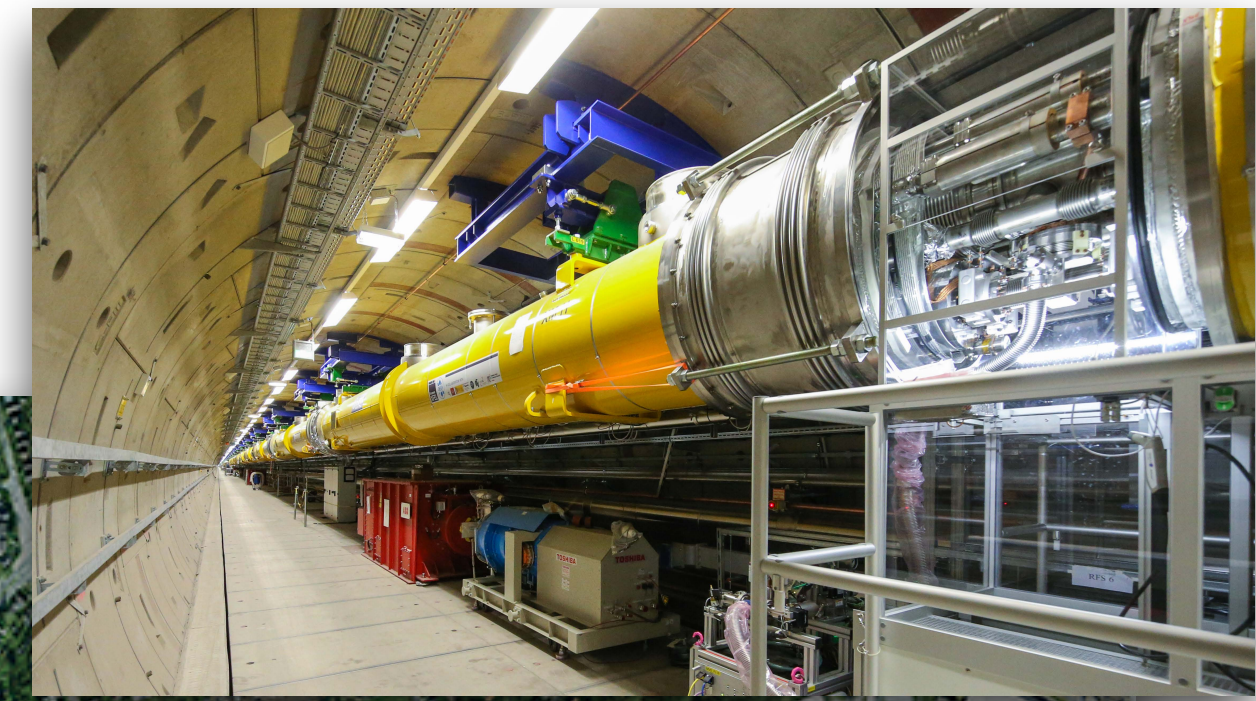
The Schwinger field may be approached/reached only in a highly-boosted system, e.g. the one produced at LUXE

- never been reached in a clean environment*
- test basic predictions in a novel QM regime
- relevant to many areas in physics

potential for seeing effects of new physics!



LUXE @ the Eu.XFEL



Conceptual Design Report for the LUXE Experiment

H. Abramowicz¹, U. Acosta^{2,3}, M. Altarelli⁴, R. Aßmann⁵, Z. Bai^{6,7}, T. Behne⁵, Y. Benhammou¹, T. Blackburn⁸, S. Boogert⁹, O. Borysov⁵, M. Borysova^{5,10}, R. Brinkmann⁵, M. Bruschi¹¹, F. Burkart⁵, K. Büßer⁵, N. Cavanagh¹², O. Davidi⁶, W. Decking⁵, U. Dosselli¹³, N. Elkina³, A. Fedotov¹⁴, M. Firlej¹⁵, T. Fiutowski¹⁵, K. Fleck¹², M. Gostkin¹⁶, C. Grojean¹⁵, J. Hallford^{5,17}, H. Harsh^{18,19}, A. Hartin¹⁷, B. Heinemann^{15,20}, T. Heinzl²¹, L. Helary⁵, M. Hoffmann^{5,20}, S. Huang¹, X. Huang^{5,15,20}, M. Idzik¹⁵, A. Ilderton²¹, R. Jacobs⁵, B. Kämpfer^{2,3}, B. King²¹, H. Lahno¹⁰, A. Levanon¹, A. Levy¹, I. Levy²², J. List⁵, W. Lohmann²⁵, T. Ma²³, A.J. Macleod²¹, V. Malka⁶, F. Meloni⁵, A. Mironov¹⁴, M. Morandin¹³, J. Moron¹⁵, E. Negodin⁵, G. Perez⁶, I. Pomerantz¹, R. Pöschl²⁴, R. Prasad⁵, F. Quéré²⁵, A. Ringwald⁵, C. Rödel²⁶, S. Rykovanov²⁷, F. Salgado^{18,19}, A. Santra⁶, G. Sarri¹², A. Sävert¹⁸, A. Sbrizzi²⁸, S. Schmitt⁵, U. Schramm^{2,3}, S. Schuwalow⁵, D. Seipt¹⁸, L. Shaimerdenova²⁹, M. Shchedrolosiev⁵, M. Skakunov²⁹, Y. Soreq²³, M. Streeter¹², K. Swientek¹⁵, N. Tal Hod⁶, S. Tang²¹, T. Teter^{18,19}, D. Thoden⁵, A.I. Titov¹⁶, O. Tolbanov²⁹, G. Torggrimsso³, A. Tyazhev²⁹, M. Wing^{5,17}, M. Zanetti¹³, A. Zarubin²⁹, K. Zeil³, M. Zepf^{18,19}, and A. Zhemchukov¹⁶

¹Tel Aviv University, Tel Aviv, 6997801, Israel
²TU Dresden, 01062 Dresden, Germany
³Helmholtz-Zentrum Dresden-Rossendorf, 01328 Dresden, Germany
⁴Max Planck Institute for Structure and Dynamics of Matter, 22761 Hamburg, Germany
⁵Deutsches Elektronen-Synchrotron (DESY), 22607 Hamburg, Germany
⁶Weizmann Institute of Science, Rehovot, 7610001, Israel
⁷Department of Physics, Southern University of Science and Technology, Shenzhen 518055, China
⁸Johns Hopkins Institute at Royal Holloway, Department of Physics, Royal Holloway, Egham, TW20 0EX, Surrey, UK
⁹Institute for Nuclear Research NASU (KINR), Kyiv, 03680, Ukraine
¹⁰INFN and University of Bologna, Bologna, Italy
¹¹INFN and University of Padova, Padova, Italy
¹²National Research Nuclear University MEPhI, Kashirskoe sh. 31, Moscow, 115409, Russia
¹³Suda Institute for Nuclear Research (SINR), Dubna 141980, Russia
¹⁴University College London, London, WC1E 6BT, UK
¹⁵Helmholtz-Institut Jena, 07743 Jena, Germany
¹⁶Albert-Ludwigs-Universität Freiburg, Freiburg, Germany
¹⁷University of Liverpool, Liverpool, UK
¹⁸CEA, CNRS, Université Paris-Saclay, CEA Saclay, 91191 Gif-sur-Yvette, France
¹⁹Institute of Nuclear Physics, TU Darmstadt, 64289 Darmstadt, Germany
²⁰Skolkovo Institute of Science and Technology (Skoltech), Moscow 121205, Russia
²¹INFN Trieste, Trieste, Italy
²²National Research Tomsk State University NI TSU, TSU, Russia

Accepted by European Physics Journal ST

Passed a detailed review process by an international committee of experts

Got the “Critical Decision 0” (CD0) approval from the DESY directorate



$$\epsilon_{\text{Laser}} \rightarrow \epsilon_{\text{Laser}} \times \frac{E_e \sim 10 \text{ GeV}}{m_e \sim 0.5 \text{ MeV}} \sim \epsilon_{\text{Laser}} \times 10^4$$

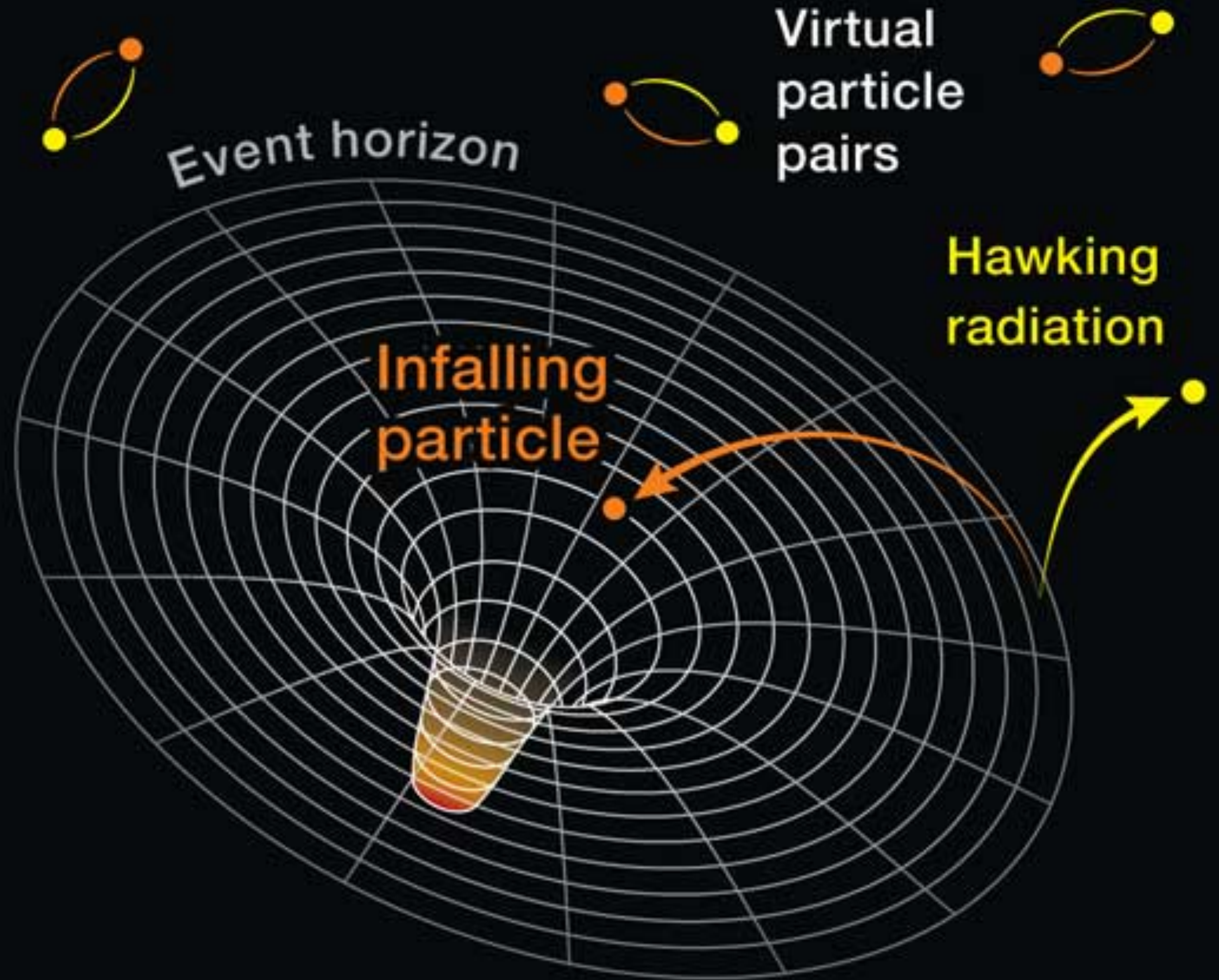
Electrons	E_e up to 16.5 GeV, with $N_e = 1.5 \times 10^9$ e-/bunch and a bunch charge up to 1.0 nC, 1/2700 bunches/train, $\sim 1+9$ Hz (collisions+background), spot $r_{xy}=5 \mu\text{m}$, $l_z=24 \mu\text{m}$
Laser	Ti-Sapphire, 800 nm, 40/350 TW, up to ~ 10 J, ~ 10 Hz repetition, 60% losses ~ 30 -200 fs pulse length, down to $3 \times 3 \mu\text{m}^2$ FWHM spot with up to $I \sim 10^{21}$ W/cm ²



LUXE

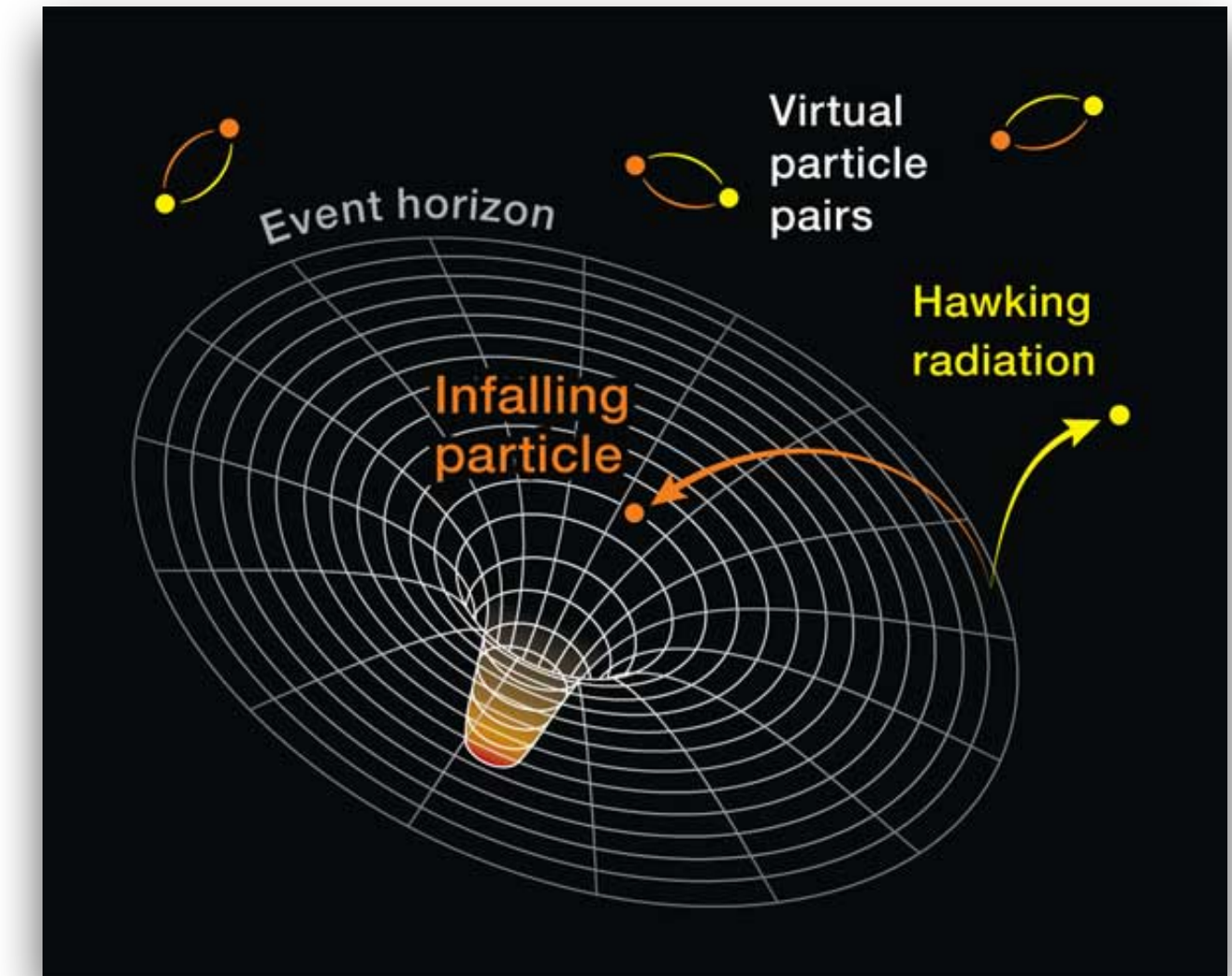
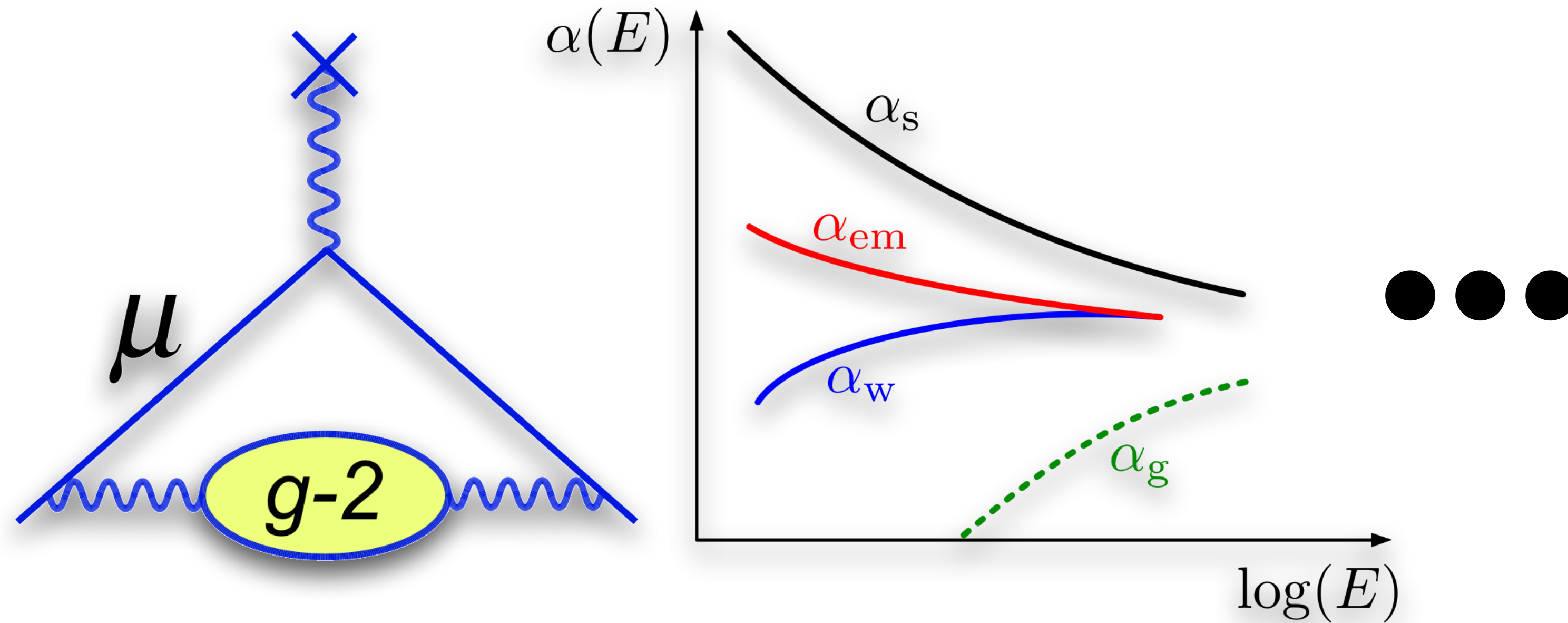
Install and start operation in 2024

The Hawking equivalent



- ◉ **Outside observer:** the BH has radiated a particle so the energy must come from it
- ◉ **Looking at the system:** the BH energy has decreased so its mass must decrease

Why strong field physics?



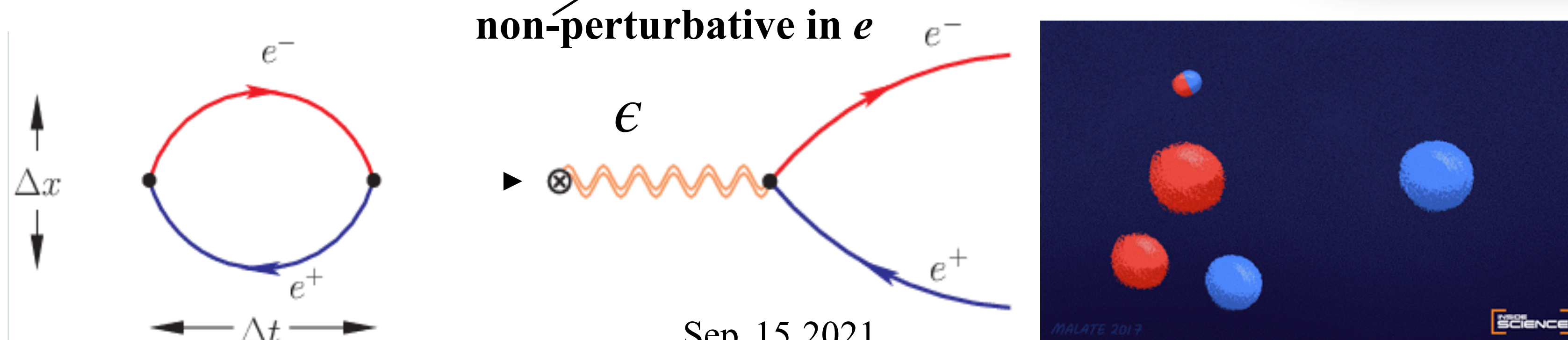
- Reaching ϵ_S is equivalent e.g. to the measurement of the anomalous magnetic moment or the coupling constant and deviations could be a hint for new physics
- Non-perturbative QFT is still being actively developed
- Can provide insight into the vacuum state / Higgs mechanism
- Schwinger effect proposed as mechanism for reheating in the early universe
- New physics opportunities with strong field (ALPs, mCPs,...)

The Schwinger mechanism simplified

- Force of external static electric field is: $F = e\epsilon$
- Energy to separate the virtual pair in a distance d : $E = F \cdot d = e\epsilon \cdot d$
- Energy required to materialise as a real pair: $E = 2m_e c^2$
- Condition to materialise as a real pair in distance d : $e\epsilon d = 2m_e c^2$
- Compton wavelength (typical scale): $\lambda_C = \hbar / (m_e c)$
- Probability for d :

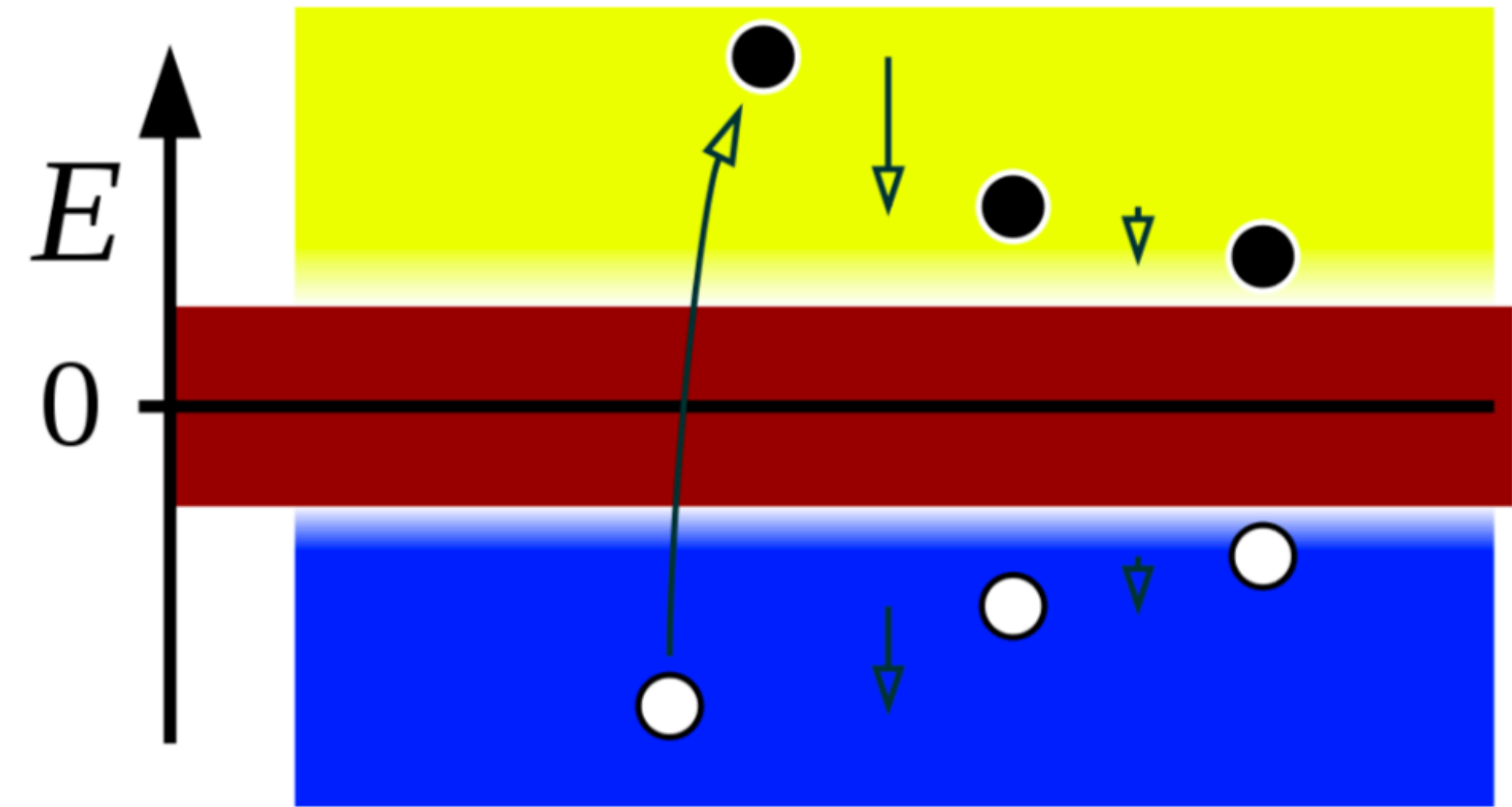
$$P \propto \exp\left(-\frac{d}{\lambda_C}\right) = \exp\left(-2 \frac{m_e^2 c^3}{\hbar e \epsilon}\right) = \exp\left(-2 \frac{\epsilon_S}{\epsilon}\right)$$

$$\epsilon_S = \frac{m_e^2 c^3}{\hbar e} \simeq 1.3 \cdot 10^{18} \frac{\text{V}}{\text{m}}$$



The Furry Picture vacuum

The 2nd quantisation of the Dirac field relies on a gap between the positive and negative energy solutions



- ◉ The external field “closes” this energy gap
- ◉ Electrons are lifted from the sea to leave the vacuum charged
- ◉ The VEV of the EM current must no longer vanish
- ◉ Separation into creation and destruction operators is problematic
- ◉ This point is the limit of the validity of the Furry picture

The Furry Picture

- If the external field is sufficiently strong: quantum interactions with it leave it essentially unchanged and it can be considered to be a classical background field

- Separate the gauge field to external and quantum parts:

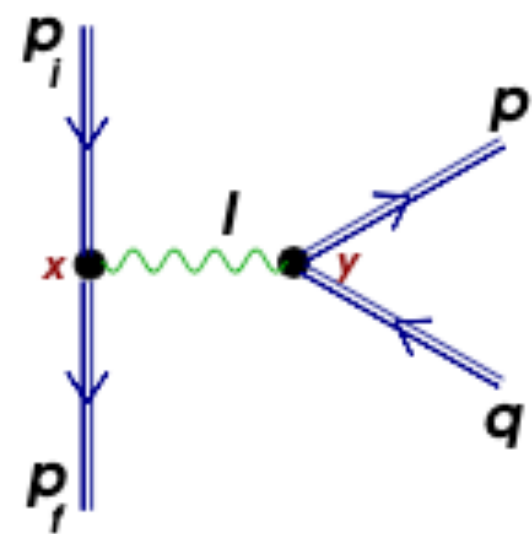
$$\mathcal{L}_{\text{Int}} = \bar{\psi}(i\partial - m)\psi - \frac{1}{4}F_{\mu\nu}^2 - e\bar{\psi}(\mathbf{A}_{\text{ext}} + \mathbf{A})\psi \text{ and shift } \mathbf{A}_{\text{ext}} \text{ to the Dirac component: } \mathcal{L}_{\text{FP}} = \bar{\psi}^{\text{FP}}(i\partial - e\mathbf{A}_{\text{ext}} - m)\psi^{\text{FP}} - \frac{1}{4}F_{\mu\nu}^2 - e\bar{\psi}^{\text{FP}}\mathbf{A}\psi^{\text{FP}}$$

- The FP Lagrangian satisfies the Euler-Lagrange equation.

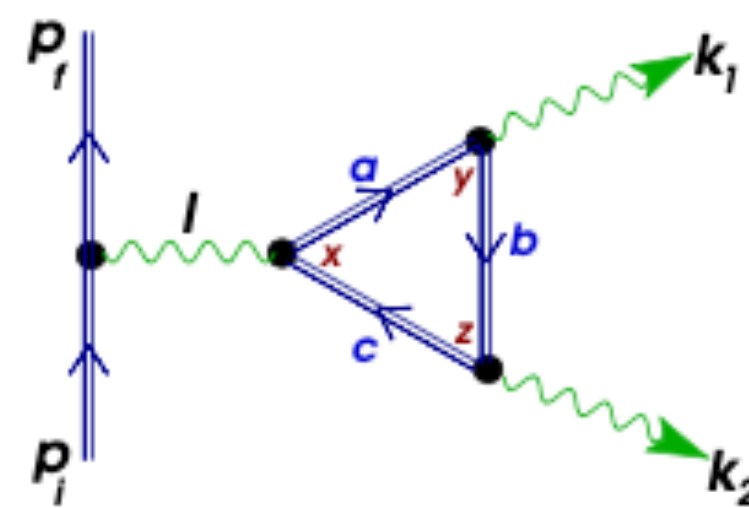
- New equation of motion for the non-perturbative (bound) Dirac field (wrt \mathbf{A}_{ext}) and new solutions ψ^{FP} : $(i\partial - e\mathbf{A}_{\text{ext}} - m)\psi^{\text{FP}} = 0$

- Exact solutions exist for a certain classes of external fields (plane waves, Coulomb fields and combinations) [Volkov Z Physik 94 250 (1935), Bagrov & Gitman 1990]:

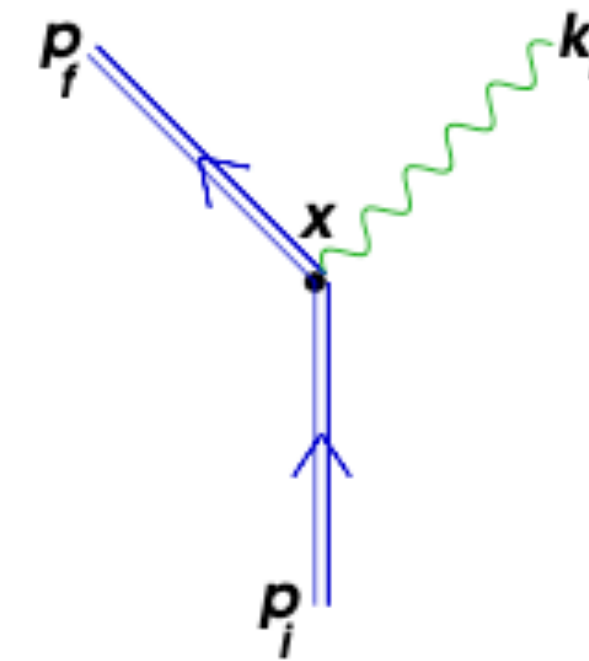
$$\psi^{\text{FP}} = \mathbf{E}_p e^{-ipx} u_p \text{ with } \mathbf{E}_p = \text{Exp} \left[-\frac{1}{2k \cdot p} (e\mathbf{A}_{\text{ext}} \not{k} + i2e(\mathbf{A}_{\text{ext}} \cdot p) - ie^2 \mathbf{A}_{\text{ext}}^2) \right]$$



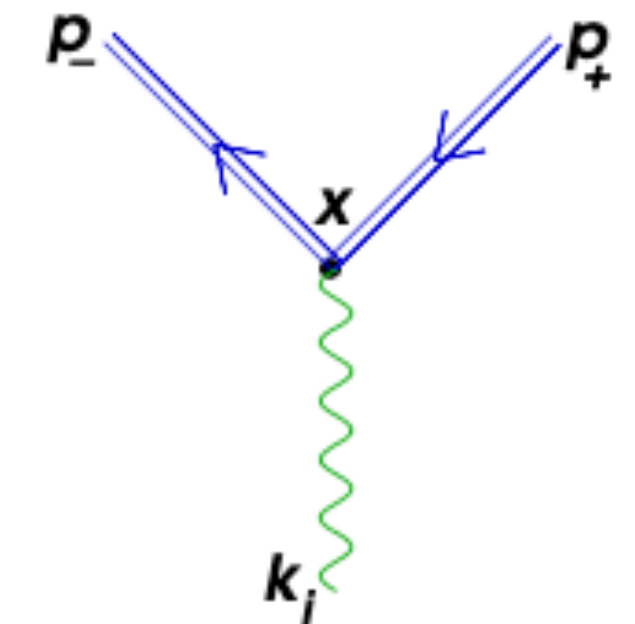
Trident process (vacuum resonance)



Photon splitting (vacuum birefringence)



High intensity Compton scatter (HICS)



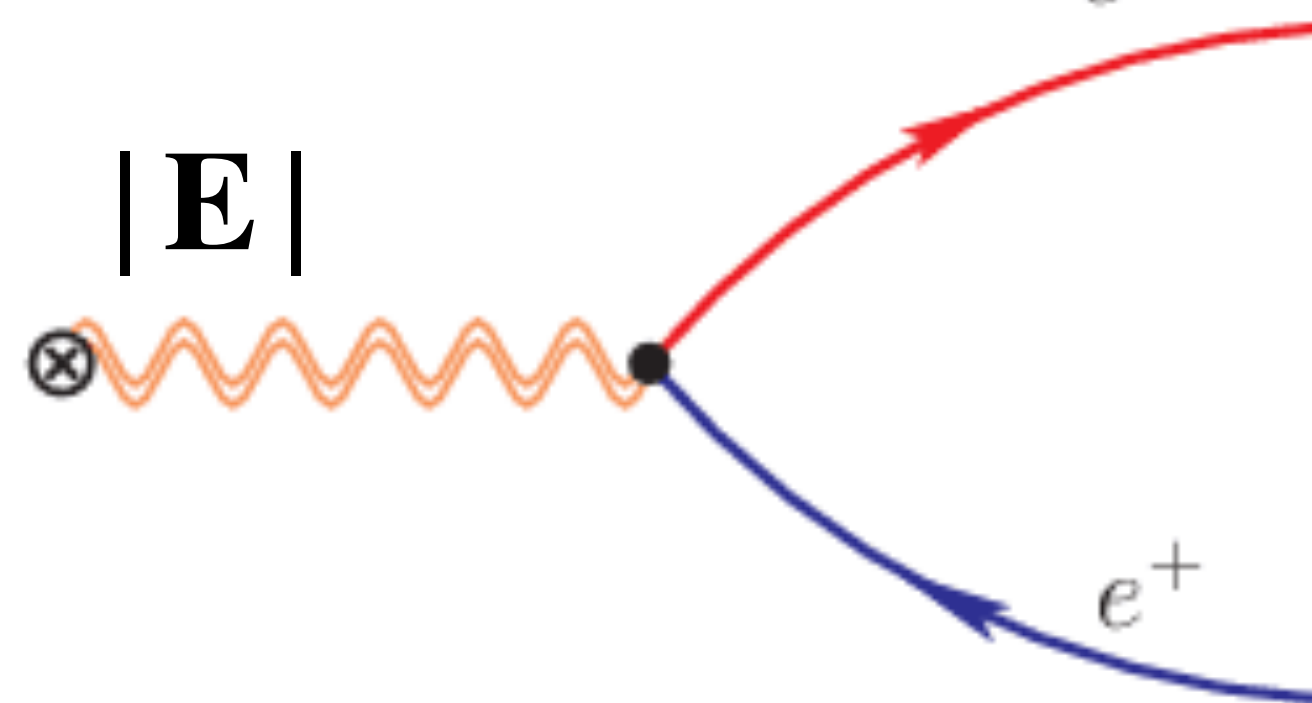
One photon pair production (OPPP)

Boiling point of QED

- **Weak fields:** many accurate predictions of observables through ordinary perturbative expansion in the EM coupling (α_{EM})
- **Strong fields:** observables become inaccessible through ordinary perturbative expansion and there's no experimental verification
- **For example:** the spontaneous e^+e^- pair production (SPP) rate per unit volume in strong static E-field is:

$$\frac{\Gamma_{\text{SPP}}}{V} = \frac{m_e^4}{(2\pi)^3} \left(\frac{|\mathbf{E}|}{E_c} \right)^2 \sum_{n=1}^{\infty} \frac{1}{n^2} e^{-n\pi \frac{E_c}{|\mathbf{E}|}} \sim e^{-\frac{\pi m_e^2}{e|\mathbf{E}|}}$$

non-perturbative in α



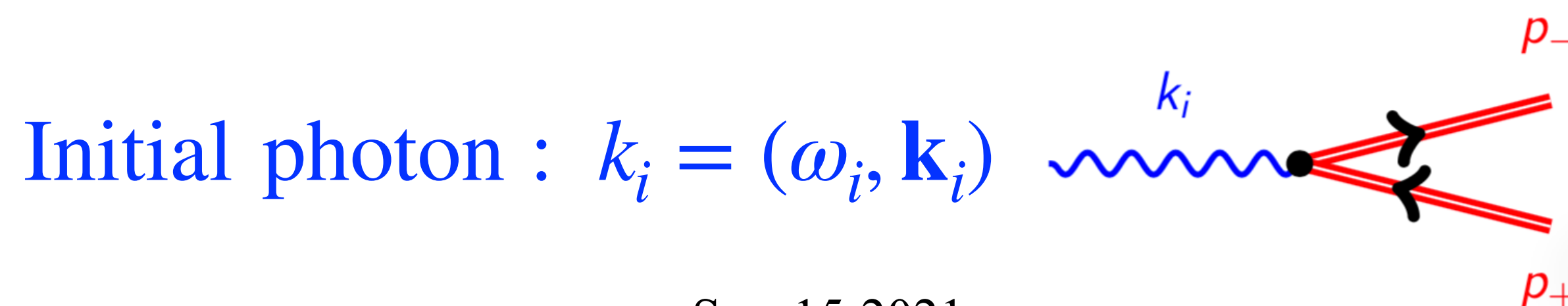
But how to produce static E-field of the order of $\sim 1.3 \times 10^{18}$ V/m ???

Lasers strong field “how-to”

- Laser-assisted one photon pair production, OPPP (SPP \rightarrow OPPP)
 - the laser’s E-field frequency is ω , with momentum $k = (\omega, \mathbf{k})$
 - the laser’s E-field strength is $|\epsilon|$, with $I \sim |\epsilon|^2$
 - The e^+e^- pair picks up momentum from the laser photons
- OPPP rate is a function of the laser intensity ξ and the photon recoil χ :

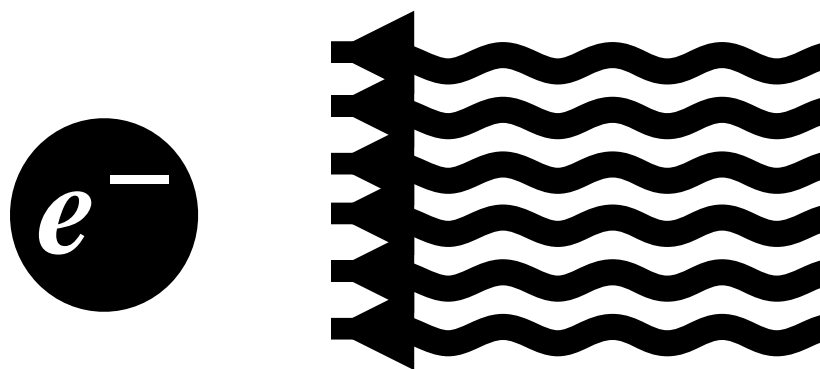
Dimensionless and Lorentz-invariant

$$\left\{ \begin{array}{l} \text{Laser intensity : } \xi = \frac{e |\epsilon|}{\omega m_e} = \frac{m_e |\epsilon|}{\omega \epsilon_S} \\ \text{Photon recoil : } \chi_\gamma = \frac{k \cdot k_i}{m_e^2} \xi = (1 + \cos \theta) \frac{\omega_i |\epsilon|}{m_e \epsilon_S} \end{array} \right.$$



$$\Gamma_{\text{OPPP}} = \frac{\alpha m_e^2}{4\omega_i} F(\xi, \chi_\gamma)$$

Understanding ξ

Electron “at rest”  Infinite E-field plane wave with frequency ω

The electron will oscillate with frequency ω and radiate in turn: $eE = m_e a$

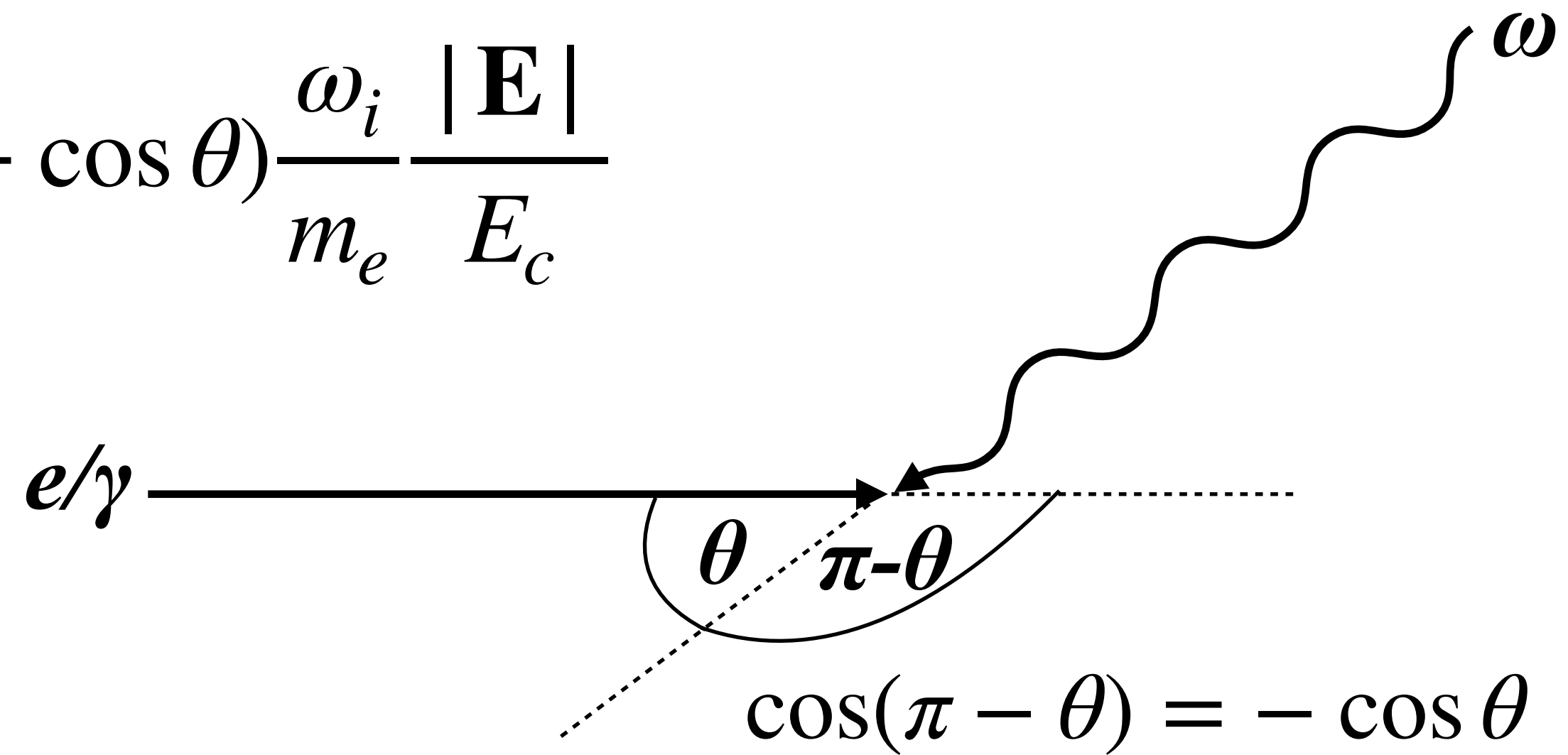
The electron’s maximum velocity is: $v_{\max} = a \cdot \Delta t = \frac{eE}{m_e} \cdot \frac{1}{\omega}$

Normalise to c : $\xi \equiv \frac{v_{\max}}{c} = \frac{eE}{\omega m_e c}$ (dimensionless & Lorentz-invariant)

ξ reaches unity for e.g. a $\lambda = 800$ nm laser at an intensity of $I \sim 10^{18}$ W/cm²

Understanding χ

Recoil parameter: $\chi = \frac{k \cdot k_i}{m_e^2} \xi = (1 + \cos \theta) \frac{\omega_i}{m_e} \frac{|\mathbf{E}|}{E_c}$



Scattering geometry: $k \cdot k_i = \omega\omega_i - |\mathbf{k}| |\mathbf{k}_i| \cos(\pi - \theta) = \omega\omega_i (1 + \cos \theta)$

$$\chi = \frac{k \cdot k_i}{m_e^2} \xi = \frac{\omega\omega_i (1 + \cos \theta)}{m_e^2} \frac{e\epsilon}{\omega m_e c} = (1 + \cos \theta) \frac{\omega_i}{m_e} \frac{\epsilon}{\epsilon_S}$$

$\frac{1}{\epsilon_S} = \frac{e}{m_e^2}$

←

$\hbar = c = 1$

OPPP rate: $\Gamma_{\text{OPPP}} \propto F(\xi, \chi_\gamma)$

Sum on number of absorbed laser γ 's

J_n are Bessel functions

$$F_\gamma(\xi, \chi_\gamma) = \sum_{n > n_0}^{\infty} \int_1^{v_n} \frac{dv}{v \sqrt{v(v-1)}} \left[2 J_n^2(z_v) + \xi^2 (2v-1) (J_{n+1}^2(z_v) + J_{n-1}^2(z_v) - 2J_n^2(z_v)) \right]$$

threshold number of absorbed γ 's

$$n_0 \equiv \frac{2\xi(1+\xi^2)}{\chi_\gamma}, \quad z_v \equiv \frac{4\xi^2 \sqrt{1+\xi^2}}{\chi_\gamma} [v(v_n - v)]^{1/2}, \quad v_n \equiv \frac{\chi_\gamma n}{2\xi(1+\xi^2)}$$

As the laser intensity ξ increases

- the threshold number of absorbed photons increases
- more terms in the summation drop out of the probability

Assumption 1: the laser E-field is a circularly polarised infinite plane wave

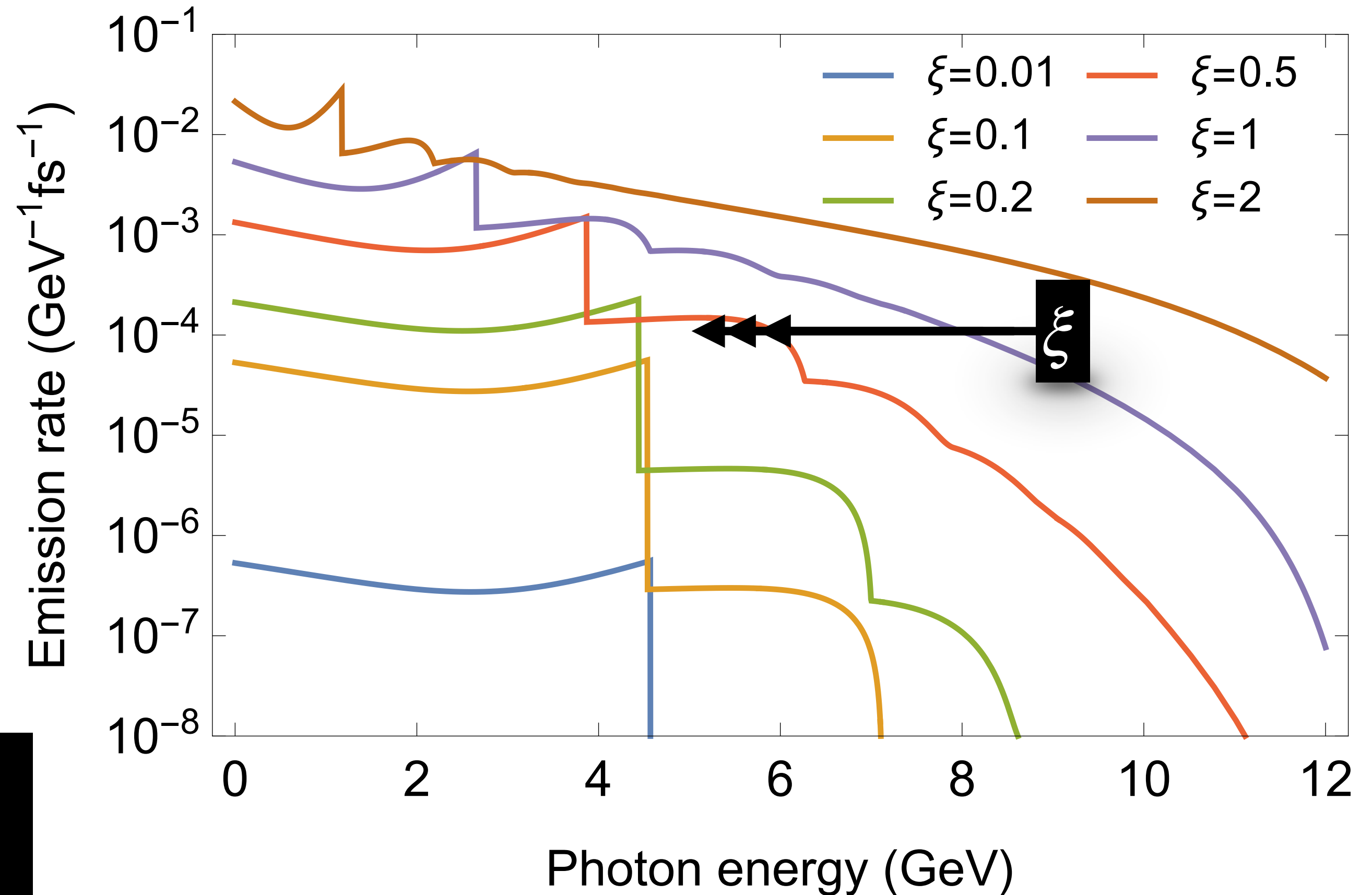
Assumption 2: we can produce a mono-energetic photon beam with $\sim O(10 \text{ GeV})$

Compton edges

- With increasing laser intensity ξ :
- higher order (n) contributions become more prominent
- edge shifts to lower energies due to electron's higher effective mass
- Cannot go much beyond $\xi \sim 1$ to produce high energy photons

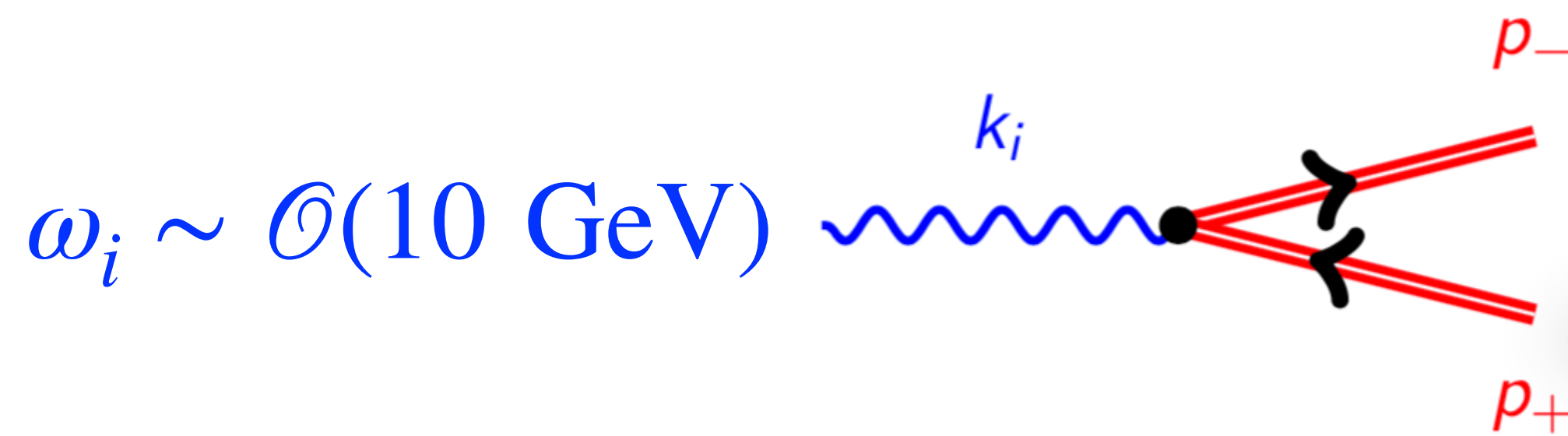
The rate is a series of Compton edges for $n=1,2,3,\dots$ absorbed photons and the edges shift down with increasing ξ

16.5 GeV electron, 800 nm laser, 17.2° crossing angle



Γ_{OPPP} asymptotically

$$\Gamma_{\text{OPPP}} \rightarrow \frac{3}{16} \sqrt{\frac{3}{2}} \alpha m_e (1 + \cos \theta) \frac{|\epsilon|}{\epsilon_S} \exp \left(-\frac{8}{3} \frac{1}{1 + \cos \theta} \frac{m_e \epsilon_S}{\omega_i |\epsilon|} \right)$$

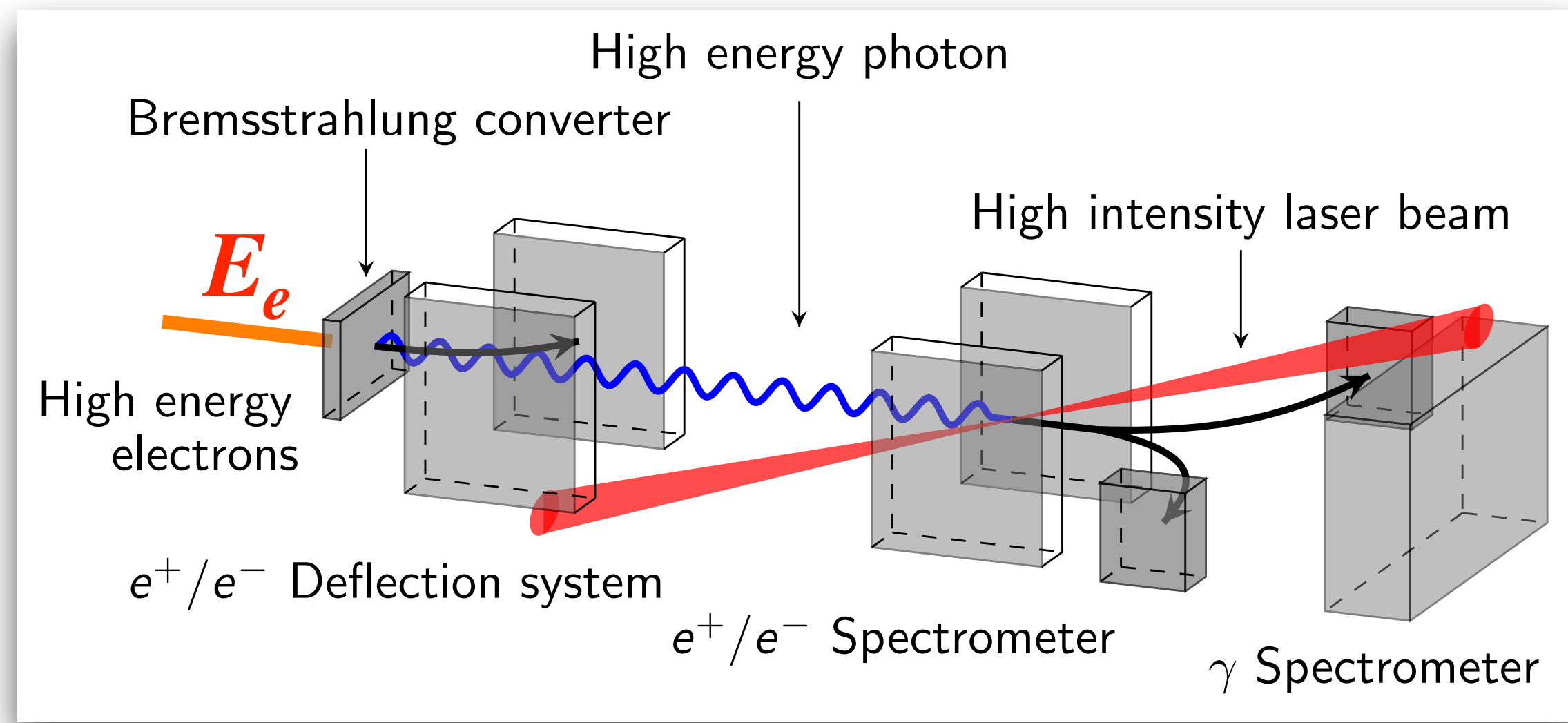


e^+e^- pair is boosted and the E-field is enhanced

- Unlike SPP, the e^+e^- pair (in its rest frame) experiences an E-field enhanced by the relativistic boost factor: $|\epsilon| \rightarrow |\epsilon| \times \omega_i/m_e$
- However, mono-energetic photon beams with energies in the $\omega_i \sim \mathcal{O}(10 \text{ GeV})$ range are not available...

High-energy photons?

- An $\sim \mathcal{O}(10 \text{ GeV})$ electron beam can be sent onto a high-Z target
- Converted into a collimated high-energy γ -beam (Bremsstrahlung)
- These photons are crossed with the high-intensity laser beam
- Laser-assisted bremsstrahlung photon pair production (BPPP)



E_e is the energy of the incident electrons

$$\text{Recall : } \Gamma_{\text{OPPP}} = \frac{\alpha m_e^2}{4\omega_i} F(\xi, \chi_\gamma(\omega_i))$$

$$\Gamma_{\text{BPPP}} = \frac{\alpha m_e^2}{4} \int_0^{E_e} \frac{d\omega_i}{\omega_i} \frac{dN_\gamma}{d\omega_i} F_\gamma(\xi, \chi_\gamma(\omega_i))$$

Bremsstrahlung "PDF"

Asymptotically

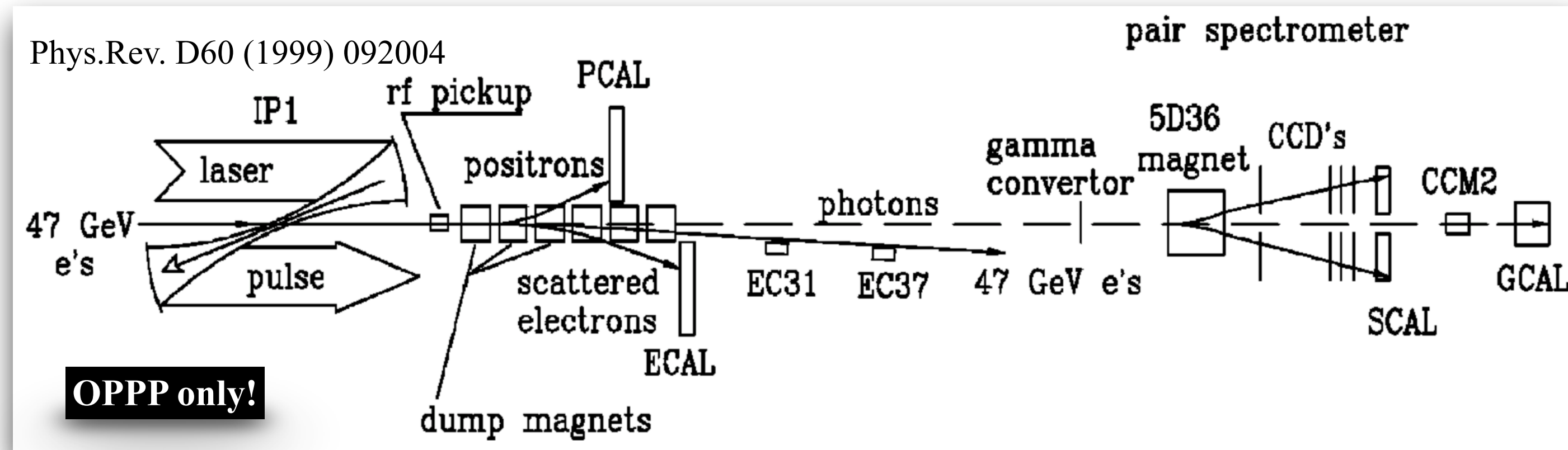
- For a target of thickness $X \ll X_0$, where X_0 is the radiation length:

$$\omega_i \frac{dN_\gamma}{d\omega_i} \approx \left[\frac{4}{3} - \frac{4}{3} \left(\frac{\omega_i}{E_e} \right) + \left(\frac{\omega_i}{E_e} \right)^2 \right] \frac{X}{X_0}$$

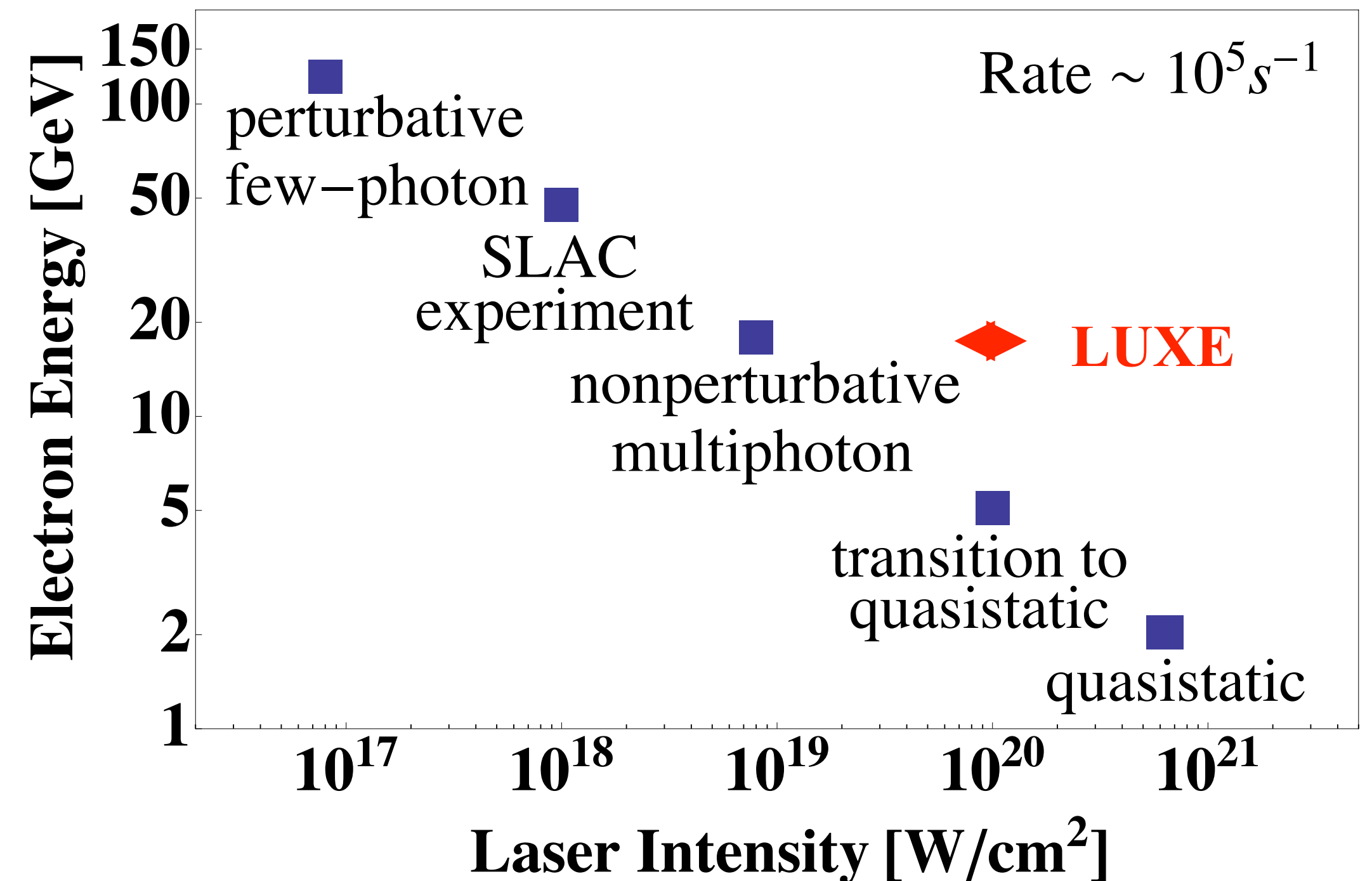
- Similarly to OPPP, replacing χ_γ with χ_e , the BPPP rate is:

$$\Gamma_{\text{BPPP}} \longrightarrow \frac{\alpha m_e^2}{E_e} \frac{9}{128} \sqrt{\frac{3}{2}} \frac{X}{X_0} \chi_e^2 e^{-\frac{8}{3\chi_e} \left(1 - \frac{1}{15\xi^2} \right)}$$

History: E144 @ SLAC



- 46.6 GeV electron beam
- 5×10^9 electrons per bunch
- Bunch rates up to 30 Hz
- Terawatt laser pulses
- Intensity of $\sim 0.5 \times 10^{18}$ W/cm²
- Frequency of 0.5 Hz for wavelengths 1053 nm, 527 nm
- electrons-laser crossing angle: 17°



History: E144 @ SLAC

OPPP only!

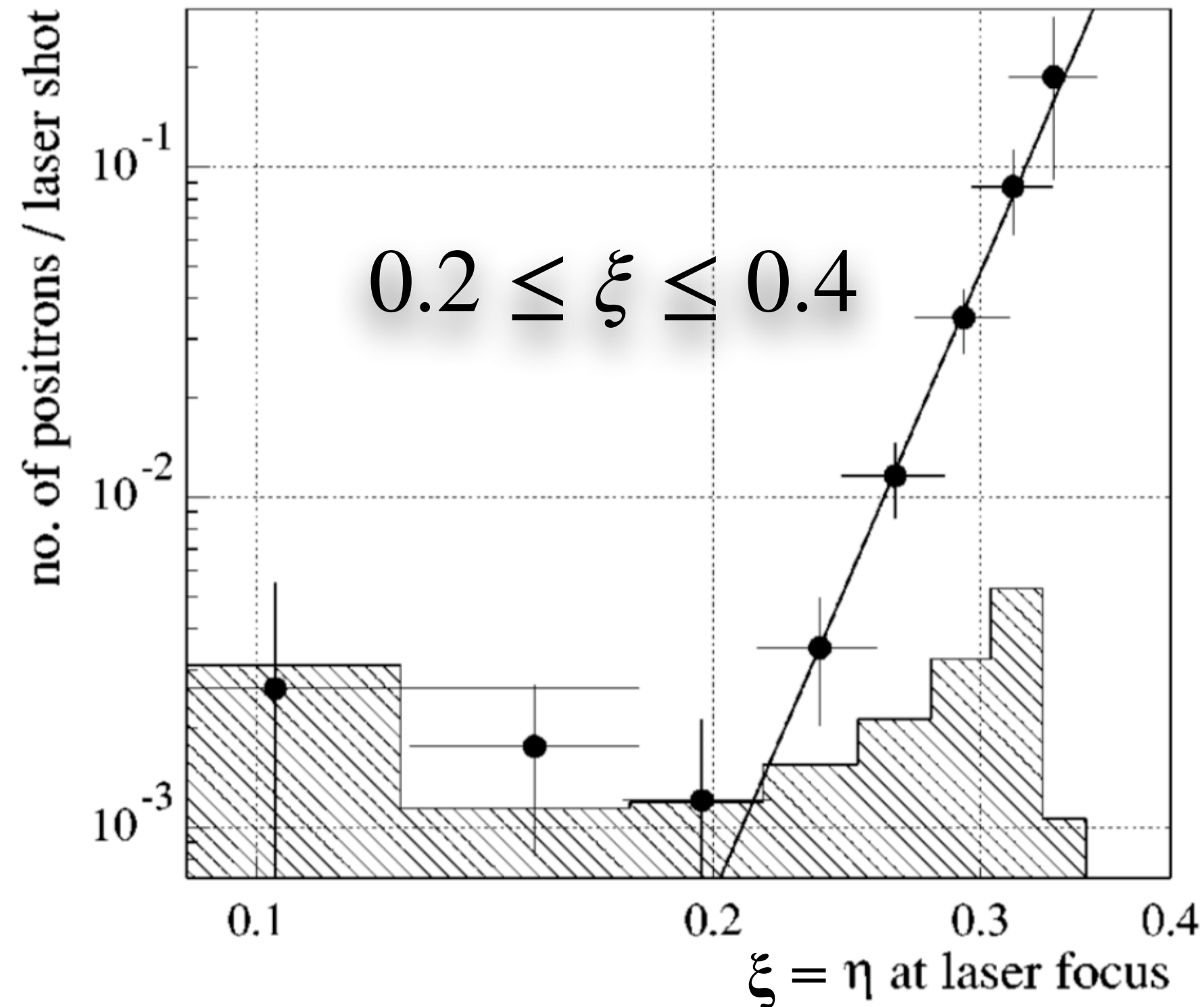


FIG. 44. The dependence of the positron rate per laser shot on the laser field-strength parameter η . The line shows a power law fit to the data. The shaded distribution is the 95% confidence limit on the residual background from showers of lost beam particles after subtracting the laser-off positron rate.

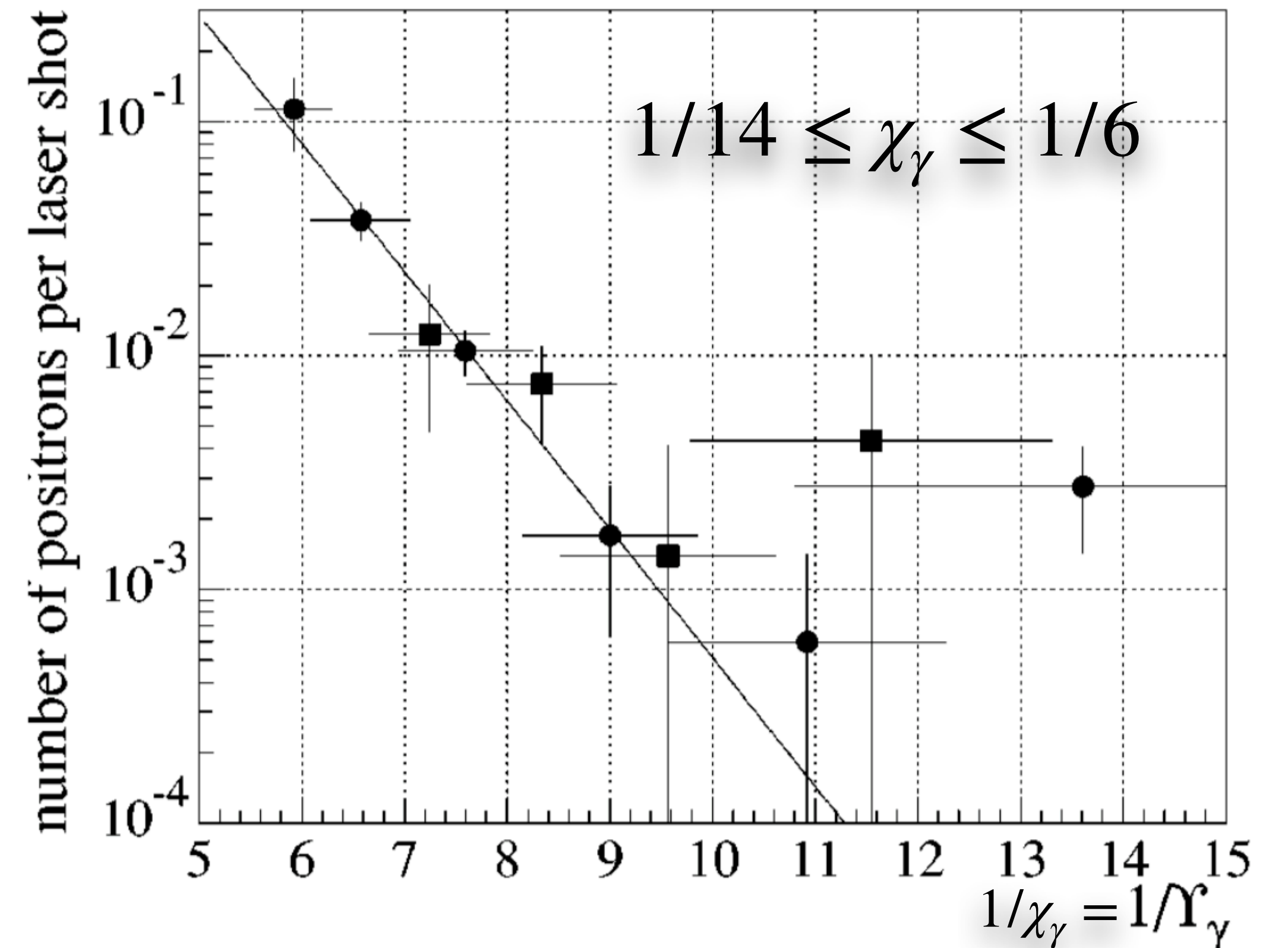


FIG. 49. Number of positrons per laser shot as a function of $1/\Upsilon_\gamma$. The circles are the 46.6 GeV data whereas the squares are the 49.1 GeV data. The solid line is a fit to the data.

Phys.Rev. D60 (1999) 092004

Sep 15 2021

History: E144 @ SLAC

- ◉ Measured non-linear Compton scattering with $n = 4$ photons absorbed and pair production (with $n = 5$)
- ◉ Observed the strong rise $\sim \xi^{2n}$ but not asymptotic limit (still perturbative)
- ◉ Measurement well described by theory
- ◉ Large uncertainty on the laser intensity
- ◉ Did not achieve the critical field - the peak E-field of the laser: 0.5×10^{18} V/m

Mass shift

- Electron motion in a circularly polarised field, ϵ_L , with frequency ω_L :

- Force: $F_{\perp} = e\epsilon_L = m_e a = m_e v^2/R \implies R = m_e v^2/e\epsilon_L$

- Velocity: $v = \omega_L R = \omega_L m_e v^2/e\epsilon_L \implies v = e\epsilon_L/\omega_L m_e = \xi$

- Momentum: $p_{\perp} = m_e v = m_e \xi$

- Energy: $E = m_e^2 + \vec{p}^2 = m_e^2 + p_{\perp}^2 + p_{\parallel}^2 = m_e^2 (1 + \xi^2) + p_{\parallel}^2 = \bar{m}_e^2 + p_{\parallel}^2$

- Mass shift:

$$m_e \longrightarrow \bar{m}_e = m_e \sqrt{1 + \xi^2}$$

- The 4-momentum of the electron inside an EM wave is altered due to continuous absorption and emission of photons

- the laser photon 4-momentum is: k_{μ}

- outside the field, the (free) charged particle 4-momentum is: p_{μ}

- inside the field, the effective 4-momentum (q_{μ}) and mass are:

$$q_{\mu} = p_{\mu} + \frac{\xi^2 m_e^2}{2(k \cdot p)} k_{\mu} \implies \bar{m}_e = \sqrt{q_{\mu} q^{\mu}} = m_e \sqrt{1 + \xi^2}$$

Mass shift \longrightarrow kinematic edge

- ◉ if n is the number of absorbed laser photons in the nonlinear Compton process, the energy-momentum conservation: $q_\mu + nk_\mu = q'_\mu + k'_\mu$

- ◉ The maximum value for the scattered photon energy, ω' , corresponds to the minimum energy, or, “kinematic edge” of the scattered electron. It depends on the number of absorbed laser photons:

$$\omega'_{\min} = \frac{\omega}{1 + 2n(k \cdot p)/\bar{m}_e^2}, \text{ where } \bar{m}_e = m_e \sqrt{1 + \xi^2}$$

- ◉ This energy decreases with increasing number of photons absorbed
- ◉ The electron is effectively getting more massive with ξ and recoils less
 - ◉ the min energy of the scattered electron (kinematic edge) is higher

Electric field vs Intensity

$$I = (1 - f_{\text{Losses}}) \times \frac{E_{\text{pulse}}}{T_{\text{pulse}} \times S_{\text{pulse}}} \rightarrow \frac{(1 - 60\%) \times 9 \text{ [J]}}{30 \text{ [fs]} \times (3 \times 3 \text{ [\mu m}^2\text{)])}}$$

$$I = 0.4/30 \text{ [J/fs/\mu m}^2\text{]} \sim 1.33 \times 10^{-2} \times 10^{15} \times 10^8 \text{ [J/s/cm}^2\text{]}$$

$$I = 1.33 \times 10^{21} \text{ [J/s/cm}^2\text{]} = 1.33 \times 10^{21} \text{ [W/cm}^2\text{]}$$

$$\epsilon_L = \sqrt{\frac{I}{cn\epsilon_0}} \xrightarrow[n=1]{\sim} \sqrt{\frac{1.33 \times 10^{21}}{(2.99 \times 10^8) \times (8.85 \times 10^{-12})}} \left[\sqrt{\frac{(\text{N} \cdot \text{m/s})/\text{cm}^2}{(\text{m/s}) \times (\text{N/V}^2)}} \right] \sim 0.71 \times 10^{12} \text{ [V/cm]}$$

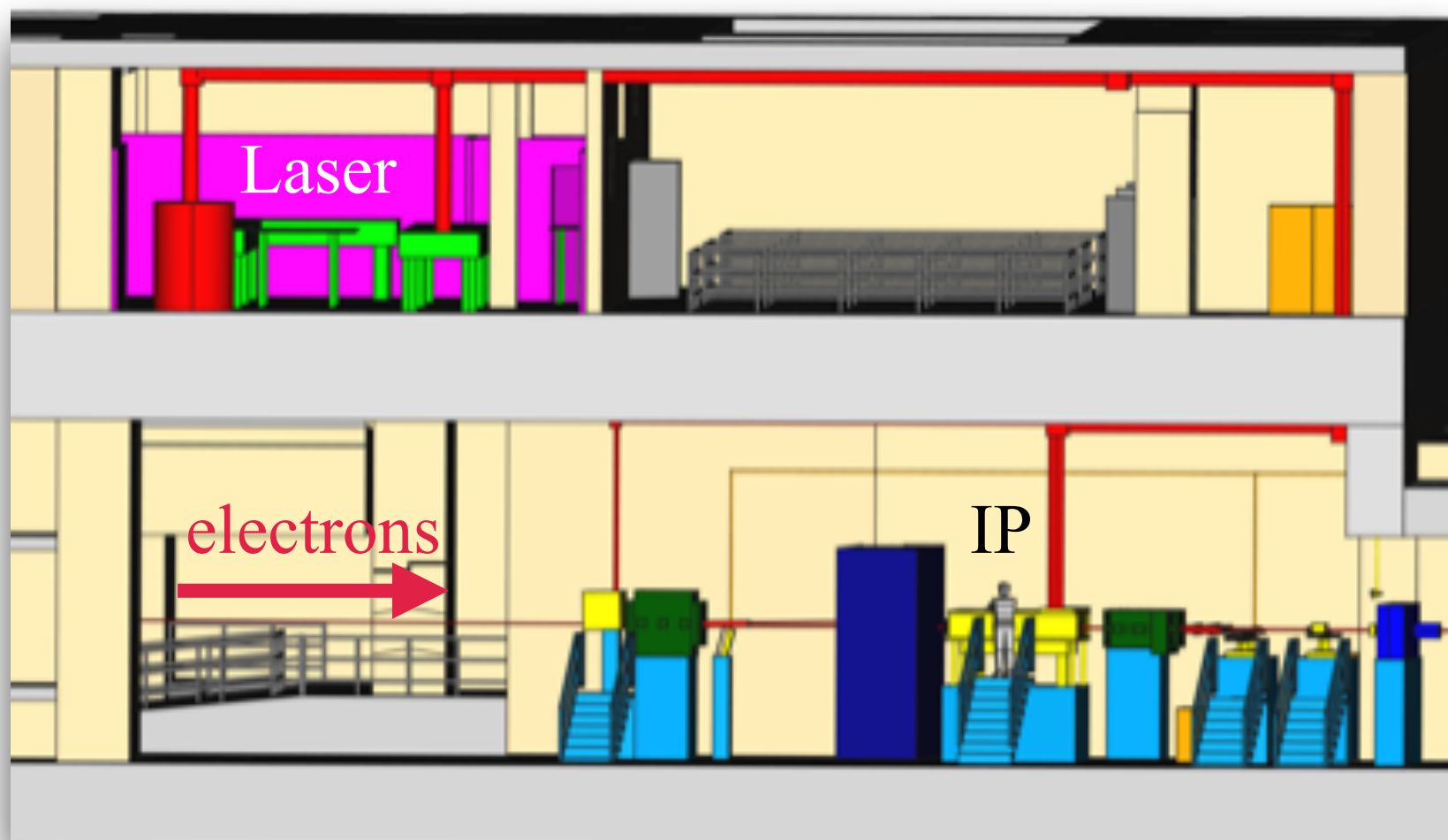
Boost : $\epsilon_L \rightarrow \epsilon'_L = \epsilon_L \times (3.23 \times 10^4) \sim 2.3 \times 10^{16} \text{ [V/cm]} = 1.77 \times \epsilon_{\text{Schwinger}}$

$$\epsilon_{\text{Schwinger}} \sim 1.3 \times 10^{16} \text{ [V/cm]}$$

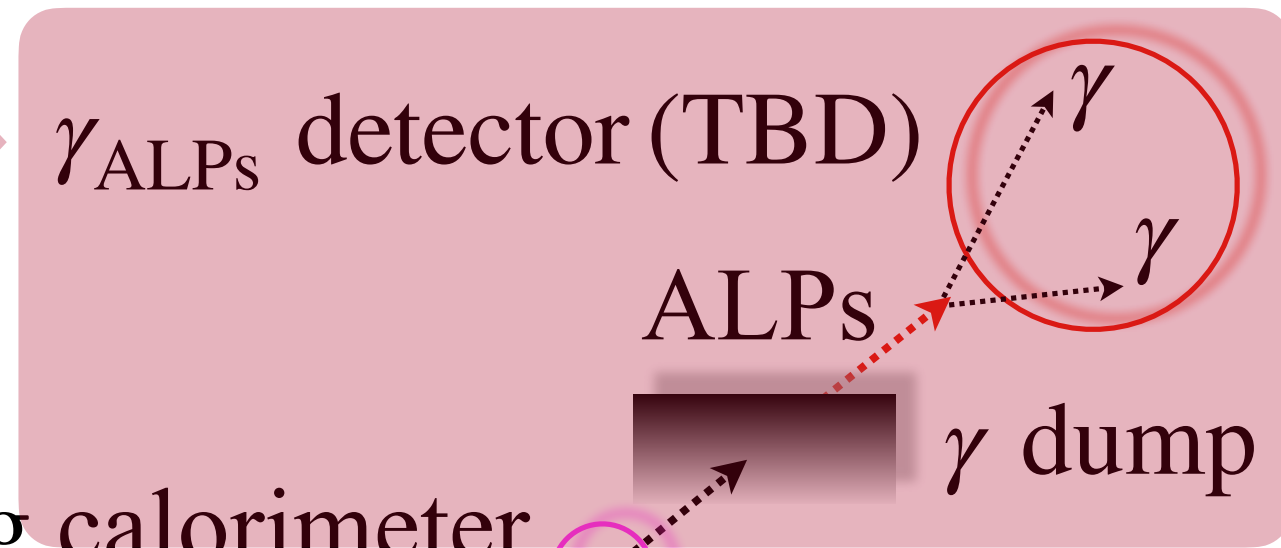
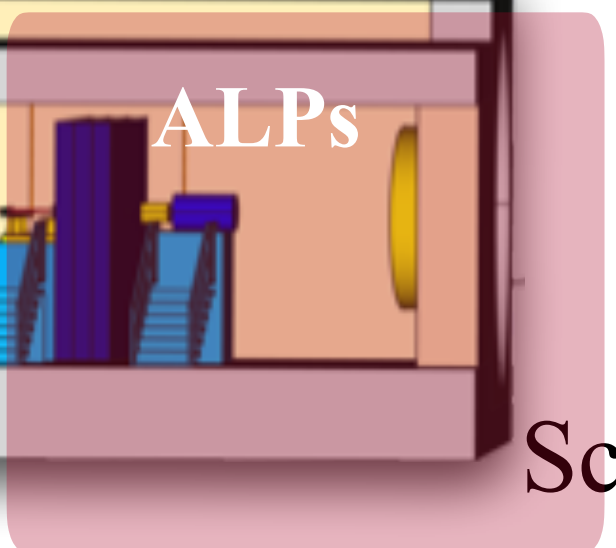
$$c = 2.99 \times 10^8 \text{ [m/s]}$$

$$\epsilon_0 = 8.85 \times 10^{-12} \text{ [N/V}^2\text{]}$$

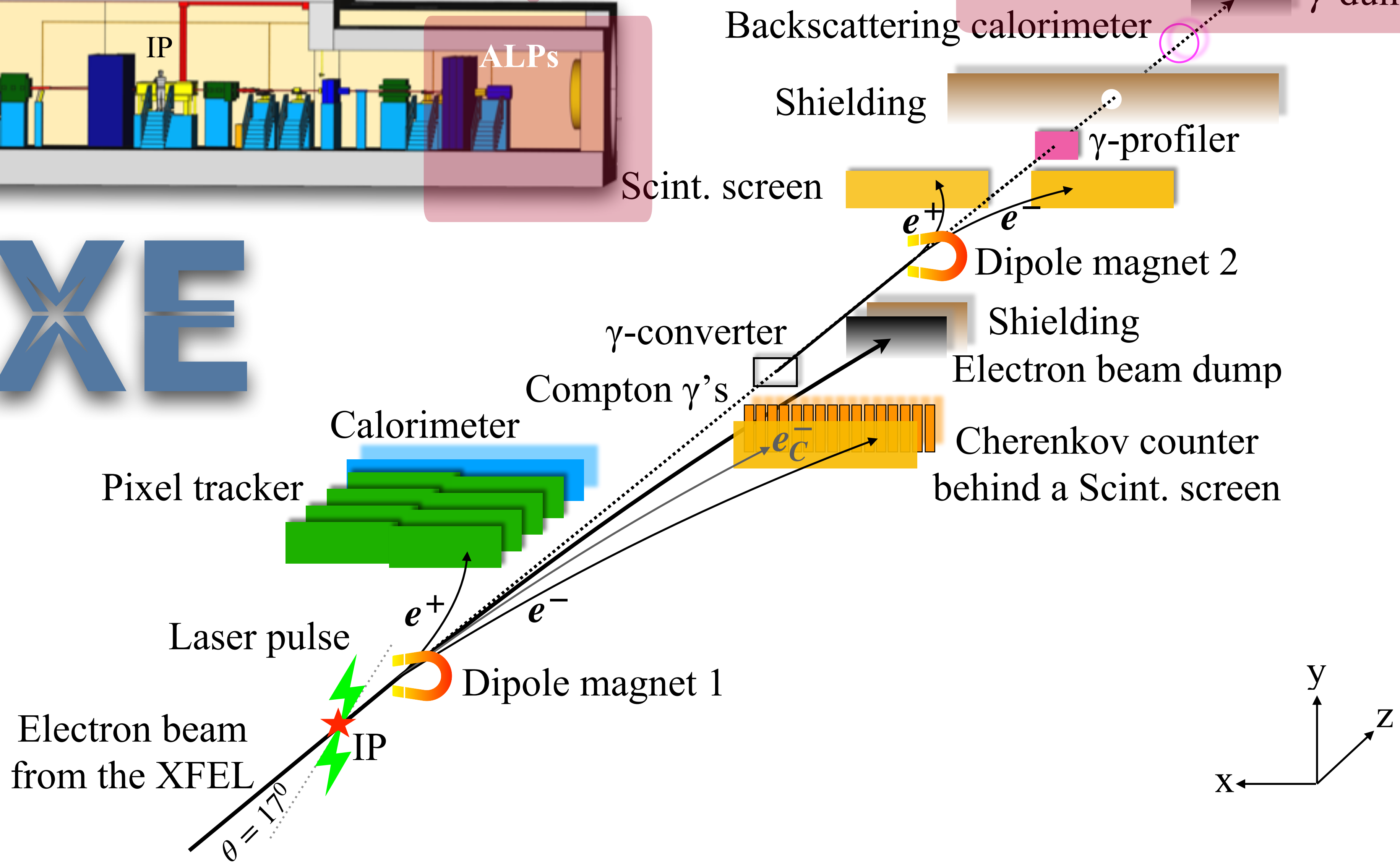
$$[I] = [\text{W}] = [\text{N} \cdot \text{m/s}]$$



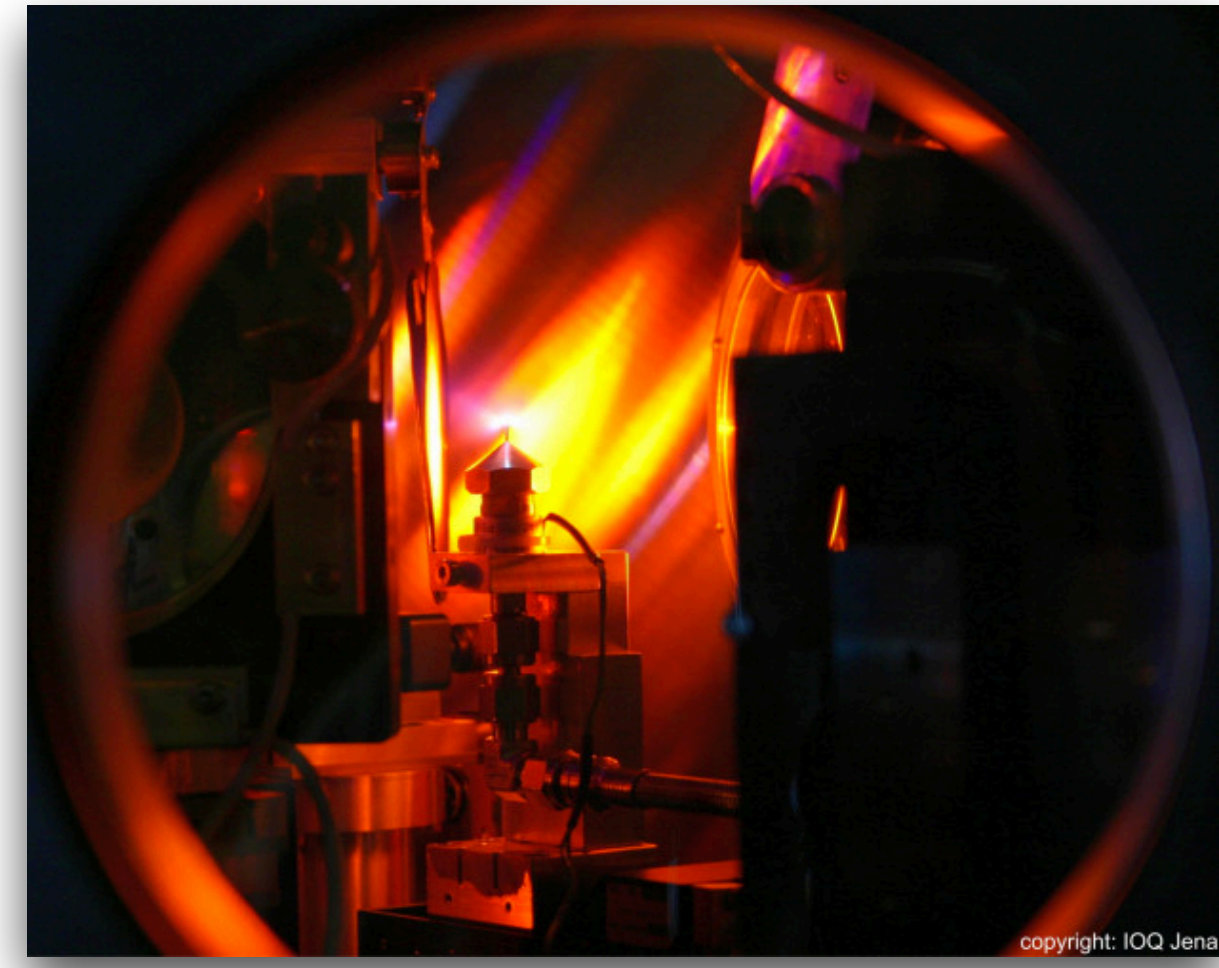
Today's talk focus



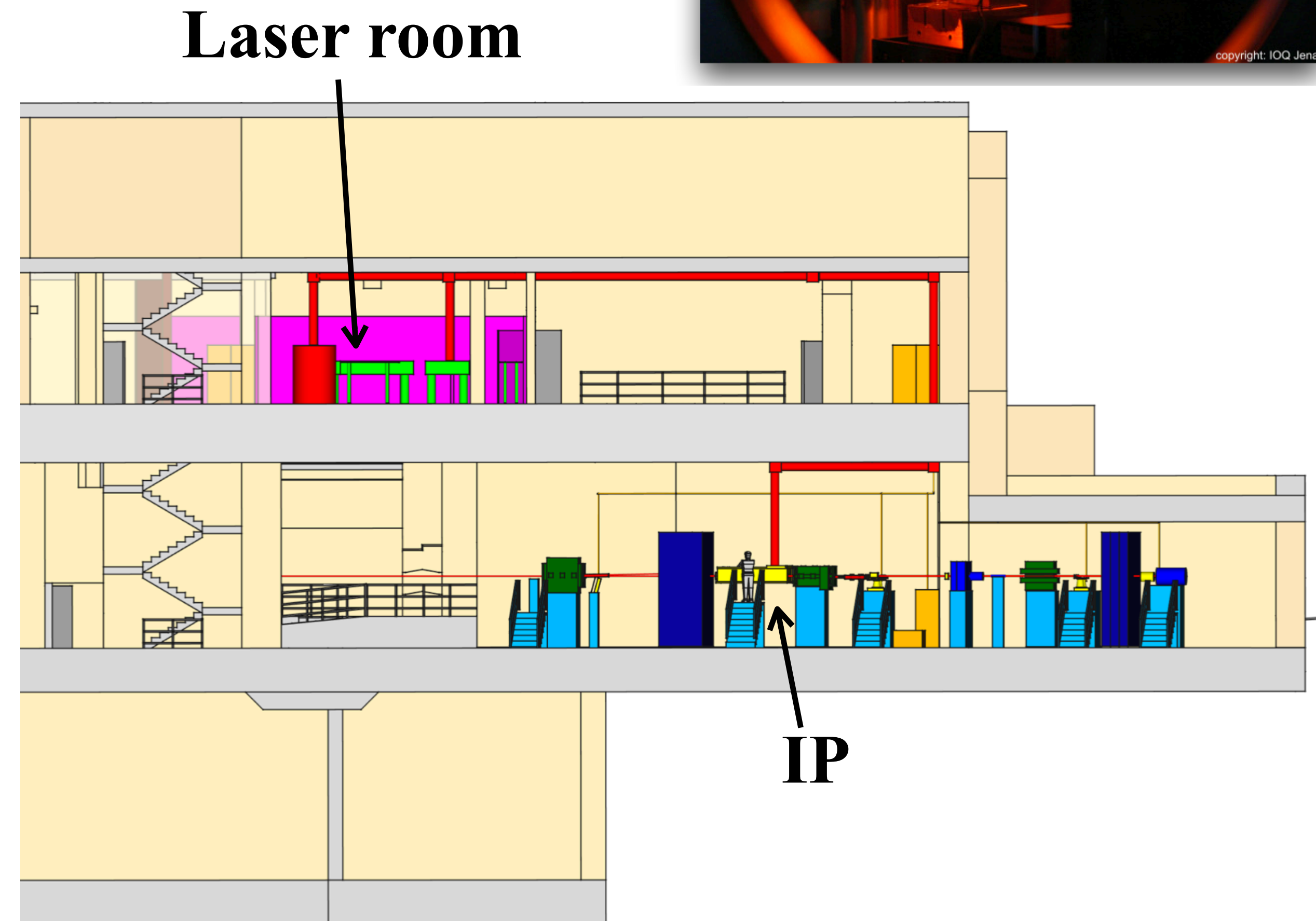
LUXE



Laser



- ◉ Phase-I: the JETi40 40 TW laser loaned to LUXE by Helmholtz Institute Jena
- ◉ Phase-II: looking up towards a 350 TW laser with as small as $3 \times 3 \mu\text{m}^2$ spot size
- ◉ Challenge: exact knowledge of the intensity at the IP
 - ◉ with the laser being ~ 10 's of meters away from it
 - ◉ and with a remote diagnostics system



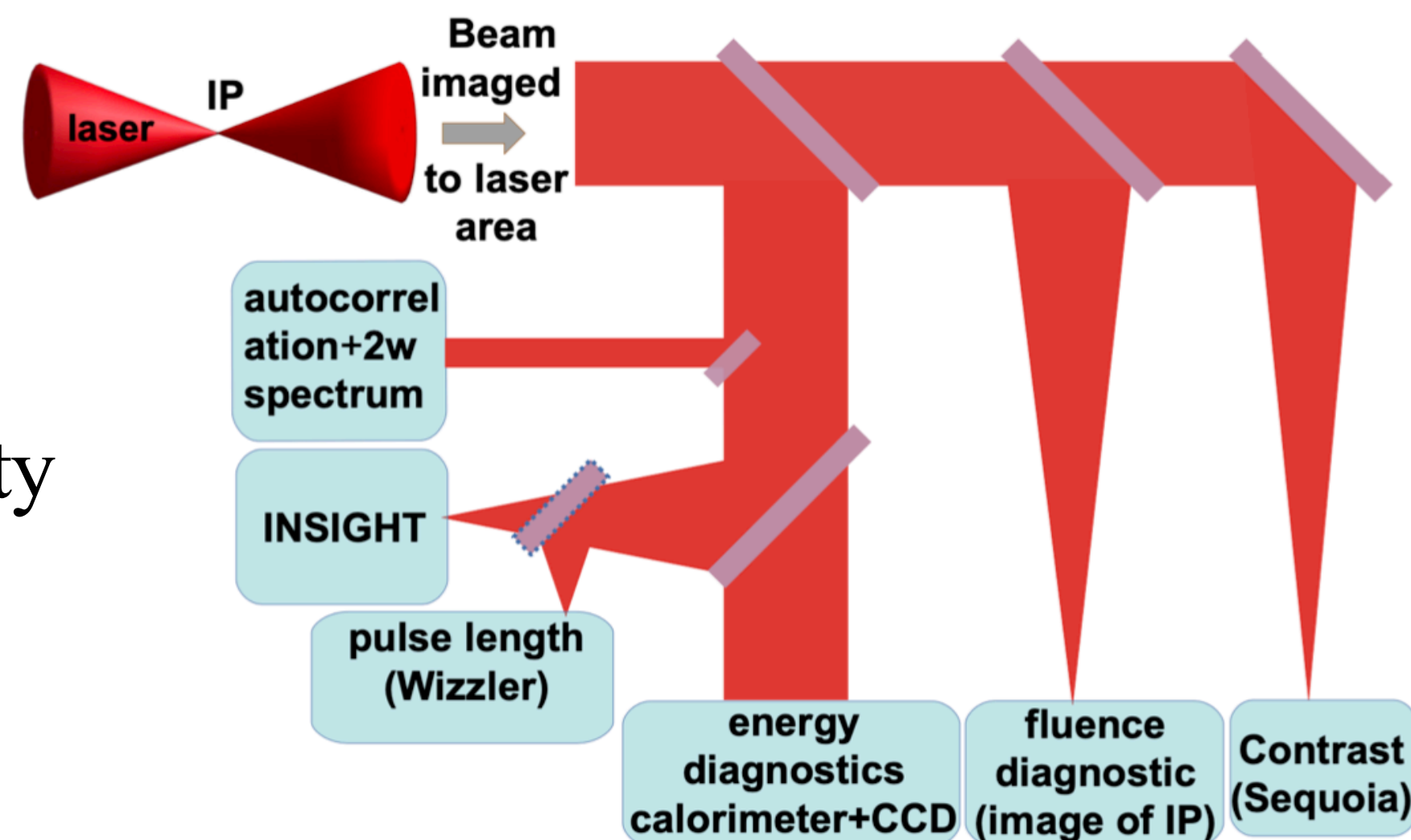
Laser diagnostics

- Measure laser parameters to infer the intensity, I
 - can be indirect and direct, relative and absolute
- Small fluctuations in I lead to large rate fluctuations
 - air movement, vibrations, temp-drift, pump discharge variations, etc.
- The laser beam will be attenuated and imaged on the return path to the diagnostics 10s of meters away from the IP

$$I = \frac{E}{A \times \tau}$$

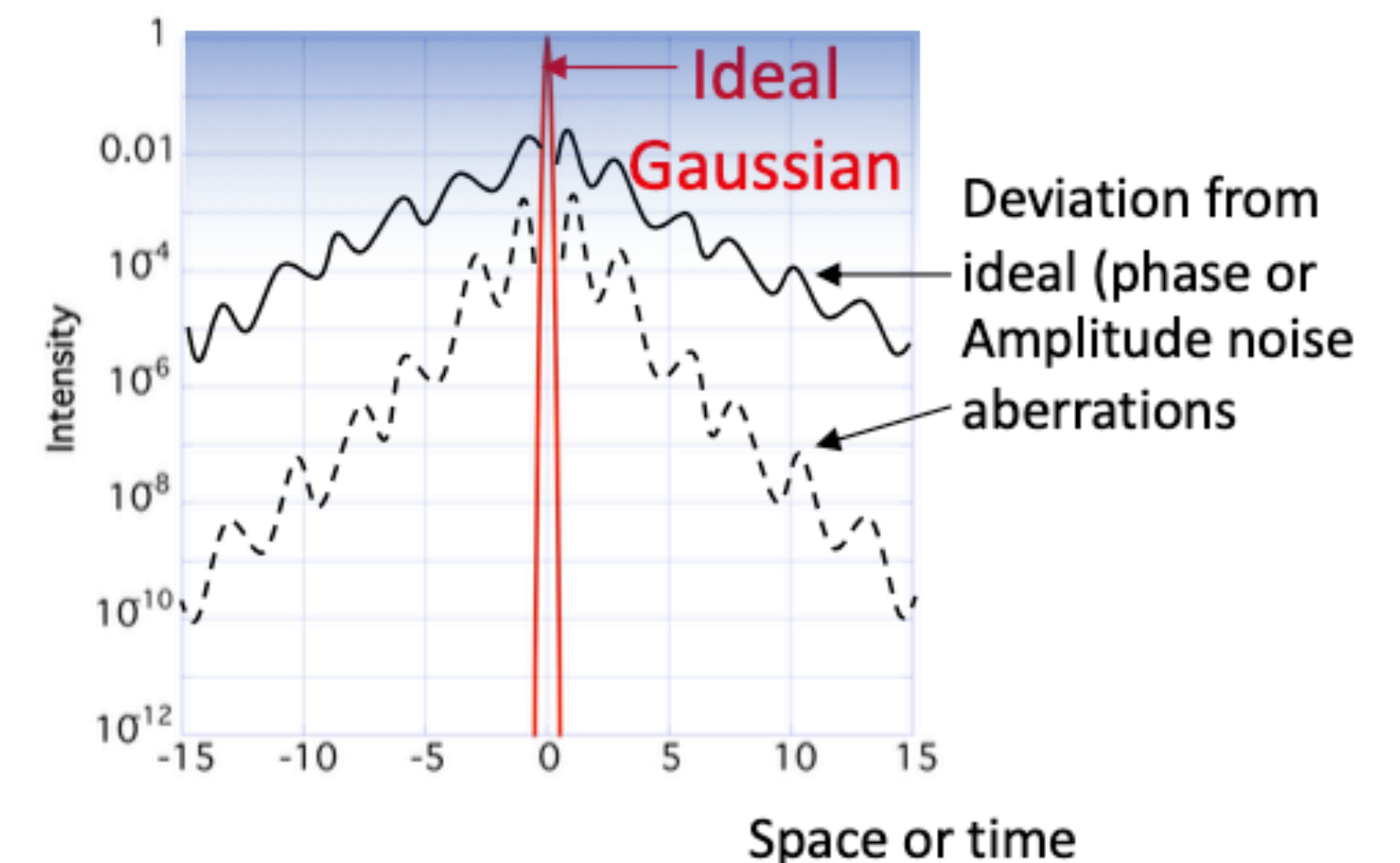
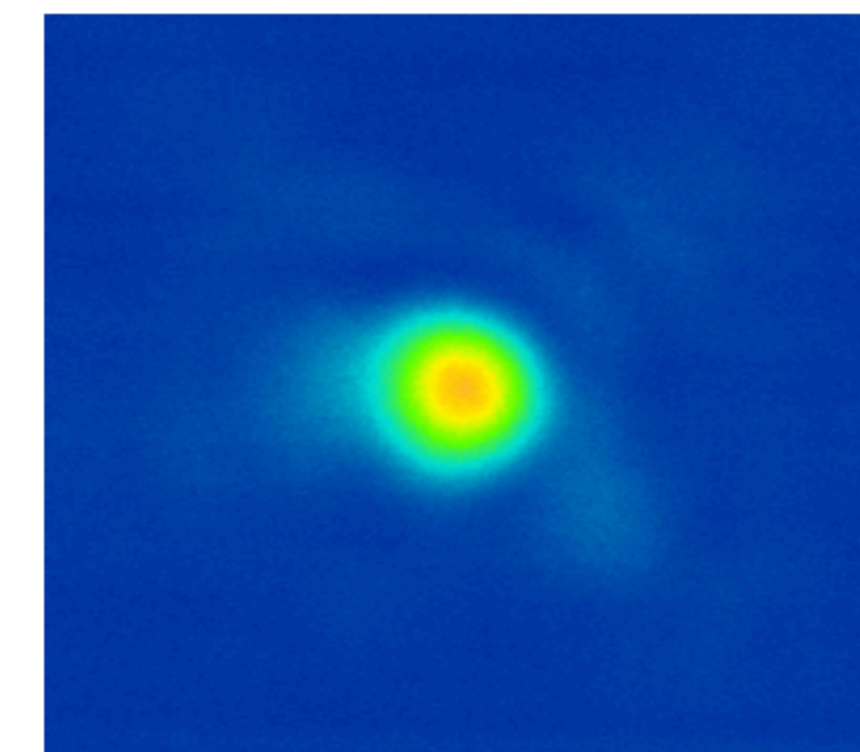
← pulse energy

← pulse spot size × duration

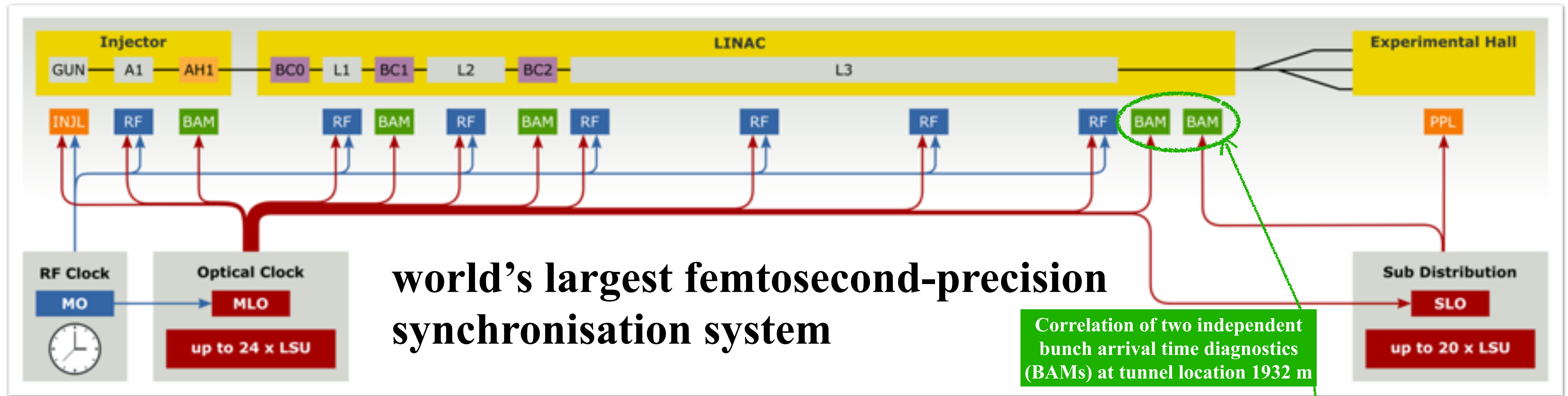


Diagnostics

- relative intensity
- pulse duration
- beam size



Synchronisation & Trigger

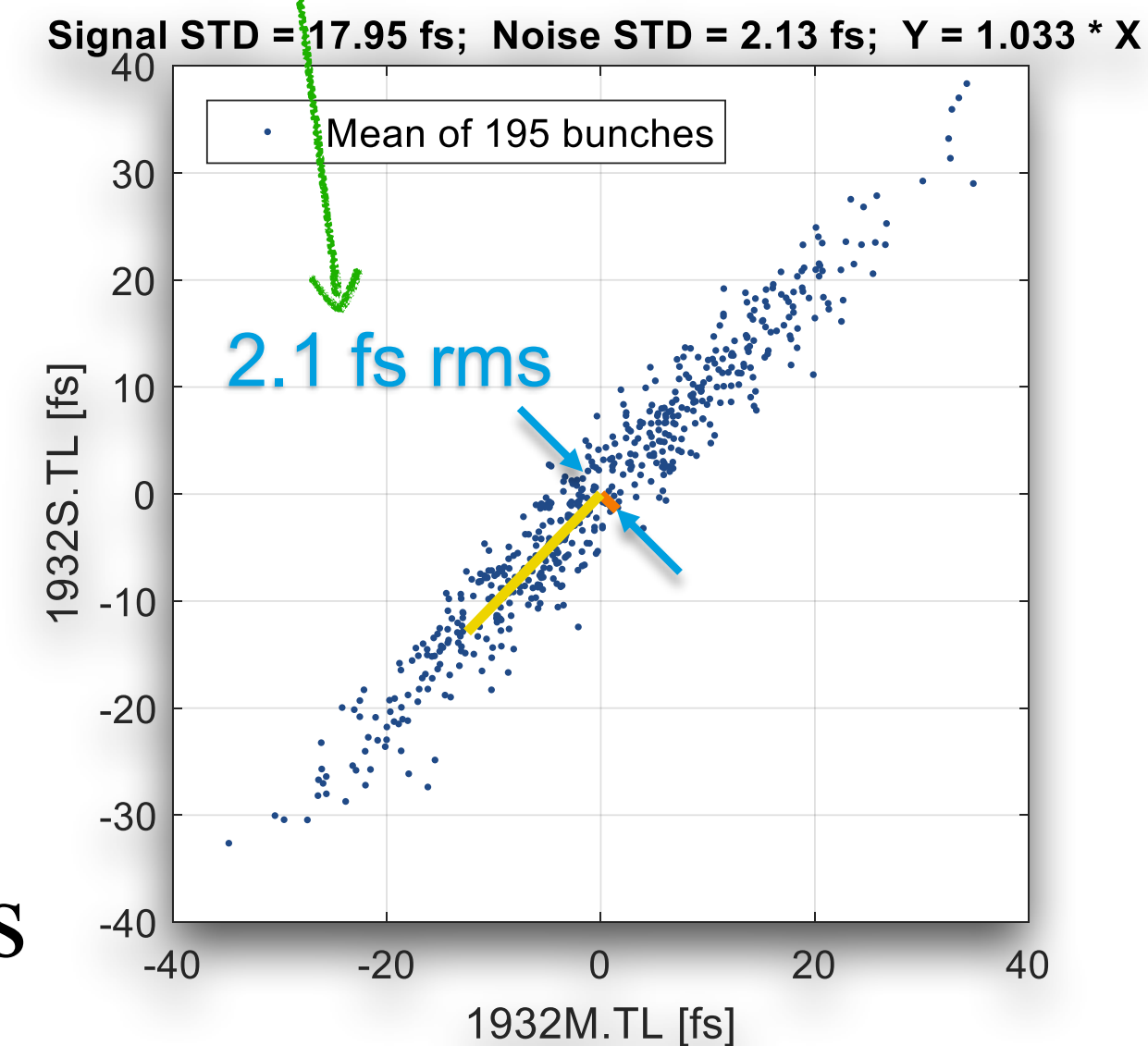


Synchronisation of the XFEL:

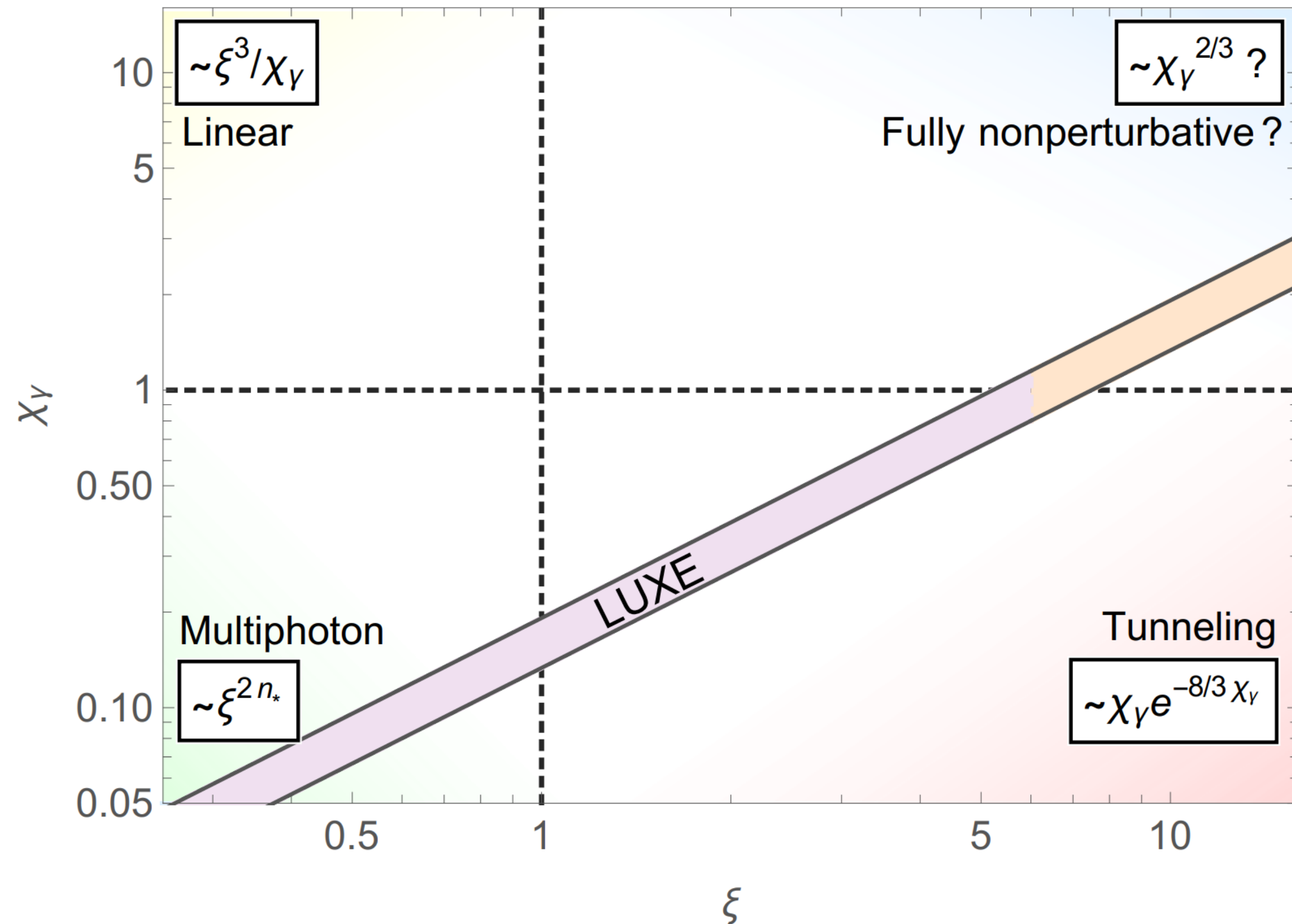
- Optical clock (master laser oscillator, MLO) provides stable pulsed optical reference (Phase-locked to radio frequency (RF) oscillator (MO))
- Optical reference distributed via length-stabilised optical fibre links for laser locking and RF re-sync

LUXE's laser oscillator:

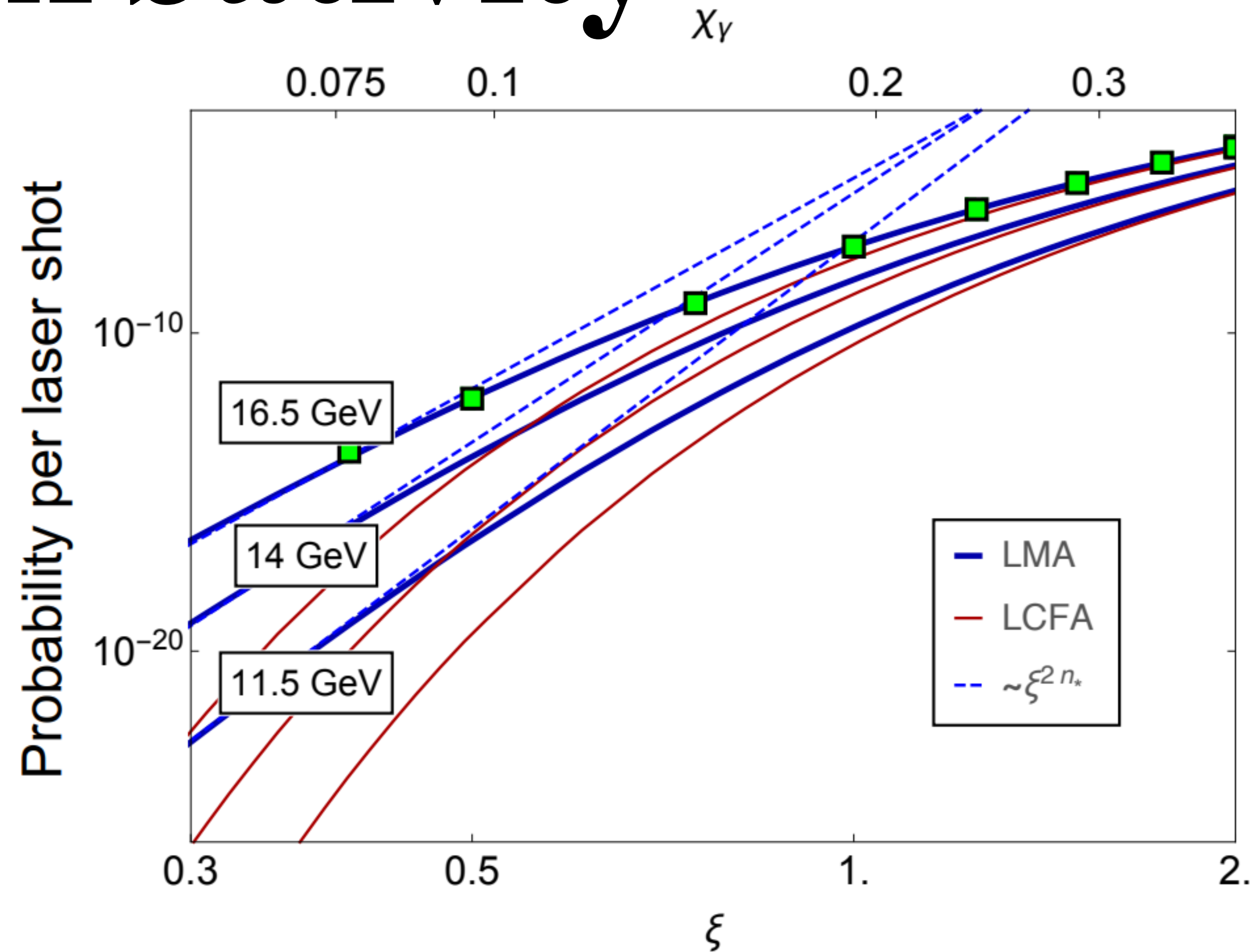
- connected to the optical sync system, which will in turn trigger the detectors



Non-perturbativity

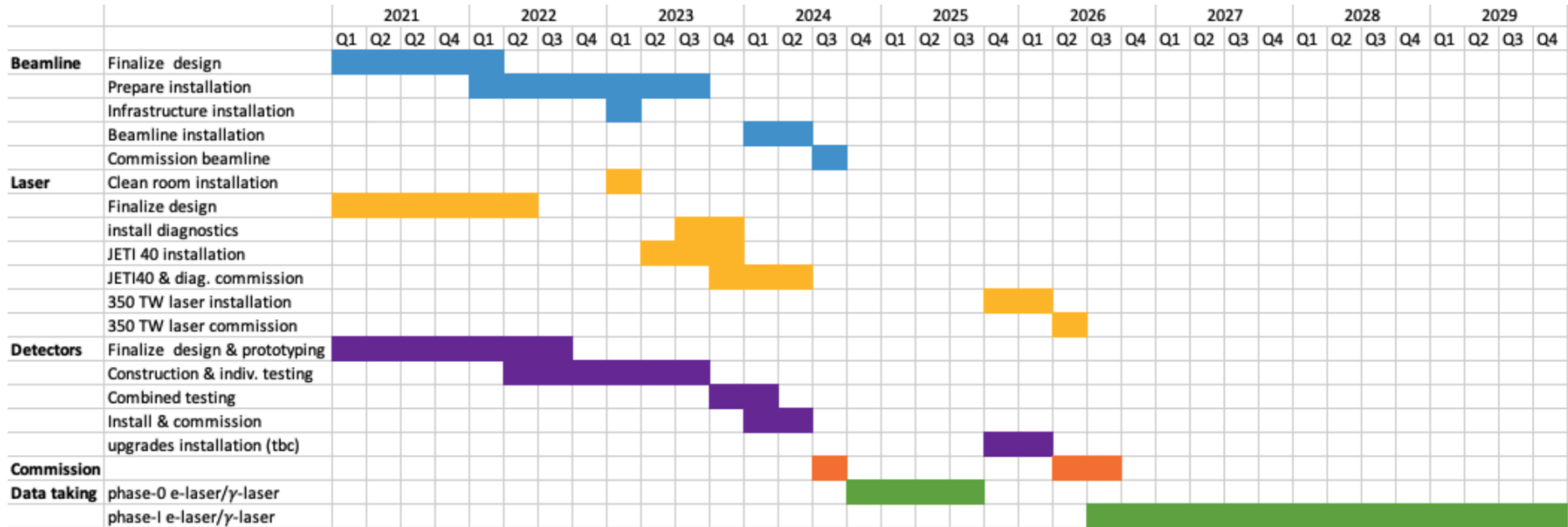


The parameter region LUXE will probe, compared to the asymptotic scaling of the Breit-Wheeler process at large and small ξ and χ parameters



The dependency of probability for the Breit-Wheeler process on the intensity parameter ξ for a probe photon colliding at 17.2 degrees with otherwise standard laser pulse parameters. The blue dashed lines indicate multi-photon scaling and the plot markers are the analytical QED plane-wave results for a photon energy of 16.5 GeV

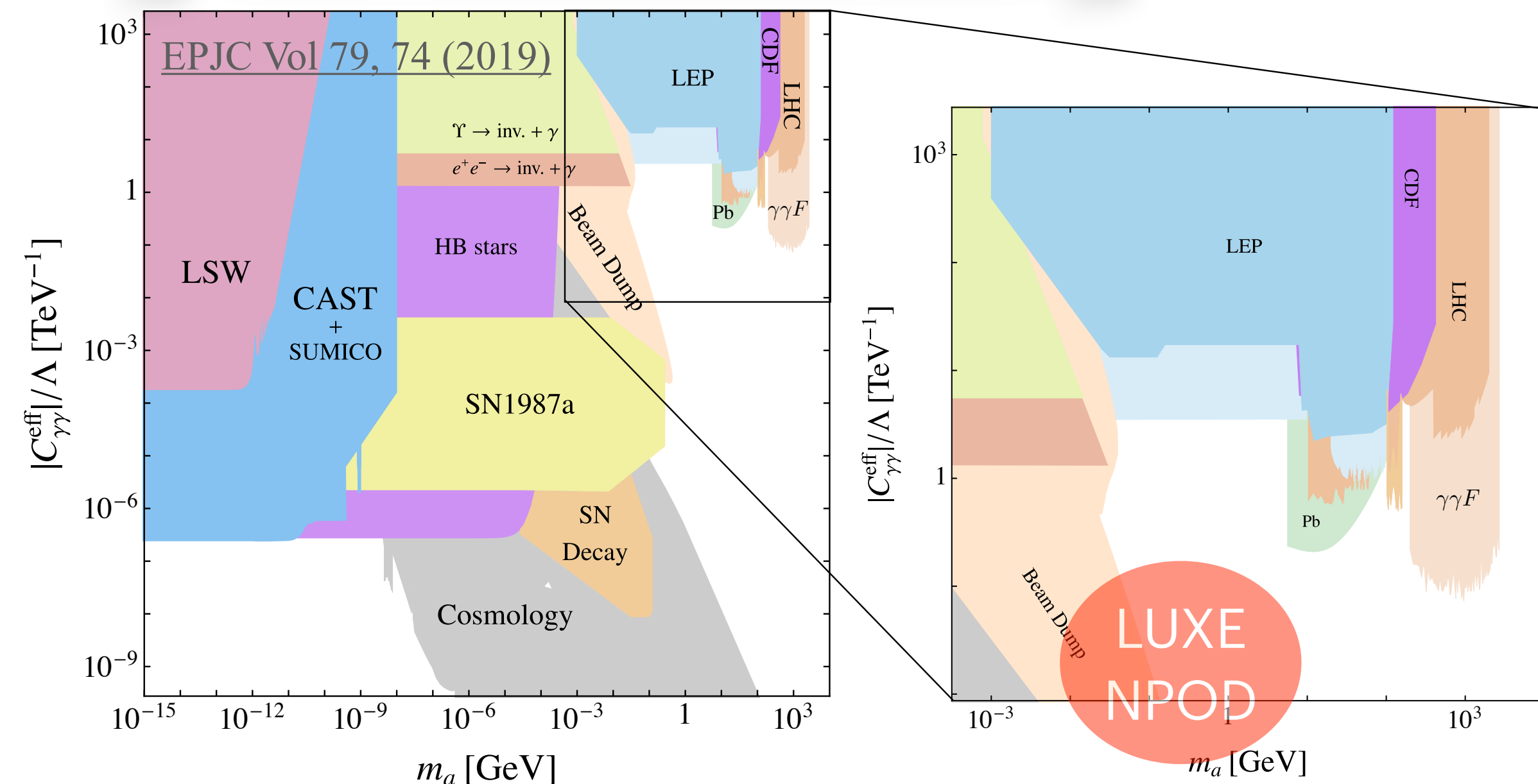
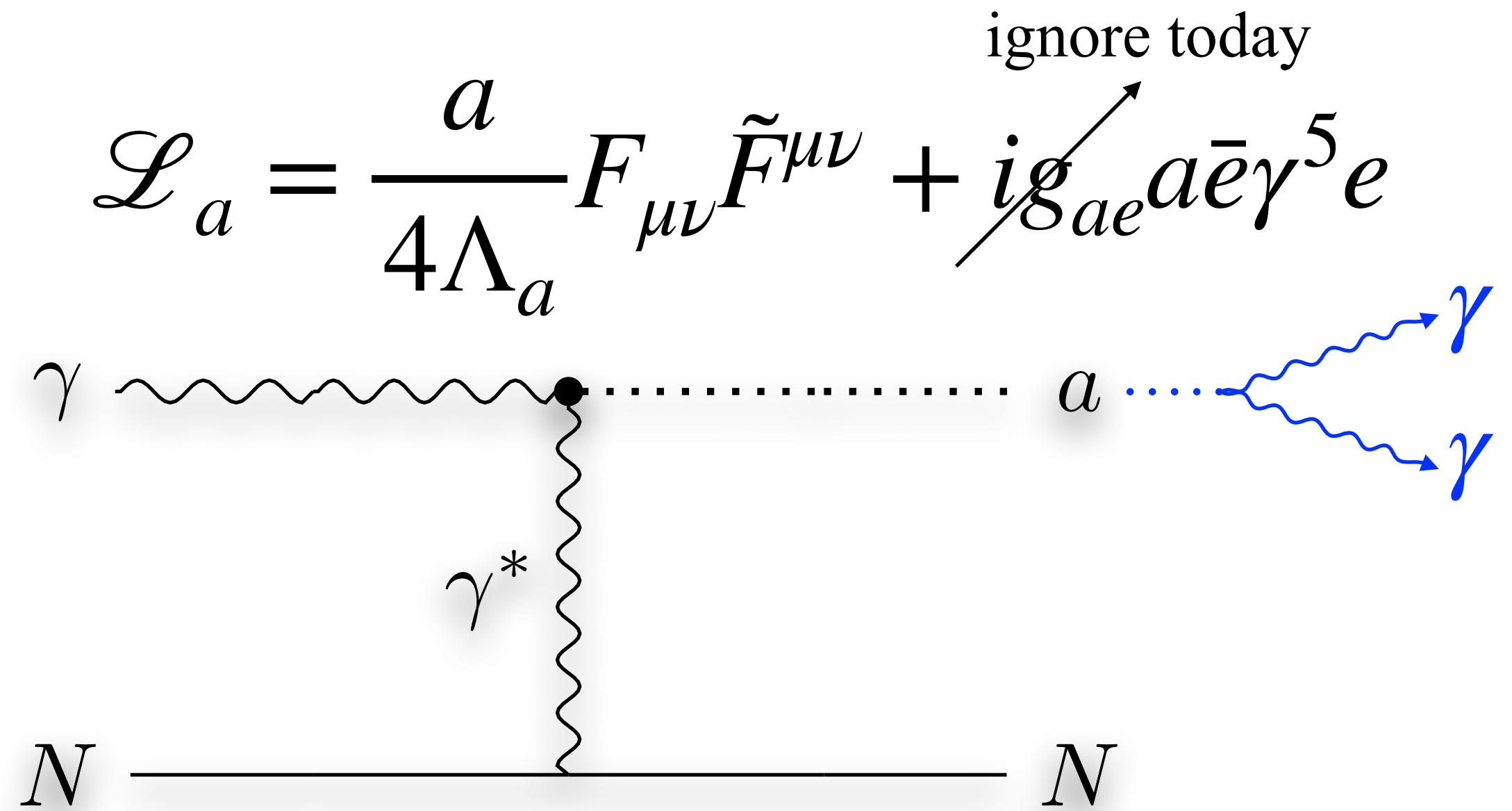
LUXE Planning



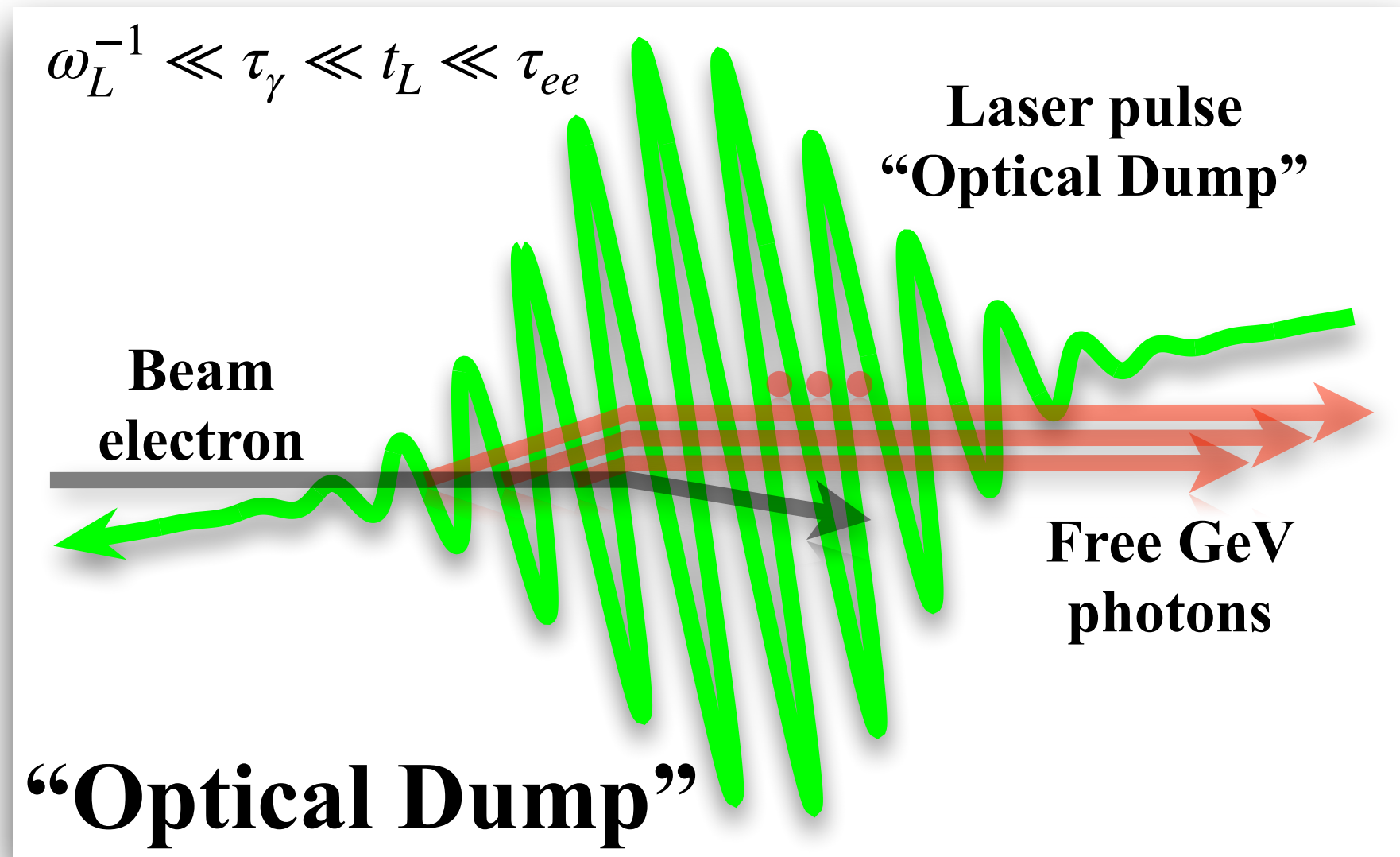
- CDR released in Feb 2021 & passed an international review. Now working toward TDR for 2022
- Experiment must be installed by 2024 during the long shutdown of the Eu.XFEL
- Phase-0: data taking in 2024 with the 40 TW laser in e-laser mode and move to γ -laser in 2025
- Phase-1: upgrade laser to 350 TW in 2026 and run until the Eu.XFEL needs the tunnel (~2029)

New Physics at LUXE

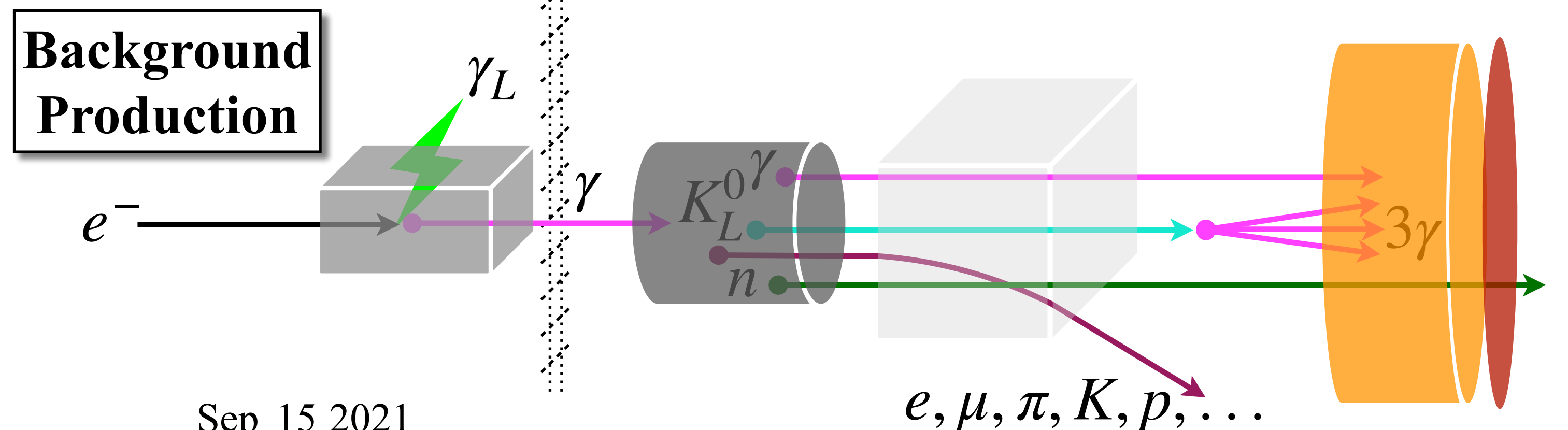
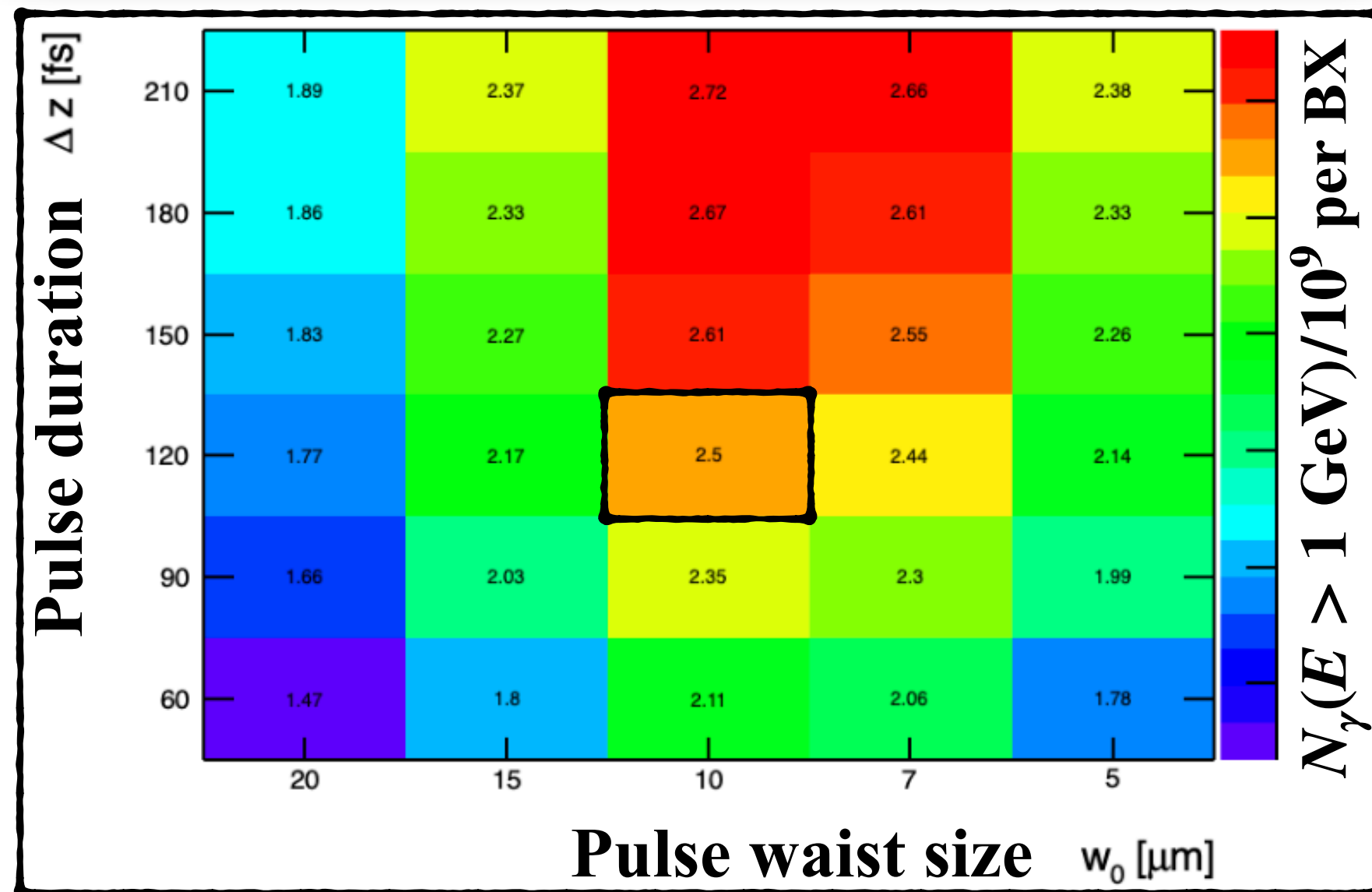
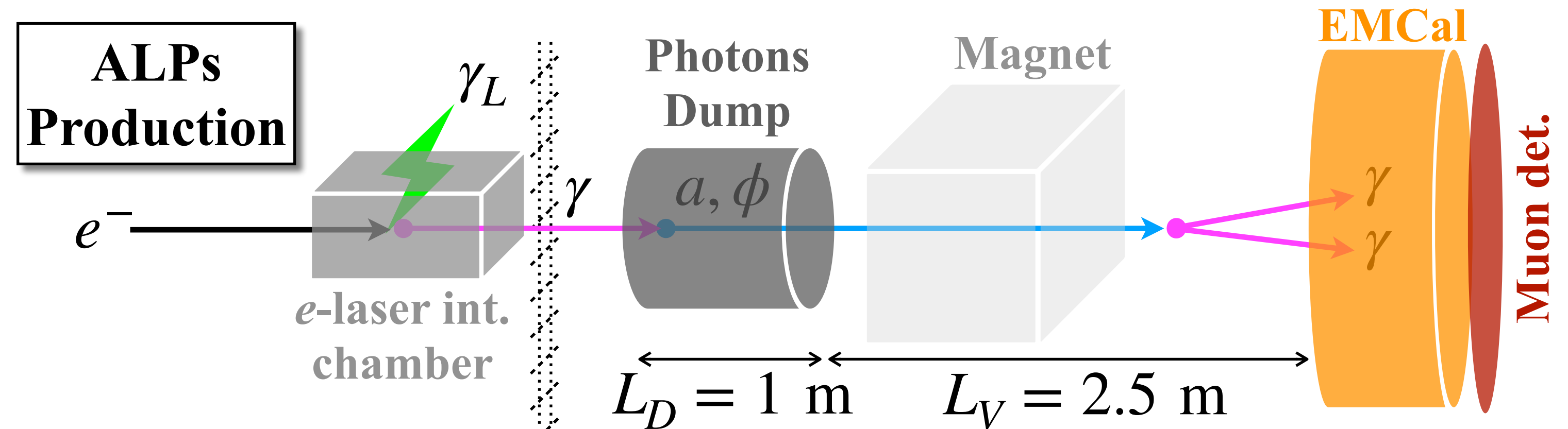
- Focus on axion-like particles (ALP) search
- in many motivated extensions of the SM
- addresses the strong CP & the hierarchy problems, valid dark matter candidate,...
- everything will apply also to scalars with $a \rightarrow \phi$, $\tilde{F}_{\mu\nu} \rightarrow F_{\mu\nu}$, $i\gamma^5 \rightarrow 1$
- Focusing on the Primakoff production with a displaced decay to 2 hard photons
- See backup for ALP production discussion



New Physics @ Optical Dump

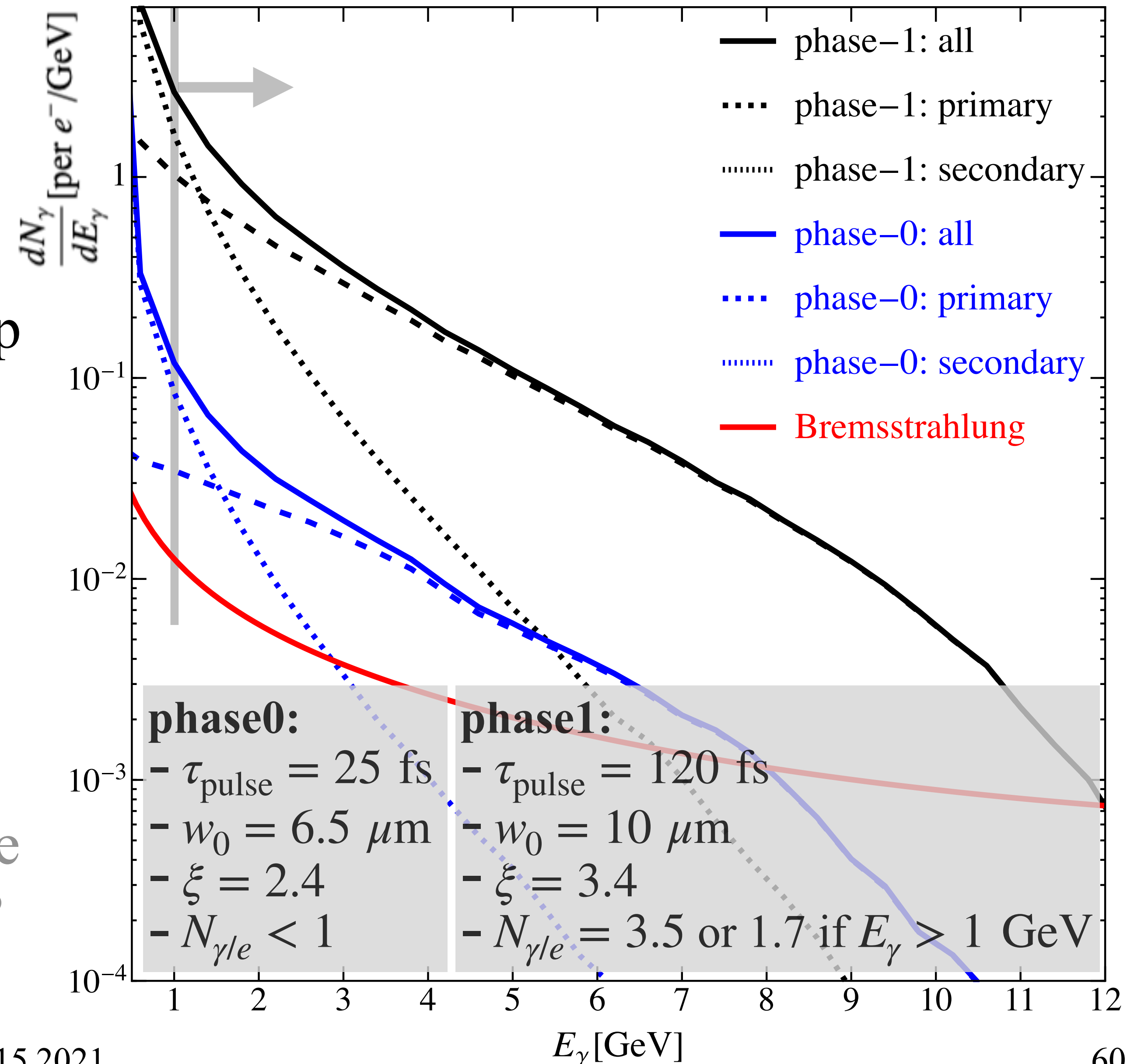


$$N_a \approx \mathcal{L}_{\text{eff}} \int dE_\gamma \frac{dN_\gamma}{dE_\gamma} \sigma_a(E_\gamma, Z) \left(e^{-\frac{L_D}{L_a}} - e^{-\frac{L_V + L_D}{L_a}} \right) \mathcal{A}$$



Photon spectra for ALPs production

- Showing spectra per primary electron
 - “primary” from the IP and
 - “secondary” from the shower in the dump
- “Many” photons per electron (phase-1):
 - ~ 3.5 for ($E_\gamma > 0$ GeV)
 - ~ 1.7 for ($E_\gamma > 1$ GeV)
- Not shown: spectra for the electrons-on-dump case. One expects a factor of ~ 2 more photons - more signal!, **what about bkg?**



ALPs production

$$N_a \approx \mathcal{L}_{\text{eff}} \int dE_\gamma \frac{dN_\gamma}{dE_\gamma} \sigma_a(E_\gamma, Z) \left(e^{-\frac{L_D}{L_a}} - e^{-\frac{L_V + L_D}{L_a}} \right) \mathcal{A} \quad \mathcal{L}_{\text{eff}} = N_e N_{\text{BX}} \frac{9\rho_W X_0}{7A_W m_0} \quad L_a = c\tau_a \frac{p_a}{m_a} \quad p_a \approx \sqrt{E_\gamma^2 - m_a^2}$$

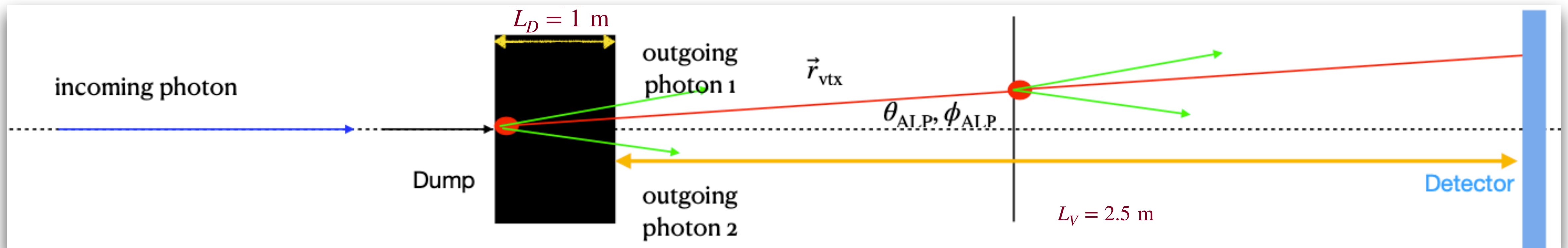
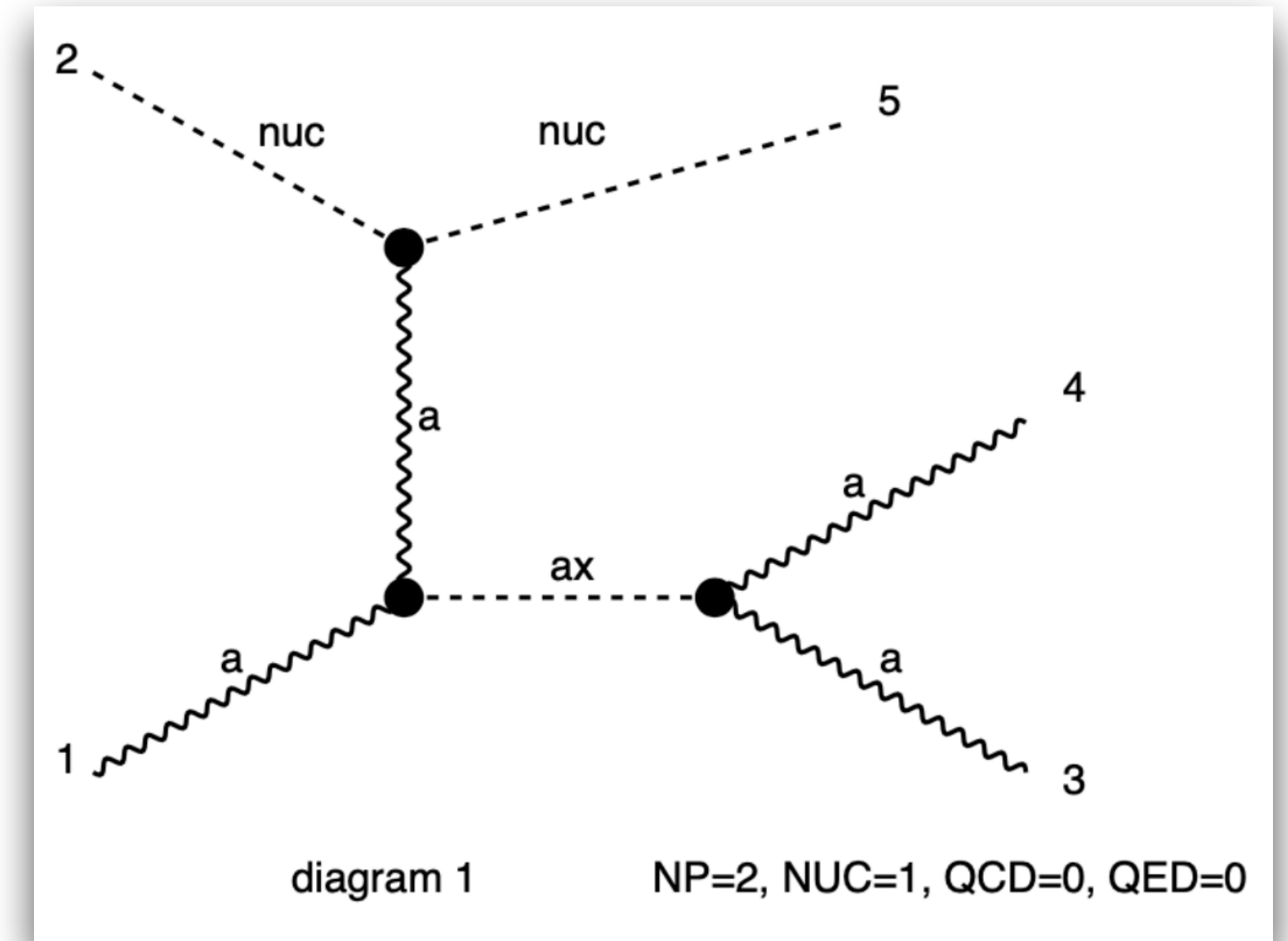
- $N_e = 1.5 \times 10^9$ is the number of electron per bunch and $N_{\text{BX}} (= 10^7)$ is the number of BXs assumed
- E_γ is the incoming photon energy
- \mathcal{L}_{eff} is the effective luminosity, where ρ_W is the Tungsten density, A_W is its mass number and X_0 is its radiation length. $m_0 \sim 930$ MeV is the nucleon mass
- L_a is the ALP propagation length, where τ_a is its proper lifetime and p_a is its momentum
- $\sigma_a(E_\gamma, Z)$ is the Primakoff production cross section of the ALP in the dump
- \mathcal{A} is the angular acceptance times efficiency of the detector
- dN_γ/dE_γ is the differential photon flux per initial electron, includes photons from the electron-laser interaction, as well as secondary photons produced in the EM shower which develops in the dump
- $L_D = 1$ m is the dump's length. The dump is positioned ~ 13 m away from the electron-laser interaction region
- $L_V = 2.5$ m is the length of the decay volume
- The decay rate of the ALP into two photons is $\Gamma_{a \rightarrow \gamma\gamma} = m_a^3 / (64\pi\Lambda_a^2)$

Scalar and Naturalness

- The $\phi - \gamma$ coupling induces quadratically divergent, additive contribution to the scalar mass-square, $\delta m_\phi^2 \sim \Lambda_{\text{UV}}^4 / (16\pi^2 \Gamma_\phi^2)$
- Λ_{UV} is the scale in which NP is required to appear in order to cancel the quadratic divergences
- This leads to a naturalness bound:
$$\Gamma_\phi \gtrsim 4 \times 10^5 \text{ GeV} \left(\frac{\Lambda_{\text{UV}}}{\text{TeV}} \right)^2 \frac{200 \text{ MeV}}{m_\phi}$$
- LUXE-NPOD is expected to reach the sensitivity required to probe the edge of the parameter space of natural models in its phase-1

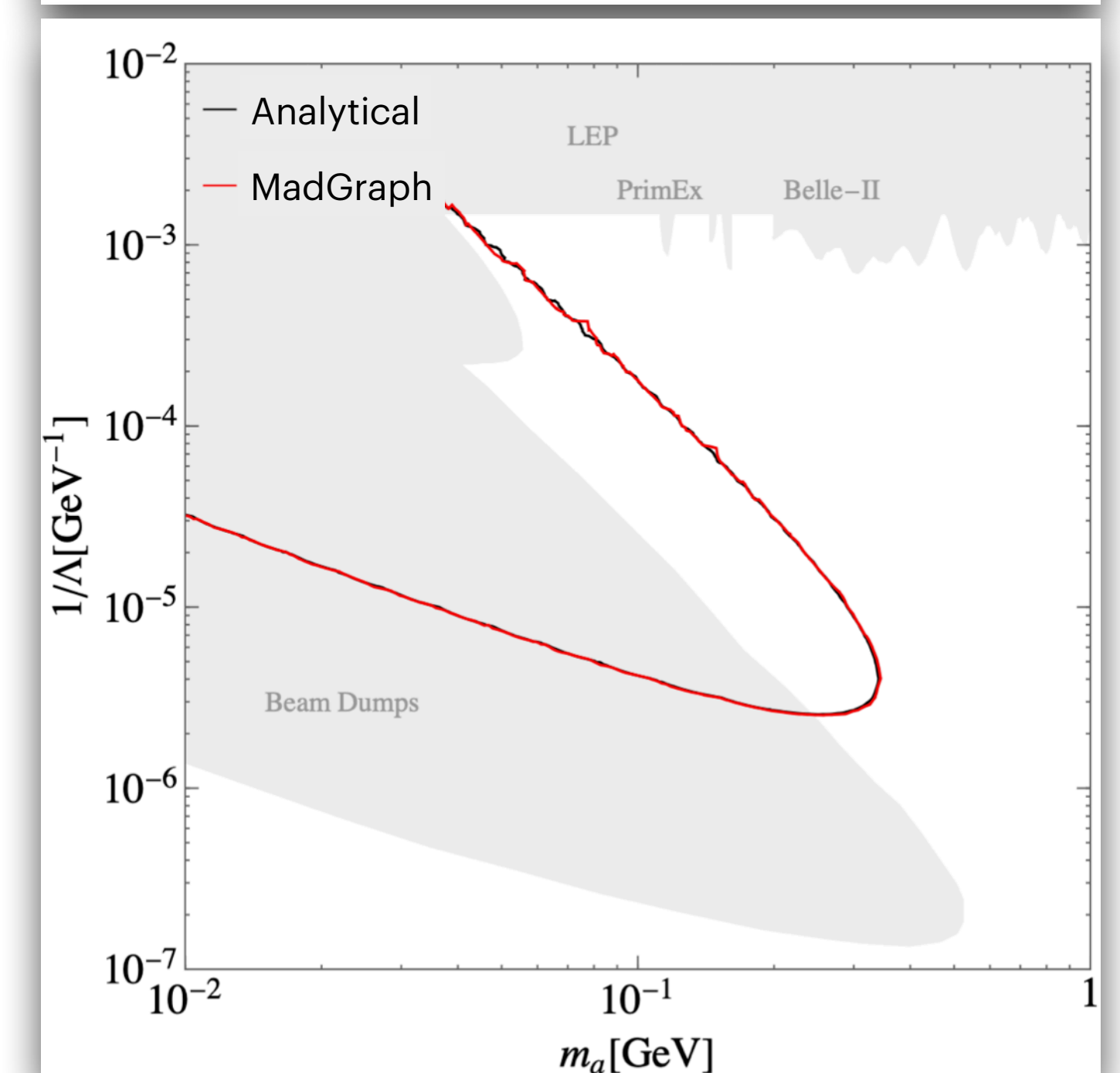
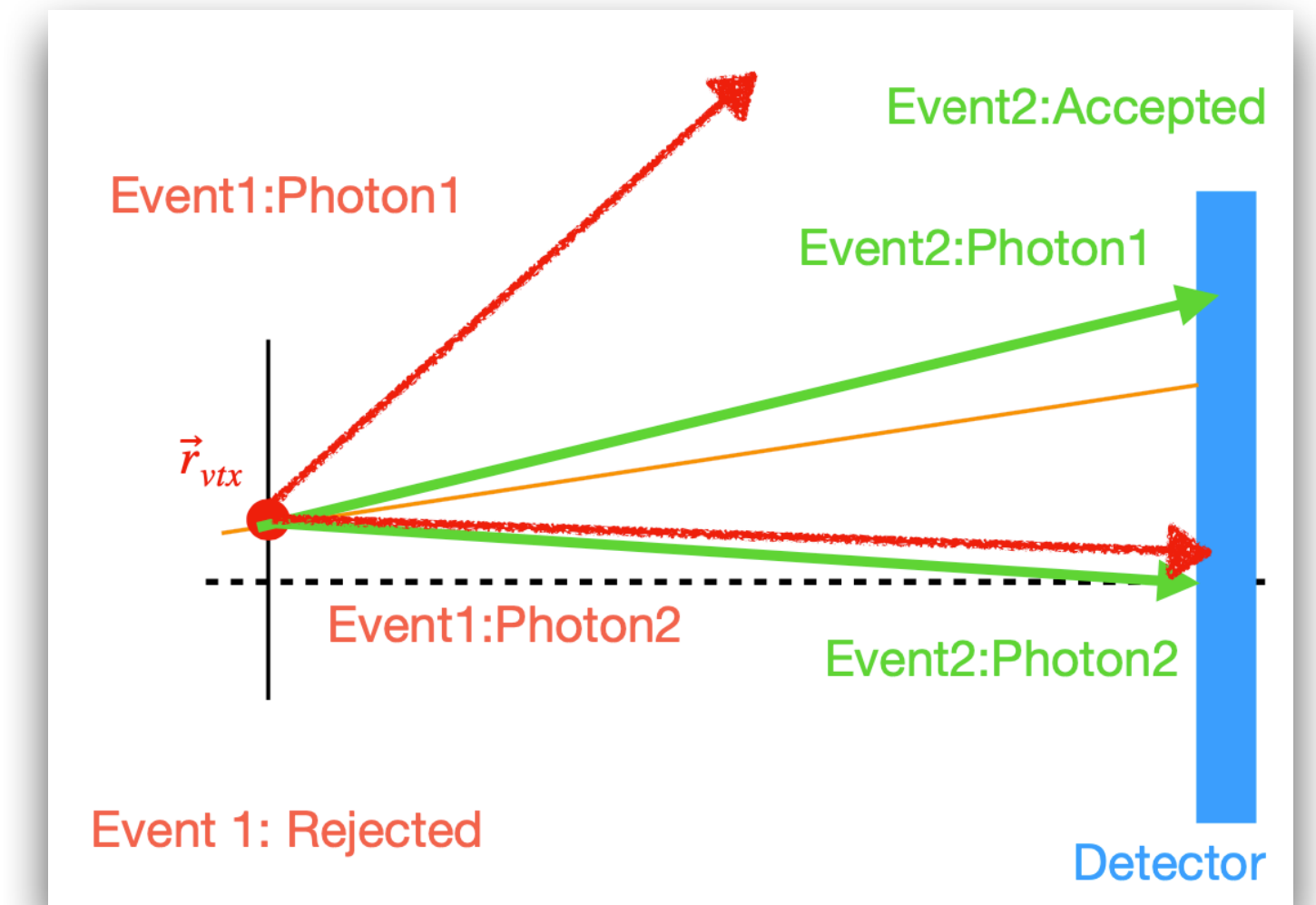
Signal MC prod. with MadGraph

- Generate this process: $a \text{ nuc} \rightarrow ax \text{ nuc}$ where a is photon, nuc is the nucleus of the tungsten dump and ax is the ALP (Primakoff production)
- The nuclear form factor was obtained from Iftah Galon and implemented in the model
- MadGraph does not smear the vertex position, so all collisions happen at $z=0, t=0$
- Moreover MadGraph decays the ALP instantaneously
- The 2 photons are produced at $z=0$ and hence we need to displace them according to the ALP's lifetime

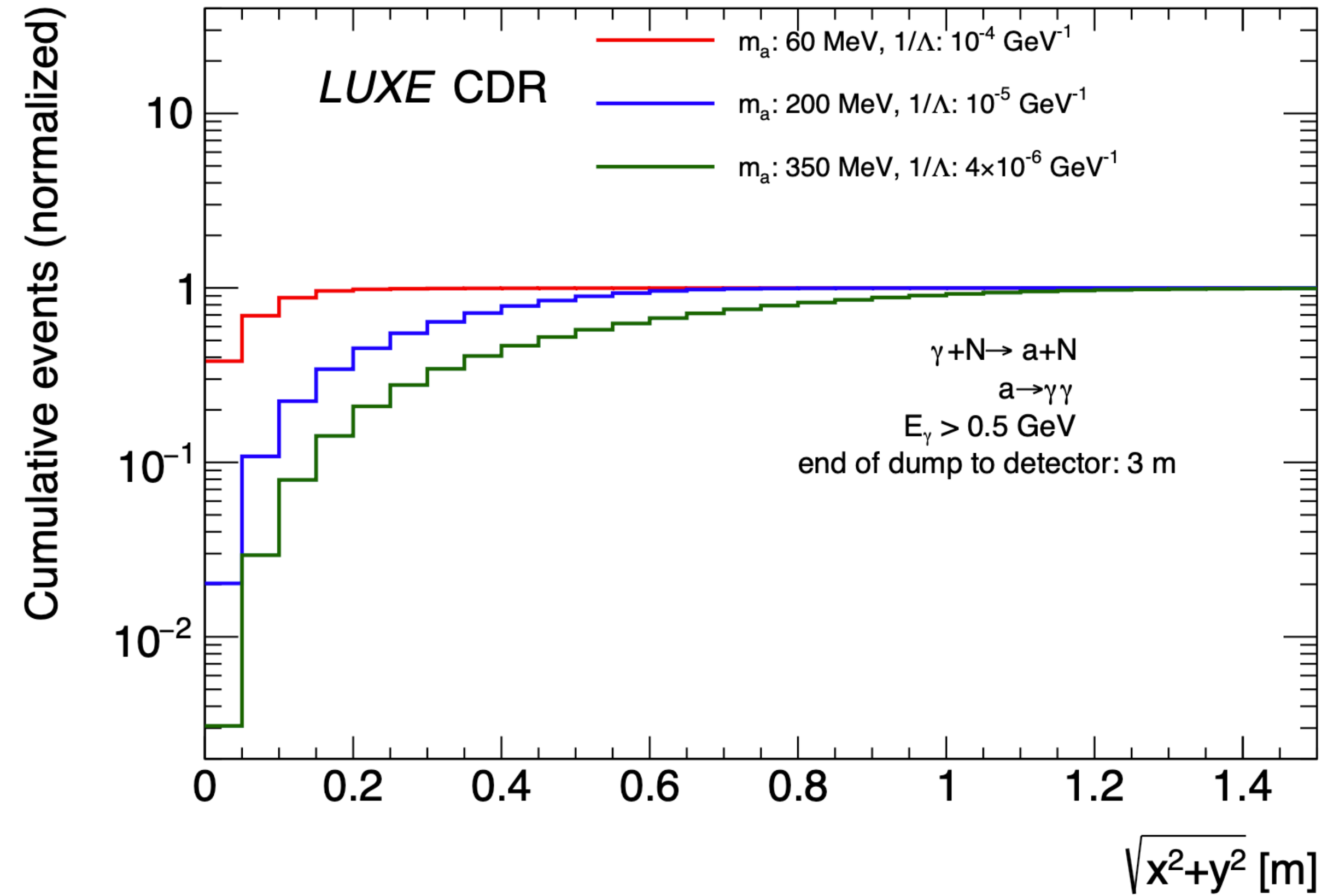
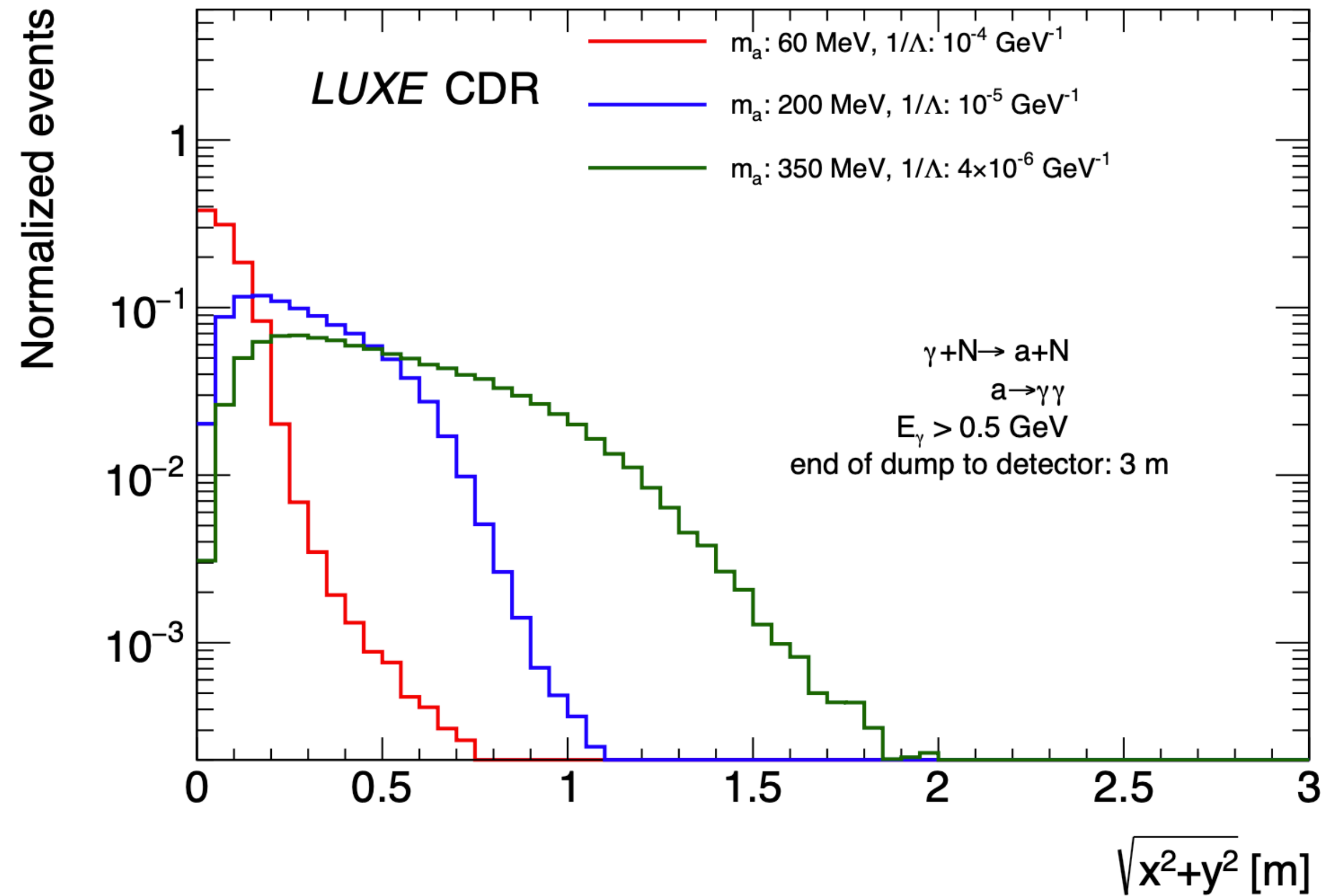


Signal MC prod. with MadGraph

- The distance of decay (r_{vtX}) for each ALP is obtained by randomly drawing a length from the decay length distribution of the ALP, where:
 - the decay length is $L_a = c\tau_a p_a/m_a$
 - the direction is determined by the momentum of ALP
 - r_{vtX} is randomly drawn number from e^{-L_a}
- Once \vec{r}_{vtX} is obtained, the two photons are shifted to that position
 - if $L_D < r_{\text{vtX}} \cos \theta_a < L_D + L_V$ we proceed to next stage, otherwise the event is rejected
 - given the opening angle of the photons and the distance they still need to travel to detector, we check if the photons impinge the detector or not.
 - if both photons impinge the detector and $E_\gamma > 0.5$ GeV, then that event is accepted
- The acceptance \mathcal{A} is the number of events with both photons passing the energy cut and geometric constraints divided by the total number of events generated
- Once the geometric acceptance is obtained, the factor is multiplied by the effective luminosity and the cross-section of production to get the number of ALP events (see earlier slide) where $N_a = \mathcal{L}_{\text{eff}} \sum_i \sigma_i \mathcal{A}_i N_{\gamma,i}$ and where the sum is over sum over the incoming photon beam energy distribution $N_{\gamma,i}$

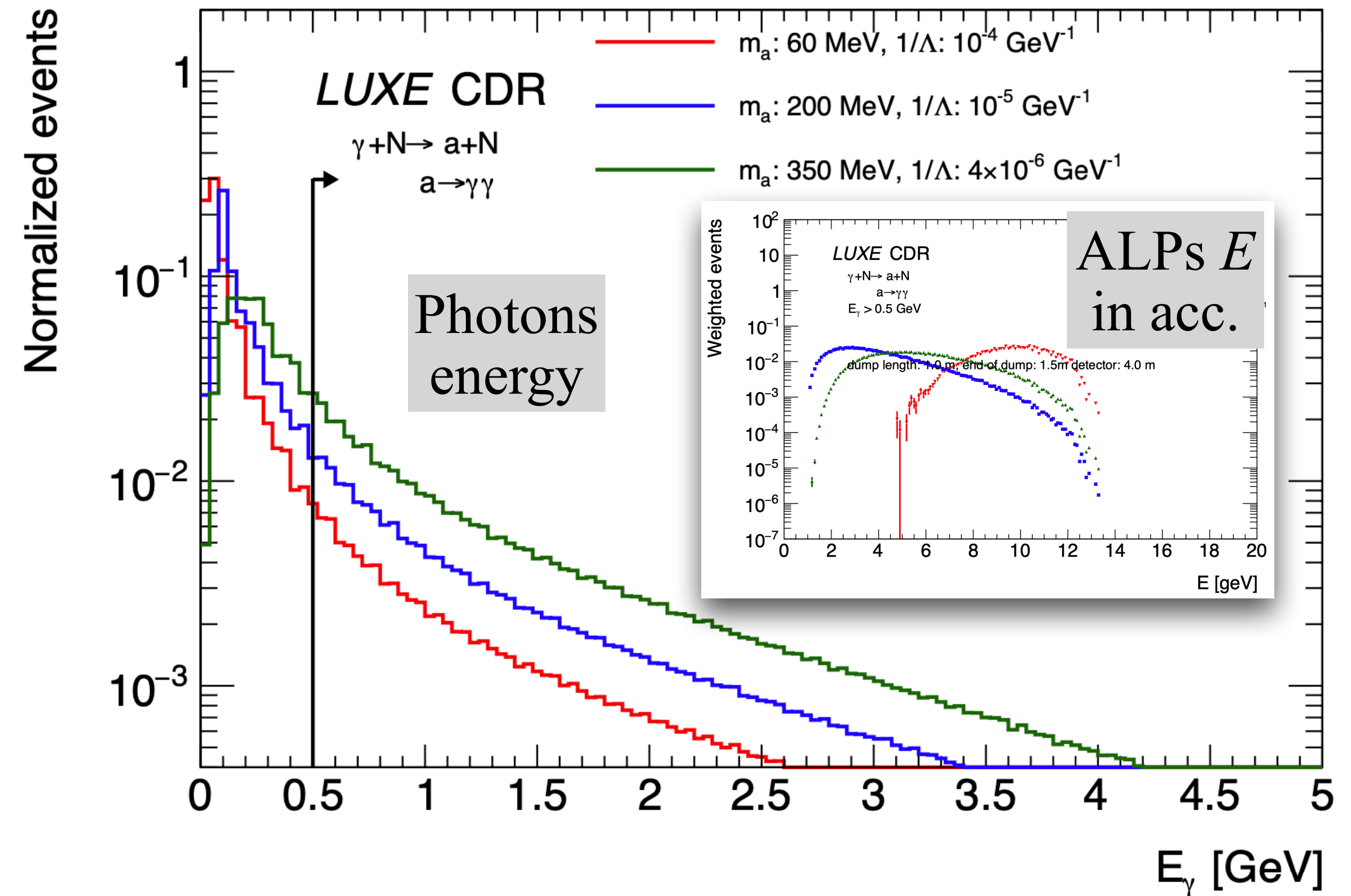
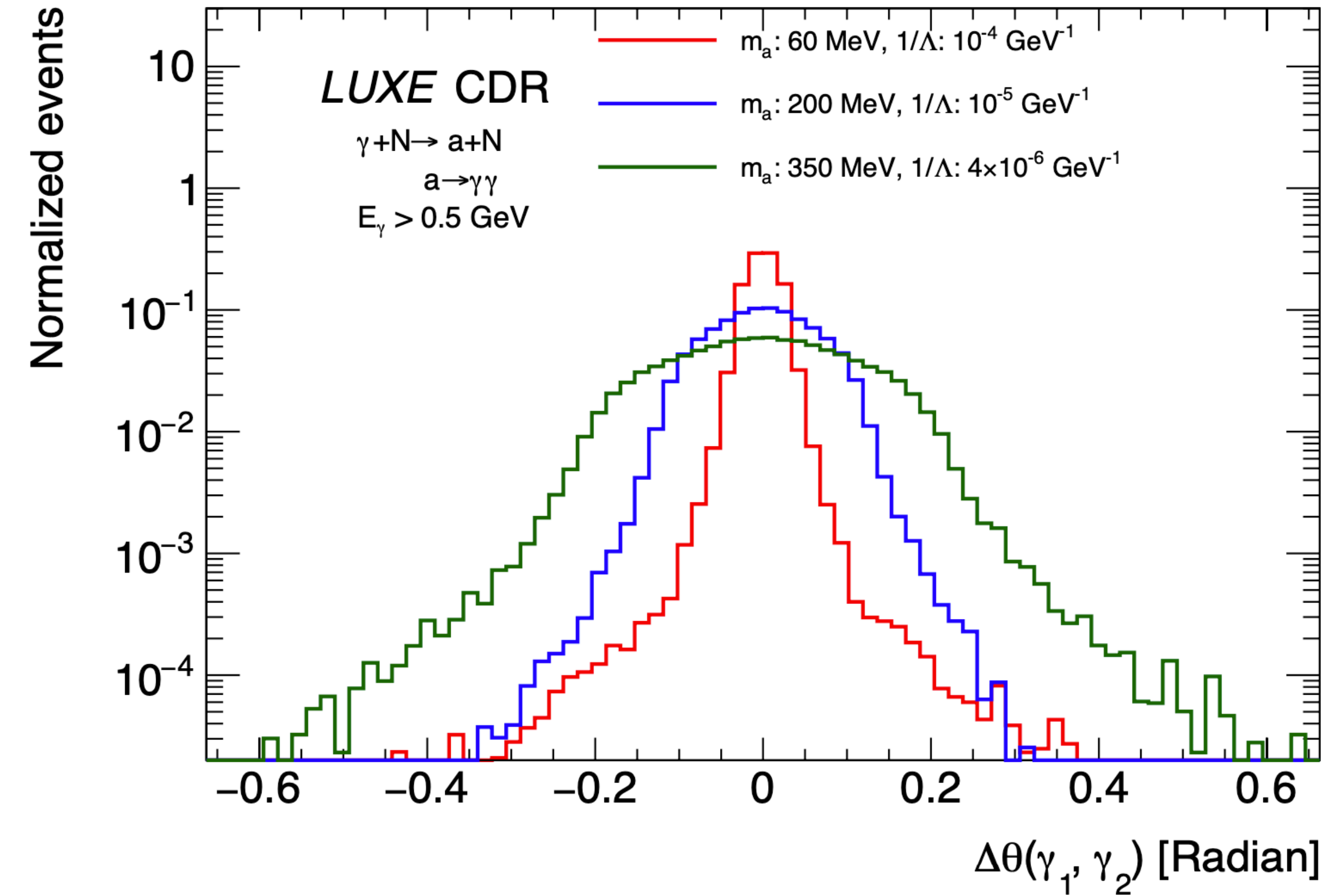


Signal MC prod. with MadGraph

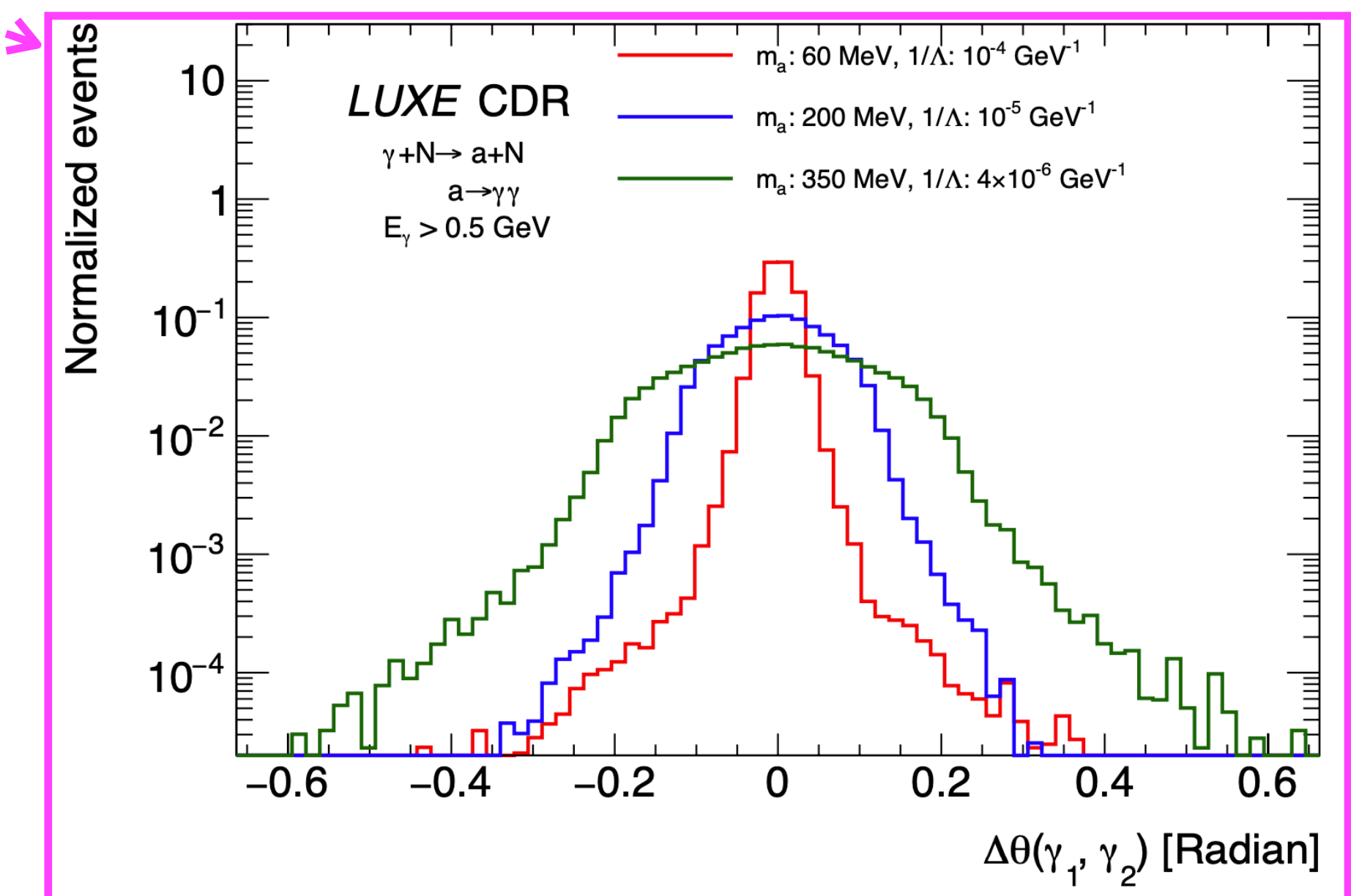
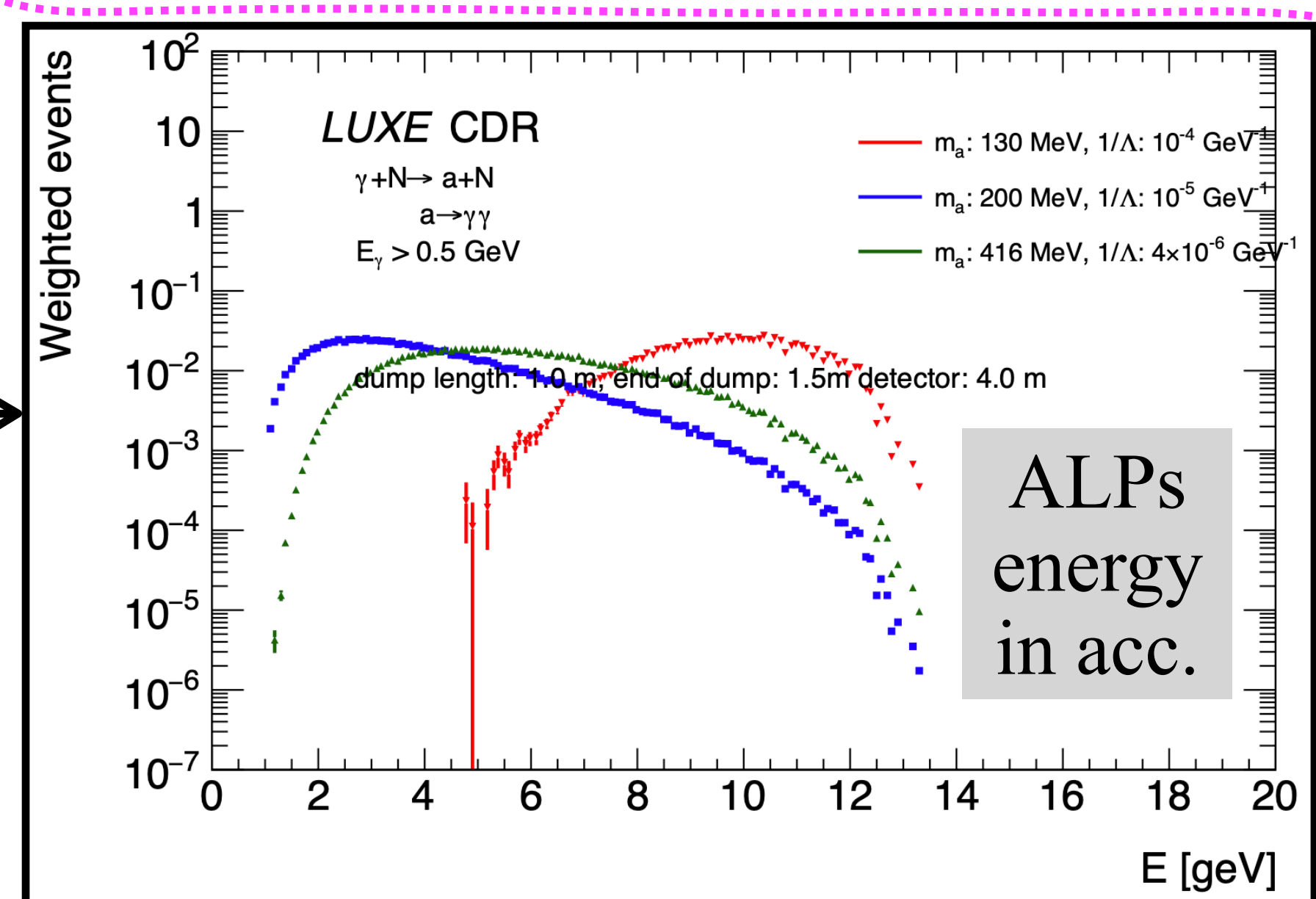
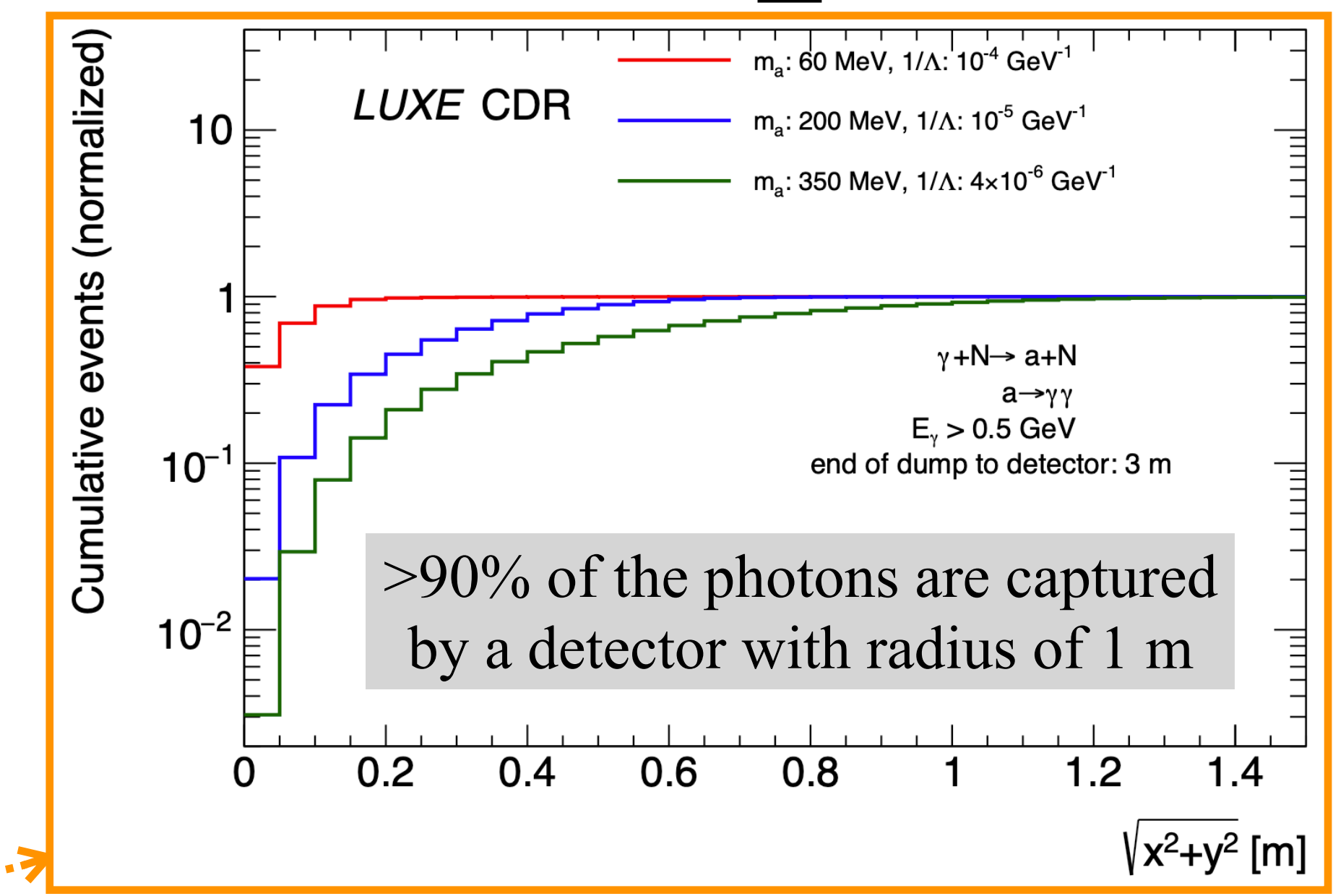
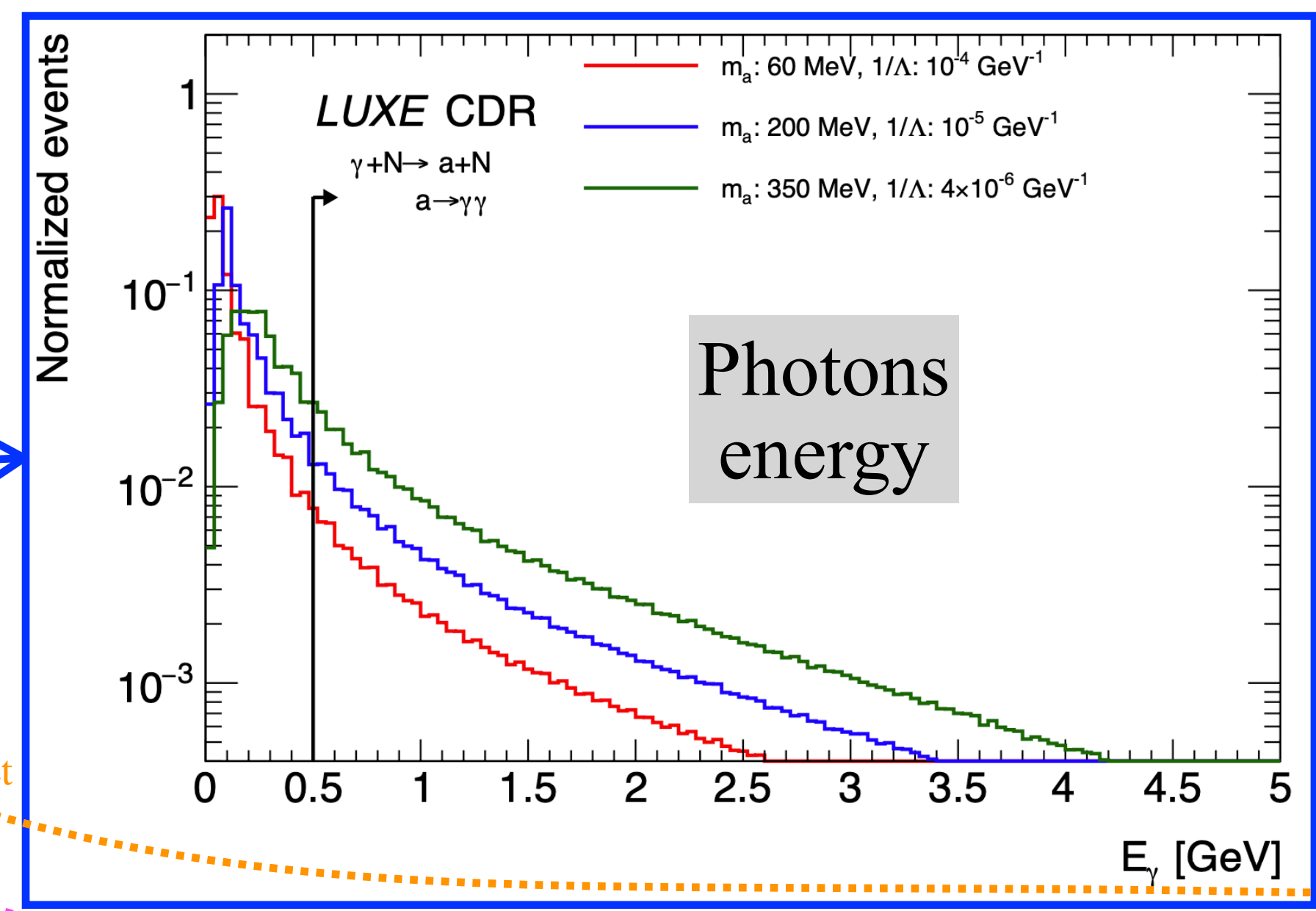
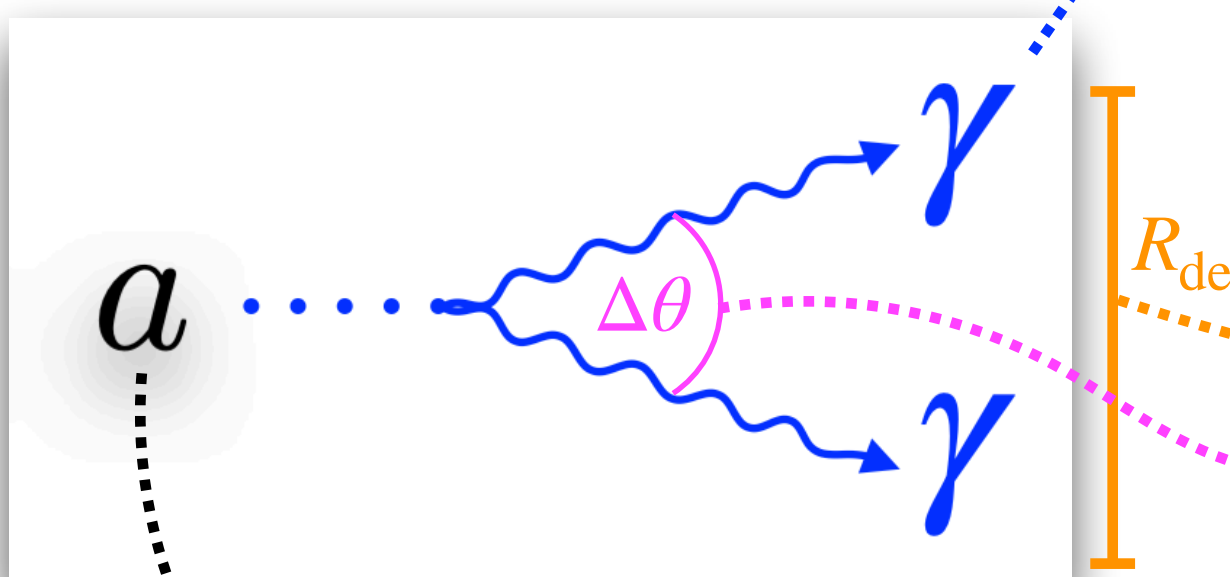


More than 90% of the photons are captured by a detector with radius of 1 m

Signal MC prod. with MadGraph



Signal MC with MadGraph

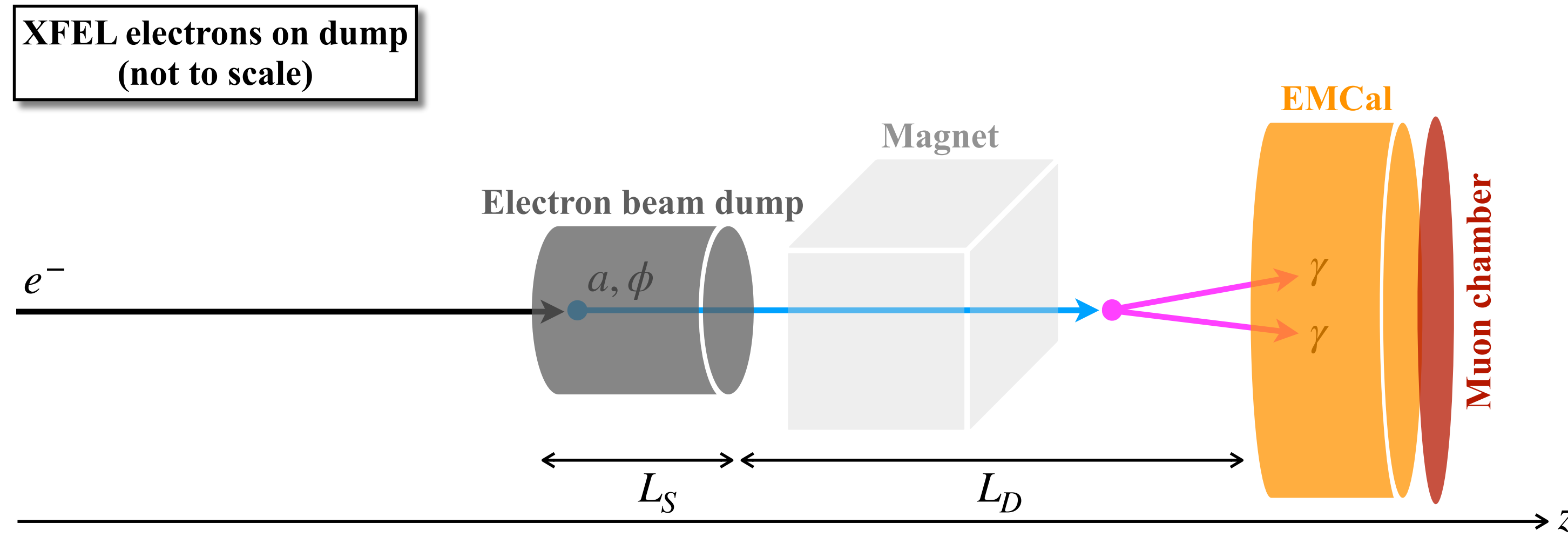


Time scales @ LUXE-NPOD

- The relevant time scale of LUXE's 800 nm laser itself is $\omega_L^{-1} \sim 0.4$ fs
- The laser pulse duration is $t_L \sim \mathcal{O}(10 - 200)$ fs
- The (Compton scattering) photon production timescale is $\tau_\gamma \sim \mathcal{O}(10)$ fs
- The (Breit-Wheeler) pair production timescale is $\tau_{ee} \sim \mathcal{O}(10^4 - 10^6)$ fs

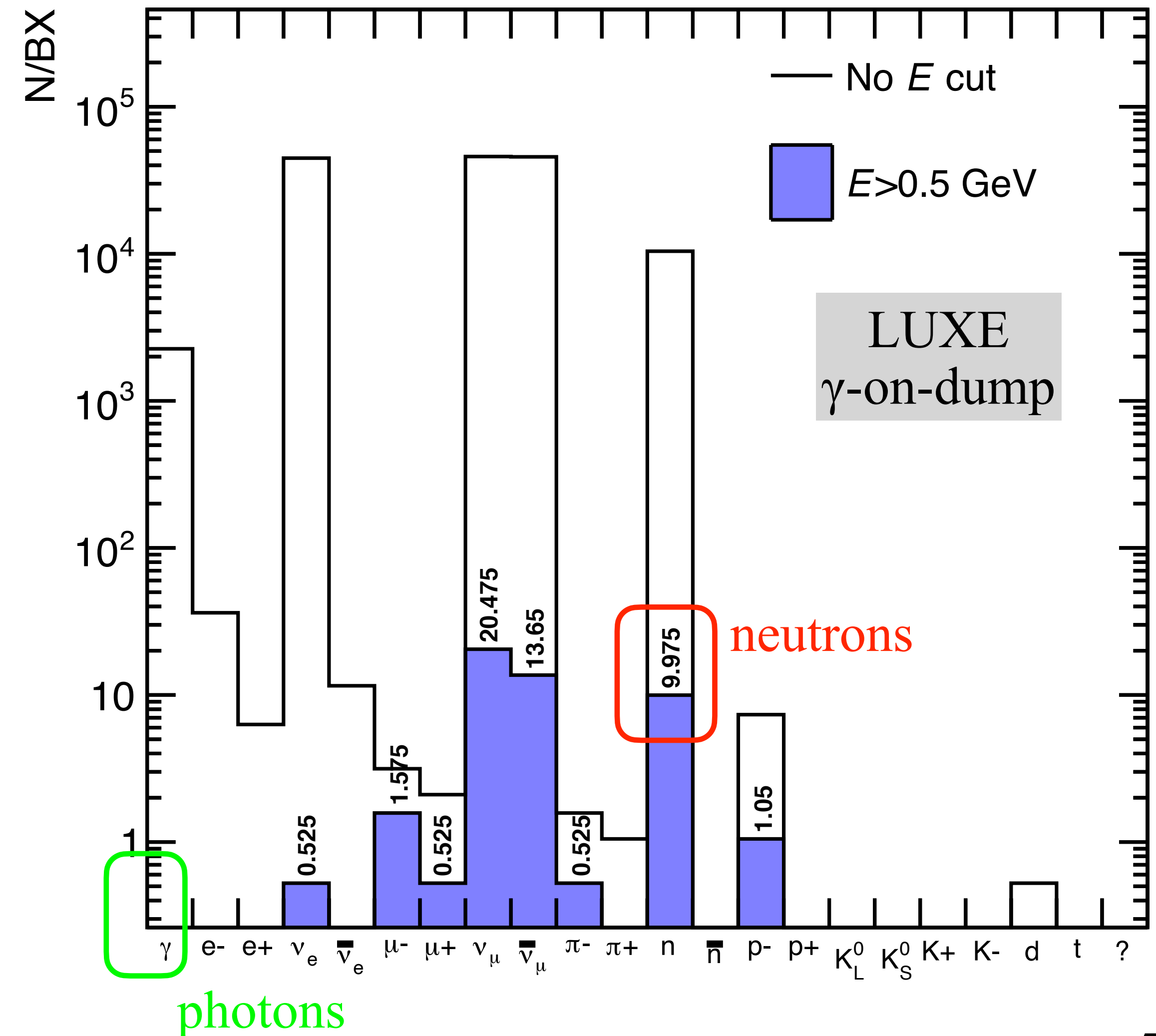
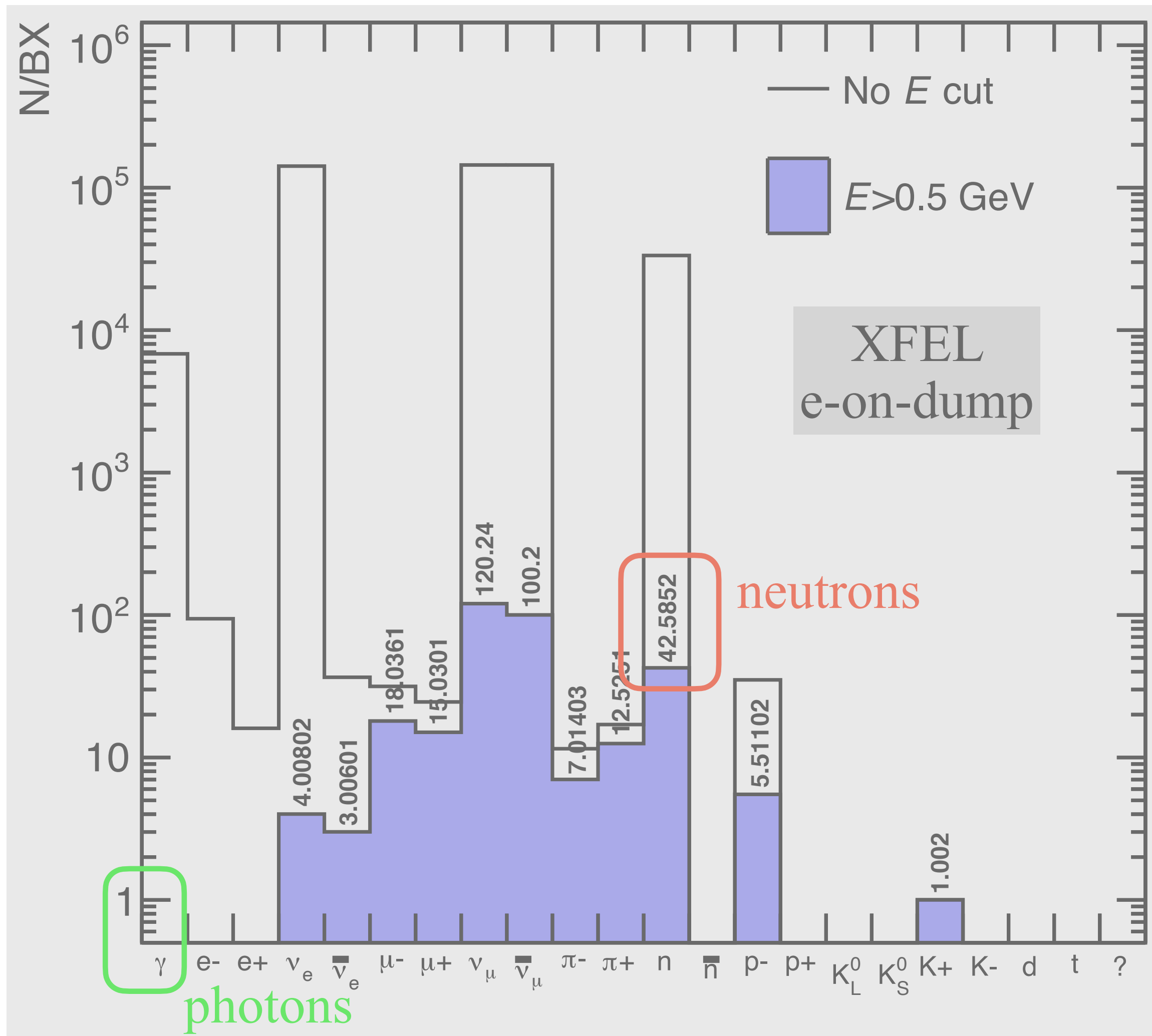
- Therefore: $\omega_L^{-1} \ll \tau_\gamma \ll t_L \ll \tau_{ee}$

Why not electrons-on dump?



Particles from e/γ -beam on 1m W dump

Each simulation in the following is equivalent to about 2 BXs (i.e. $3e9$ primary e 's)
 Showing the number of particles - only those which arrive at the detector surface



Probability to get 2 real photons

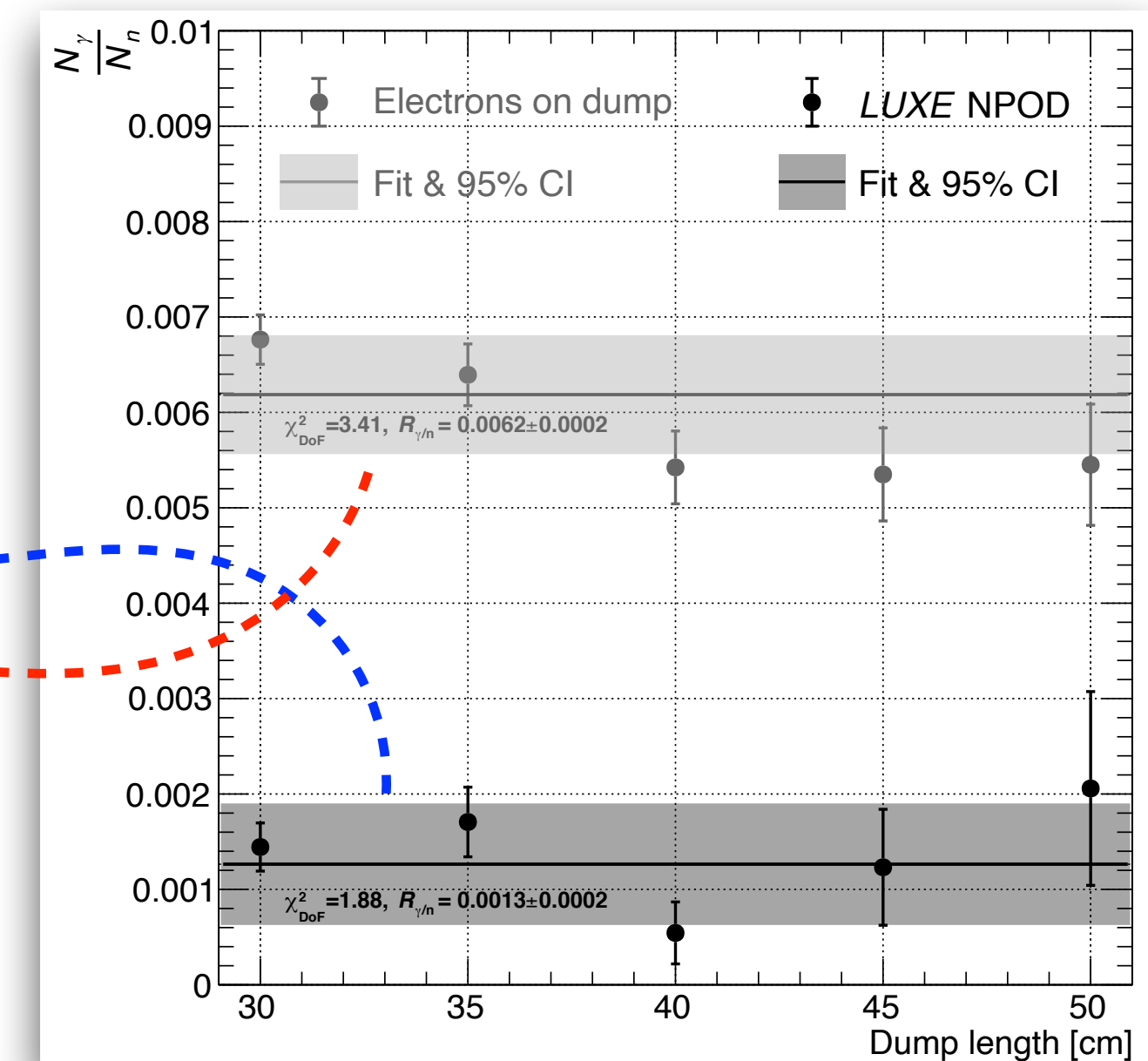
- $$P_{m_\gamma} = \frac{\lambda_\gamma^{m_\gamma} e^{-\lambda_\gamma}}{m_\gamma!}$$

- $\lambda_\gamma = 0.013 \pm 0.004$ since the fit gives $R_{\gamma/n} = 0.0013 \pm 0.0002$ and

since $N_n \simeq 10$, with $\lambda_\gamma = N_n R_{\gamma/n} \left(1 \pm \sqrt{\frac{1}{N_n} + \frac{\Delta^2 R_{\gamma/n}}{R_{\gamma/n}}} \right)$

(or in the e-on-dump case: $\lambda_\gamma \simeq 0.26 \pm 0.04$ for $R_{\gamma/n} \simeq 0.0062 \pm 0.0002$ and $N_n \simeq 42.6$)

- $$P_{2\gamma} = \frac{\lambda_\gamma^2 e^{-\lambda_\gamma}}{2!} \simeq 8.34 \times 10^{-5} \quad (\text{or in the e-on-dump case: } 2.7 \times 10^{-2})$$



Probability to get 2 fake photons

- $P_{n \rightarrow \gamma} = f_{n \rightarrow \gamma}$

- $\lambda_n = \lambda_n(1 \text{ m}) = 10$ (or in the e-on-dump case: $\lambda_n \simeq 42.6$)

- $P_{2n \rightarrow 2\gamma} = \sum_{m_n=2}^{\infty} \frac{\lambda_n^{m_n} e^{-\lambda_n}}{m_n!} C(2, m_n, P_{n \rightarrow \gamma})$

- $P_{2n \rightarrow 2\gamma} = \sum_{m_n=2}^{\infty} \left(\frac{\lambda_n^{m_n} e^{-\lambda_n}}{m_n!} \right) \left(\frac{m_n!}{2!(m_n-2)!} P_{n \rightarrow \gamma}^2 \times (1 - P_{n \rightarrow \gamma})^{m_n-2} \right) = \sum_{m_n=2}^{\infty} \frac{\lambda_n^{m_n} e^{-\lambda_n} \times P_{n \rightarrow \gamma}^2 \times (1 - P_{n \rightarrow \gamma})^{m_n-2}}{2!(m_n-2)!}$

- $P_{2n \rightarrow 2\gamma} = \frac{P_{n \rightarrow \gamma}^2 e^{-\lambda_n} \lambda_n^2}{2} \left(1 + \lambda_n(1 - P_{n \rightarrow \gamma}) + \frac{\lambda_n^2(1 - P_{n \rightarrow \gamma})^2}{2!} + \dots \right) = \frac{P_{n \rightarrow \gamma}^2 e^{-\lambda_n} \lambda_n^2}{2} \left(\sum_{k=0}^{\infty} \frac{(\lambda_n(1 - P_{n \rightarrow \gamma}))^k}{k!} \right) = \frac{P_{n \rightarrow \gamma}^2 e^{-\lambda_n} \lambda_n^2}{2} \underbrace{\sum_{k=0}^{\infty} \frac{x^k}{k!}}_{e^x}$

- $P_{2n \rightarrow 2\gamma} = \frac{P_{n \rightarrow \gamma}^2 \lambda_n^2 e^{-\lambda_n} e^{\lambda_n(1 - P_{n \rightarrow \gamma})}}{2} = P_{n \rightarrow \gamma}^2 e^{-\lambda_n P_{n \rightarrow \gamma}} \frac{\lambda_n^2}{2} = 50 f_{n \rightarrow \gamma}^2 e^{-10 f_{n \rightarrow \gamma}}$ (or in the e-on-dump case: $\frac{42.6^2}{2} f_{n \rightarrow \gamma}^2 e^{-42.6 f_{n \rightarrow \gamma}}$)

Probability to get 1 real + 1 fake photons

◦ For photons: $\lambda_\gamma = 0.013 \pm 0.004$, $P_{m_\gamma} = \frac{\lambda_\gamma^{m_\gamma} e^{-\lambda_\gamma}}{m_\gamma!} \Rightarrow P_{1\gamma} = \lambda_\gamma e^{-\lambda_\gamma}$

◦ For neutrons: $P_{n \rightarrow \gamma} = f_{n \rightarrow \gamma}$, $\lambda_n = 10 \pm 2.3$, $P_{1n \rightarrow 1\gamma} = \sum_{m_n=1}^{\infty} \frac{\lambda_n^{m_n} e^{-\lambda_n}}{m_n!} C(1, m_n, P_{n \rightarrow \gamma})$

$$P_{1n \rightarrow 1\gamma} = \sum_{m_n=1}^{\infty} \left(\frac{\lambda_n^{m_n} e^{-\lambda_n}}{m_n!} \right) \left(\frac{m_n!}{1!(m_n-1)!} P_{n \rightarrow \gamma} \times (1 - P_{n \rightarrow \gamma})^{m_n-1} \right) = \sum_{m_n=1}^{\infty} \frac{\lambda_n^{m_n} e^{-\lambda_n} \times P_{n \rightarrow \gamma} \times (1 - P_{n \rightarrow \gamma})^{m_n-1}}{(m_n-1)!}$$

$$P_{1n \rightarrow 1\gamma} = P_{n \rightarrow \gamma} e^{-\lambda_n} \lambda_n \left(1 + \lambda_n (1 - P_{n \rightarrow \gamma}) + \frac{\lambda_n^2 (1 - P_{n \rightarrow \gamma})^2}{2!} + \dots \right) = P_{n \rightarrow \gamma} e^{-\lambda_n} \lambda_n \left(\sum_{k=0}^{\infty} \frac{(\lambda_n (1 - P_{n \rightarrow \gamma}))^k}{k!} \right) = P_{n \rightarrow \gamma} e^{-\lambda_n} \lambda_n \underbrace{\sum_{k=0}^{\infty} \frac{x^k}{k!}}_{e^x}$$

$$P_{1n \rightarrow 1\gamma} = P_{n \rightarrow \gamma} \lambda_n e^{-\lambda_n} e^{\lambda_n (1 - P_{n \rightarrow \gamma})} = P_{n \rightarrow \gamma} e^{-\lambda_n P_{n \rightarrow \gamma}} \lambda_n$$

◦ For one neutron and one photon: $P_{n+\gamma \rightarrow 2\gamma} = P_{1n \rightarrow 1\gamma} \cdot P_{1\gamma} = \left(\lambda_n f_{n \rightarrow \gamma} e^{-\lambda_n f_{n \rightarrow \gamma}} \right) \cdot \left(\lambda_\gamma e^{-\lambda_\gamma} \right) \simeq 0.128 f_{n \rightarrow \gamma} e^{-10 f_{n \rightarrow \gamma}}$

(or in the e-on-dump case: $1.12 f_{n \rightarrow \gamma} e^{-42.6 f_{n \rightarrow \gamma}}$)

Magnet requirements

Circle equation wrt the origin at the centre of the circle defined by the track: $X^2 + Z^2 = R^2$

Therefore: $Z_{\text{exit}} = L_B$ and hence $X_{\text{exit}} = \sqrt{R^2 - L_B^2}$

The tangent equation is: $Z = m_T \cdot X + c_T$. The tangent gradient, m , is -1 over the gradient of the radius line itself, at the point where the tangent is defined at the point $(Z_{\text{exit}}, X_{\text{exit}})$, i.e.:

$$m_T = -1/m_R = -1/(\Delta Z/\Delta X)_{\text{radius slope}} = -\frac{(X_{\text{exit}} - 0)}{(Z_{\text{exit}} - 0)} = -\frac{\sqrt{R^2 - L_B^2}}{L_B} = -\sqrt{\frac{R^2}{L_B^2} - 1}$$

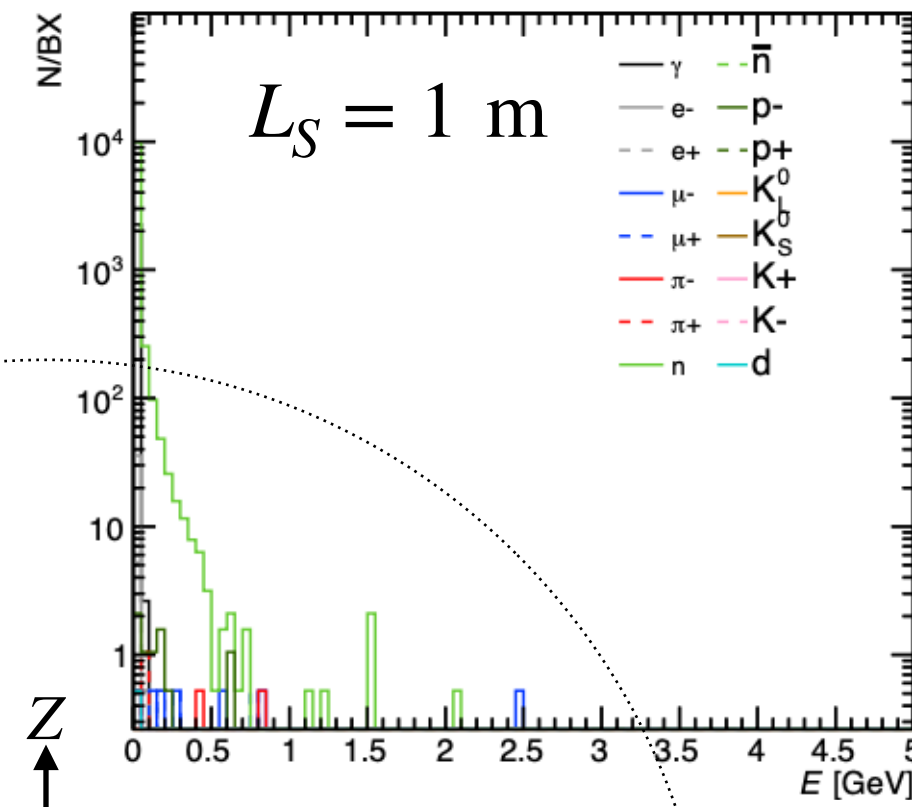
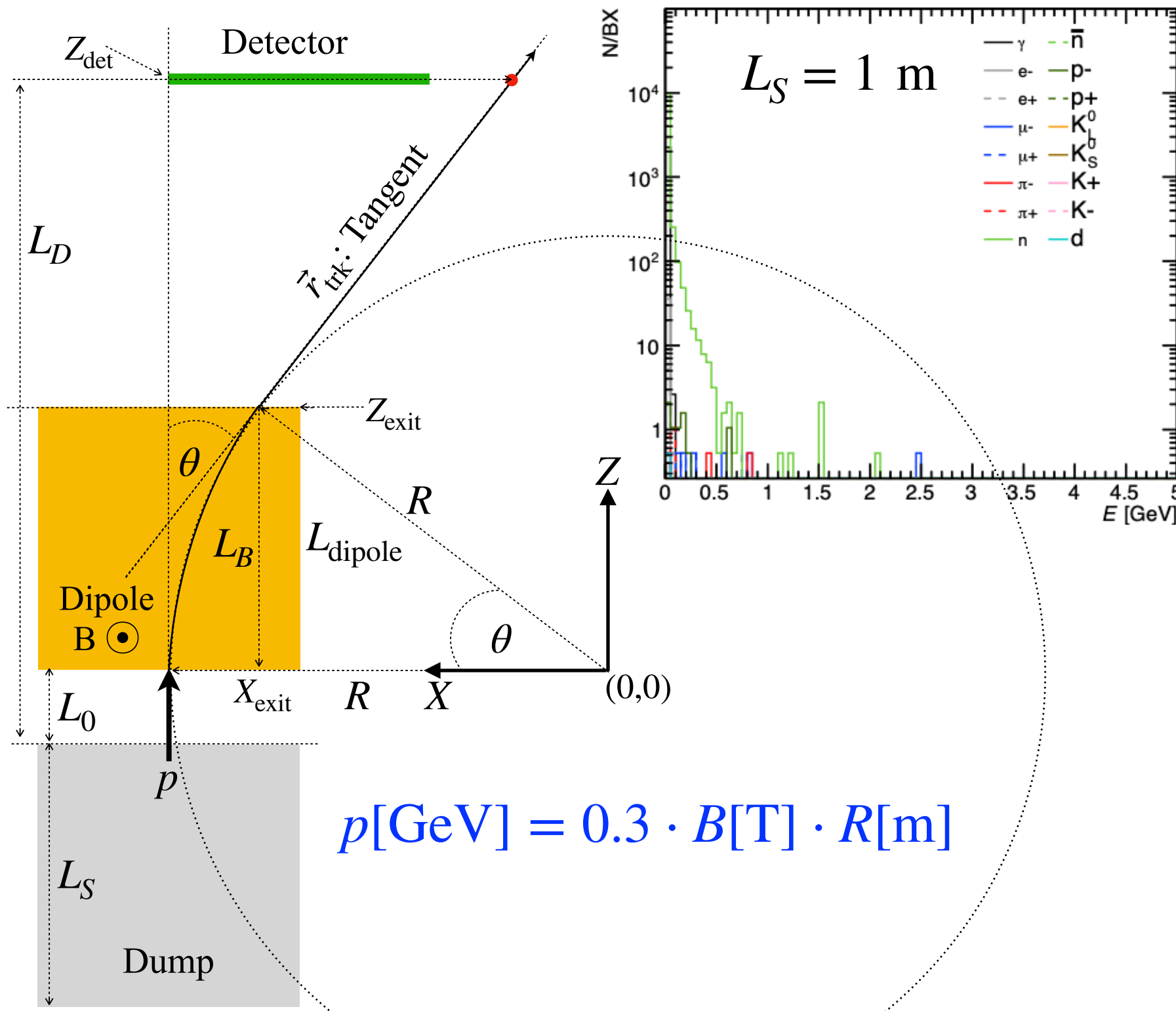
Using the point $(Z_{\text{exit}}, X_{\text{exit}})$ again we get the intersection of the tangent: $c_T = Z - m_T \cdot X$

$$c_T = L_B - \left(-\sqrt{\frac{R^2}{L_B^2} - 1}\right) \cdot \sqrt{R^2 - L_B^2} = L_B + \frac{R^2 - L_B^2}{L_B} = \frac{R^2}{L_B}$$

Hence, the prediction along the tangent at some point Z_{tangent} is: $X = \frac{Z - c_T}{m_T}$

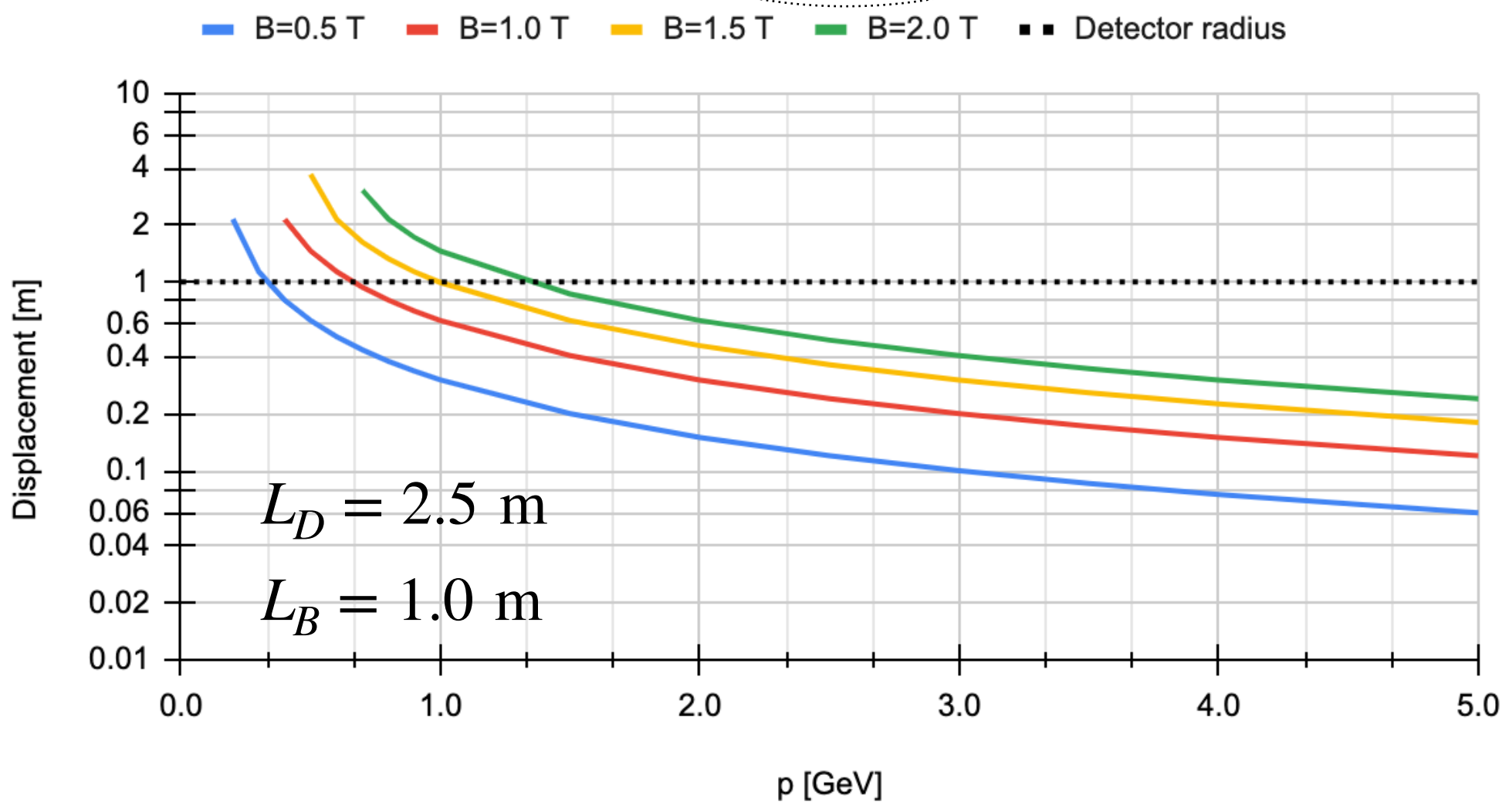
$$X_{\text{tangent}} = \left(\frac{R^2}{L_B} - Z_{\text{tangent}}\right) \frac{L_B}{\sqrt{R^2 - L_B^2}} \text{ and so putting } Z_{\text{tangent}} = Z_{\text{det}} = L_D - L_0 \simeq L_D$$

$$\text{we get that } X_{\text{tangent}} \simeq \left(\frac{(p/0.3B)^2}{L_B} - L_D\right) \frac{L_B}{\sqrt{(p/0.3B)^2 - L_B^2}}$$



$$p[\text{GeV}] = 0.3 \cdot B[\text{T}] \cdot R[\text{m}]$$

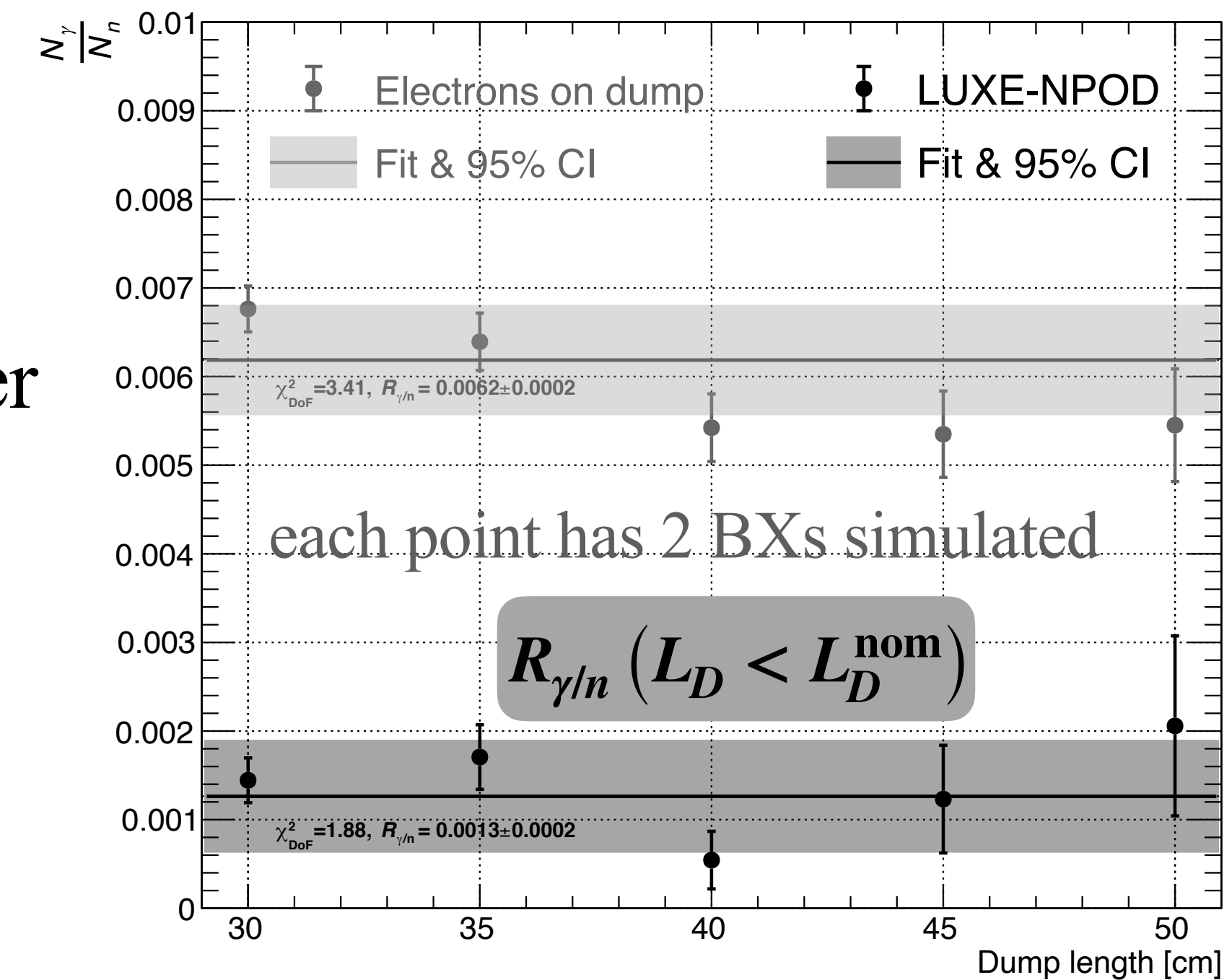
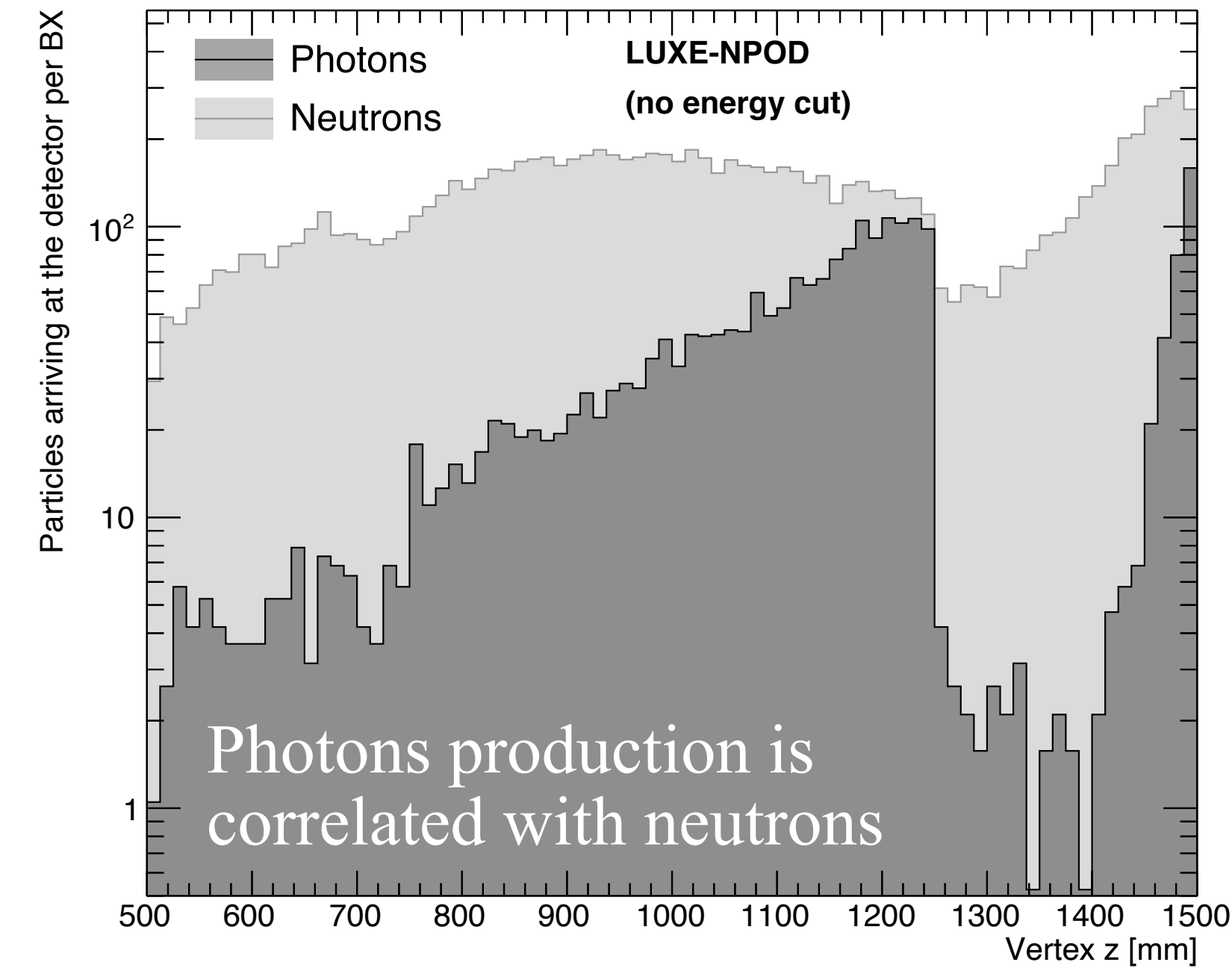
Displacement in x at the detector face



Background estimation

- Background is mostly neutrons and photons
 - we get 0 photons and 10 neutrons per BX for 2 BXs simulated
- This is inaccurate: need many more BXs for a proper estimate
 - however, the simulation is very intensive computationally
- Instead, we see that the photon production is correlated with the neutrons production (in hadronic processes)
- N_γ can be extrapolated from the photons-to-neutrons ratio of shorter L_D dumps than the nominal, where we have enough photons:

$$N_\gamma(L_D^{\text{nom}}) \simeq N_n(L_D^{\text{nom}}) \times R_{\gamma/n}(L_D < L_D^{\text{nom}})$$



Background estimation

- Assuming
 - one year of running with $T \sim 10^7$ live seconds, i.e. recorded BXs
 - rejection is $R_{\text{sel}} \lesssim 10^{-3} - 10^{-4}$ from kinematics & timing
 - neutron-to-photon fake rate is $f_{n \rightarrow \gamma} \lesssim 10^{-3} - 10^{-4}$
- Number of bkg two-photon events is $N_{\text{bkg}} = P_{\text{bkg}} R_{\text{sel}} T_{\text{operation}}$
 - bkg = 2γ
 - bkg = $2n \rightarrow 2\gamma$ (sub-dominant)
 - bkg = $\gamma + n \rightarrow 2\gamma$
- The probabilities are given by Poisson and Binomial laws:

$$P_{N_\gamma} = \frac{\mu_\gamma^{N_\gamma} e^{-\mu_\gamma}}{N_\gamma!}$$

$$P_{N_n \rightarrow N_\gamma} = \sum_{k_n=N_n}^{\infty} \frac{\mu_n^{k_n} e^{-\mu_n}}{k_n!} B(N_n, k_n, f_{n \rightarrow \gamma})$$

$$P_{n+\gamma \rightarrow 2\gamma} = P_{1n \rightarrow 1\gamma} \cdot P_{2\gamma}$$

Assumptions	Value
T_{op}	1E+07
R_{sel}	5E-04
$f_{n \rightarrow \gamma}$	5E-04

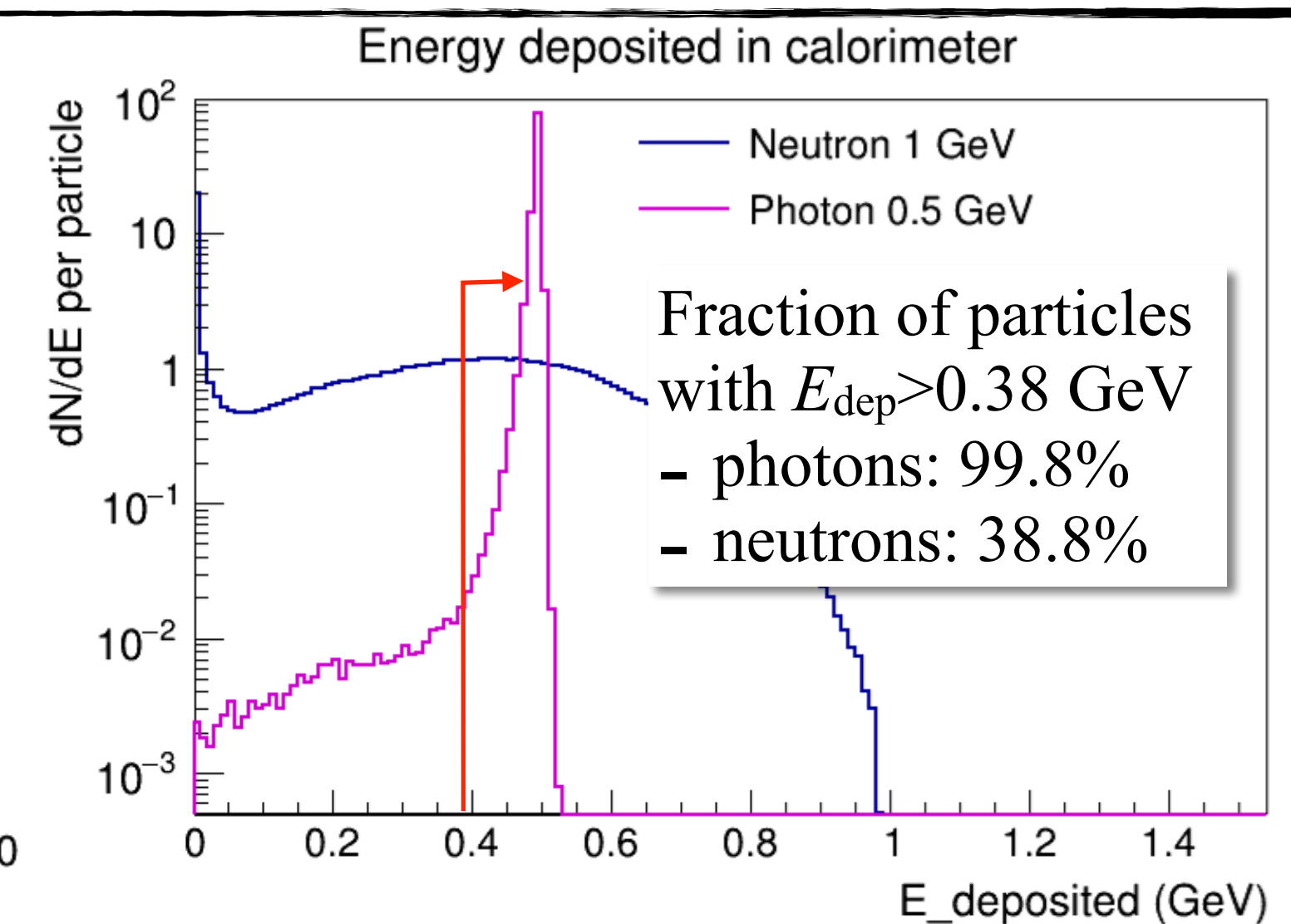
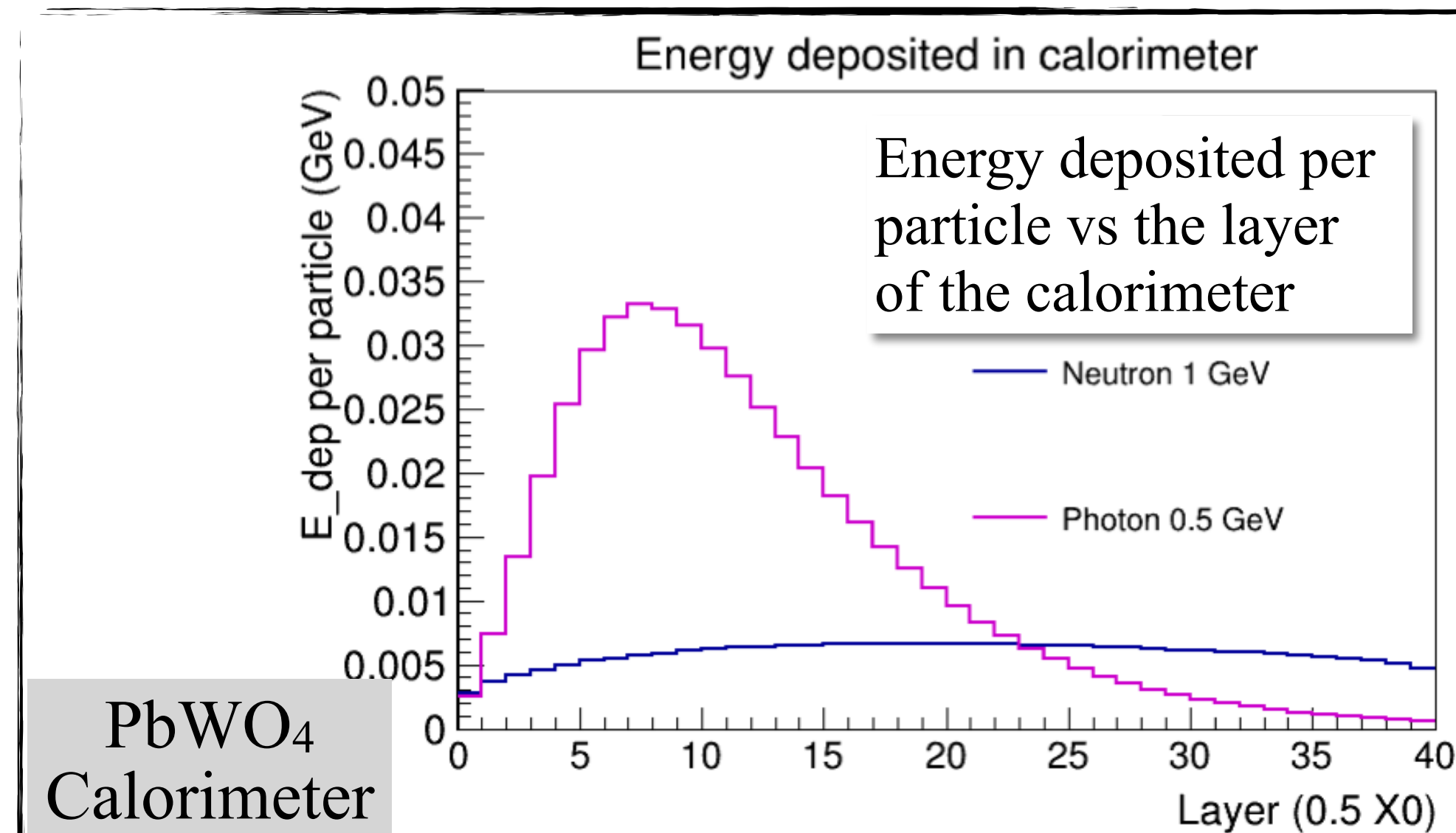
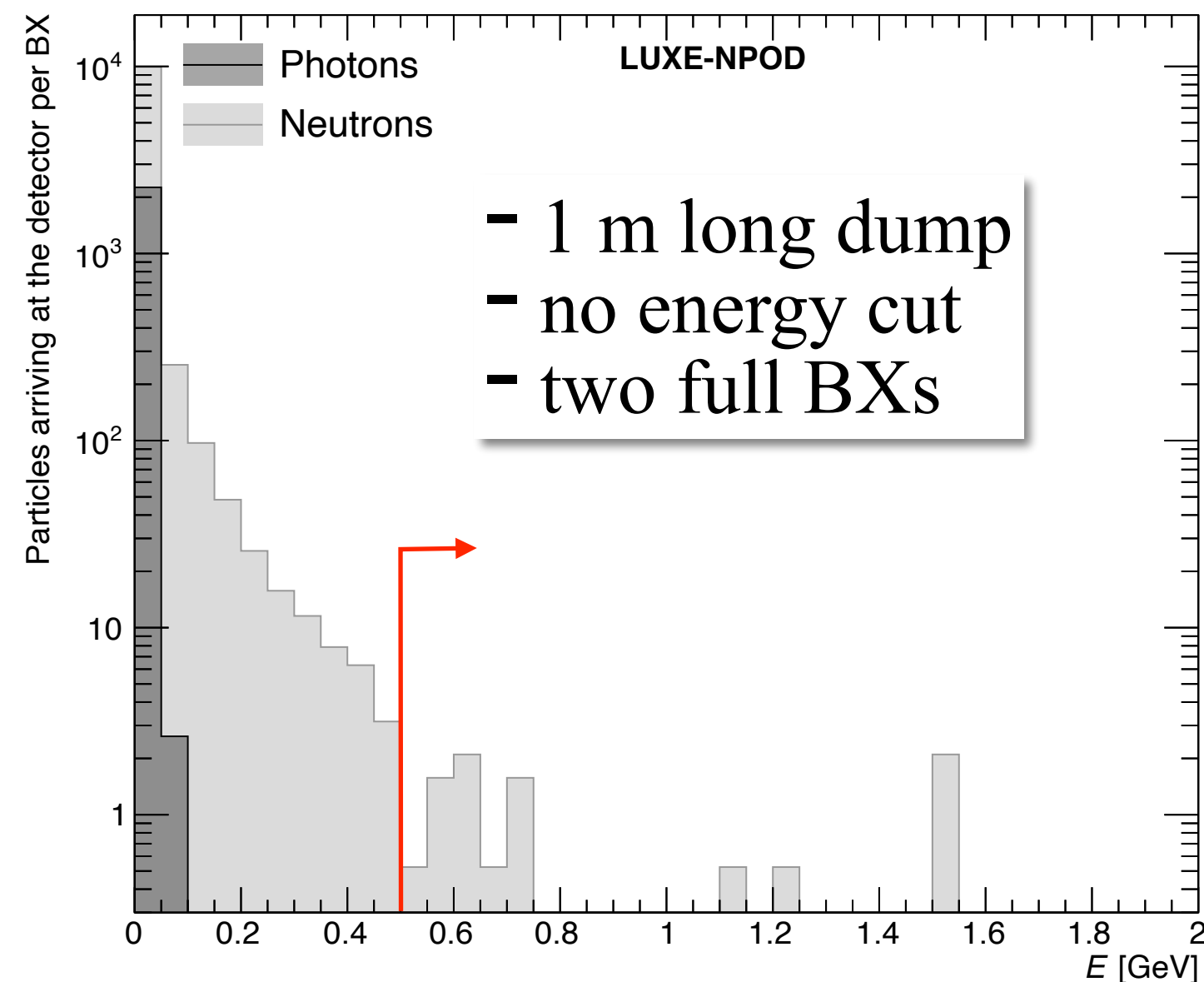
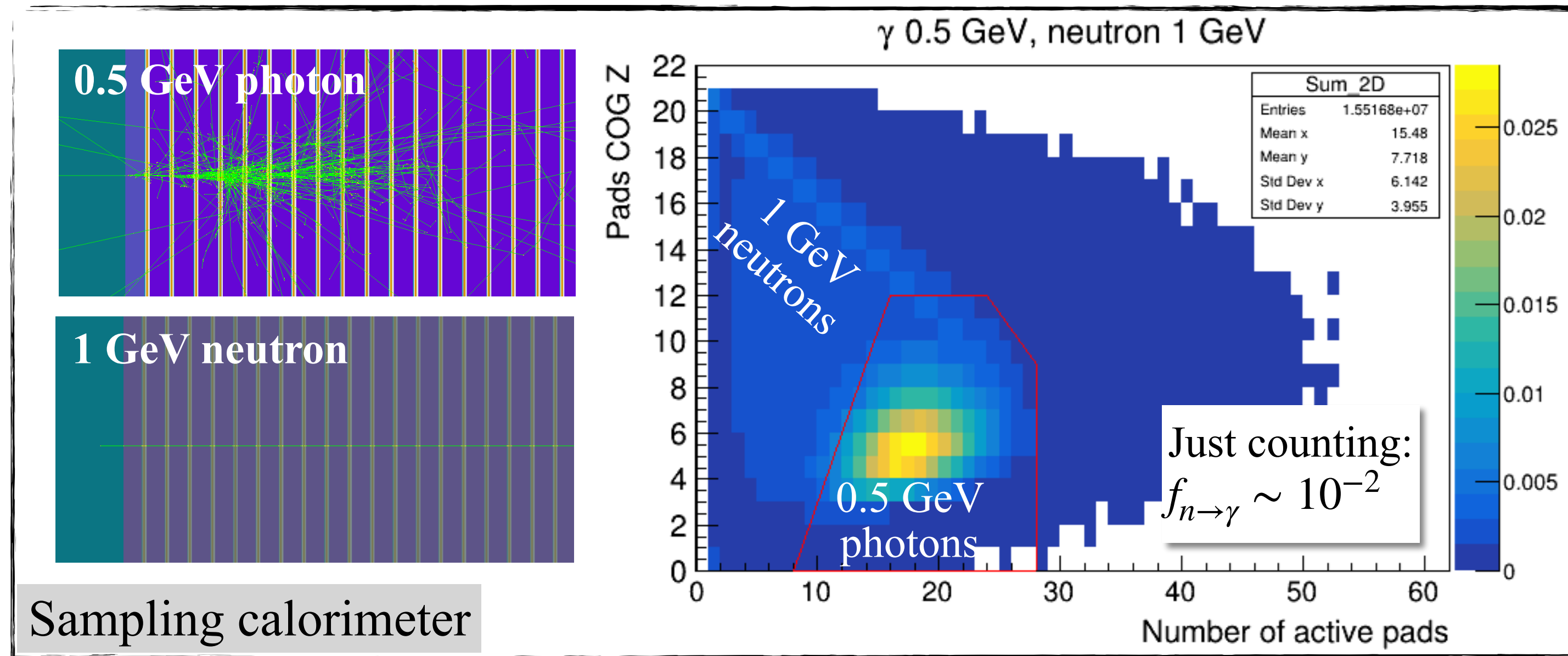
Parameter	LUXE NPOD	Electrons on dump
$R_{\gamma/n}$ (fit)	0.0013	0.0062
μ_n (count)	9.8	42.6
μ_γ (extrap.)	0.013	0.264

Max N_{bkg}	LUXE NPOD	Electrons on dump
$N_{2\gamma}$	0.4	133.9
$N_{2n \rightarrow 2\gamma}$	0.1	1.1
$N_{\gamma+n \rightarrow 2\gamma}$	0.3	21.1

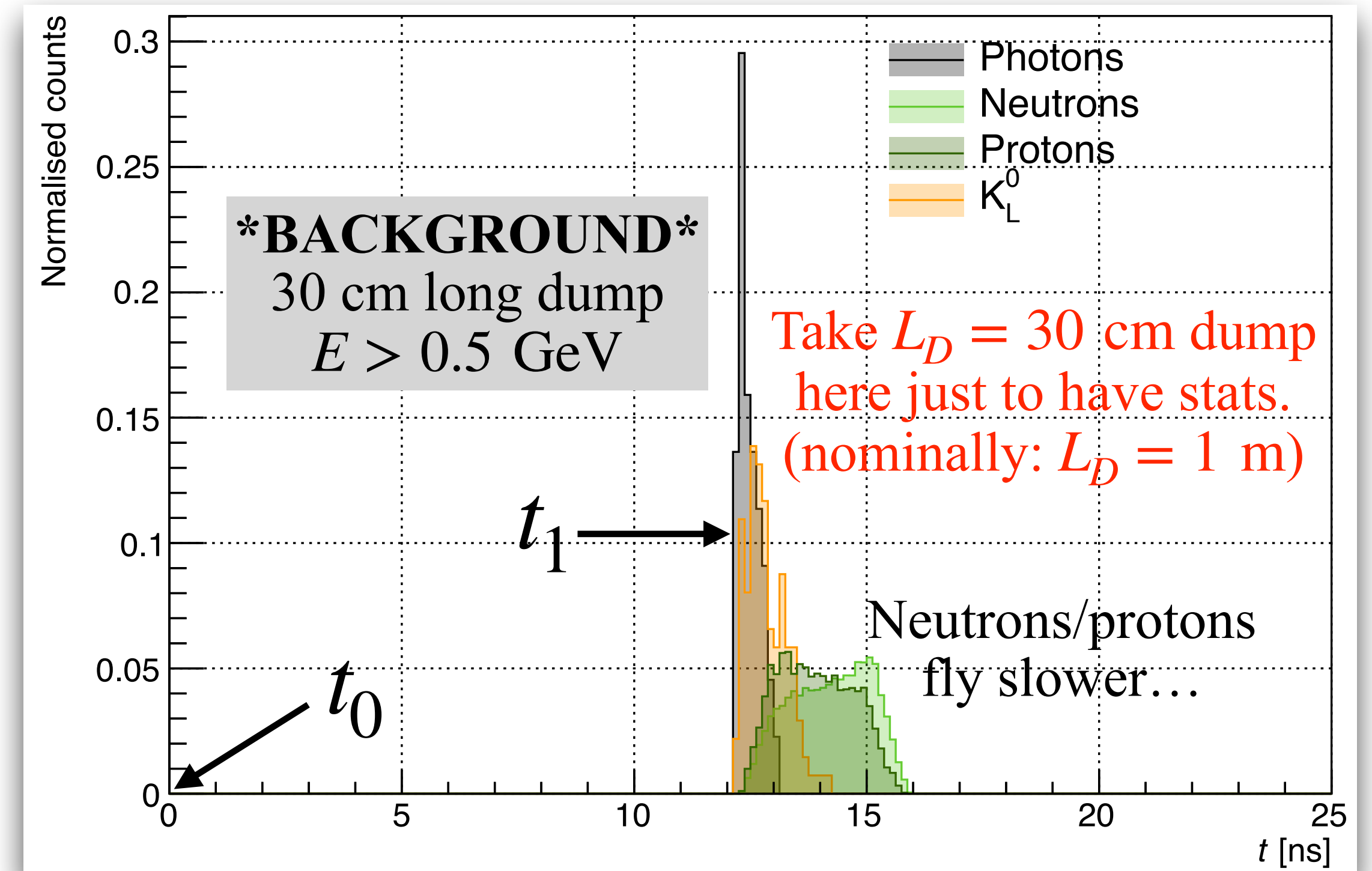
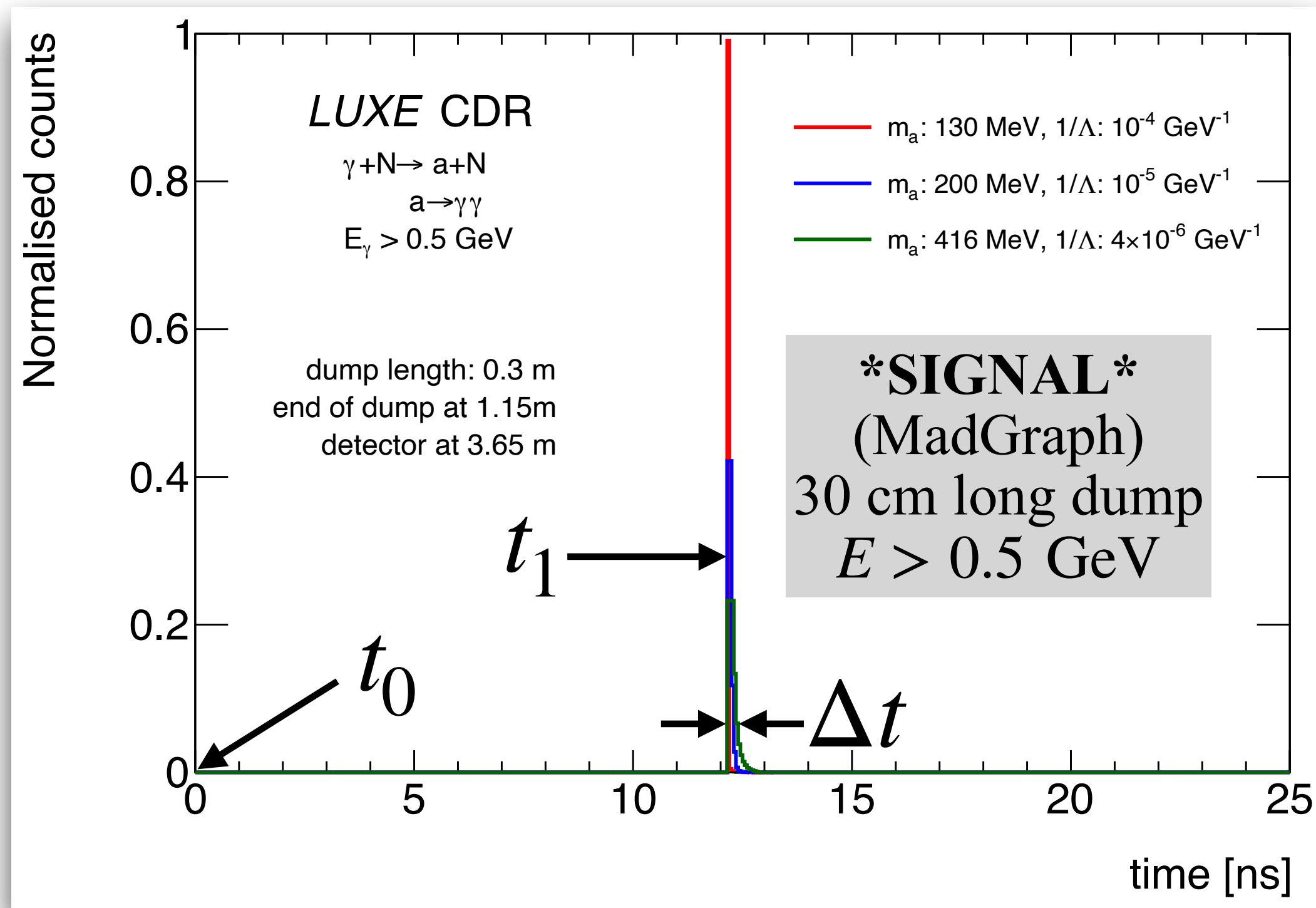
$$N_{\text{bkg}}^{\text{tot}} < 1$$

Fake photons from neutrons

- Most neutrons are very soft
- Very different shower shapes (γ vs n)
 - harder neutrons are more similar
- Study done by **Sasha Borysov** (Staff scientist candidate at the faculty)



Exploiting timing information



- The time it takes a bkg photon to fly from z_0 at t_0 to the detector face at $z_1 = z_D + L_D/2 + L_V = 3.65 \text{ m}$, is $t_1 = t_0 + (12 + \Delta t) \text{ ns}$
 - for $z_0 = 0, t_0 = 0, z_D = 1 \text{ m}, L_D = 0.3 \text{ m}$ and $L_V = 2.5 \text{ m}$
- We trigger at t_0 (Eu.XFEL clock) and open a short time window Δt
 - most signal (and bkg) photons will **arrive within $\Delta t \simeq 0.5 \text{ ns}$**
 - almost all bkg hadrons will arrive after that - **need $\lesssim 0.1 \text{ ns}$ resolution**

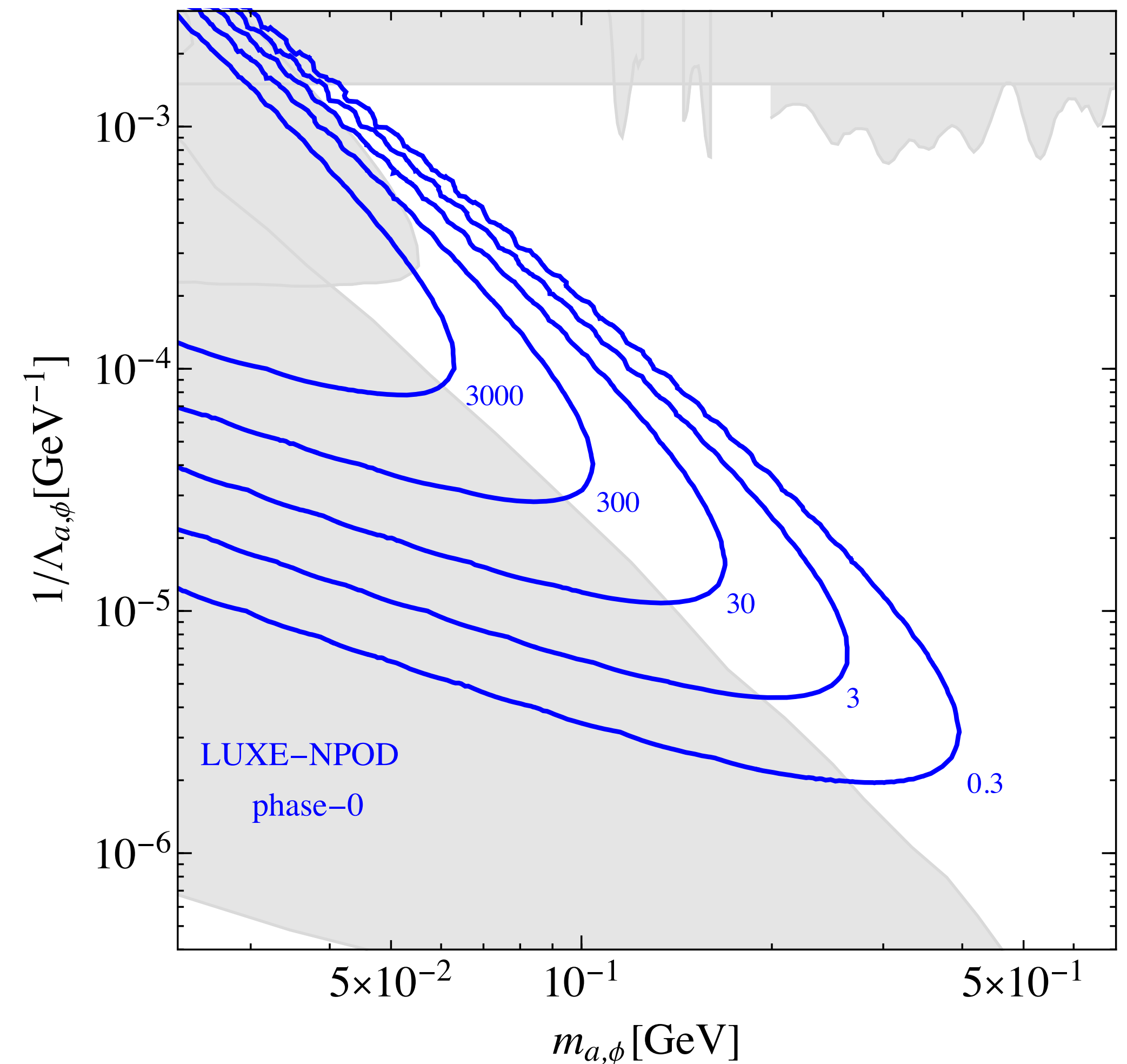
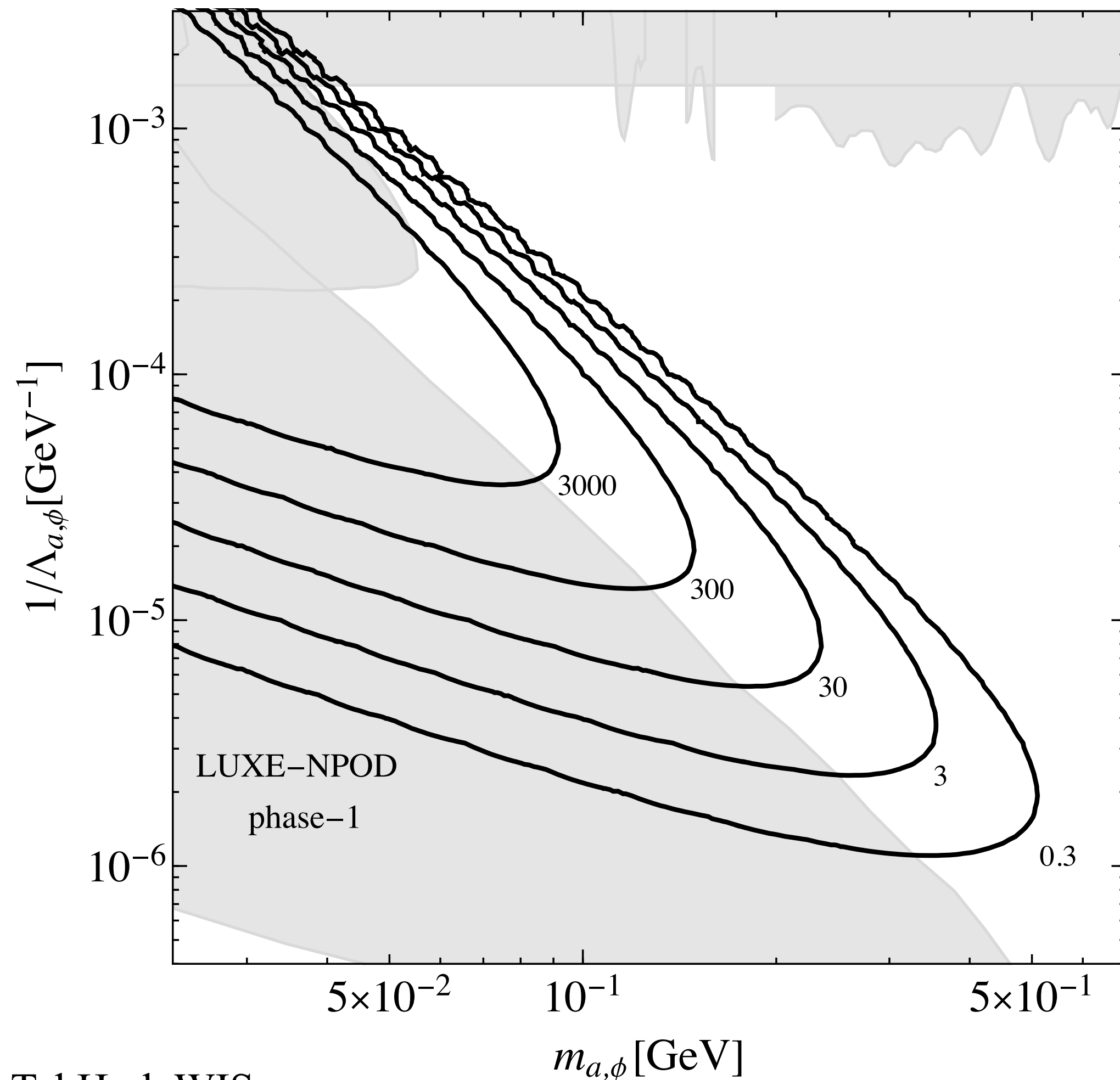
Δt [ns]	Background rejection \sim [%]				Signal efficiency [%] for $m_a: 1/\Lambda_a$		
	γ	n	p	K_L	130:1e-4	200:e-5	416:e-5
0.1	57	99.9	99.9	87	99.6	84	46
0.5	16	96	94	52	100	100	99
1.0	0	80	70	13	100	100	100

$R_{sel}^{\text{neutrons}} \sim 10^{-3}$

Contours of the expected number of $a, \phi \rightarrow 2\gamma$ events, $N_{a,\phi}$, for phase-0 and phase-1

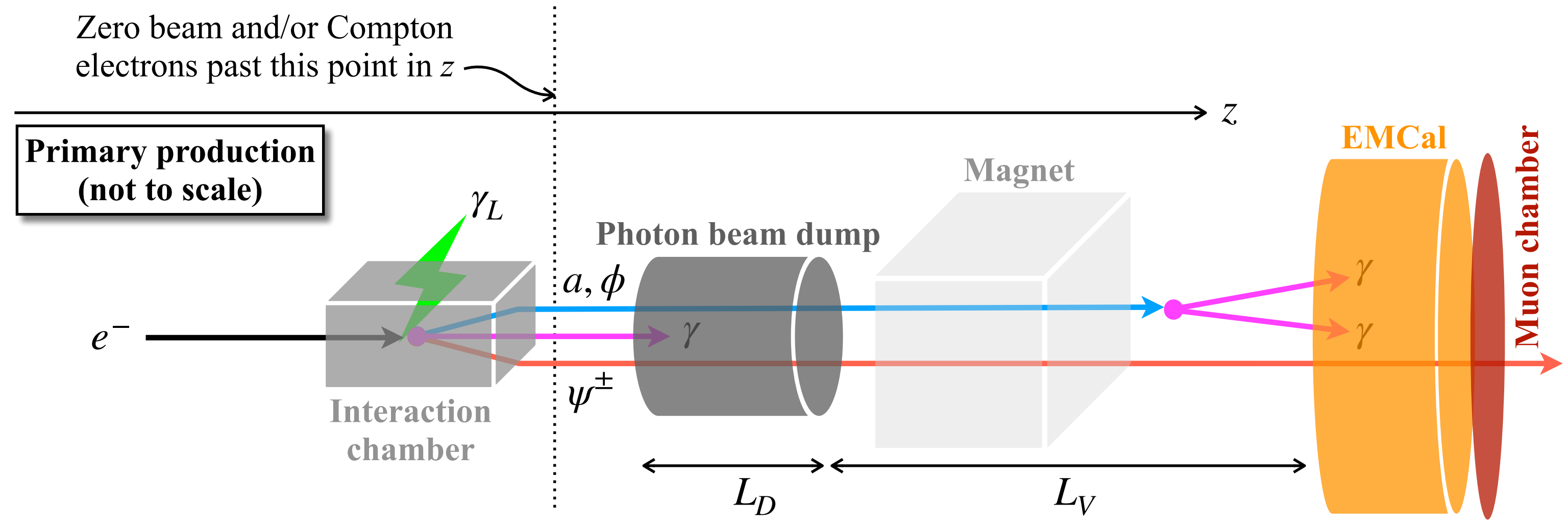
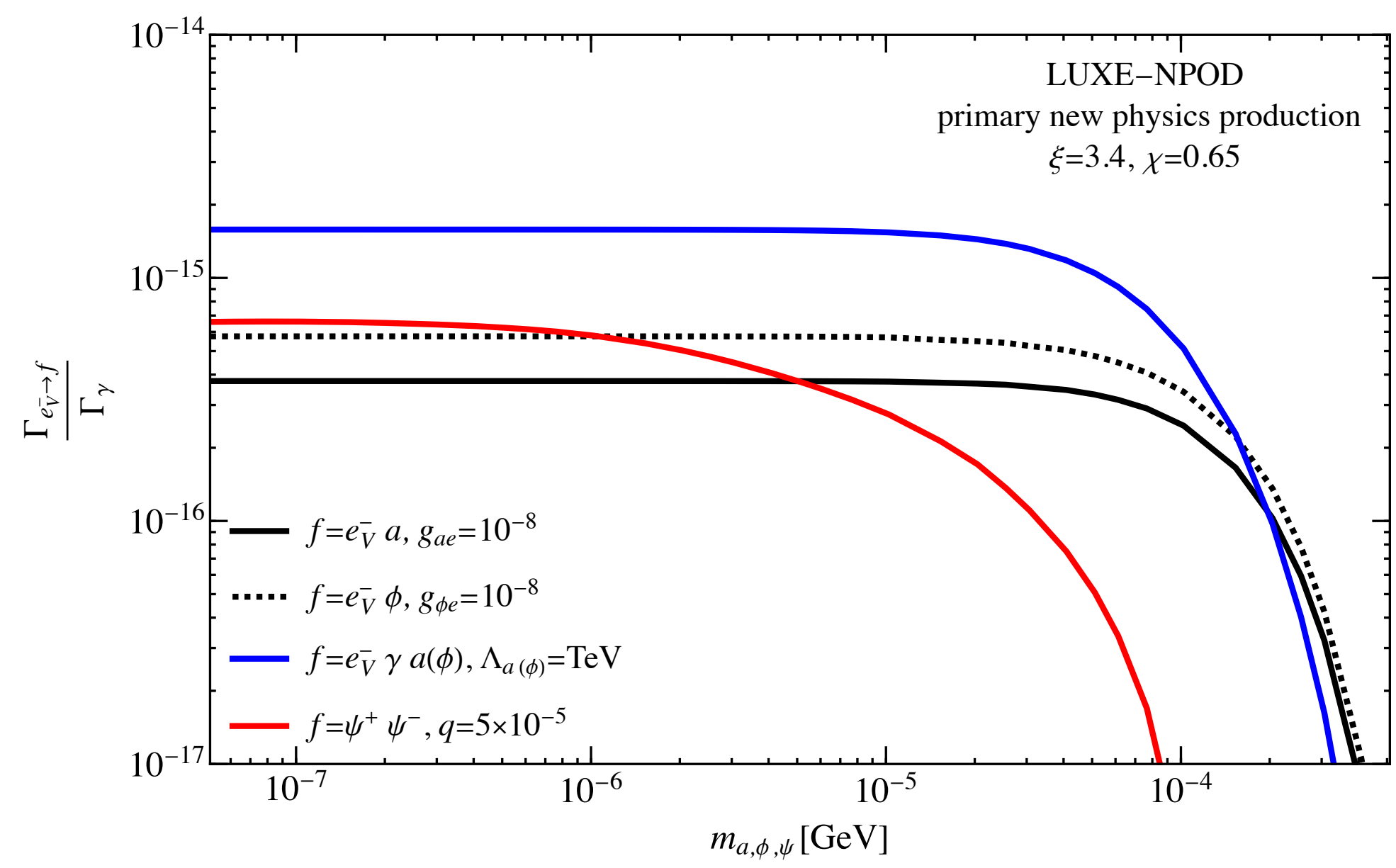
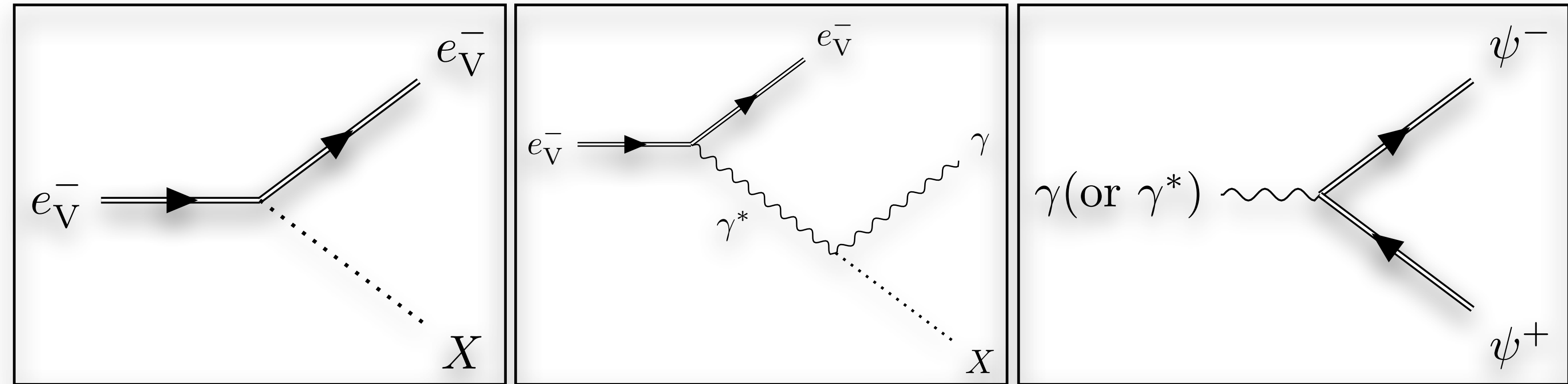
The lines correspond to 1 year of data taking.

The nominal curve is for $N_{a,\phi} = 3$ which is the 95 % CL equivalent for background free search



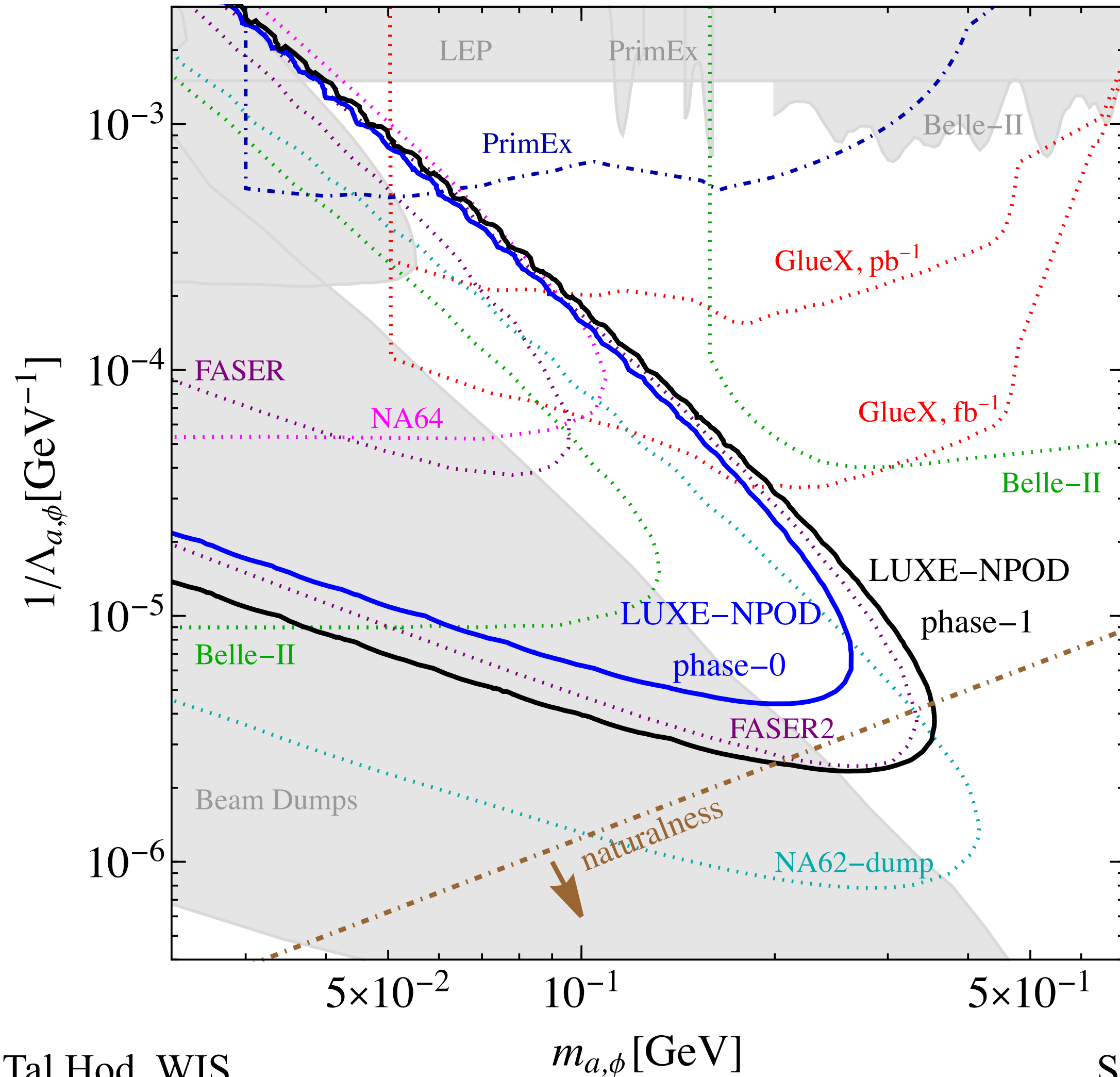
New Physics production at the IP

- Axion-like particles (ALPs)
 - or scalars ($X = a, \phi$)
- Milli-charged particles (mCPs)
 - $m_\psi \ll m_e$ and $q_\psi \equiv qe \ll e$



LUXE-NPOD

Setting the number of observed signal-like events to $N_a = 3$, which is the 95 % CL equivalent for background free search



LUXE-NPOD: new physics searches with an optical dump at LUXE

Zhaoyu Bai,^{1,2,*} Thomas Blackburn,^{3,†} Oleksandr Borysov,^{4,‡} Oz Davidi,^{2,§} Anthony Hartin,^{5,¶} Beate Heinemann,^{4,6,**} Teng Ma,^{7,††} Gilad Perez,^{2,‡‡} Arka Santra,^{2,§§} Yotam Soreq,^{7,¶¶} and Noam Tal Hod^{2,***}

¹Department of Physics, Southern University of Science and Technology, Shenzhen 518055, China

²Department of Particle Physics and Astrophysics, Weizmann Institute of Science, Rehovot 7610001, Israel

³Department of Physics, University of Gothenburg, SE-41296 Gothenburg, Sweden

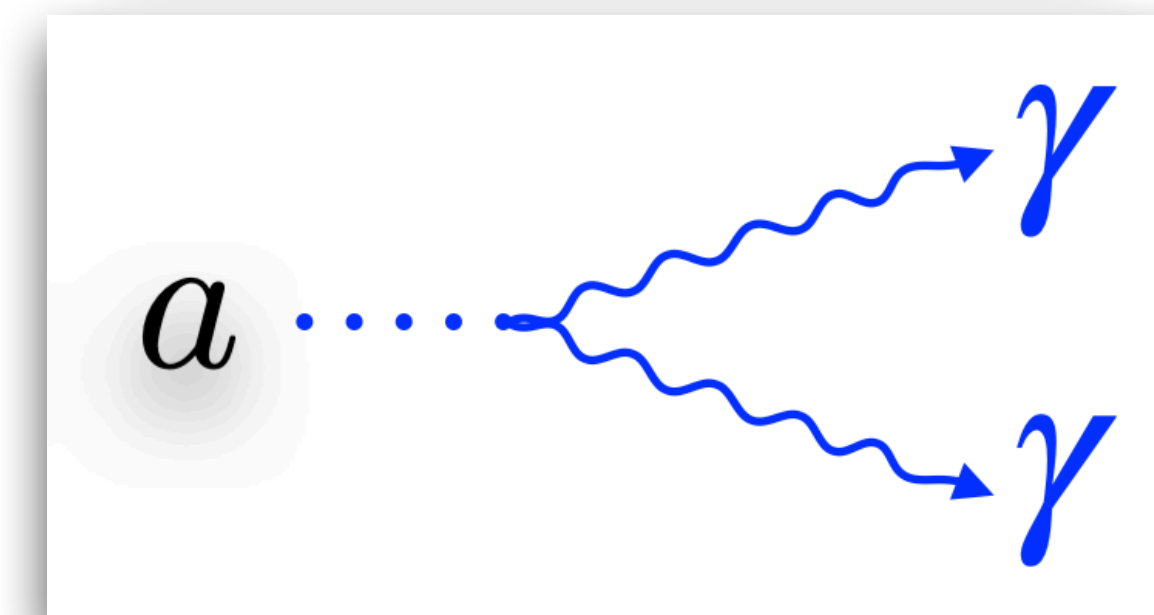
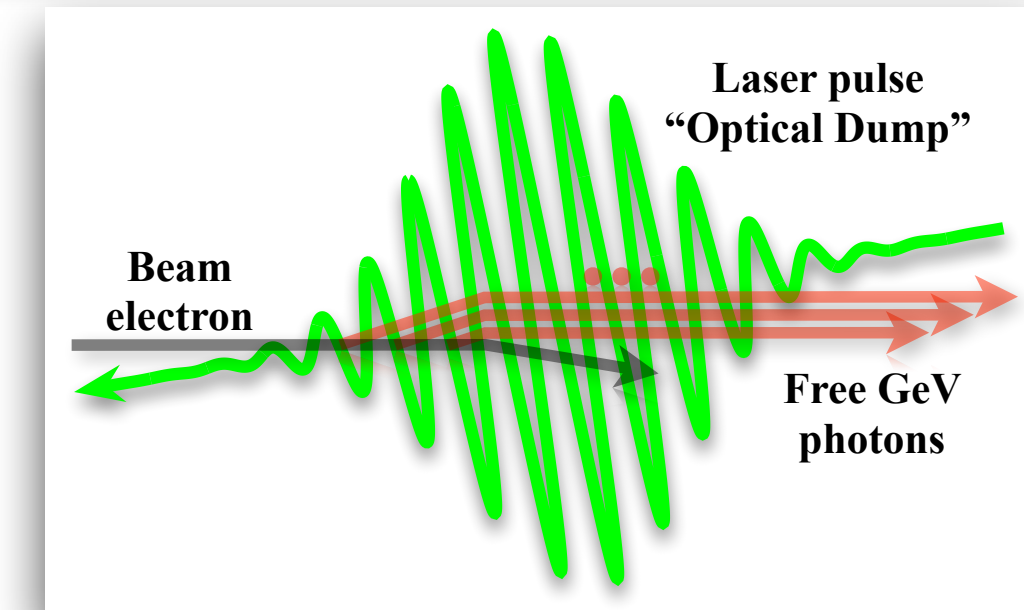
⁴Deutsches Elektronen-Synchrotron DESY, 22607 Hamburg, Germany

⁵University College London, Gower Street, London WC1E 6BT, United Kingdom

⁶Albert-Ludwigs-Universität Freiburg, 79104 Freiburg, Germany

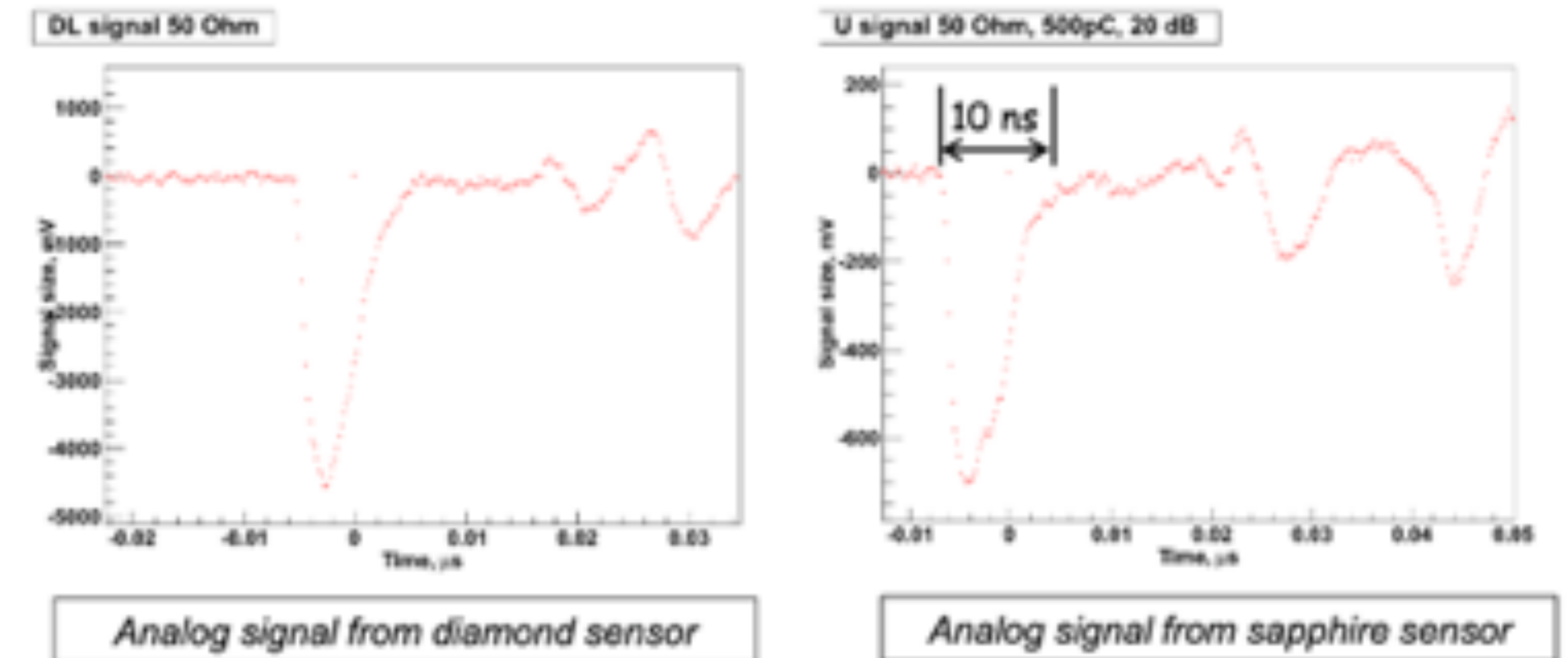
⁷Physics Department, Technion—Israel Institute of Technology, Haifa 3200003, Israel

We propose a novel way to search for feebly interacting massive particles, exploiting two properties of systems involving collisions between high energy electrons and intense laser pulses. The first property is that the electron-intense-laser collision results in a large flux of hard photons, as the laser behaves effectively as a thick medium. The second property is that the emitted photons free-stream inside the laser and thus for them the laser behaves effectively as a very thin medium. Combining these two features implies that the electron-intense-laser collision is an apparatus which can efficiently convert UV electrons to a large flux of hard, co-linear photons. We further propose to direct this unique large and hard flux of photons onto a physical dump which in turn is capable of producing feebly interacting massive particles, in a region of parameters that has never been probed before. We denote this novel apparatus as “optical dump” or NPOD (new physics search with optical dump). The proposed LUXE experiment at Eu.XFEL has all the required basic ingredients of the above experimental concept. We discuss how this concept can be realized in practice by adding a detector after the last physical dump of the experiment to reconstruct the two-photon decay product of a new spin-0 particle. We show that even with a relatively short dump, the search can still be background free. Remarkably, even with a 40 TW laser, which corresponds to the initial run, and definitely with a 350 TW laser, of the main run with one year of data taking, LUXE-NPOD will be able to probe uncharted territory of both models of pseudo-scalar and scalar fields, and in particular probe natural of scalar theories for masses above 100 MeV.



Profiler - why Sapphire Al_2O_3 ?

Material properties	sapphire	diamond	silicon
density [g/cm ³]	3.98	3.52	2.33
bandgap [eV]	9.9	5.47	1.12
energy to create an eh pair [eV]	27	13	3.6
dielectric constant	9.3–11.5	5.7	11.7
dielectric strength [V/cm]	4.0E+05	1.0E+06	3.0E+05
resistivity [Ohm cm] at 20 C	1.0E+16	1.0E+16	1.0E+05
electron mobility [cm ² /(V s)] at 20 C	600	2800	460
MIP eh created [eh/ μm]	22	36	73



- High radiation resistance: ~ 10 MGy
- Leakage current does not increase with dose
- High e-h creation energy
- Low collection efficiency ($\sim 10\%$)
- Fast response
 - low electron mobility compensated by reduced distance travelled by electrons
- Low Cost: 1€/cm² (compared to diamond 3000 €/cm²)
- Intensively tested as beam halo and beam loss monitors at CMS (LHC)

S. Schuwalow et al.: Investigation of a direction sensitive sapphire detector stack at the 5 GeV electron beam at DESY-II / JINST 10 P08008